# Advanced LIGO Optics Workshop at Caltech Nov ‘06

LIGO-T060297-00-D

## *Summary Report*

Report by David Ottaway and Gregg Harry Get Report

## *Talk List*

### Coating Session

| | | |
|---|---|---|
| Coating Overview | Gregg Harry | Get Talk |
| Some Q’s and first dn/dT for tantala | Andri Grettarson | Get Talk |
| 3rd Generation Coating Issues | Stuart Reid | Get Talk |
| Results from the TNI | Eric Black | |
| More Absorption at H1 | David Ottaway | Get Talk |

### Scatter Session

| | | |
|---|---|---|
| Losses in LHO HR Surfaces | Bill Kells | Get Talk |
| Scatter measurement set-up at Caltech | LiyuanZhang | Get Talk |
| New FFT for advLIGO | Hiro Yamamoto | Get Talk |
| Techniques at Southern University | Steve Macquire | |

## Stable/Marginally Stable Recycling Cavities

| | | |
|---|---|---|
| Overview | Peter Fritschel | Get Talk |
| Report from UFL | Guido Mueller | Get Talk |

## Parametric Instabilities

| | | |
|---|---|---|
| Time Domain Issues in Parametric Instability | David Ottaway | Get Talk |
| Recycling and Parametric Instability | Bill Kells | Get Talk |
| Analysis of Parametric Oscillatory Instability in Signal Recycled LIGO Interferometer with Different Arms | Sergey Vyatchanin | Get Talk |
| Passive Parametric Instability Control | SlawekGras | Get Talk |
| Ring Dampers at the TNI | Akira Villar | Get Talk |
| Experimental Investigation of Parametric Instabilities at Gingin Facility | Li. Ju | Get Talk |

# Summary of the Advanced LIGO Optics Meeting

November, 2006 at Caltech, Report by David Ottaway and Gregg Harry

Attendees: Sergey Vyatchanin (MSU), Guido Mueller(UFL), Gregg Harry (MIT), Peter Fritschel (MIT), Hiro Yanmamoto (Caltech), Bill Kells (Caltech), David Ottaway (MIT), Slawek Gras (UWA), Phil Willems (Caltech), Helena Armadula (Caltech), Liyan Zhang (Caltech), Eric Black (Caltech), Garilyn Billingsley, Norna Robertson (Stanford), Steve Maquire (South. Univ.), Stuart Reid (Glasgow), Muzammil Arain (UFL), Iain Martin (Glasgow) and Akira Villar(Caltech)

This meeting was held to discuss key topics of importance to the Optics used in Advanced LIGO. The aim of the meeting was to explore the following key questions in coatings, scatter, parametric instability and recycling cavity geometries:

1. TNI Results imply that the doped tantila coating loss is lower than inferred from Q measurements – why ?
2. Why is the absorption in the H1 ITMs higher than that measured in the lab (Unacceptable for Advanced LIGO) ?
3. Why is the scatter in the in-situ Core Optics higher than measured in the lab (Unacceptable for Advanced LIGO) ?
4. Does the choice of a stable/marginally stable recycling cavity have implications for Parametric Instability (PI) ?
5. What are the implications of the recycling cavities on PI ?
6. What are the implications of asymmetries in the IFO on PI ?
7. Do we know whether PI can be killed by mechanical damping methods ?
8. Others ??

A summary of the discussions is as follows:

## *Coating Issues*

Gregg Harry presented an overview of the recent achievements and brought us up to date on the current open issues. His presentation is an excellent summary on what has been tried in the coating program and what remains to be tried.

Andri Grettarson reported that measurements done at Embry Riddle have shown that the new titanium doped tantala coating known as LMA 5** does not improve the coating thermal noise over a standard Titanium doped Tantala coating. This is counter to measurements taken at LMA and Glasgow, which do indicate an improvement in the mechanical loss. Unfortunately this sample has a smear on it. The coating experts in the room did not feel that this would be enough to significantly downgrade the mechanical loss, however it is one possible reason to explain the discrepancy. Another key difference between Andri's 5** result and

Glasgow/LMA was Andri had only 1/4 lambda thick tantala while Glasgow/LMA was more like 1 micron.

In addition to the coating mechanical loss measurements, Andri reported on some very preliminary results on the effort to measure the dn/dT of Tantala. This was done by heating the sample in an oven with a high thermal mass and watching the reflectivity of a multi-layer dielectric coating change as the oven cools. This measurement produced a very clear signal that sets the dn/dT of tantala at 8.8e-5, which agrees favorably with an existing measurement of 1e-4. Given our current understanding of the thermo-refractive noise this value of dn/dT would pose significant problems for Advanced LIGO. However using this theory the TNI measurements set upper limits on dn/dT at the level of 1e-5 so there is a clear discrepancy here. Andri will re-check his measurements and check this result. If the result still stands the theory will need to be re-examined.

Eric Black gave a presentation on the results of the TNI. The TNI has reported results that show excellent agreement between results and theory for the case of thermo-elastic noise in sapphire and coating thermal noise in standard silica-tantalum coatings. However when the coating thermal noise of the titanium doped tantalum coating were measured in the TNI the amplitude of the thermal noise was found to be approximately 30 % lower than what would have been predicted based on the Q measurements.

Eric presented an overview of the calibration of the TNI. This is quite a complicated procedure and it was mentioned that a simple one would reduce error propagation. In addition to this it was asked if the radius of curvature of the TNI mirrors was accurately known. The TNI cavities have a g factor close to unity (g =0.99) to increase the spot size on the mirrors. The discrepancy between Q/theory numbers and the TNI measurements can be explained by a 30 % error in the spot size value in the TNI which would result from a 1% change in the ROC of the TNI Mirrors ( R=1m). It was agreed that these parameters would be checked thoroughly so that we could determine if the TNI has uncovered a hole in our understanding of coating thermal noise.

David Ottaway presented results of recent measurements of the absorption at LHO. The measured absorption was found to be around 4.5 ppm. This value is appreciably higher than the 1.5 ppm that was measured by Sam Waldman in August 2005 after the installation of the new ITMX and the drag wiping of the ITMY. Tracking of the power applied to the TCS system during the science run indicated that this change in absorption was not caused by a gradual accumulation of absorbing material over the science run. The replacement ITMX substrate and coating absorption was measured at Caltech before its installation at LHO. The numbers gave a coating referred absorption of 1ppm. These results appear to not be consistent with the TCS applied to the optics during various running periods. These results need to be better understood. It was also mentioned that the other IFO mirrors should be measured. Phil Willems and Sam Waldman intend to carry

this out in the next commissioning break at LLO. Absorption at the 5 ppm level is unacceptable for Advanced LIGO high power (180 Watt input) operation.

Stuart Reid presented a talk on third generation technologies. He broke the technologies down into two types, the first being those that could be easily retrofitted into Advanced LIGO and those that would require a radical departure from the Advanced LIGO topology such as diffractive gratings. The European gravitational wave community is looking for near term funding to start a design study on a third generation interferometer that could have a radically different topology from Advanced LIGO/Virgo. A couple of meeting attendees expressed a hope that new topology work would not hinder to much the work to develop technology improvements that could be retrofitted to Advanced LIGO

## *Scattering*

Bill presented an overview of the scattering situation as we currently understand it. The main point of this are:

1. When the optics are measured in-situ by measuring the intensity of the scattered light through a viewport the result is found to be approximately 80 ppm per optic.
2. It has not yet been determined whether the scatter on the installed Initial LIGO optics is limited by micro-roughness or point scatterers, although the latter is suspected.
3. An upper limit on the spatial size of the point scatters can be provided by observing the beam splitter and the folding mirrors. The mirrors swing freely through the standing wave electric field caused by the counter propagating electric fields in the recycling cavity. Careful observation of the light irradiating shows complete darkness of these points as they swing through a null in the electric field. At this pattern effectively moves transversely across the mirror an upper limit on the size of the point scatterers can be obtained from this observation.

Hiro Yamamoto updated us on the latest results from the FFT modeling of the fields circulating in Initial LIGO. The improvement that Hiro made this time is to include the as-built phase maps of the H1 optics. He calculates the recycling gain versus additional loss (on top of the phase maps):

| Loss | Recycling gain |
|---|---|
| 0 | 88.1 |
| 25ppm | 61.4 |
| 30ppm | 57.5 |
| 35ppm | 54.0 |
| 40ppm | 50.8 |

Given that the current recycling gain is around 55, the additional loss is estimated at 35ppm per optic. Accounting for optical absorption and end mirror transmission this reduces to about 30ppm. A plane wave model requires the loss to be

approximately 65 ppm to explain this recycling gain. We can attribute large scale polishing errors to approximately 30 ppm. Lab measurements of small scale scatter yield a scatter loss of 18 ppm. So with the combination of these results we appear to be short about 10 ppm in 65 ppm, which seems to be close to the accuracy of the measurements. Hiro also pointed out that for Advanced LIGO polishing the central 16 cm diameter is the most critical.

Liyuang Zhang discussed the experiment that measure scatter directly in the Caltech laboratory. He mentioned that point scatterers do not seem to be present in the lab measurements, which may also help explain the missing 10 ppm. One key point is that we still have a discrepancy between the LMA measurements (5 ppm) and the Caltech results (18 ppm). It should be noted that the LMA measurements are calibrated slightly differently way. LMA measures an angular distribution for the scatter of one point and then maps the optic out at one angle. They use a spot size on the mirror of 1mm. The selected point for the angular scatter measurement was a non-defect point on the optic. The LIGO measurement that we are comparing to was done using an integrating sphere. This integrating sphere was calibrated by observing the signal from a scattering surface that scatters 100% of the light. I could easily imagine that this may be a significant source of discrepancy between the two measurements. The other method of calibration for the Caltech experiment is to measure the signal from a sample coating from REO whose loss had been measured in the high finesse cavity. Peter suggested that when doing the cavity measurement you could simultaneously take a scatter measurement
It was also mentioned that it is well known that the 1 inch sample routinely measure lower loss than larger samples. This has been attributed to the fact that small optics can be cleaned prior to coating using spin polishing, which unfortunately is not available for use on larger diameter optics.

Steve McGuire then talked about his X-ray measurements, and two proposals for new work. A few new things I learned about the X-ray data is that the unlabelled peaks at lower energy are likely from silicon, phosphorous, and aluminum. The structural data was best fit by having 6 oxygen atoms around each tantala atom. There was some discussion about the fact that the Formula 1 coating had a double peak where all the other samples had a single peak. Formula 1 also showed the highest iron and chromium peaks, which may or may not be related. Gregg suggested to Steve that he might look at the bond stucture of silica, to see if we can match that up with our understanding of mechanical loss in fused silica. Gregg thinks it may be worthwhile to do some more coordination on silica thermal noise work, especially if Hai Peng gets funded.

Then Steve talked about his proposal to use his AFM for scatter work. Their AFM can take samples up to 15 cm in diameter. Right now it is not in a clean room. There was some concern that the resolution of the AFM was so high that it might be hard to find scatter centers that are identified at Caltech. A plan arose to measure scatter on some 1 inch witness samples at Caltech, then send them to

Southern for AFM, followed by post-AFM scatter measurements, to see if there are any noticeable defects at the scatter points. Steve talked with Gari and Liyuan during breaks, and plans to spend a fair amount of time today with them looking at their lab.

The final suggestion from Steve was to look at samples with a synchrotron at Argonne that can resolve where the fluorescing materials are in the Z direction. This could help resolve, for example, whether the chromium and iron are at the surface of the substrate or are actually in the coating.

## *Stable/Marginally Stable Recycling Cavities*

Peter Fritschel gave us an overview of where we stand in the choice of stable/marginally stable signal recycling cavities.
Guido Mueller updated us on his calculations on the alignment signals for stable signal recycling cavity geometries. He made the observation that in the stable geometry that the build-up of the TEM01 modes is suppressed by a factor of 10 which makes the error signal for the differential arm signal appreciably smaller than it would otherwise be. This being said the alignment signal matrix formed by the stable recycling cavity case looked much closer to diagonal than that of a marginally stable geometry. In addition to this he pointed out that a good signal to control the signal recycling mirror remains elusive.

## *Parametric Instability – Optical Geometry Issues*

Bill Kells started this session by giving us a report on the work that one of his students did over the summer on a direct calculation of the effective gain provided by a single arm cavity on the light scattered from each of the 2000 or so mechanical modes in a test mass. This was done by using a FFT code that analyzed the case of a single arm cavity. The main result of this work was that main optical contributors to the optical side on PI are the standard optical modes and there are not an infinite number of high loss modes that conspire to significantly enhance the R value for a single mode.
Bill also described his work on the cases of signal recycling cavities. He showed that whilst signal recycling can appreciably increase the parametric gain of modes near some very narrow features, the gain between the narrow peaks is actually reduced. This result was verified by David Ottaway's code. This raises the important question of that whilst stable cavity geometries may actually increase the R value of the worst case scenario values it may also increase the amount of arm cavity operating space that allows PI free operation.
Sergey Vyachanin presented results on the work he has done on extending his analytical calculations to the case where arms asymmetries exist. He presented the somewhat surprising result that in the case of minor de-tunings (~100 Hz) that it made little difference to the likelihood of parametric instability. Bill Kells was surprised by this result and at the time of the meeting was not convinced. Sergey

also made the observation that in the case of significant asymmetries between the arms (1 kHz) that PI can be suppressed to a large degree. This observation was also made by David Ottaway in recent work. It was decided that the way forward to decide the whether PI was significantly affected by the choice of a stable or marginally stable recycling geometry was to confirm that codes of Kells and Ottaway were in agreement. Next these issues need to be examined given the likely tolerances in the parameters of Advanced LIGO.
The last talk of the session was given by David Ottaway who has studied the case of PI in the time domain to determine whether there are any “boot strapping” issues because of the fact that the 180 degree phase shift due to the opposite arm in the cavity taking a while to develop.

## *Parametric Instability – Mechanical*

Akira Villar a graduate student working on the TNI updated us on the recent attempts to decrease the mechanical Q of the modes of the TNI without significantly increasing the broadband thermal noise as measured by the TNI. The measured Qs of the TNI mirrors is in the same regime as that measured on the test masses in Initial LIGO ie Qs ~ 2e5. The most recent result from the TNI was the installation of monolithic copper rings that are installed by thermally expanding the rings and placing them around the optics. It was stated that the Qs of the test mass body modes reduce significantly but a slight thermal noise increase (2 %).

There was disagreement whether a simple coupled oscillator model that suggests that the damping method needs mass (Done by Bill Kells and Riccardo) was correct. Gregg cited results from coating thermal noise to demonstrate that this is not necessarily the case.

Slawek Gras from the University of Western Australia presented results from his analysis of the ring damper approach to passively reduce the effect of parametric instabilities in interferometers. His analysis was conducted for the case of Sapphire mirrors with no asymmetries in the arms and a power recycled interferometer. He presented results showing the number of unstable modes vs arm cavity radius of curvature. It appeared that there may have been a bug in his code because at no point was the number of unstable modes less in the case of power recycling which would be the case if the theory mentioned above was correct. Slawek agreed to look into this. His results did show an appreciable drop in Q of the test mass modes (~ 20 reduction) with only a 2% increase in thermal noise. As a result of Slawek’s talk a discussion of the right approach to ring damping on Advanced LIGO test masses ensued. It was generally agreed that we should include some form of damping on the test masses to such a level that some Q reduction is achieved (even if not enough to kill the effect completely) and not appreciably change the thermal noise. It was also noted that we should try to see whether there is any way to spoil the bulk Q of silica in a controlled way so it is still below coating thermal noise but not an order of magnitude below like it is now.

Slawek also agreed to work with the TNI folks to see if there were any practical design choices for increasing the sensitivity of the TNI measurements.

Ju Li presented results from calculations on the 3 mode parametric instability case that they hope to observe in Gin Gin. In the first round of results they have not managed to find a mode that will see appreciable Q enhancement due to parametric processes. They have seen a couple of modes where you may expect appreciable reduction in Qs due to cold damping. The UWA group has also analyzed the tranquilizer cavity approach to parametric instability case and found severe practical limitations with this approach.

It became clear that during this discussion that we should make it a priority to investigate cold damping of test mass mechanical modes using the electrostatic drive (ETM) and some other method, potentially a photon actuator (ITM). If we can demonstrate cold damping then this should be sufficient to suppress PI in any other modes. This is particularly relevant if PI is likely to be just a handful of problematic modes.

Phil then talked about his proposal to put a gold coating on the barrel. With a 1 micron thick coating and a Q of 100, Phil calculated an increase in the thermal noise by a factor of 5. Gregg was somewhat skeptical of his calculation, as he had the thermal noise linear in thickness and phi, while it should goes as the square root. Phil was going to look into this. Both 1 micron and Q of 100 are pessimistic, but not overly so. Helena, Andri and Gregg talked about getting a sample coated with gold and a nickel under layer to measure Q's. Helena found a company that should be able to do this coating. Phil also found some abstracts that indicate Boris Lunin has measured Q of gold on silica in the last year or so, wrote to Boris to see what his results are.

# Coating Development Discussion

*Gregory Harry*

**November 7, 2006**
**Optics Workshop - Caltech**

# Coating Challenges

## Problem 1a
## Coating Thermal Noises

- Limiting noise source
- Primarily caused by choice of coating materials
- Had success reducing it, but not well understood
- More than just Brownian

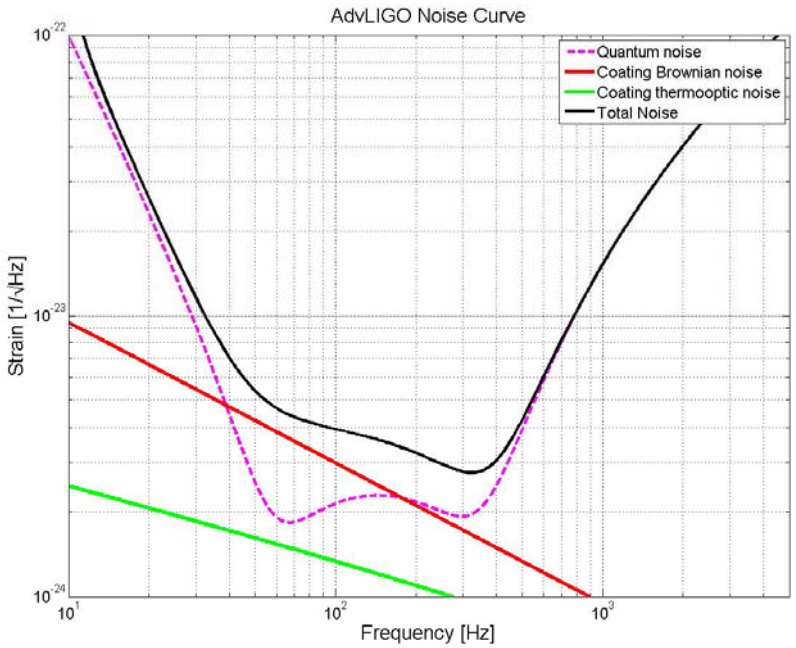


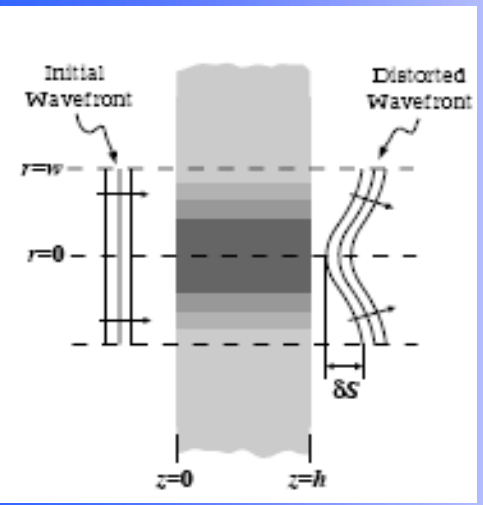


## Problem 1b
## Thermal Lensing

- Most absorption in coating
- Best coatings in spec
- Anisotropy under studied

## Other Problems

- Scatter
- Reflectivity Matching
- Uniformity
- et cetera

# Discussion Topics

- Thermorefractice noise and other thermal noise issues
  - How worrisome is thermorefractive?
  - How low can all forms of thermal noise be brought?
  - What tradeoffs might there be between parameters?
- Thermal noise interferometer
  - Can we reconcile TNI thermal noise with Q measuring?
  - What is the most efficient use of TNI time?
  - What more can we extract from existing TNI data?
- Planning for third generation coating issues
  - Are we doing too much/too little 3rd generation research?
  - What advanced ideas might be ready for AdvLIGO?
- Absorption and scatter
  - Why are the absorptions and scatter at the sites as high as they are?
  - Are they increasing with time?
  - How we can we make sure this doesn't happen in AdvLIGO?
- Coating material analysis and modeling
  - Are we doing enough material investigation?
  - How can we work closer with real material scientists?
  - Do all amorphous oxides have loss mechanisms like silica?

# Modeling and Molecular Cause of Mechanical Loss

Goal: A description of mechanical loss in thin film amorphous oxides from basic principles

## Molecular dynamics calculations beginning at University of Florida

- Have a working semi-empirical model of loss in fused silica
  - Frequency dependence from two level systems
  - Surface loss as observed phenomenon
- Develop full molecular description of silica loss
  - Surface loss caused by two member rings
- Generalize to other amorphous oxides
  - Analogous two level systems

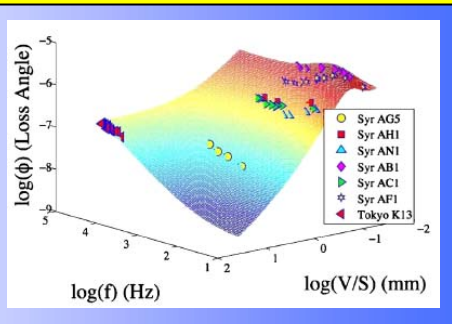


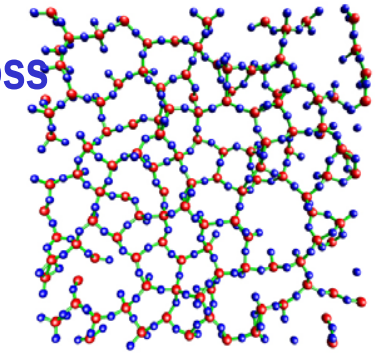

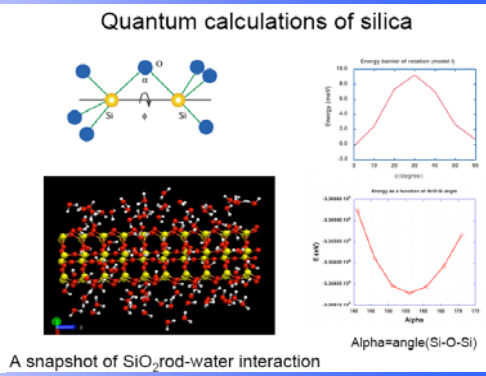


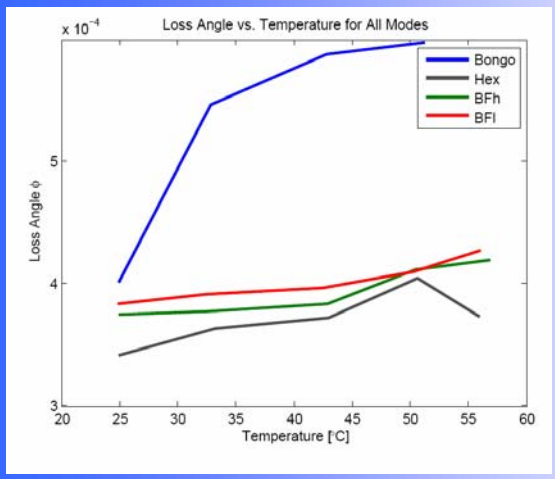


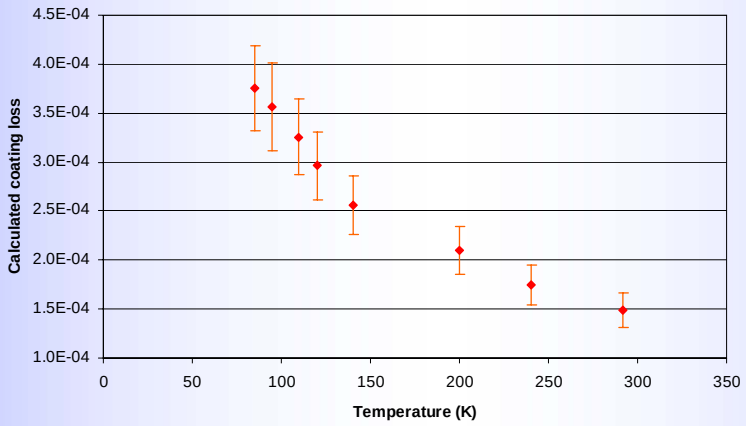


## Mechanical loss data at different temperatures

- Tantala/Silica T>300 C
- Ti doped Tantala/Silica T<300 C
- With frequency dependence, start to fit to modeling
- See talk by S Reid and F Travasso

# Some Q’s and first dn/dT for tantala

Andri M. Gretarsson

August 3, 2006

# Coating loss experiment

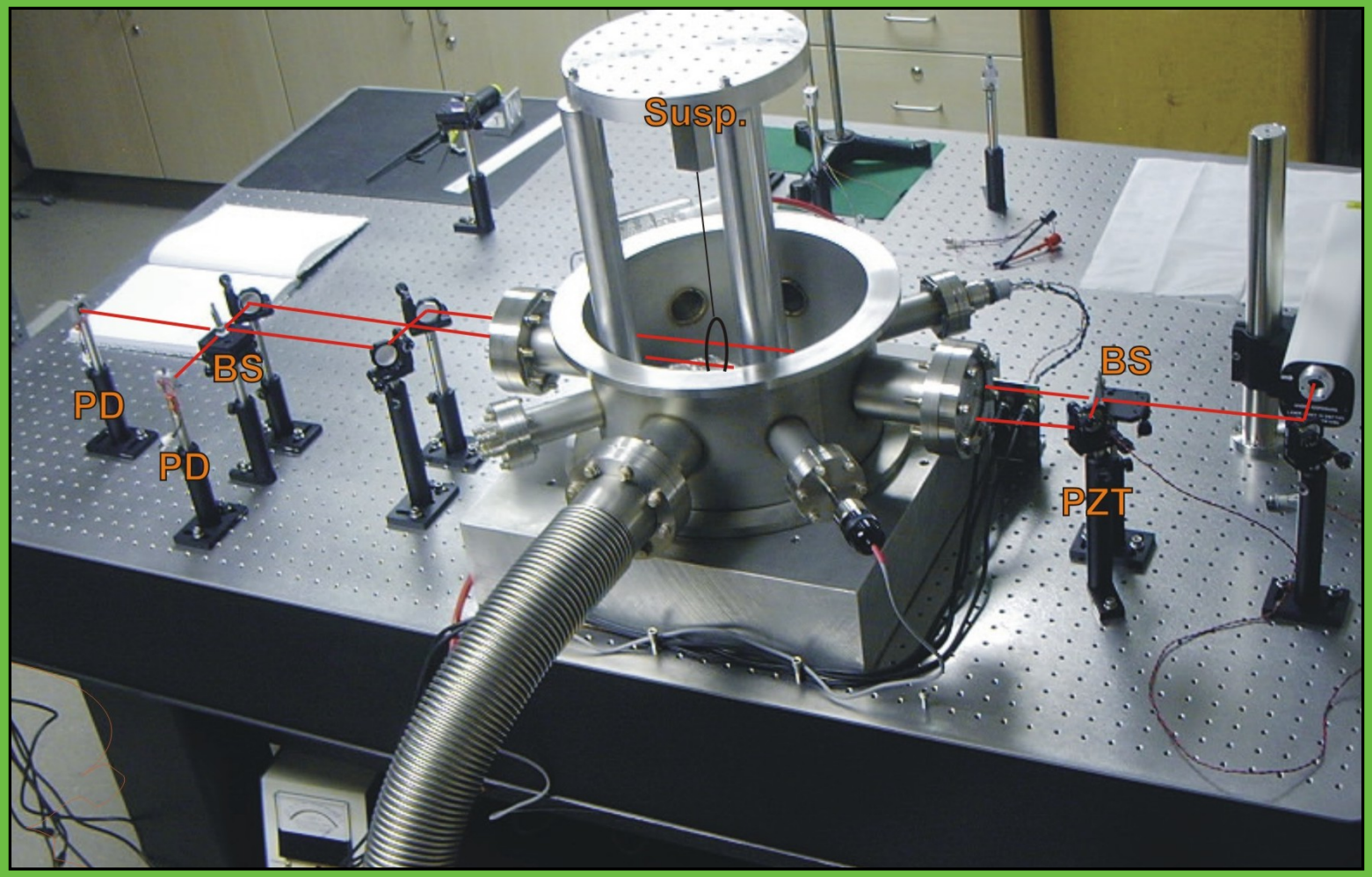

# Coating loss experiment

All fused-silica suspension

- Measured Q's of samples with 2 different coatings since August:
  - Si doped TaO & Si
  - Ti doped TaO & Si  (LMA formula 5**)

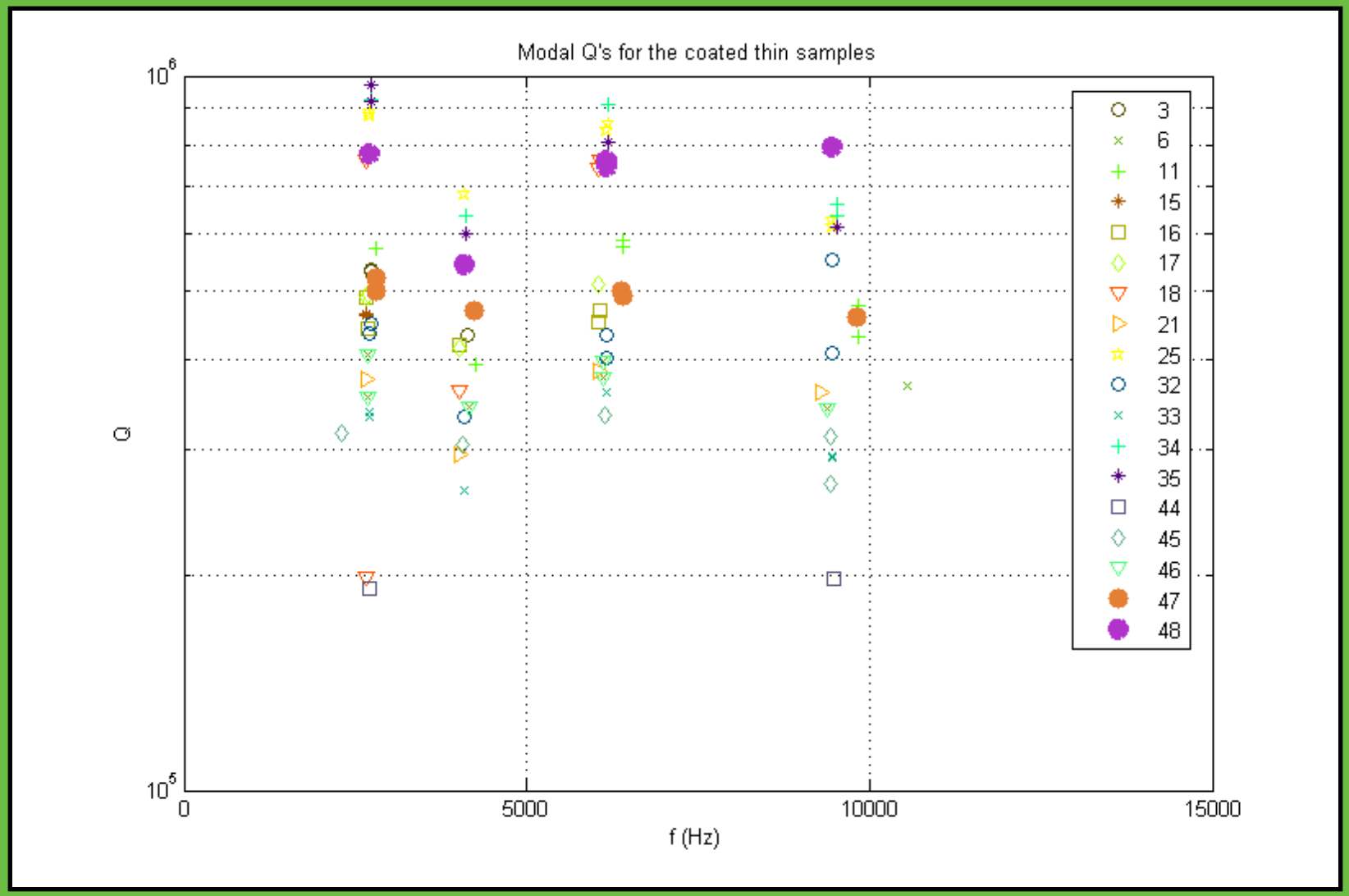

# dn/dT Experiment

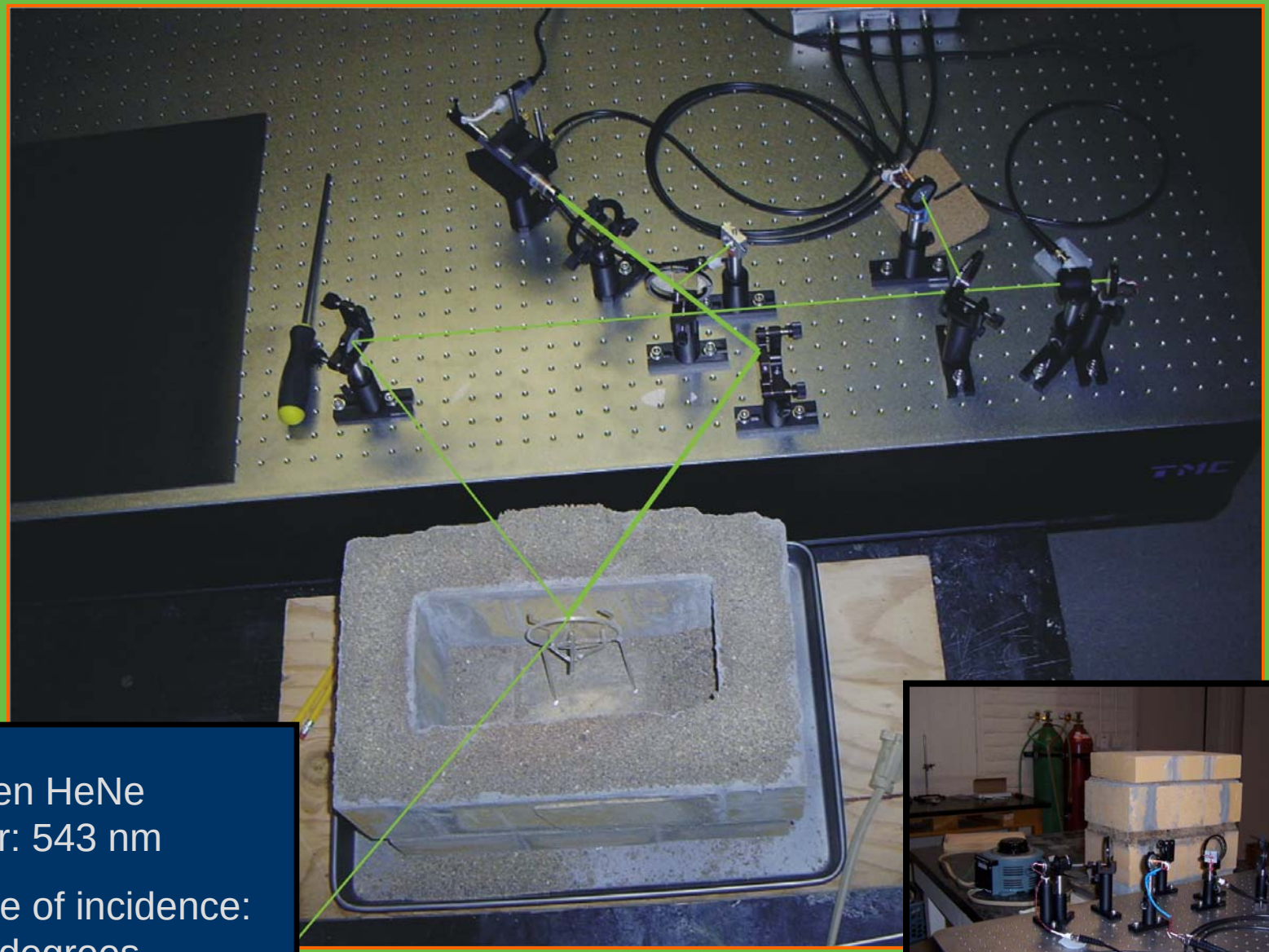



Green HeNe laser: 543 nm

Angle of incidence: ~39 degrees.

# dn/dT Experiment

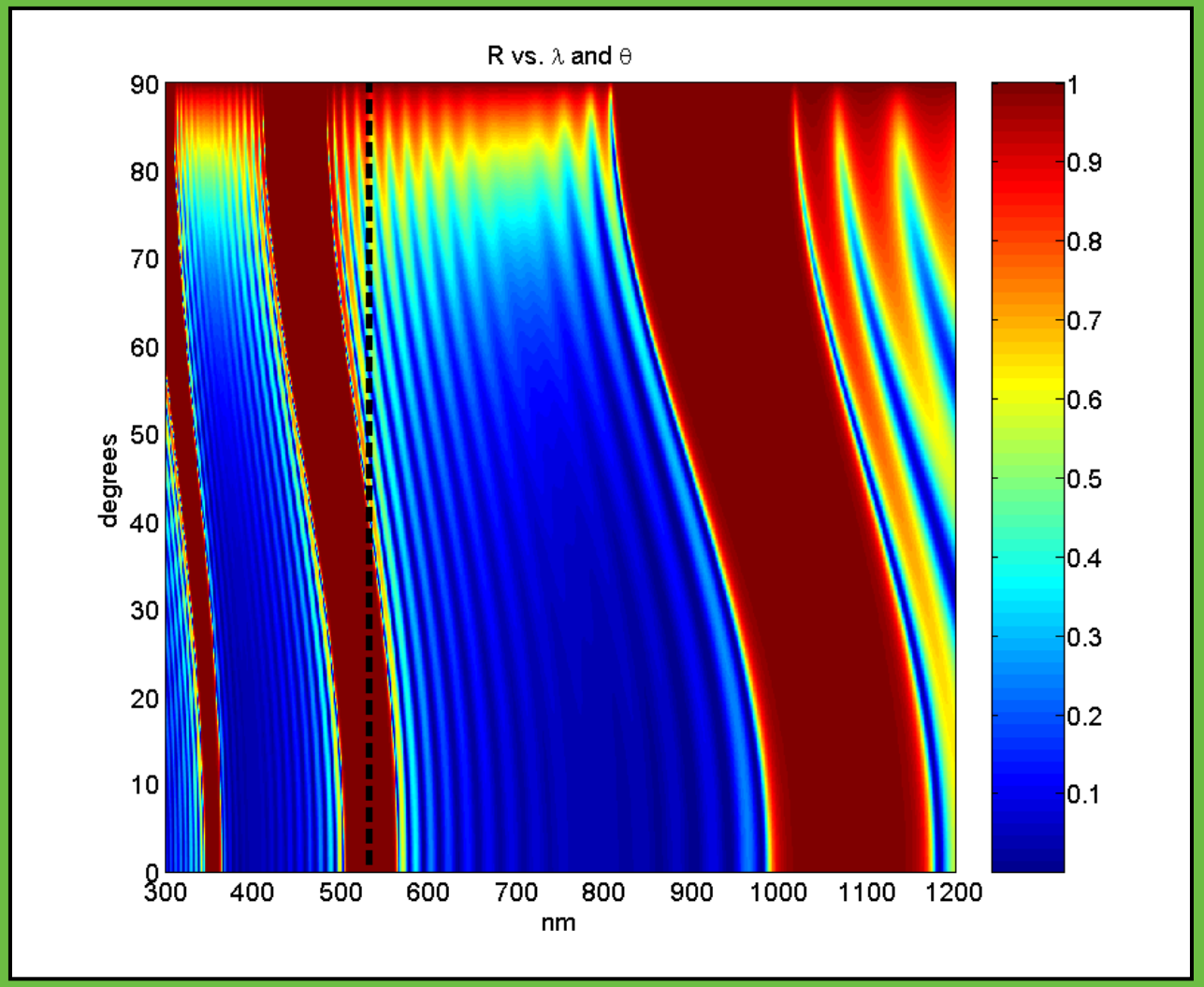

# dn/dT Experiment

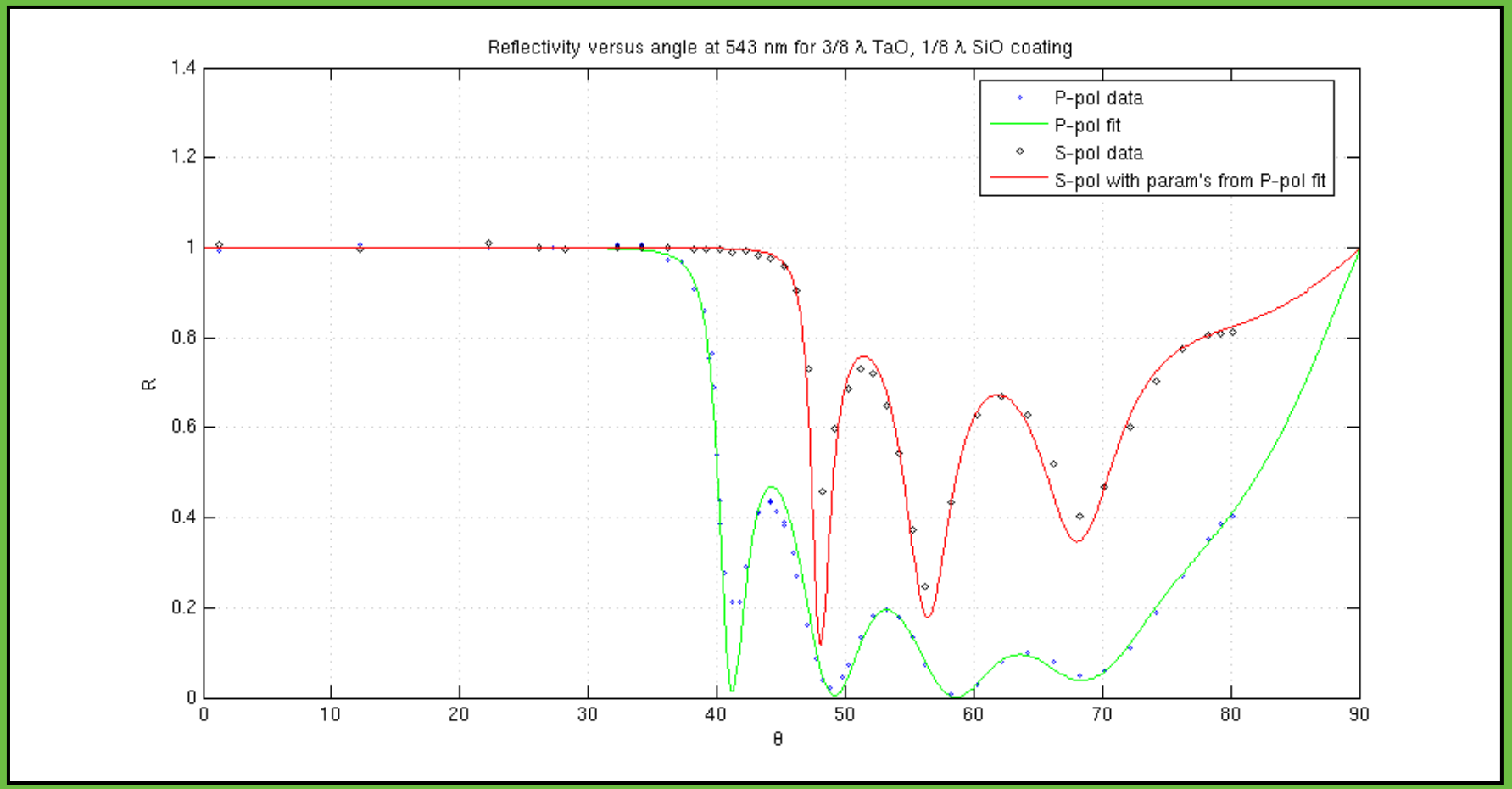

# dn/dT Experiment

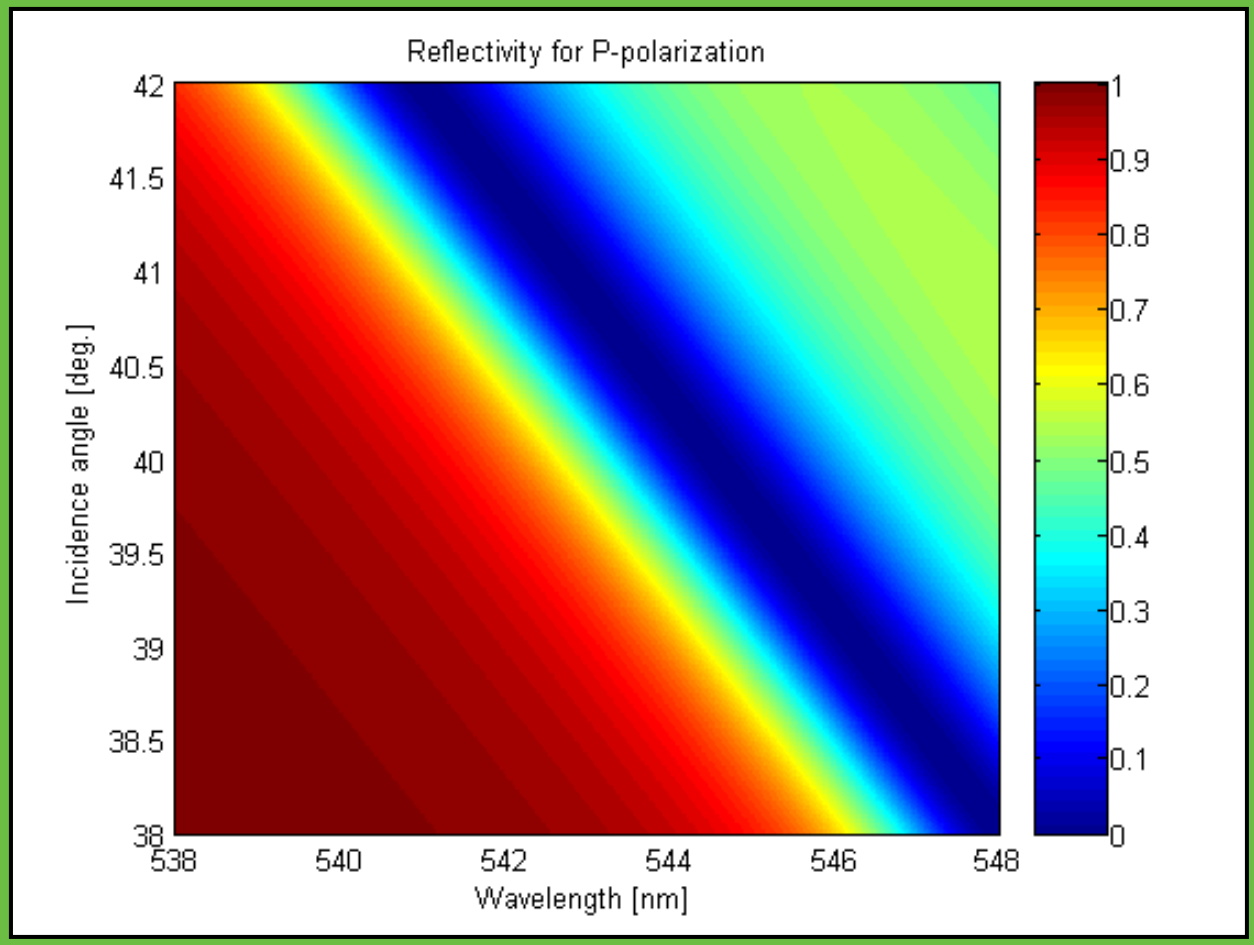

# dn/dT Results

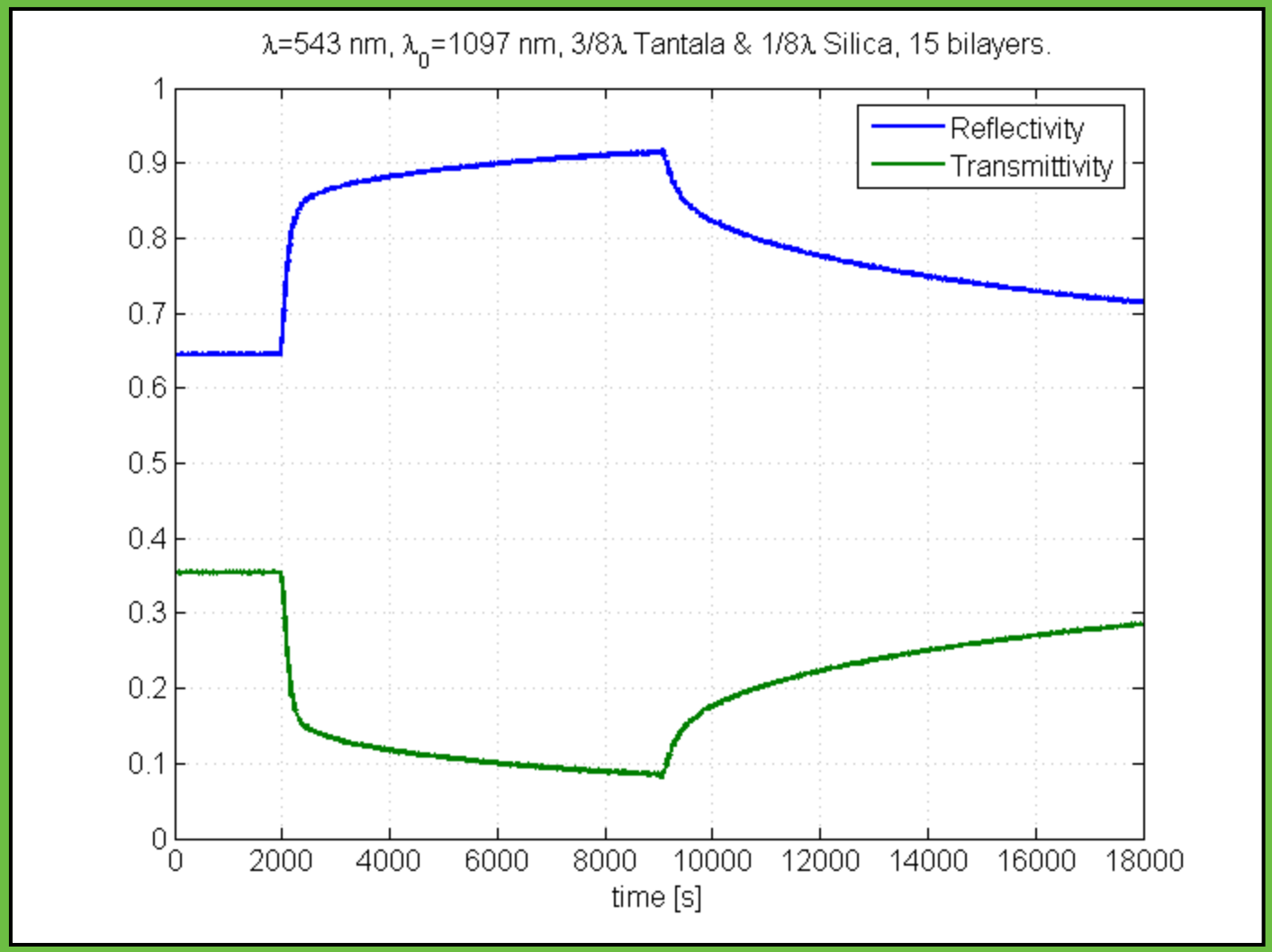

# dn/dT Results

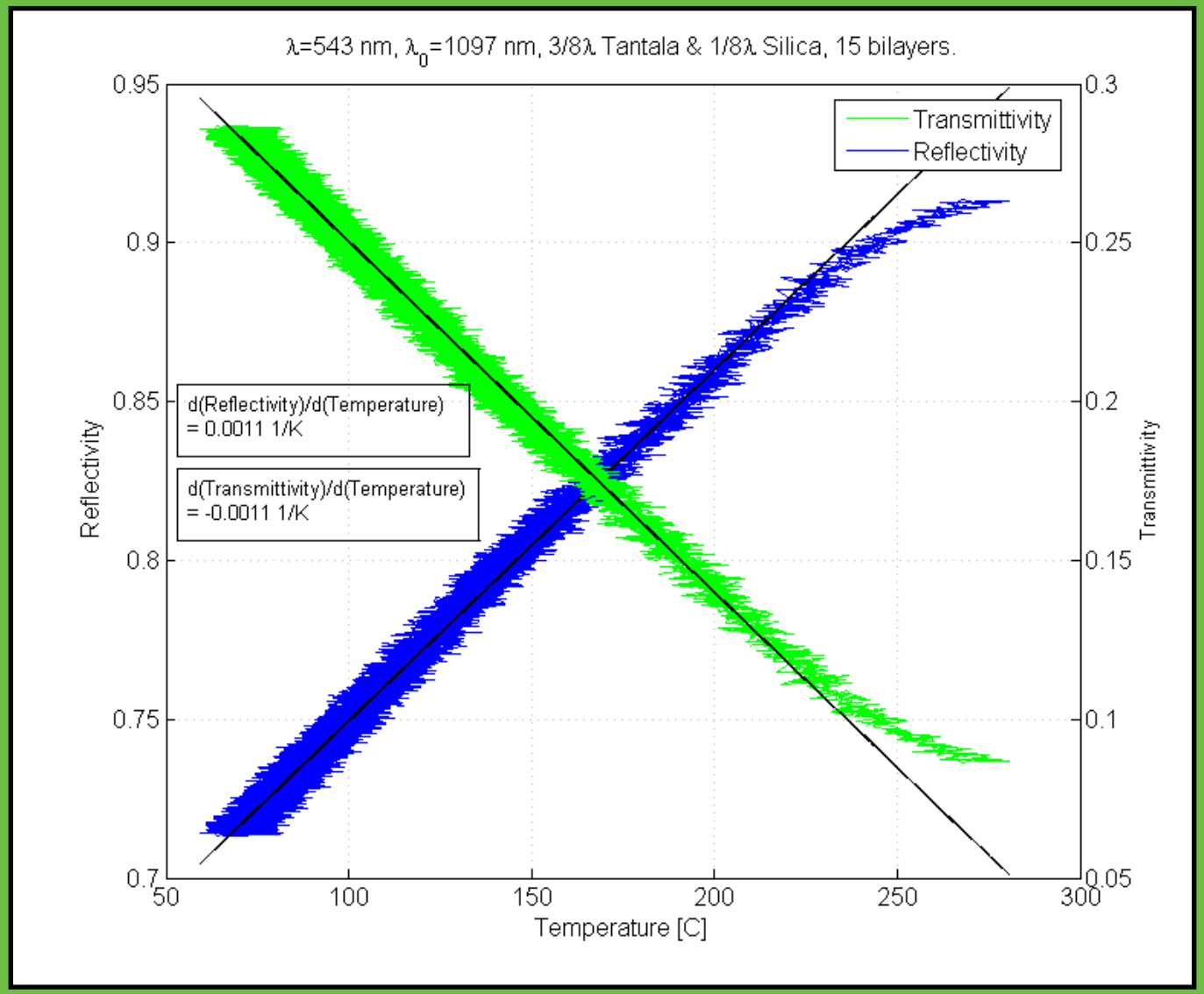

# dn/dT Theory

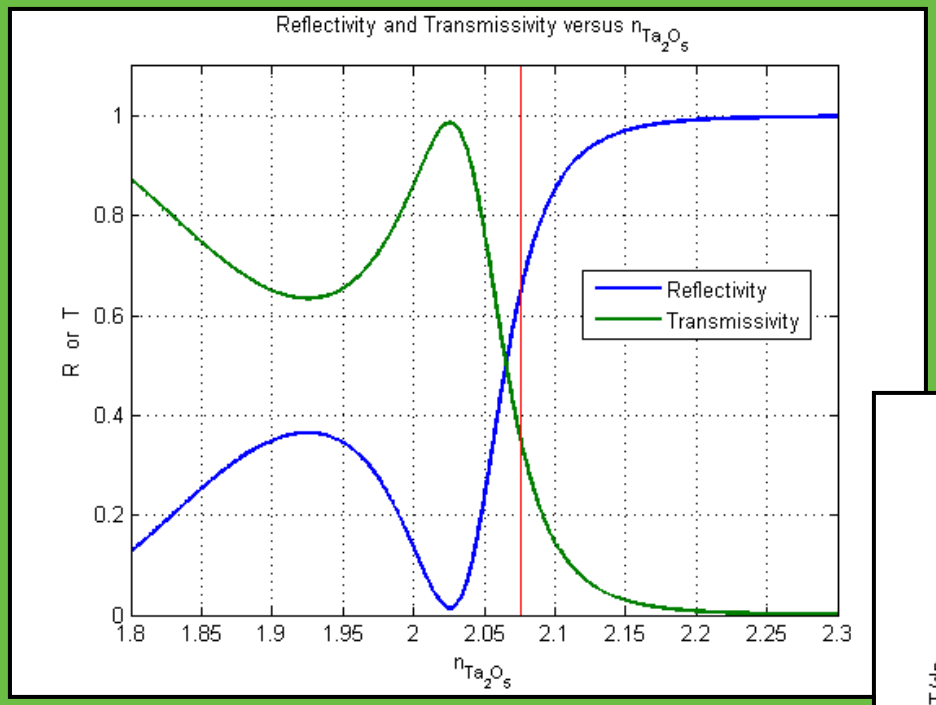
Reflectivity and Transmissivity versus $n_{Ta_2O_5}$
R or T
$n_{Ta_2O_5}$
Reflectivity
Transmissivity
0
0.2
0.4
0.6
0.8
1
1.8
1.85
1.9
1.95
2
2.05
2.1
2.15
2.2
2.25
2.3

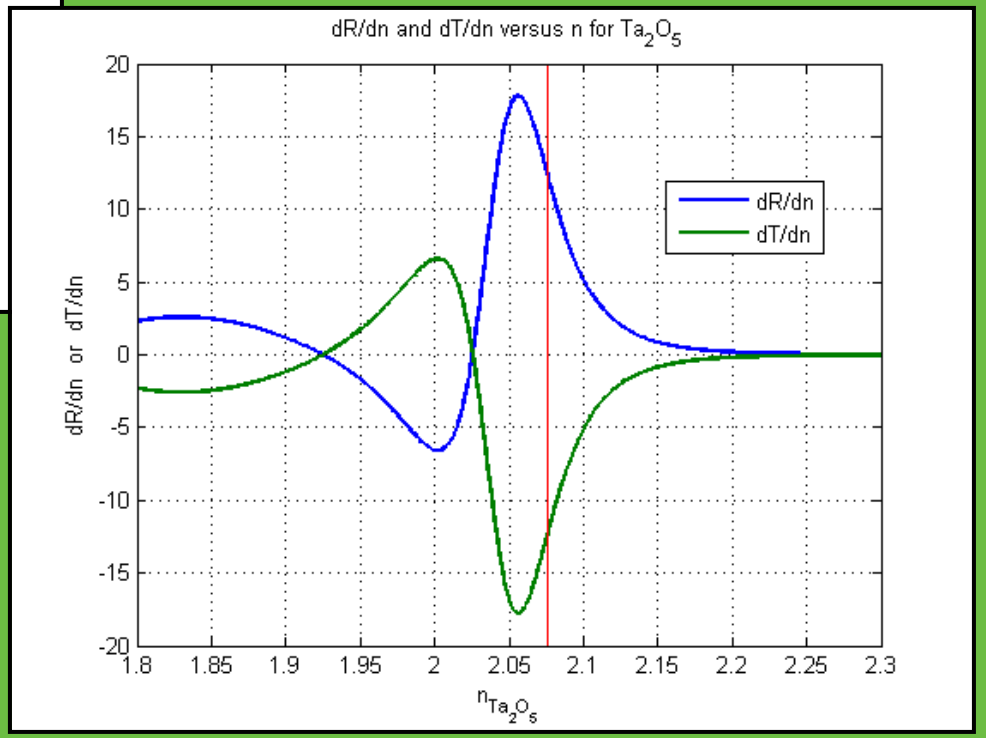
dR/dn and dT/dn versus n for $Ta_2O_5$
dR/dn or dT/dn
$n_{Ta_2O_5}$
dR/dn
dT/dn
20
15
10
5
0
-5
-10
-15
-20
1.8
1.85
1.9
1.95
2
2.05
2.1
2.15
2.2
2.25
2.3

# dn/dT Results

- Assuming
  - dn/dT of tantala dominates
  - This very new data has been understood correctly

$$\frac{dn}{dT} = \left(\frac{dR}{dT}\right) \Big/ \left(\frac{dR}{dn}\right)$$

$$= 8.8 \times 10^{-5} \ \ \mathrm{K}^{-1}$$

  - Systematic errors probably dominate.
  - Uncertainties in the few percent.

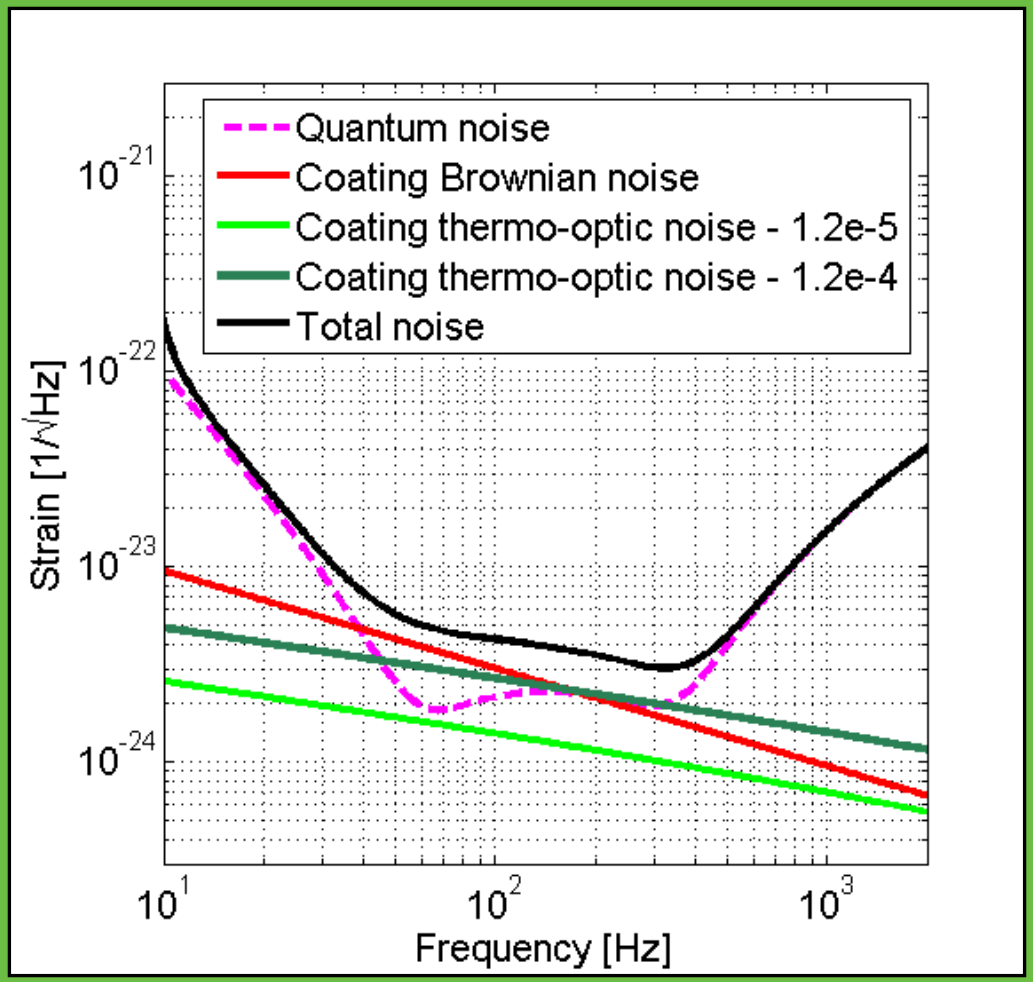

## *Thoughts*

- Maybe Inci was right.
- Coatings are limited by the materials used. 3rd generation coatings will need to be much better. We'd very much like AdLIGO coatings to be better. Are there any options beyond amorphous metal oxides?
- 3rd Gen: Cryogenic coatings...is there any data?
- Barrel coatings. How can we be absolutely sure they will not impact AdLIGO thermal noise? (Are we confident enough in our models to stake the AdLIGO optics on them?)

# 3rd Generation Coating Issues

Stuart Reid
IGR, University of Glasgow

Caltech, November 2006

# Introduction

- Coating thermal noise forms one limit to the sensitivity of Advanced LIGO in the mid-frequency range.
- To progress beyond the Advanced LIGO sensitivity level will require improvements in coating thermal noise
- 3rd generation detector designs – not yet defined, area of current study
- A number of experimental approaches are being pursued

# Status of current coating research

- $SiO_2/Ta_2O_5$ are currently the best choice from a combination of optical and mechanical properties
- Strong evidence that doping the $Ta_2O_5$ with $TiO_2$ helps
- Further optimisations ongoing through changing parameters during the coating run. Recent results from LMA for one such optimisation suggested

  $\phi_{Tantala5} \rightarrow \phi_{Tantala5^{**}}$ : $(2.4 \rightarrow 1.9)\times10^{-4}$,
  (A. Remillieux et al, 3rd ILIAS-GW meeting, Oct 06)

  $\phi_{Tantala5^{**}} \rightarrow \phi_{Tantala5^{***}}$ : $(2.1 \rightarrow 1.5)\times10^{-4} \pm \sim15\%$
  (I. Martin, Glasgow)
- Studies ongoing to try to identify loss mechanism in $Ta_2O_5$ with input from experiment and modelling (Glasgow, Florida, et al).
- Non-periodic multi-layers (Pinto et al) may allow further improvements

# 3rd generation detectors

- Research ongoing aimed at lowering thermal noise/reducing effects of high power thermal loading:
  - Use silicon optics?
  - Use diffractive optics?
  - Possibly cool to cryogenic temperatures?
  - Use of mesa-beams?
- Areas of current research relevant to coating thermal noise related to these topics:

# 1) Diffractive coatings

- Diffractive optics: potential to reduce absorption/thermal problems experienced in transmissive topologies.
  - **All-reflective: allows opaque materials (eg silicon @ 1064nm) - needs new interferometer topologies.**
- Investigations of optical properties of gratings fabricated by Institute of Applied Physics, Jena are ongoing by colleagues in Hannover.

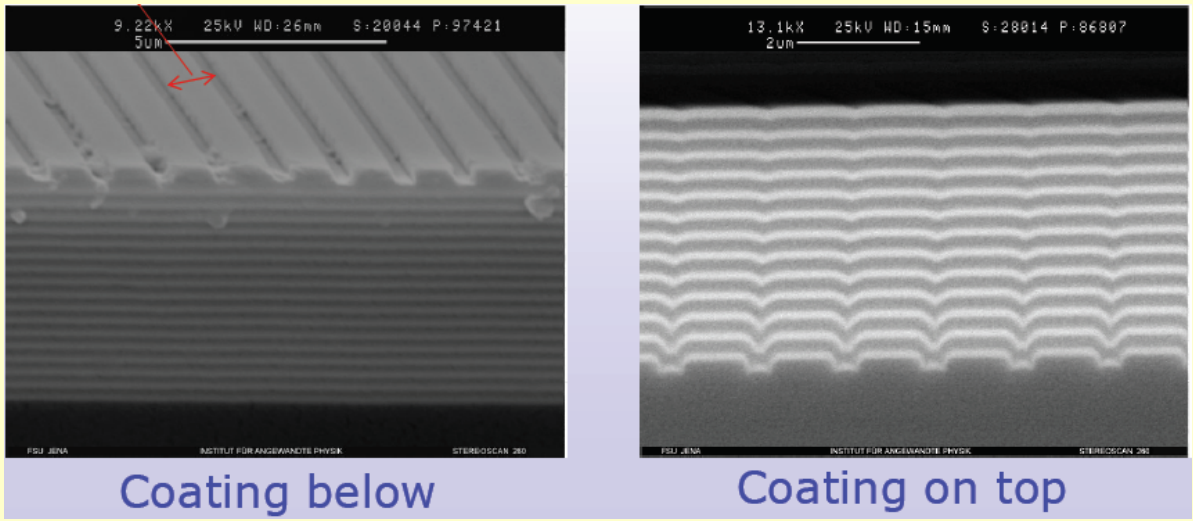


- Large gratings (metre-scale) can also be fabricated by LLNL.
- Mechanical properties of coatings applied to substrates which carry a grating are under study in Glasgow.

# 2) Total internal reflection

- The requirement for optical coatings could be eliminated in the case of total internal reflection.

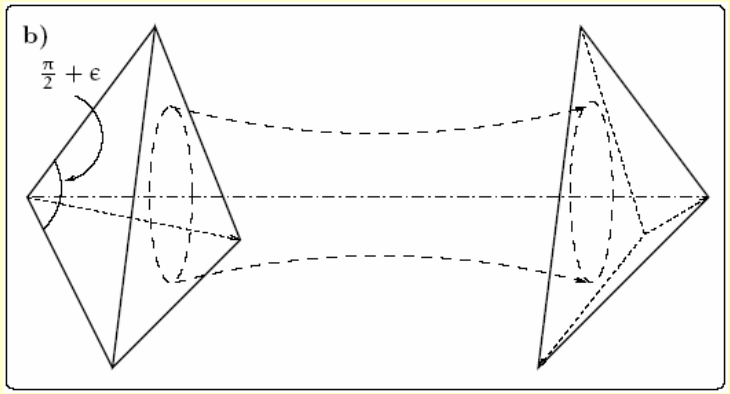


**Braginsky *et al.*, Phys.Lett. A 324 (2004) 345-360**

- Currently proposed mirror configuration:
  - **Corner cubes**
  - **Sensitivity to refractive index homogeneity an issue?**

# 3) Waveguide coatings

- Using the correct material index-thickness match, it is theoretically possible to achieve 100% reflection (when modelled as an infinite grating; the finite size of the optics and the sensitivity to misalignments need to be studied).

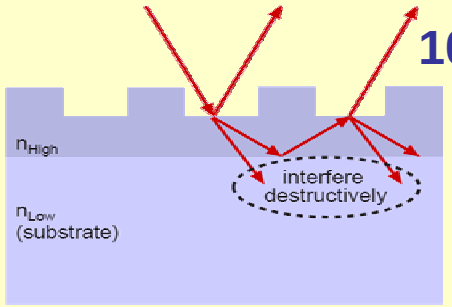


Sharon *et al*,
J. Opt. Soc. Am. A, 14 (1997)

- Optimising the parameters may allow for a significant reduction in the required coating ~0.2μm (Bunkowski *et al.*, arXiv:gr-qc/0608006)

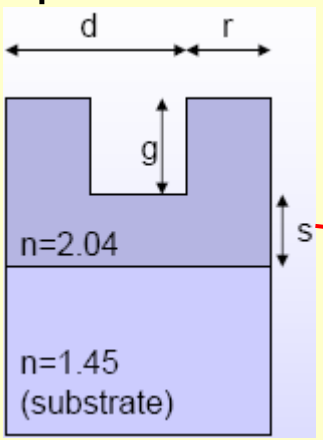


s=0

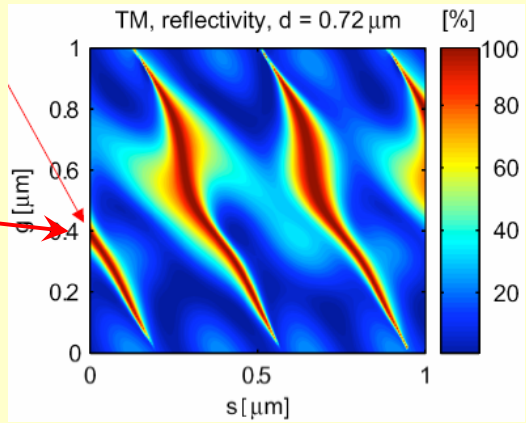


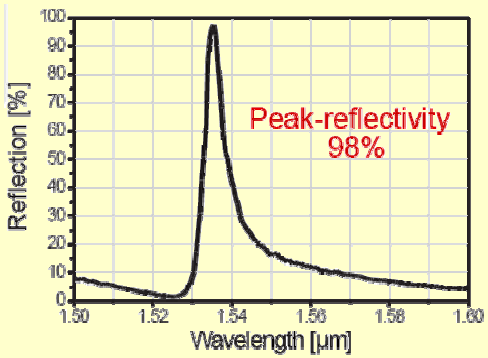


Clausnitzer et al,
J. Opt. Soc. Am. A 22 2005

**Preliminary work at Jena (98% reflectivity) and continued studies at AEI Hannover.**

# 4) The effect of cooling on multilayer optical coatings

- Current experiments suggest little or no reduction in the mechanical loss of current multi-layer coatings when cooled.
  - **Expected improvement is from the √T reduction in the thermal displacement noise.**

**Japan**
**31 alternating layers of $SiO_2$ and $Ta_2O_5$.**
**4.8μm coating on 1mm thick silica disk**

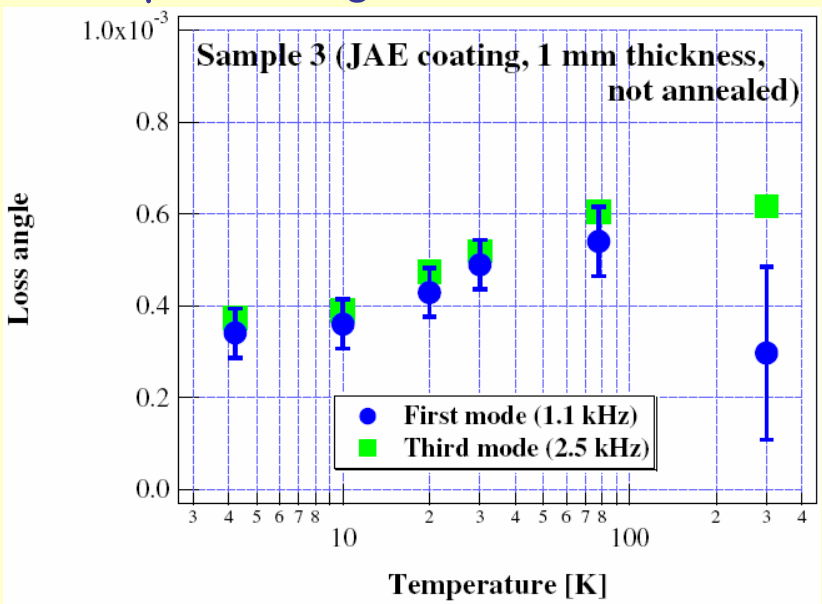


**Glasgow**
**single layer doped $Ta_2O_5$ (14.5% $TiO_2$).**
**0.5μm coating on 52μm Si cantilever**

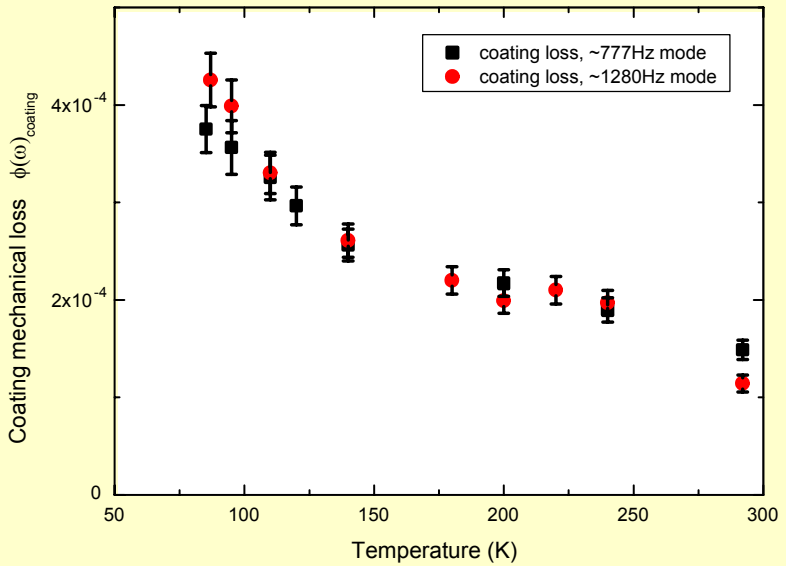


Yamamoto et al., Phys. Rev. D 74, 022002 (2006)

Martin et al., 2006 *in preparation*

# 5) Further optimisation - non-periodic multi-layers

- Studies by Pinto et al suggest by using multi-layers of 'non-standard' periodicity, that the fraction of lossy high index material may be reduced.
  - **verification will be carried out by direct thermal noise measurements here at Caltech at the TNI.**

# 6) mesa beams

- By using non-Gaussian, flat-topped beams (mesa beams) in interferometers the impact on interferometer sensitivity of noise in mirror coatings (and other noises) can be reduced.
- (see talk by J. Agresti).

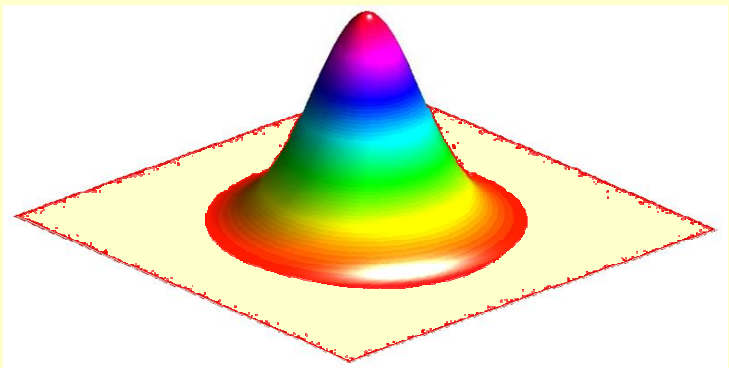

**Gaussian beam profile**

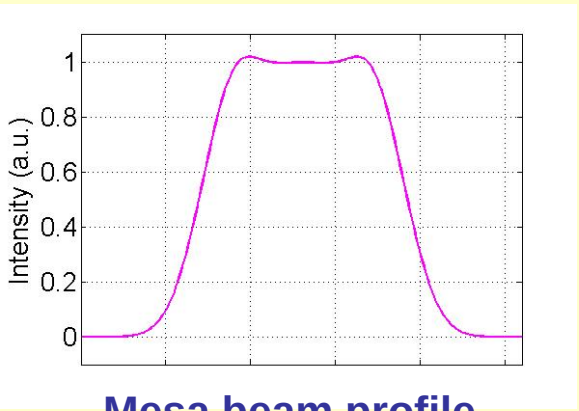


**Mesa beam profile**

Slides from Juri Agresti

# Mesa Beam and Mexican Hat mirrors

Mesa beam

Gaussian beam

$$u_{MB}(r) \propto \int_{r' \le D} d^2\vec{r}'\, e^{-\frac{(\vec{r}-\vec{r}')^2(1-i)}{2w_0^2}}$$

$$u_G(r) \propto e^{-\frac{r^2}{w^2}+\frac{ikr^2}{2R}}$$

$$w_0 = \sqrt{\frac{L}{k}}$$

The mirror shapes match the phase front of the beams.

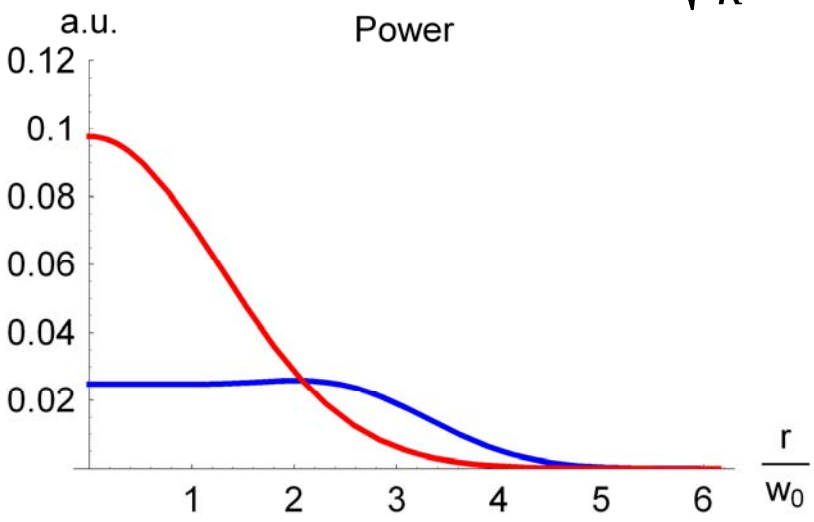


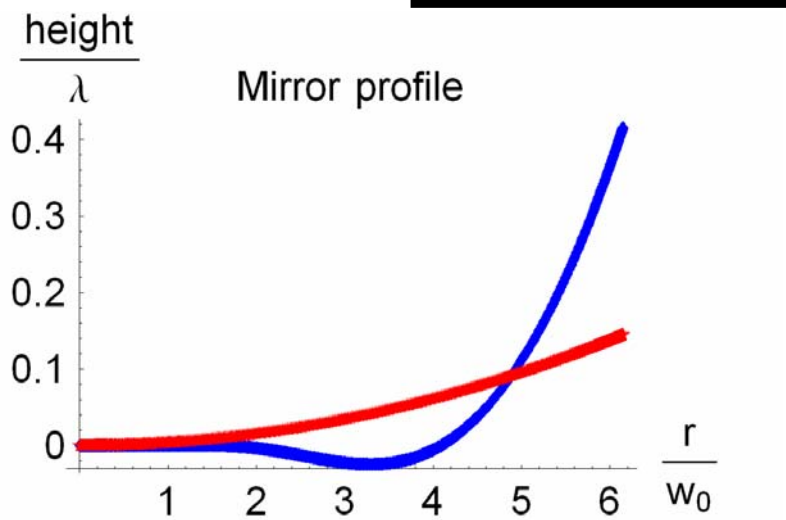

Slides from Juri Agresti

# Thermal noises for Gaussian and Mesa beam

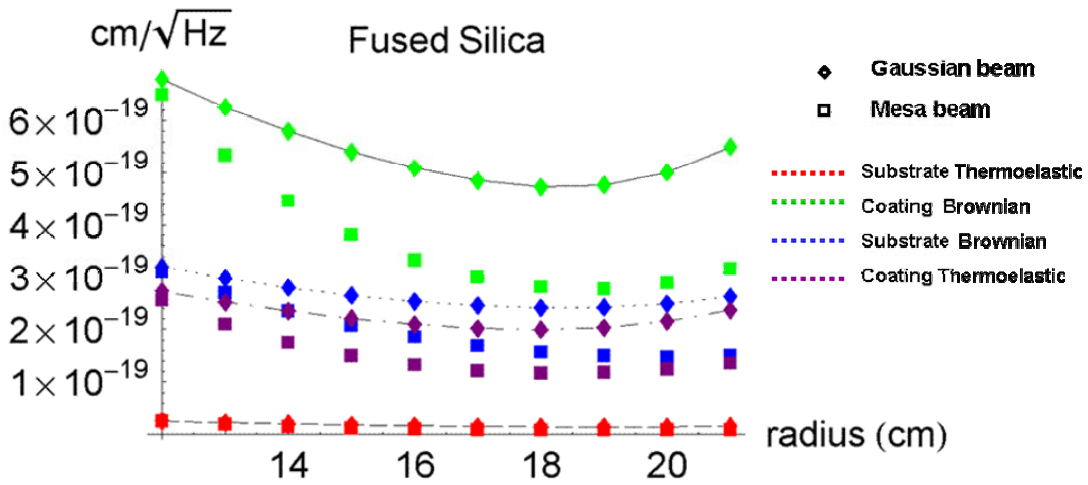


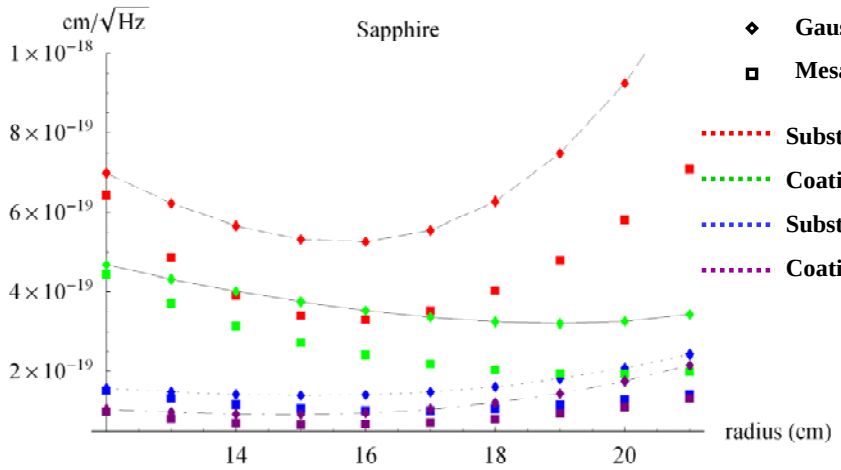


**1 ppm diffraction losses**

| FS | $\sqrt{S_X^{GB}/S_X^{MB}}$ |
|---|---|
| CB | 1.7 |
| CT | 1.7 |
| SB | 1.55 |
| ST | 1.92 |

| S | $\sqrt{S_X^{GB}/S_X^{MB}}$ |
|---|---|
| CB | 1.6 |
| CT | 1.5 |
| SB | 1.4 |
| ST | 1.4 |

**Details in http://www.ligo.caltech.edu/docs/T/T050269-00/**

Slides from Juri Agresti

# Sensitivity improvement using Mesa beam in Ad-LIGO

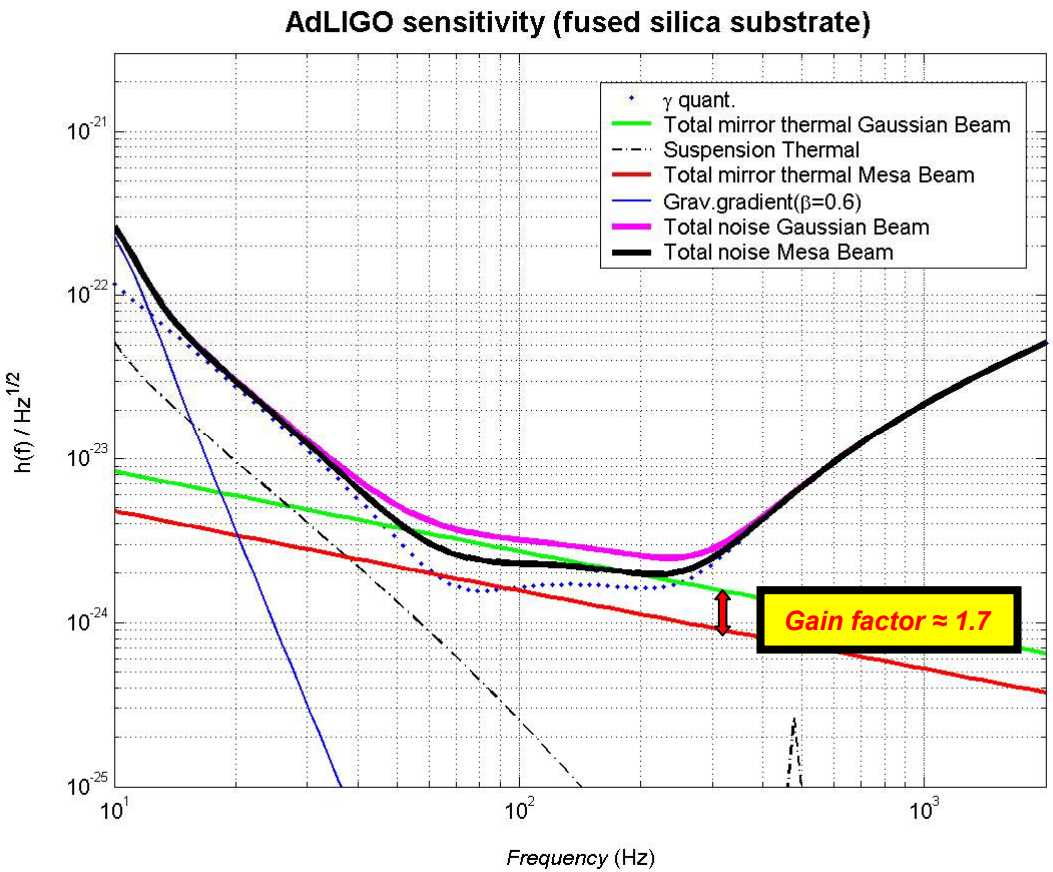


| | GB | MB |
|---|---|---|
| NS-NS range | **177** Mpc | **228** Mpc |

**Coating Thermo-refractive noise estimation**

(perfect Flat Top beam and infinite mirror)

$$\sqrt{\frac{S_X^{GB}}{S_X^{FT}}(f = 100Hz)} \approx \sqrt{3}$$

# Summary

## Future coatings

### Optimisation of multilayer optical coatings

- Doping of tantala with titania
- Non-periodic optimised thickness
- Investigations into the loss mechanism of $Ta_2O_5$ (better understanding).
- Mesa beam optical scheme
- *Cooling*

### Significant reduction in the required coating thickness

- Diffractive topology
- Total internal reflection
  - Corner cube mirrors
  - Waveguide coatings
- *Cooling*

LIGO

# More Absorption at H1

Dave Ottaway, Phil Willems and Justin Garofoli

# Review of the Spot Size Technique

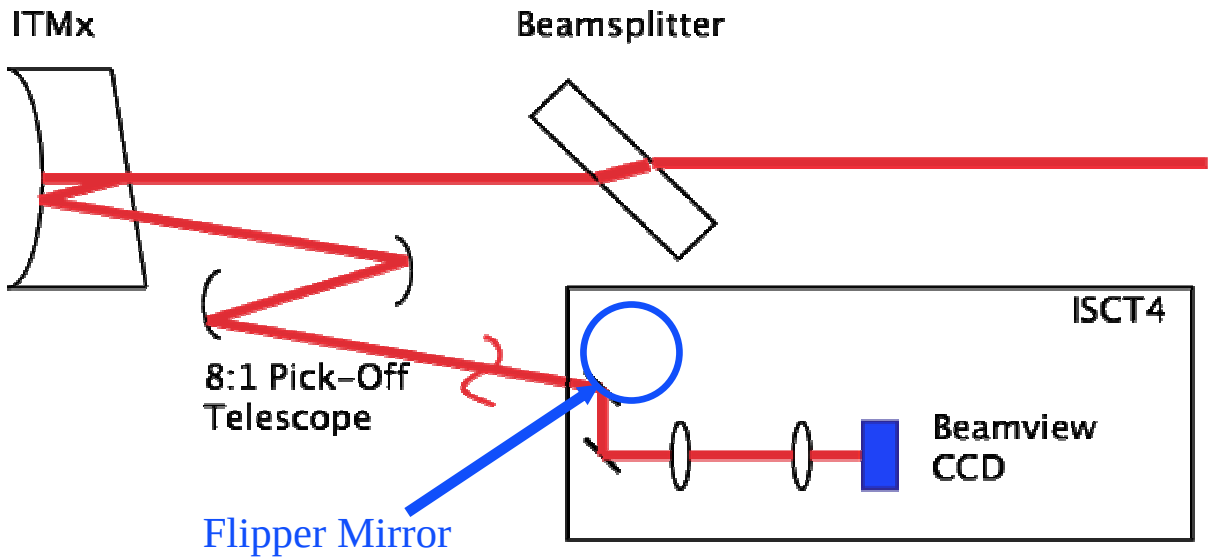


$$\omega_{out}^2 = \omega_{in}^2 \left[ \left( \frac{B}{R_{in}} + A \right)^2 + \left( \frac{\lambda B}{\pi \omega_{in}^2} \right)^2 \right]$$

- Heat the optic up using either IFO (without TCS) or TCS heating
- Watch the change in ITM lens by monitoring the change in spot size
- Technique sensitive to sub ppm absorption levels

# Absorption Data from ITMX

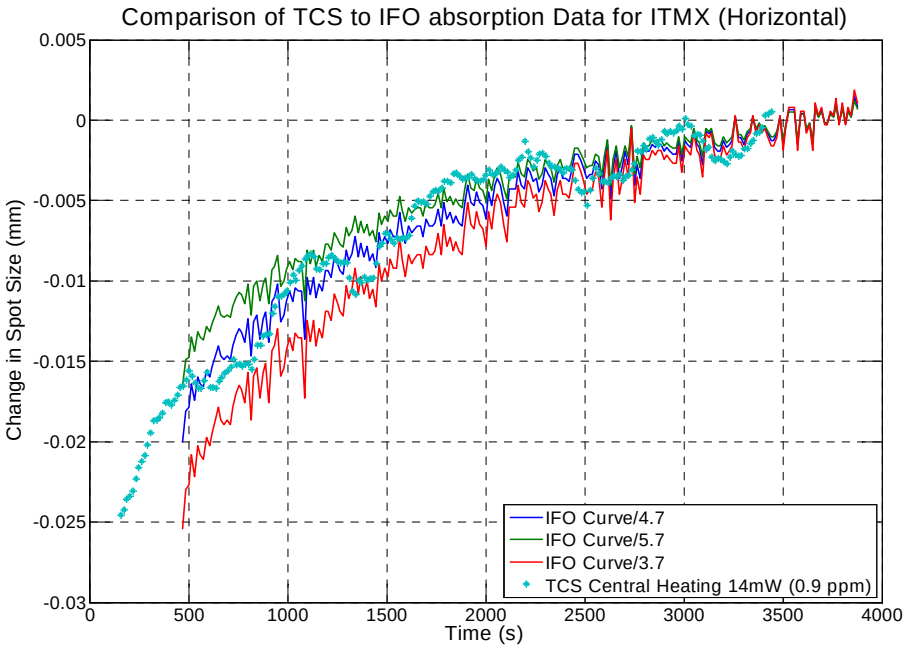


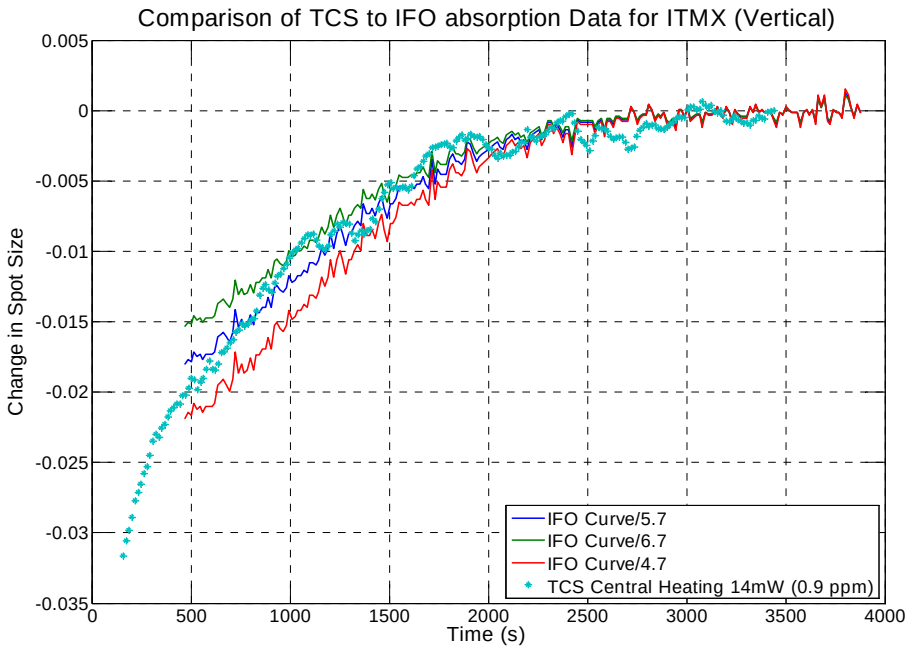


- IFO run for 2hrs in heating state
- Note different time constants between the different axis
- This is consistent with both IFO and TCS heating

- Absorption IFO is 5 +/- 1.1 ppm and 4.2 +/- 1.1 ppm
- Measurement is sensitive to sub 0.4 ppm absorption
- Better accuracy could be obtained by improved TCS measurement with more power

# Absorption in the ITMY

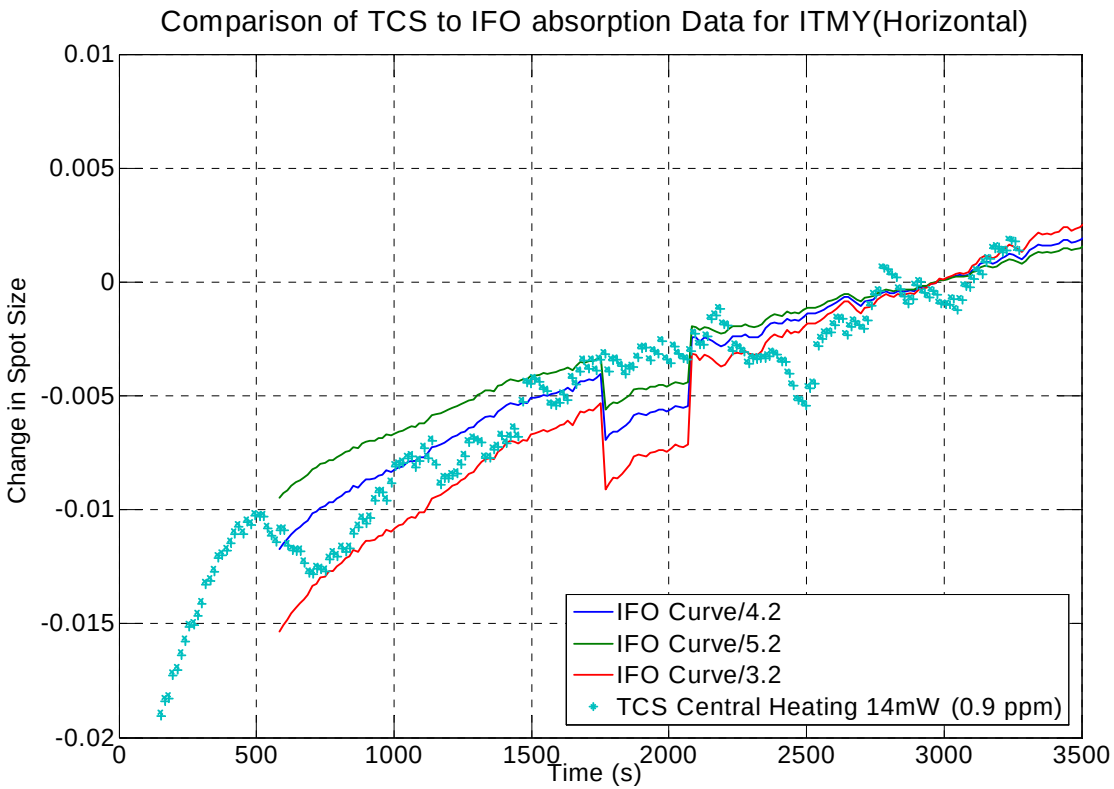


- The ITMY Vertical Data was could not be analyzed
- Absorption ITMY = 4.7 +/-1.1 ppm
- Can also be improved with increased TCS power measurement

# Requested TCS Central Heating Over the Run

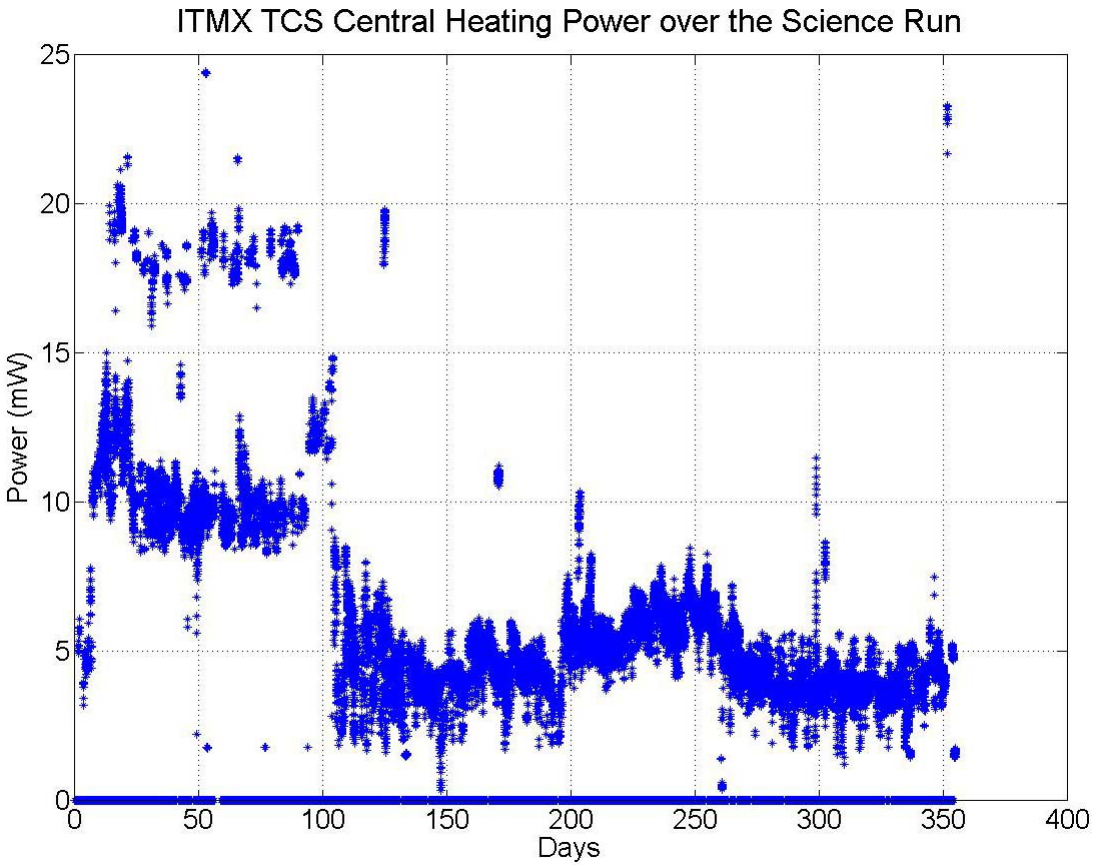


- Power measurements obtained by calibrating ITMX-PD_2
- Long term absorption changes do not explain difference between then and now
- Data is science run data, an hour after lock acquisition
- Data before science run is inconclusive

# Earlier Spot Size Data

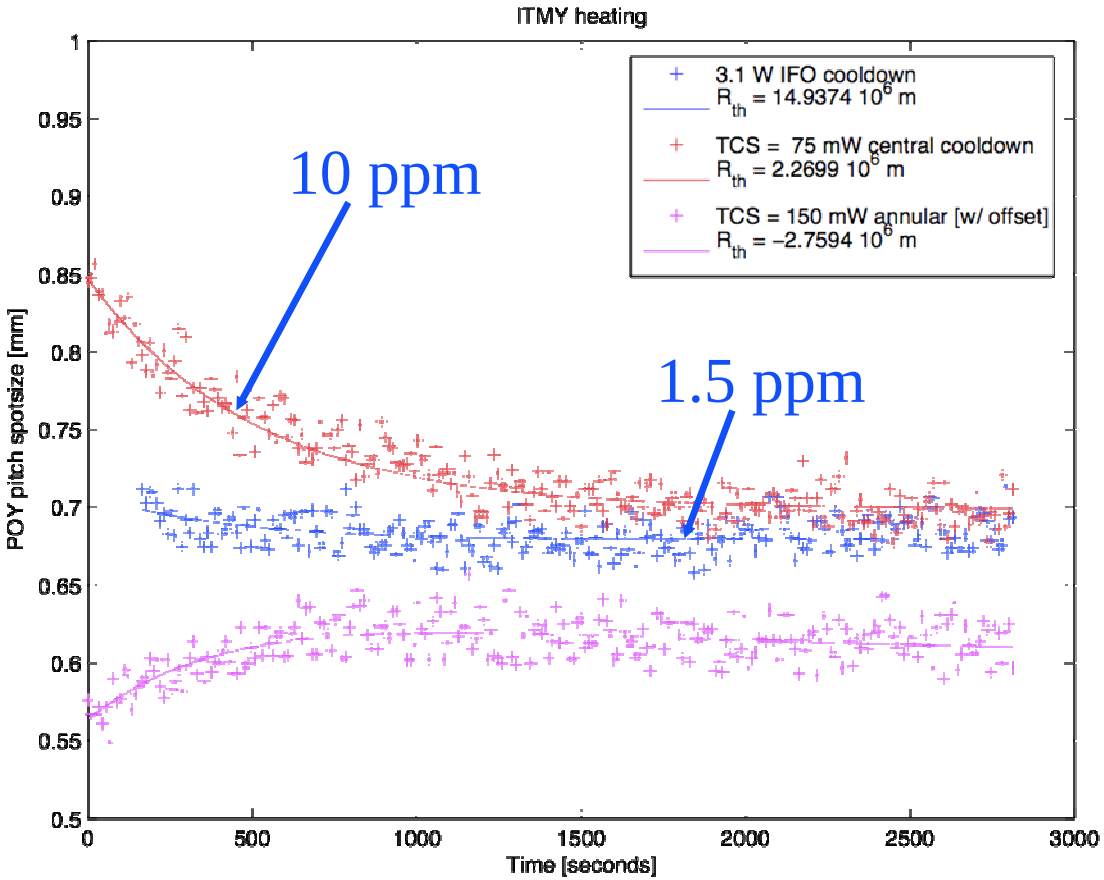


- ITMX data set an upper limit on absorption of 1.5 ppm
- Pretty unlikely that these results are consistent with the results taken now
- Has absorption suddenly got worse ??
- Data taken by Sam W

# Absorption Timeline

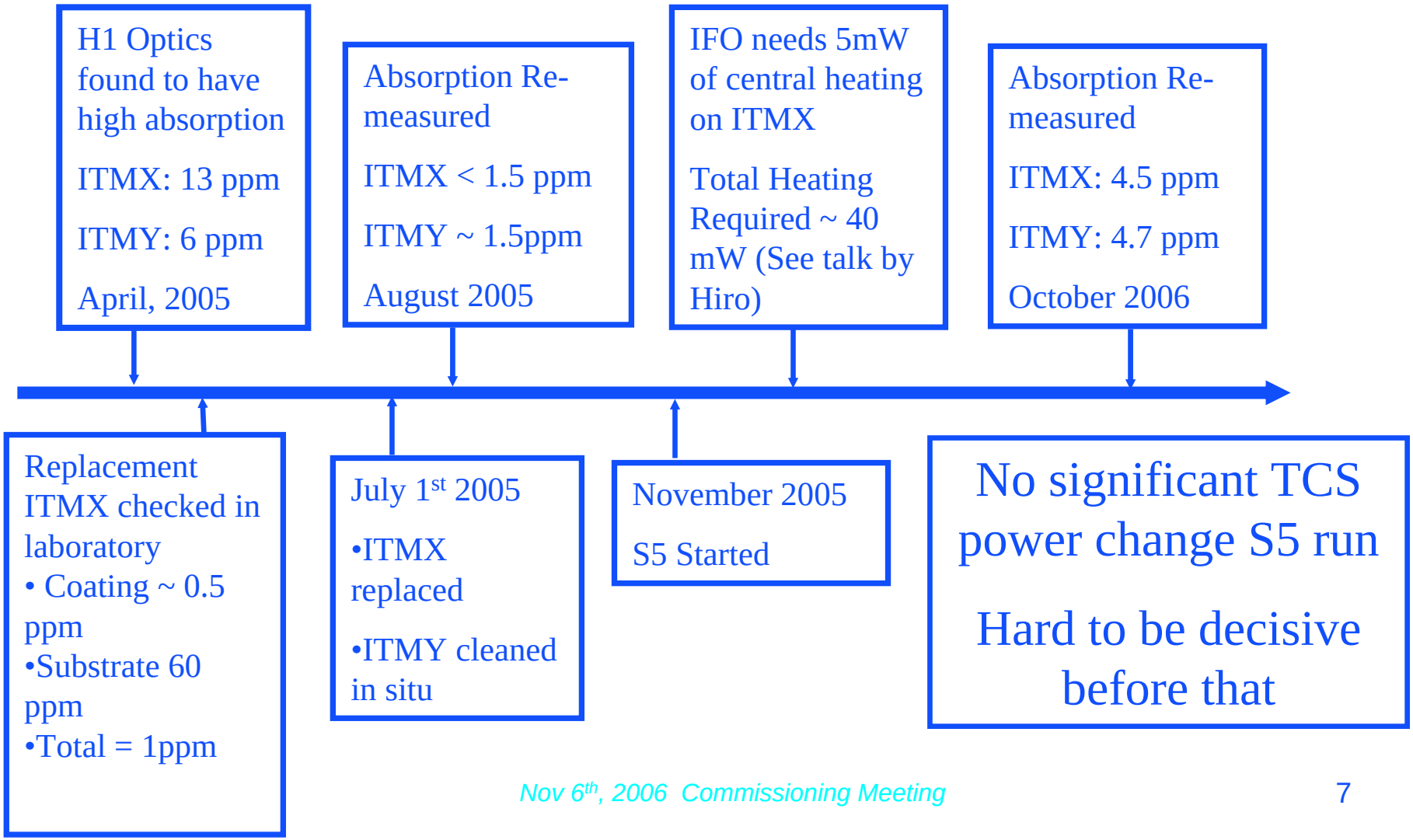

LIGO

# Conclusions

- The spot size technique is now sensitive to 0.4 ppm absorption in the optics
- H1 optics appear to be absorbing more than a year ago (From spot size measurements)
- Given that the optics appear to be absorbing 4.5 ppm. IFO appears to need 56 -> 88 mW [3.5 - 5.5ppm]. Modeling suggests 40 mW
- The inspiral range is still surprisingly sensitive to TCS setting. Turning off TCS dropped inspiral range to 8 MPc

LIGO

# Losses in LHO HR Surfaces

W. Kells

LIGO Laboratory, Caltech

# LIGO I TM Scatter loss

- "As built" optics fabrication data  scatter loss minor.
  - » Further characterization not exhaustive
  - » Recycling gain ***G*** (simulations) expected to far exceed SRD (***G*** >30)

- LHO commissioning (Sbsq. LLO): SRD achieved.
  - » Less interest in detailed characterization
  - » No evidence of degradation (scatter)
  - » Symptoms: anecdotal "point" scatter; low recycling gain; low ***V*** (~'00-'02)
  - » Direct measure of anomalous HR scatter: suspect points dominate

- Importance for Adv LIGO: bench characterization (start ~03)
  - » OTF scanning station resurrected: mixed with surface loss studies
  - » Where is the dominant "point" component?
  - » LMA, and other measurements

# Optical Loss Expectations

- Goal: $G_{RC}^{CR} \geq 30$ based on older polish/coating information
- Pathfinder development & fabrication proved much better:
  - » Micro roughness $\sigma_{rms}$ <0.24 nm $\Rightarrow$ prompt loss ~$(4\pi\sigma_{rms}/\lambda)^2$ <8ppm
    - – "blemishes" (e.g. point defects) ~1 ppm
  - » Super polished substrate 2 - 3x lower $\sigma_{rms}$

- Simulation (FFT) with Fab. Data:
  - "Figure": modal distortion
    - Hence induced diffractive loss
  - "Roughness"= prompt loss
  - Low absorption; cold "start up"
  - Witness sample reflectivities

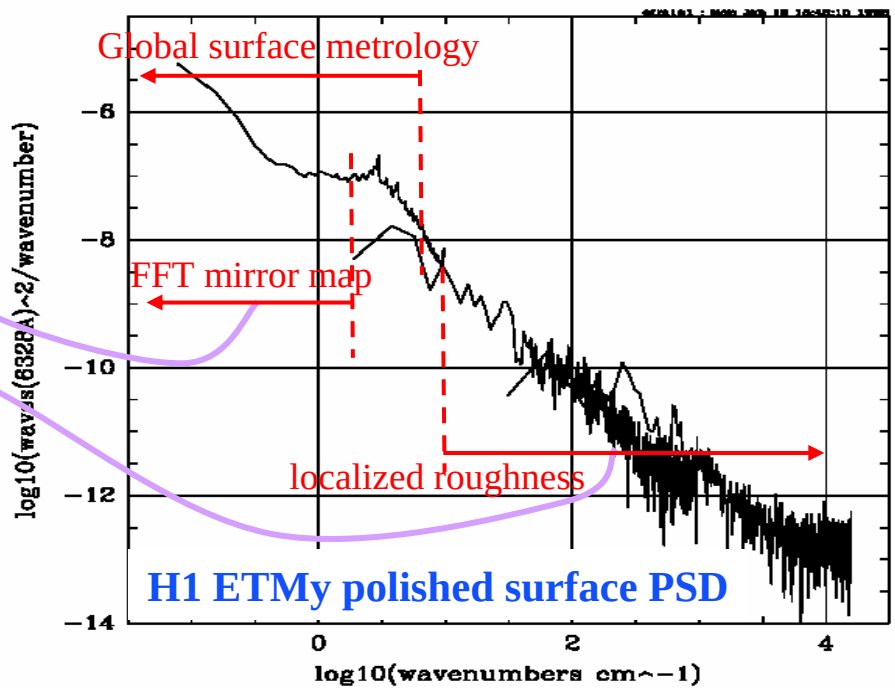


***Simulated G*** ***(at least: CR field not affected by degenerate recycling)*** ***far exceeds goals***

- **Consistent with Advanced ligo requirements**

# "As built" FFT Simulation

- FFT simulation of H1 with *no free parameters*:
  - » "Cold" state: no thermal lens (little effect on CR light)
  - » $G_{RC}^{CR}$ ~ 92 (observed ~ 41)
- FFT uses *directly measured* distortion maps of all in situ coated HR interfaces.
  - » ~13% $G_{RC}^{CR}$ degradation for full as built simulation.
  - » Consistent with very good ifo contrast defect
    - – 6 $10^{-4}$ for H1
    - – 3 $10^{-5}$ for L1
- Other in situ observations (e.g H1 arm visibilities) are consistent with arm loss needed to "match" observed $G_{RC}^{CR}$
  - » Need ~70-80 ppm/HR loss (late breaking: updated simulations (?)need only 45ppm/HR for $G$ = 45)

# In Situ Optics Performance

- $G_{RC}^{CR}$ ~41, which is:
  - » Consistent with measured arm visibilities (allowing for other losses, $V$ =.02 Requires prompt loss of 63ppm/HR)
  - » Consistent with total arm loss dominated by prompt scatter.
  - » Scatterometer data extrapolated to absolute loss
  - » Consistent with lower than anticipated contrast defect ( and small FFT dependence on maps)

Replaced ITM

| CAVITY | $V$ | $T_{ITM}$ | $T_{WITNESS}$ | Scatter |
|---|---|---|---|---|
| 2k X | .0222 | .0277 | .0283 | 0.85 |
| 2k Y | .0211 | .0272 | .0281 | 7 |
| 4k X | .0241 | .0279 | .0275 | 7.5 |
| 4k Y | .0214 | .0263 | .028 | 8.8 |

- Character of scatter: “lots” of points
  - Except for obvious blemishes all HR beam foot prints images appear ~same
  - No clearly distinguishable diffuse “background” (< 1/3 point component)
  - High extinction ratio twinkle (FM and BS)
  - Scatterometer measure as well as appearance independent of TM history.

# Scatterometer studies

- Some (H1) HR surfaces viewable @ 3 angles:

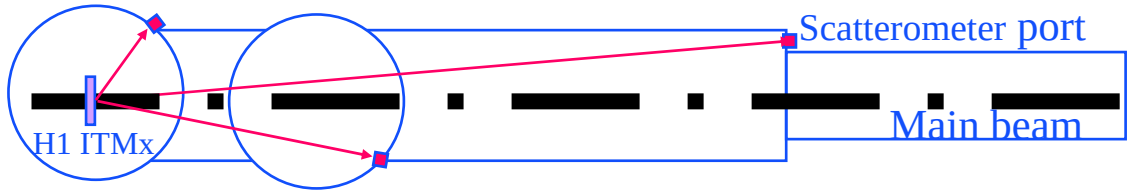


» Rough integral loss estimate for FFT input: 68ppm “base loss”

» Angular dependence more “point like”.

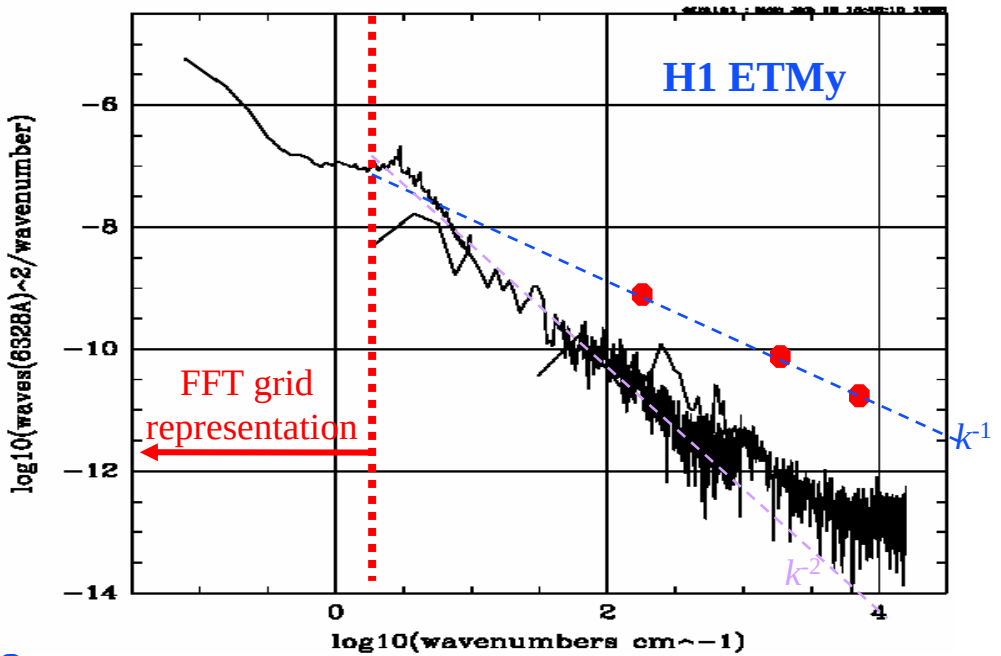


» More accurate ***comparison*** measurement of 2k ETMs (GO super polished) to 2k ITMs, 4kETMs (not super polished): no significant difference

# Analysis of the “Globular Cluster”

- Cleanest point scatter image: 2k ETMy:
  - » Grab video stills for detailed analysis:

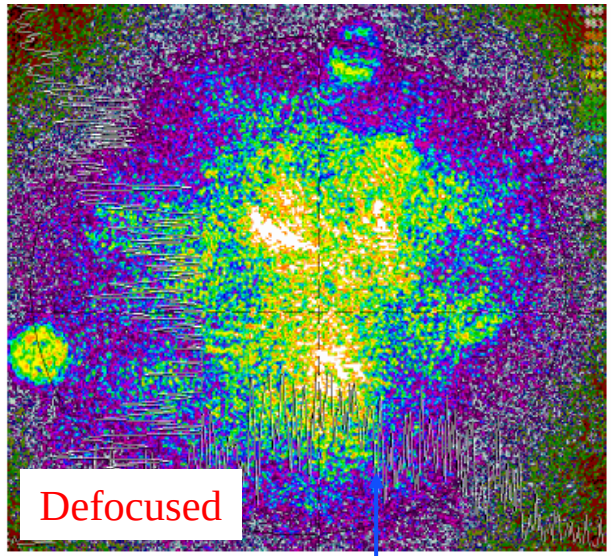


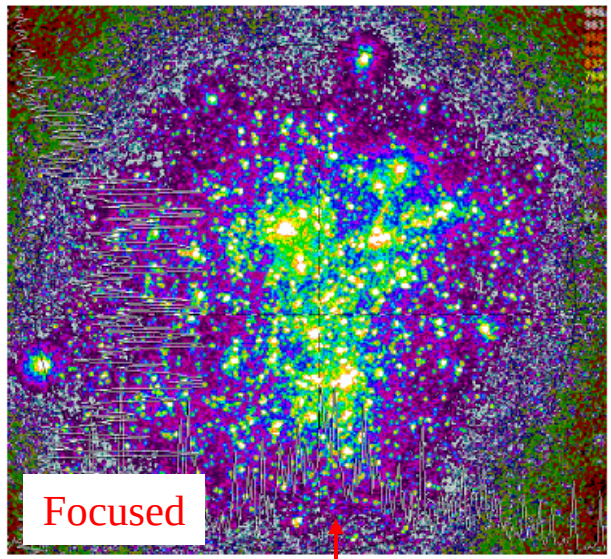


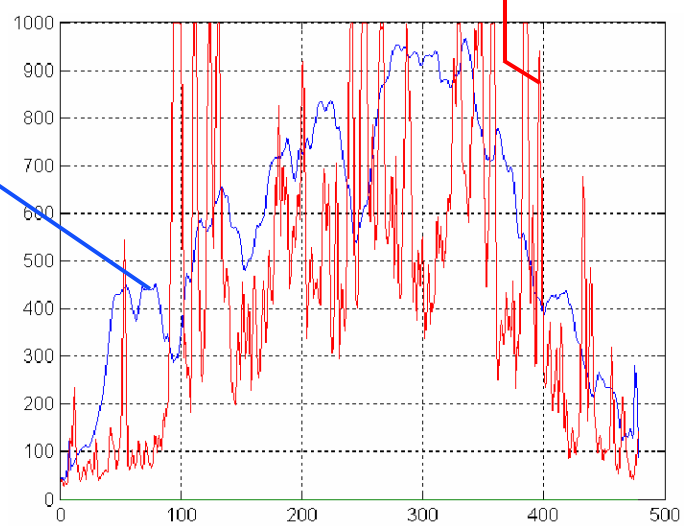


- ➢ This point defect background ~same for all optics.
- ➢ Diffuse (micro roughness) background contributes < 1/3 of total scatter.
- ➢ Blemishes (wipe streaks) don’t dominate total ?

- ➢ Puzzle: Why these point defects missed in our Lab.QA? Why not seen in LMA scans of 2ITM04 (removed from 2k, ’02)

# Why cant we “find” the point scatter ?

- Interpret histograms of BRDF vs scan pixel
  - » No clean, distinct “point” peak
  - » Some point component but not dominant
  - » Calibrated mean scatter loss <1/2 in situ implied
    (allowing for different point/roughness BRDF)
- Possibilities:
  - » Dust (cleaned away in Lab.)?
  - » In situ TMs [all] differ from those scanned
  - » Spectrum of point scatter strengths
  - » Probe beam Dia. too large (averages over points)

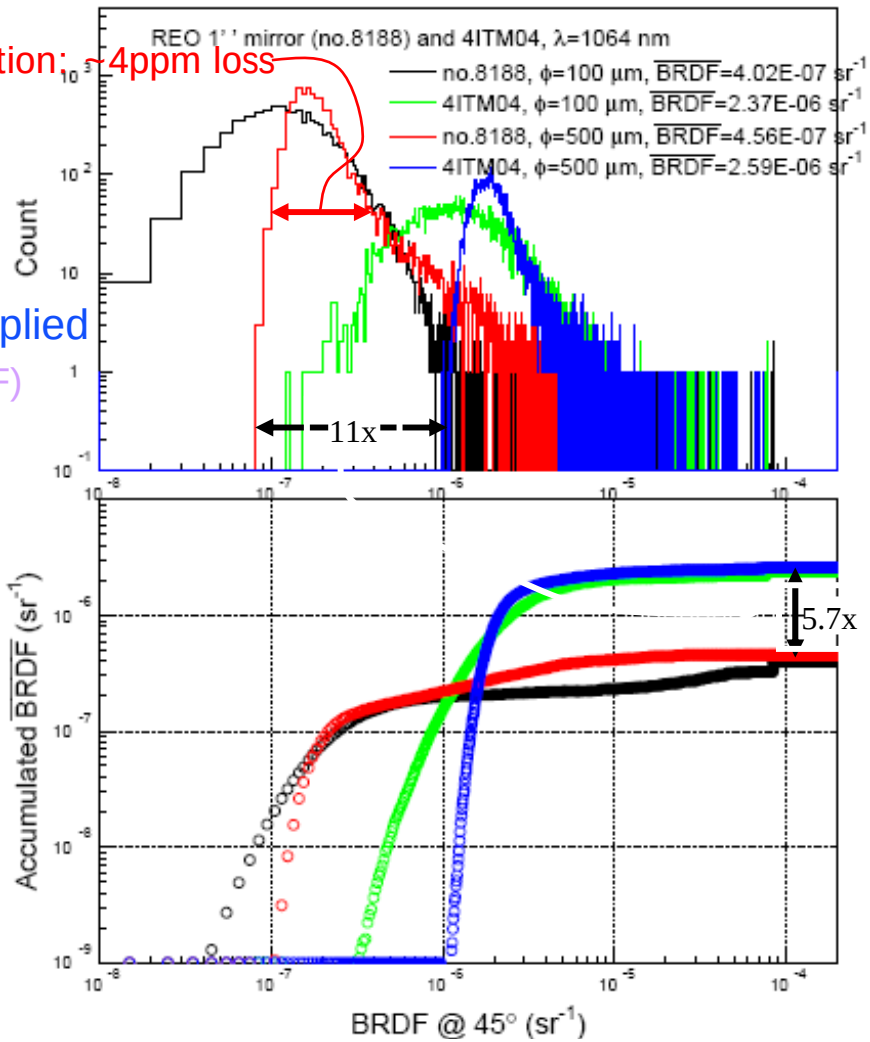

# Homogeneous roughness ?

- Expect isotropic glow from “homogeneous” polish roughness
  - » Find: “point” defect scatter dominates
  - » Bench scans (1064nm) also show excess

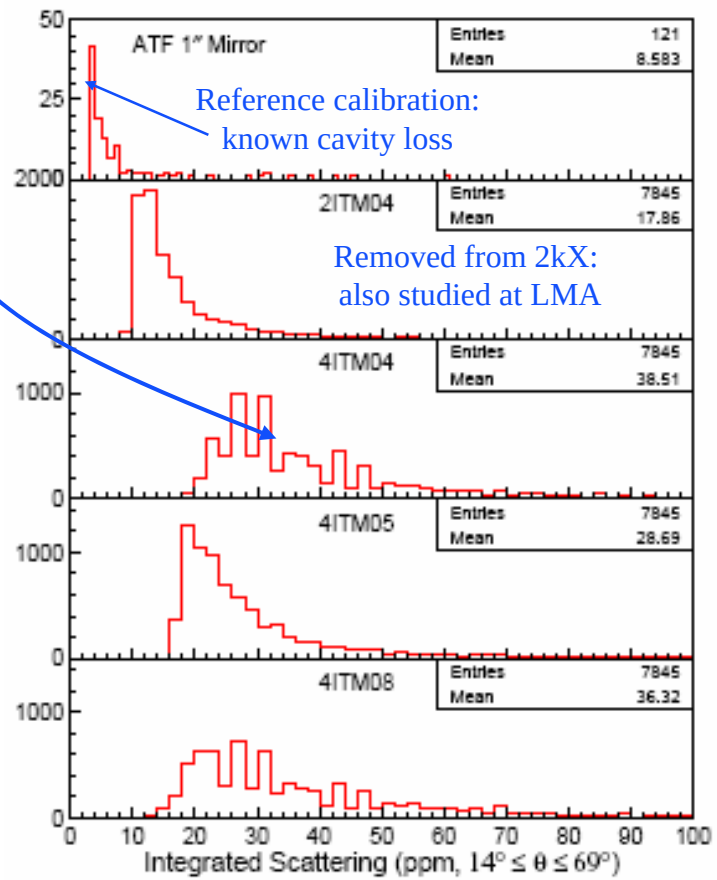


Is it just dust ??

Resonant arm, Gaussian illuminated ETM

# Contamination in LIGO I TMs

- Goal: corroborate in situ performance with bench tests
  - » Many LIGO COC optics studied
    - – Comparisons establish "typical" from anomalous
  - » Absolute calibration to various reference mirrors.
    - ➢ Components of "loss test" cavity

Example: characterize anomalous contamination of H1 ITMs.

- ➢ Absorption is lumpy but not point like
- ➢ Scatter also anomalous and correlates well spatially with absorption
- ➢ Easily removed by surface cleansing
- ➢ Fine absorbing dust, sucked in during vent?

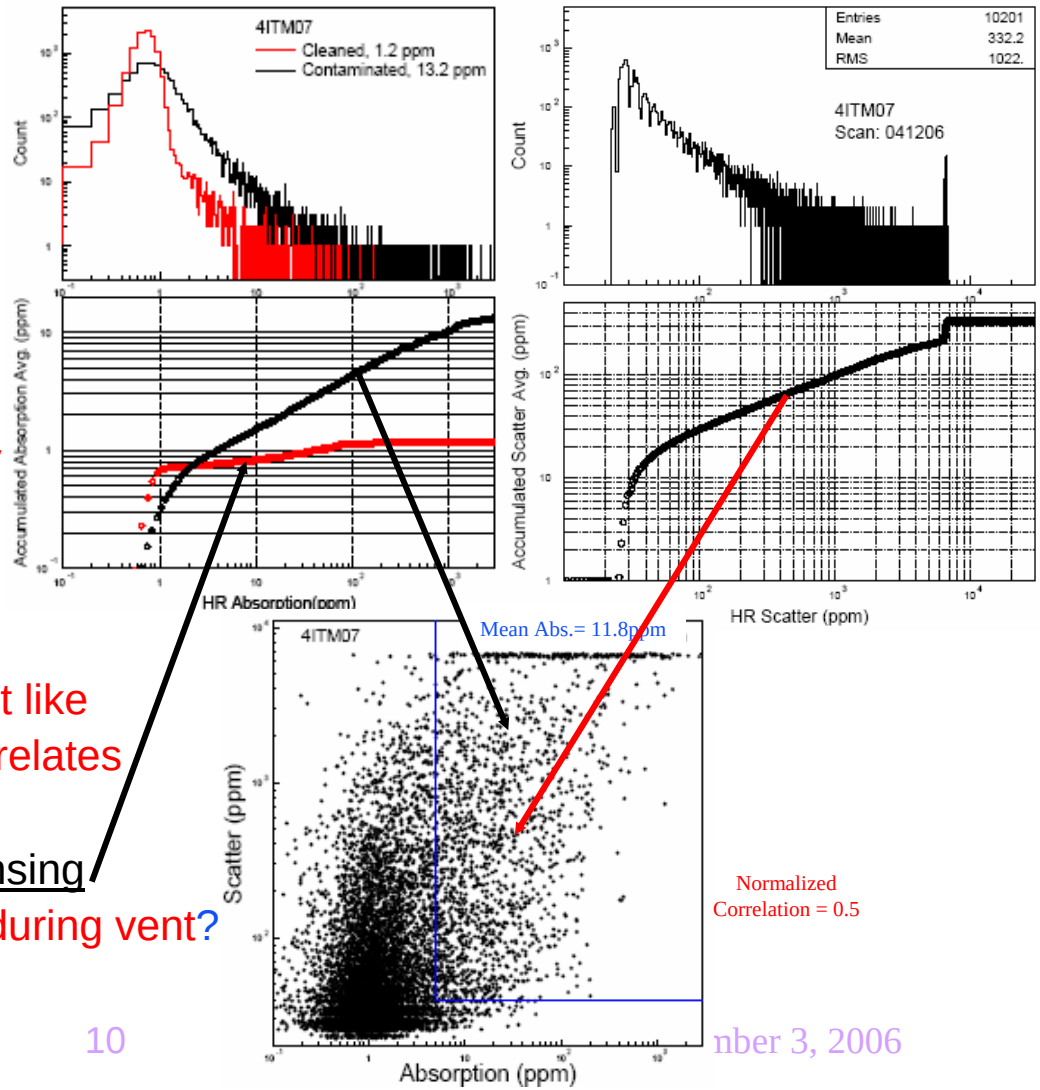

LIGO

# Scatter measurement set-up at Caltech

**Liyuan Zhang**

**On behalf of Caltech COC group**

LIGO

# Schematic of the experimental set-up

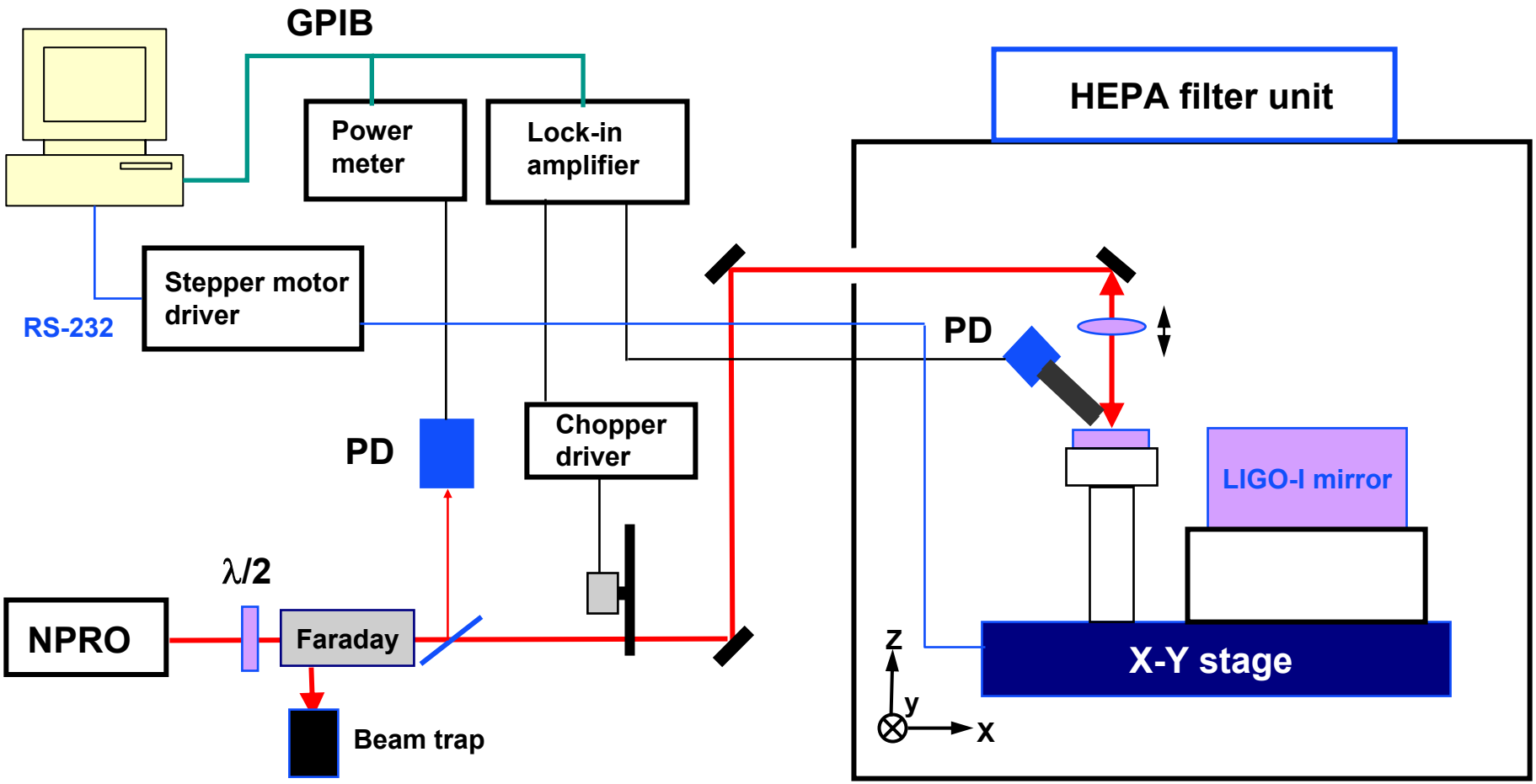

LIGO

# TIS and BRDF@45º

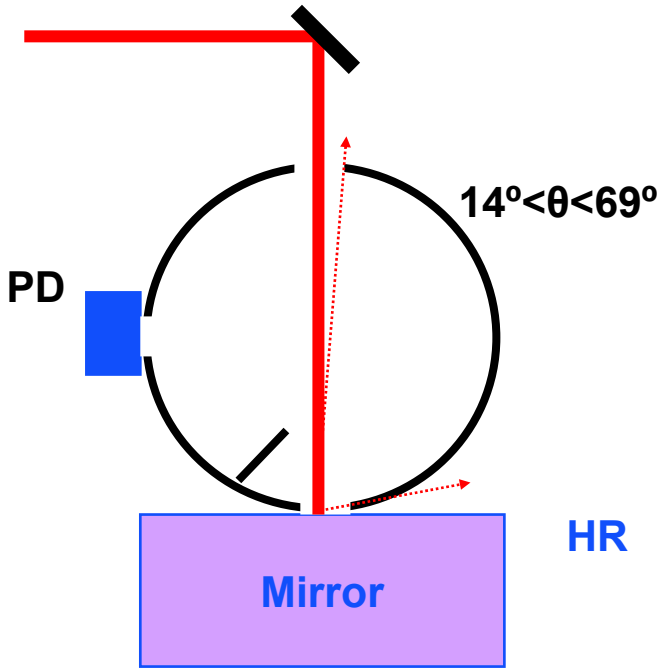


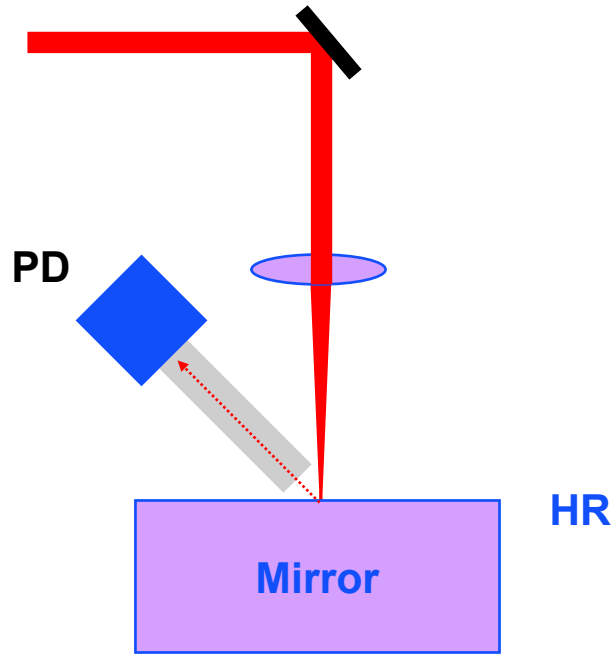


**TIS: collimated beam, Dia.~1mm, low spatial resolution, more collected scattering light.**

**BRDF @ 45 degrees: focused beam, Dia. 0.1 ~ 0.5 mm, high spatial resolution, less collected scattering light.**

LIGO

# RTS test bench

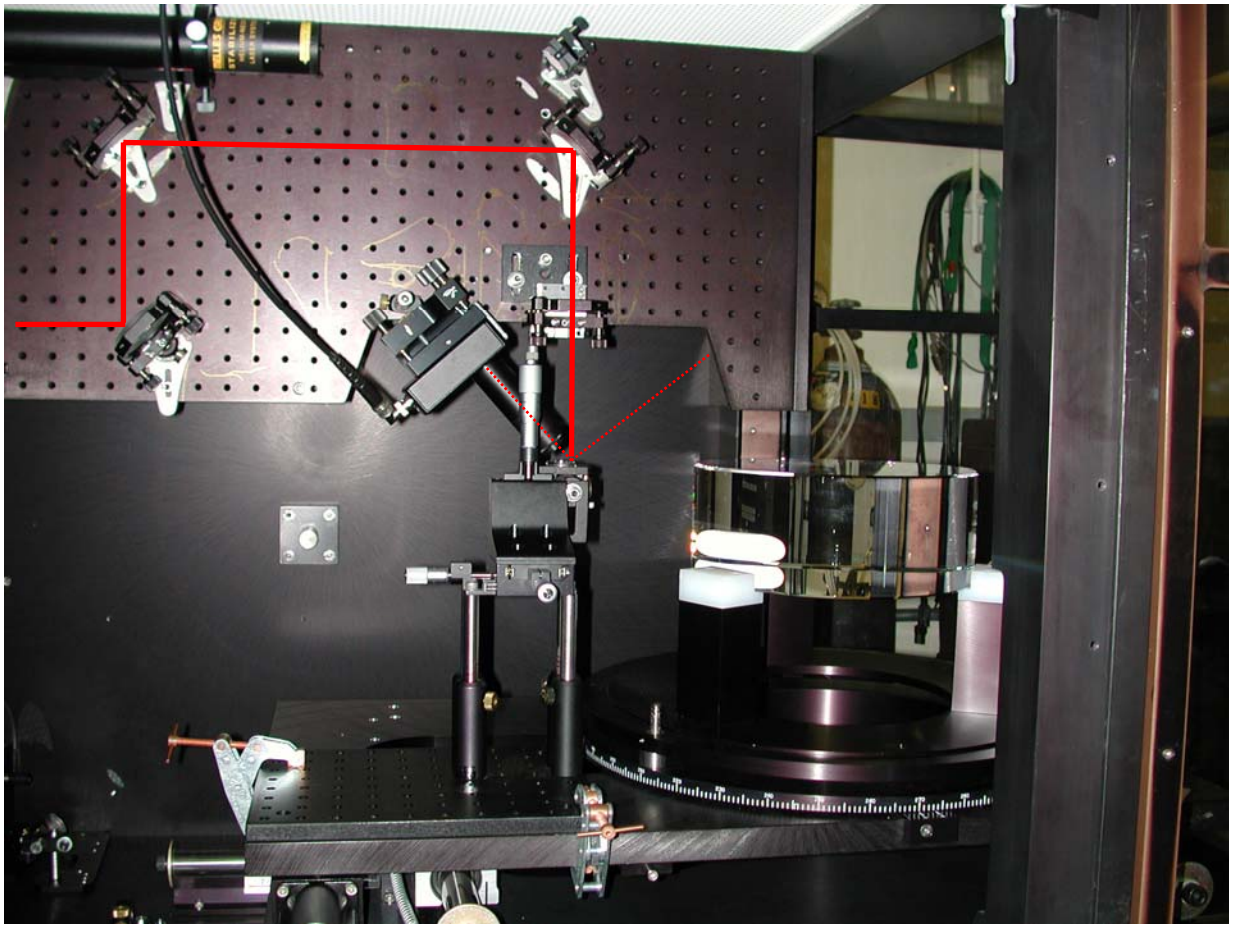

LIGO

# Results with the integrating sphere

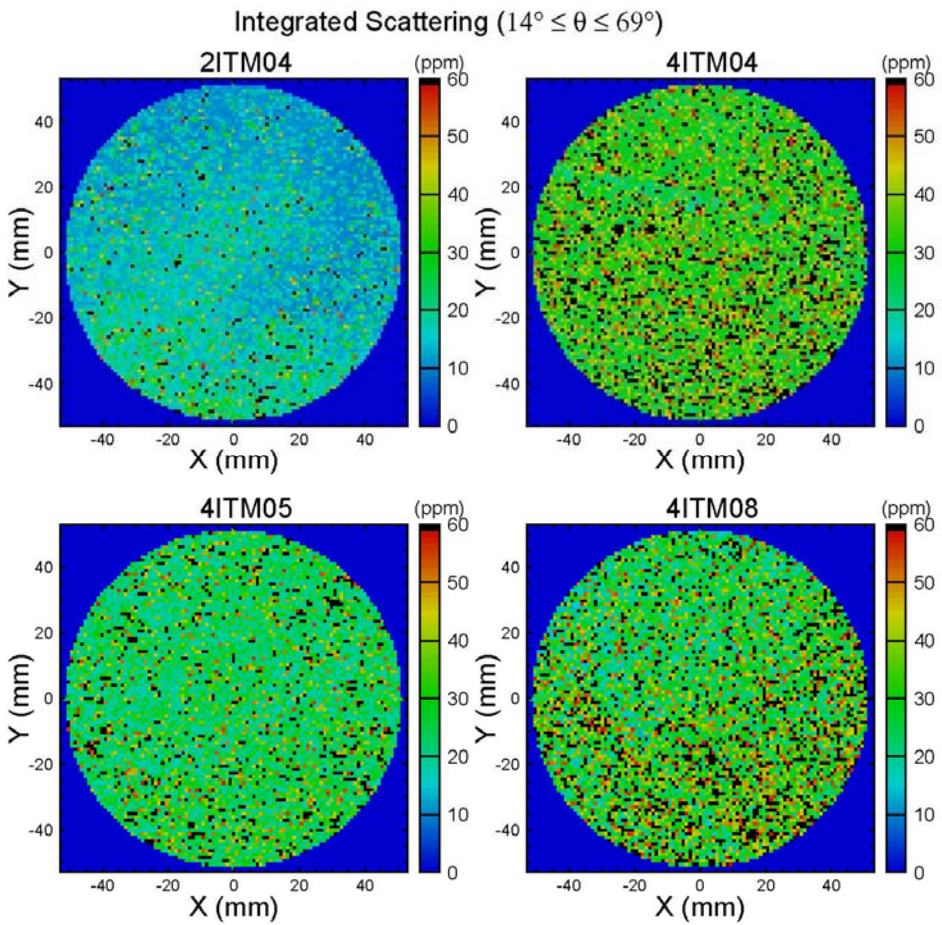


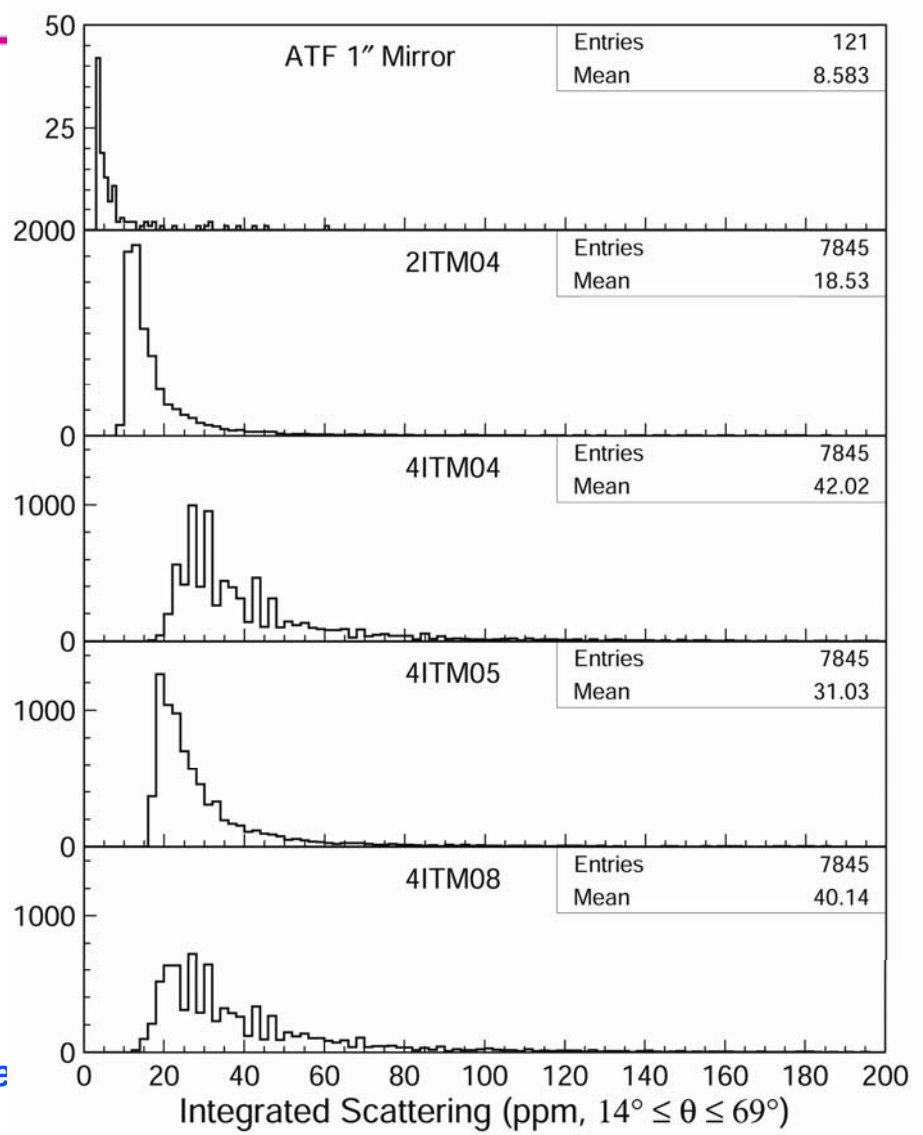

LIGO

# *Results of BDRF at 45 degrees*

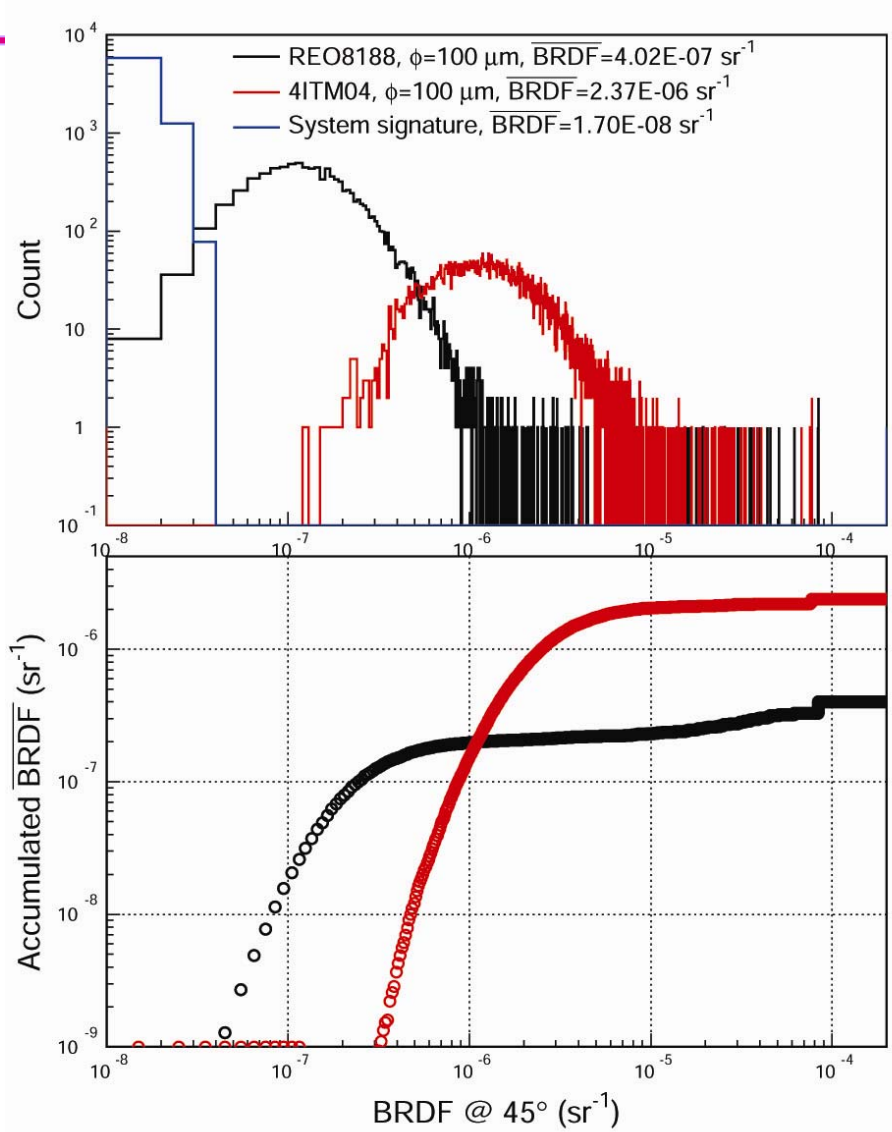


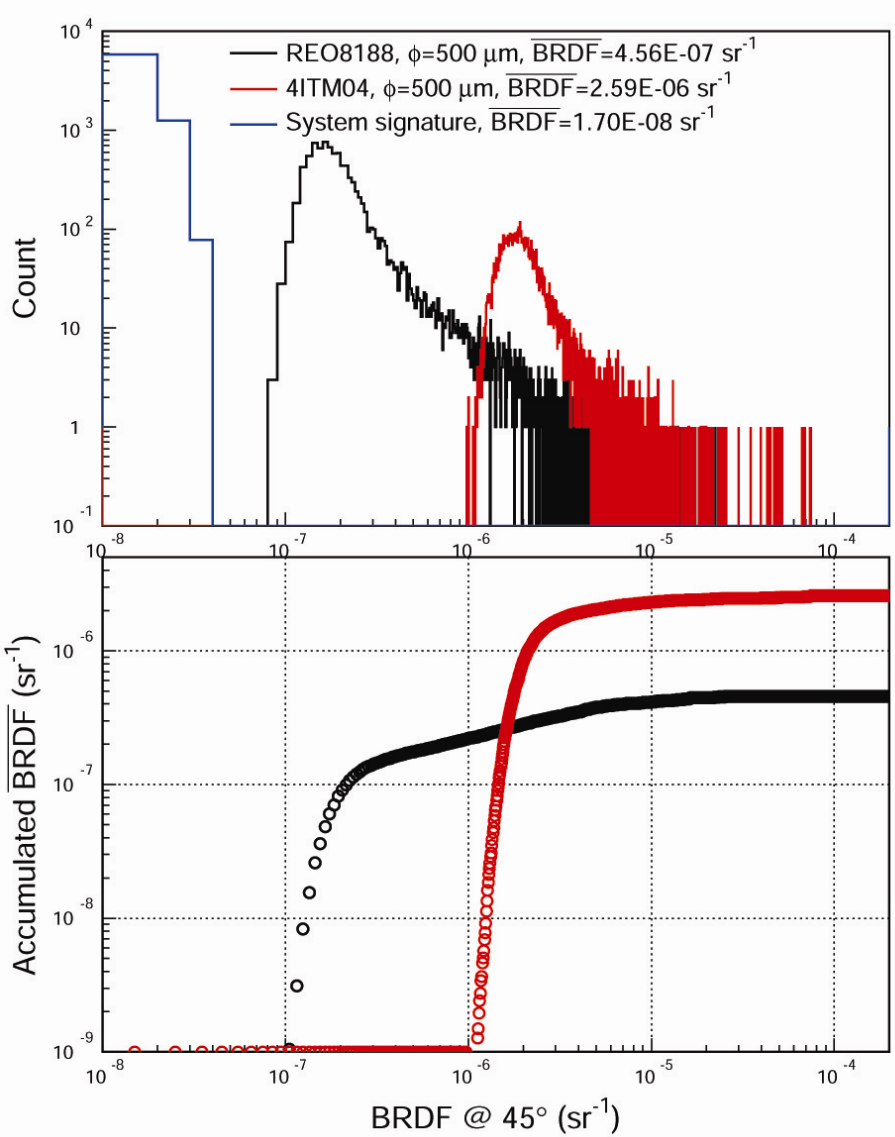

LIGO

# *Thoughts on next steps …*

- **Doing the BRDF measurement at certain angle to compare with that made *in-situ?***
- **Upgrading the integrating sphere set-up to do more complete TIS measurement?**
- **Improving the focused beam set-up to identify different scattering sources (defects)?**

LIGO

# New FFT for advLIGO

Hiro Yamamoto, Caltech/LIGO

- Introduction
  - » Requirements to be identified for AdvLIGO
  - » LIGO I research tool
- Static IFO Simulation
  - » Physics
  - » Implementation
- A few applications
  - » surface aberration and loss

LIGO

# Introduction

- LIGO I, how MIT-FFT was used
  - » Base design
    - – IFO basic parameters, surface figure requirements, etc
  - » Commissioning
    - – Thermal effect, as-built mirror effect, realistic optical gain, etc
- AdvLIGO, to be analyzed
  - » Requirement of radius of curvature of COC mirrors
    - – polishing
    - – correction by TCS
  - » Surface aberration
    - – Requirements of the surface quality to satisfy the limit of loss in arm, total of 75ppm
  - » Parametric instability
    - – highly distorted field, hard to be expressed by simple modes

LIGO

# With a little bit of reality

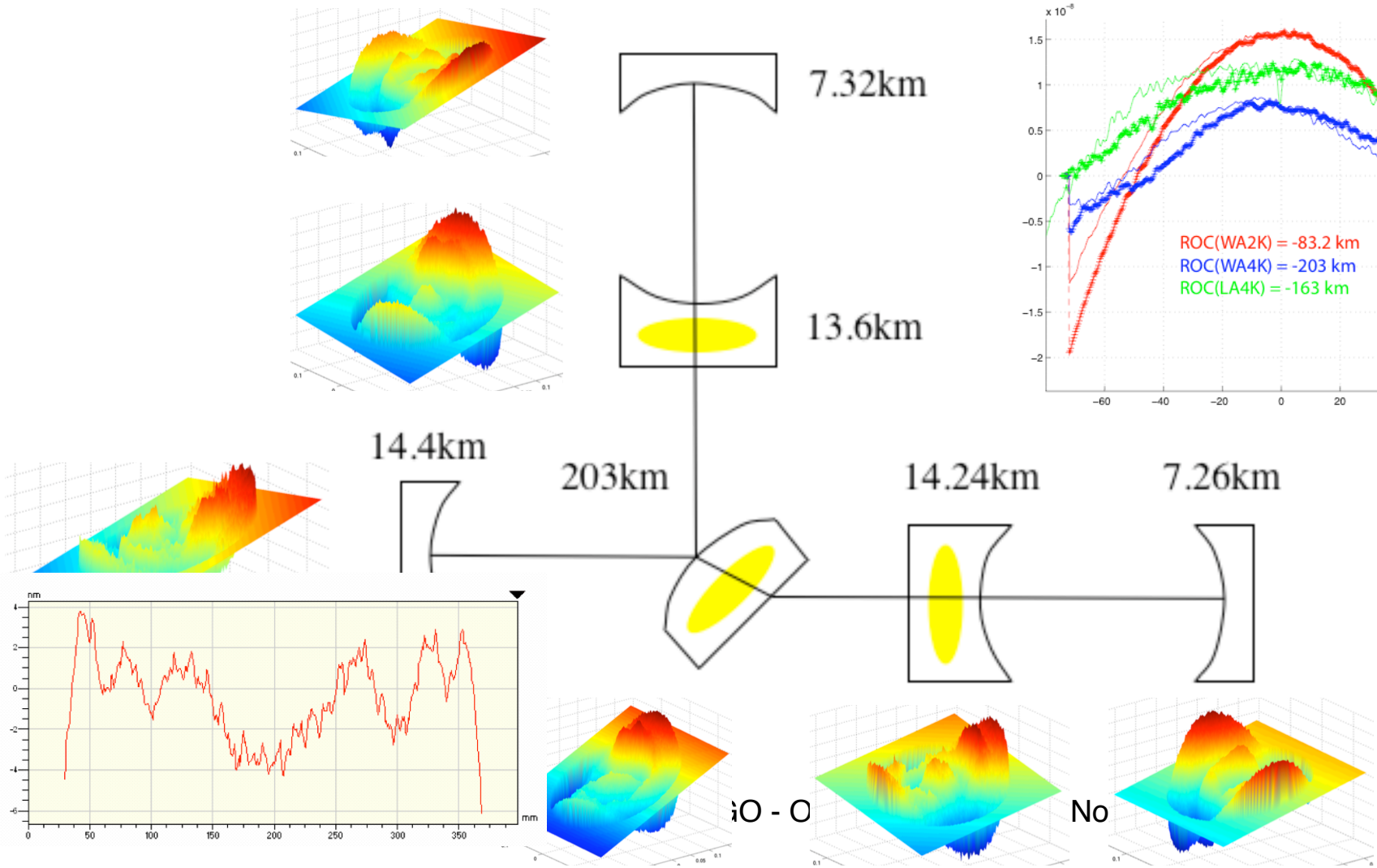




3

# LIGO I performance using old FFT

| | Lock | CR gain | Upper SB gain | Lower SB gain | Contrast Defect x$10^{-6}$ |
|---|---|---|---|---|---|
| symmetric arm, best TCS | FFT | 46 | 23.7 | 23.7 | 58 |
| As built arm, best TCS | FFT | 46 | 21.7 | 25.3 | 220 |
| As built arm, com.TCS | FFT | 46 | 19.6 | 24.6 | 233 |
| | LSC | 46 | 22.3 | 22.3 | 244 |
| As built arm, com.TCS w/ phase map | FFT | 36 | 18.3 | 23.3 | 429 |
| | LSC | 36 | 21.5 | 20.2 | 439 |

| | | | |
|---|---|---|---|
| loss / mirror | 55 | 45 | 35 |
| Rec. gain | 42.3 | 44.7 | 47.4 |

optical gain vs Spob

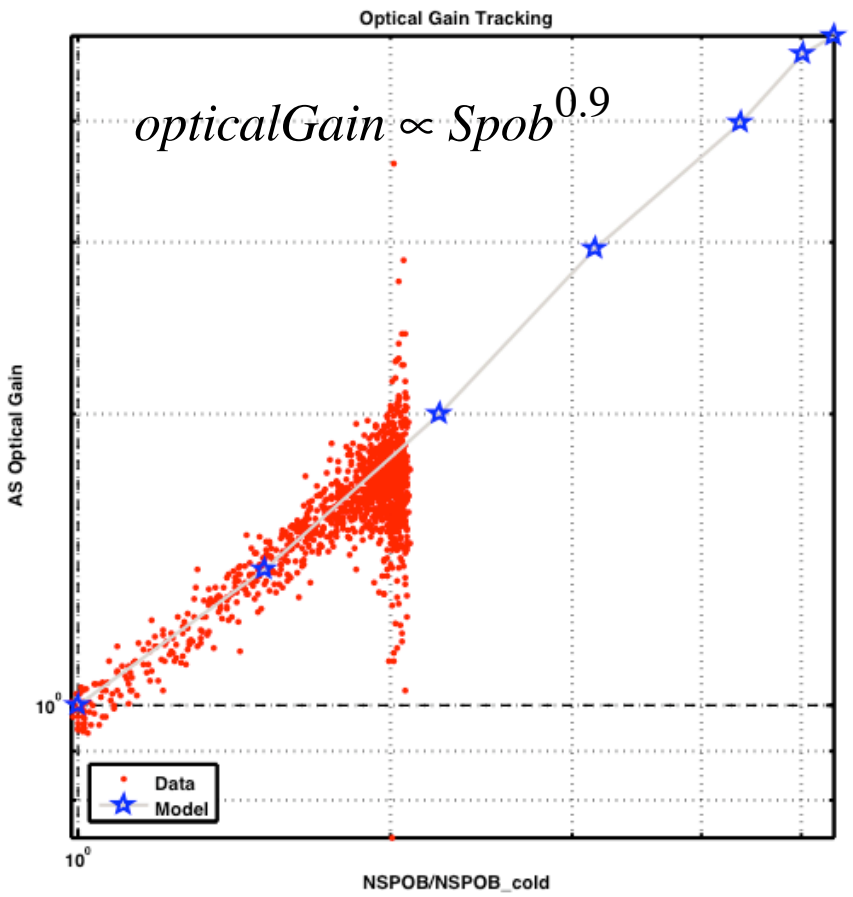


for advLIGO - Optics mtg @ CIT in Nov06

# Orange peel
## - psd shows bumps at ~0.3 cm -

loss ~ 2.4 ppm

new FFT grid size
= 0.14 ~ 0.28cm

loss ~ 1.3 ppm x 2

old FFT :
loss(35cm/256) -
loss(35cm/128)

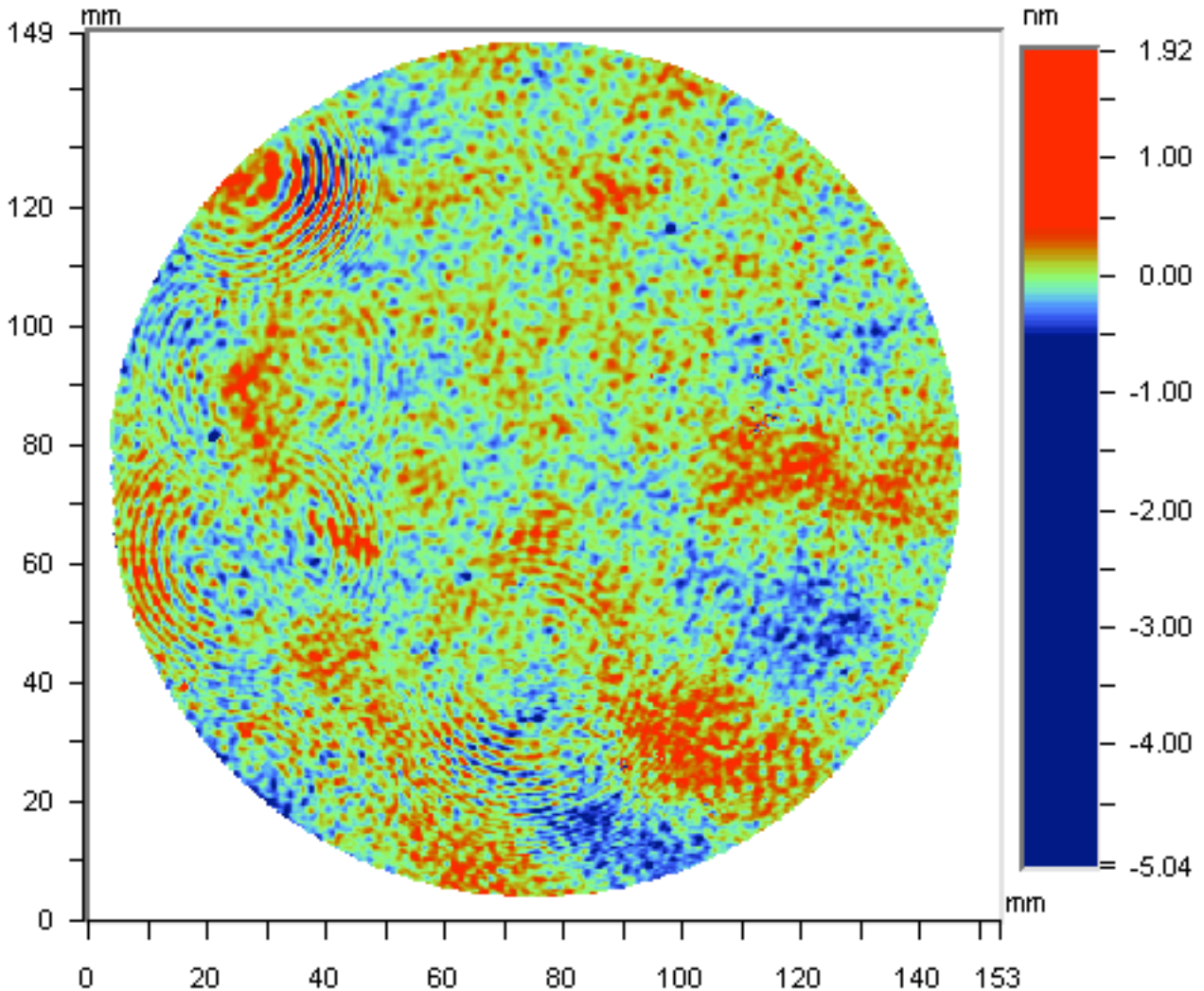


G060572

LIGO

# carrier power in dark port

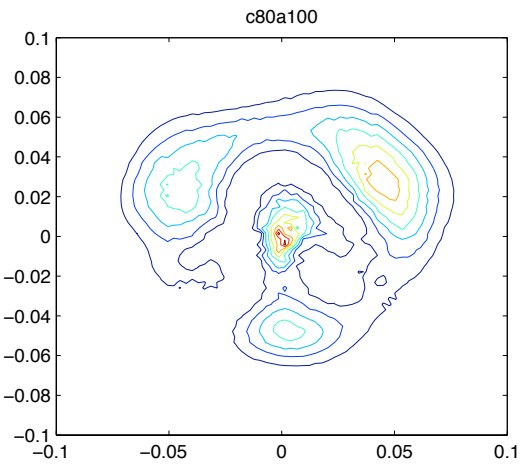


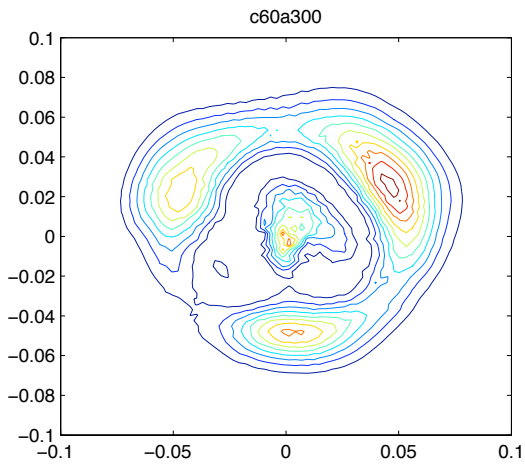


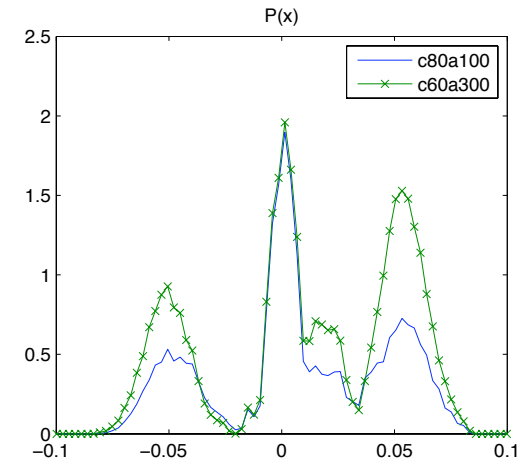


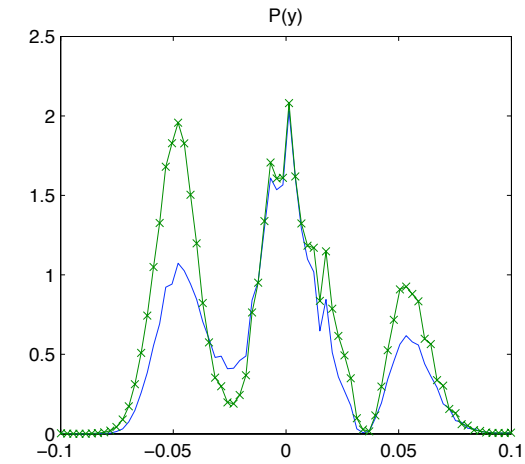


G060572

6

LIGO

# Stationary IFO Simulation

- FP completed -> advLIGO underway
  - » Object oriented code using C++
    - – ease of modification, adding compensation plate, degenerate to non-degenerate Michelson cavity, etc
- Ease of loading a variety of formats of data file
- Stationary field injection
  - » GW signal, PI excitation
- FFT using adaptive grid size
  - » The beam size changes a lot in a concentric configuration.
  - » Higher order mode needs this treatment for proper propagation.
- Cavity lock using “error” signal, similar to real LSC
- Mirror surface noise generator with proper spectrum

# Stationary IFO Simulation (1)

(4) diffractive loss = P(E41) - P(E1)

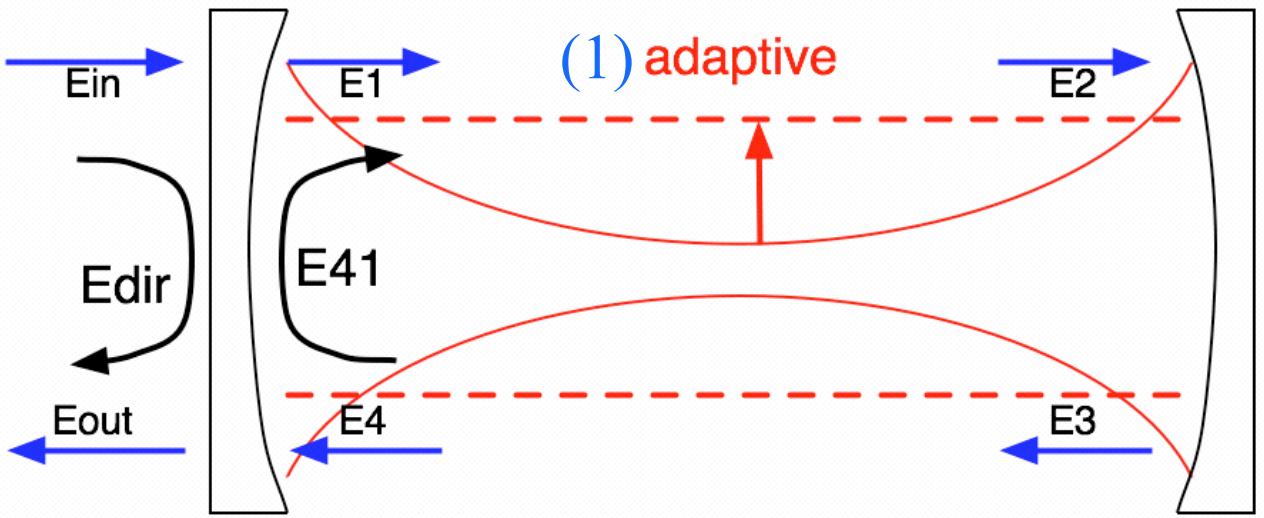


(3) Error signal = Eout * Edir

(2) A(x,y) cos( w t )

E3 = E3(0) ( 1 + i A(x,y) ( Exp( i w t ) + Exp( -i w t ) ) )

LIGO

# Stationary IFO Simulation (2)

- Any maps
  - » DATAFILE(filename), NOISEGEN(sigma,slope), formula
  - » DATAFILE can be any size
  - » ITM.opt.HR_phasemap = "DATAFILE (4ITM061stretch340.asc) - if(r<rcut,1-sup,0) *DATAFILE (ITM_N128_W1280.dat)"

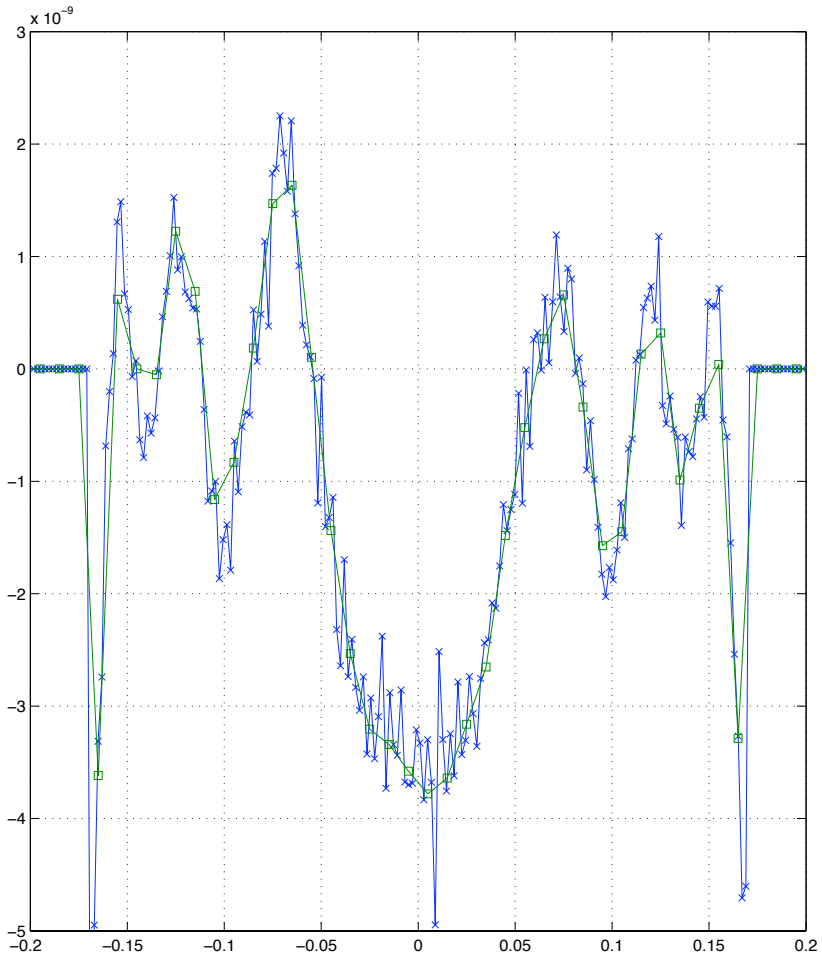

LIGO

# Input file specifying a FP

```
% Basic FFT setup
Nfft = 256
Wfft = 0.70
...
% mirror definition = [ aperture, thickness, mech, opt ]
ITM.aperture = 0.34
...
% mirror mechanical data = [ x, y, z, tX, tY, tZ ]
% mirror optoical data =
  [ T, R, ROC, reflIndex, "phasemap_xy", "phasemap_file" ]
ROC = 2076
ITM.opt.HR.ROC = ROC or
ITM.opt.HR.d = “r*r/(2*ROC)”
...
% mirror noise data = [ rand_seed, rms, power, "weightExp", WykoIndex ]
% cavity definition = [ L0, delL, matchToInput ]
% inputBeam definition =
  [ "BeamType", index1, index2, waistSize, waistPosition, matchToCavity ]
```

# 1-D spatial PSD

## LIGO I Core Optics : Lazzarini T060013

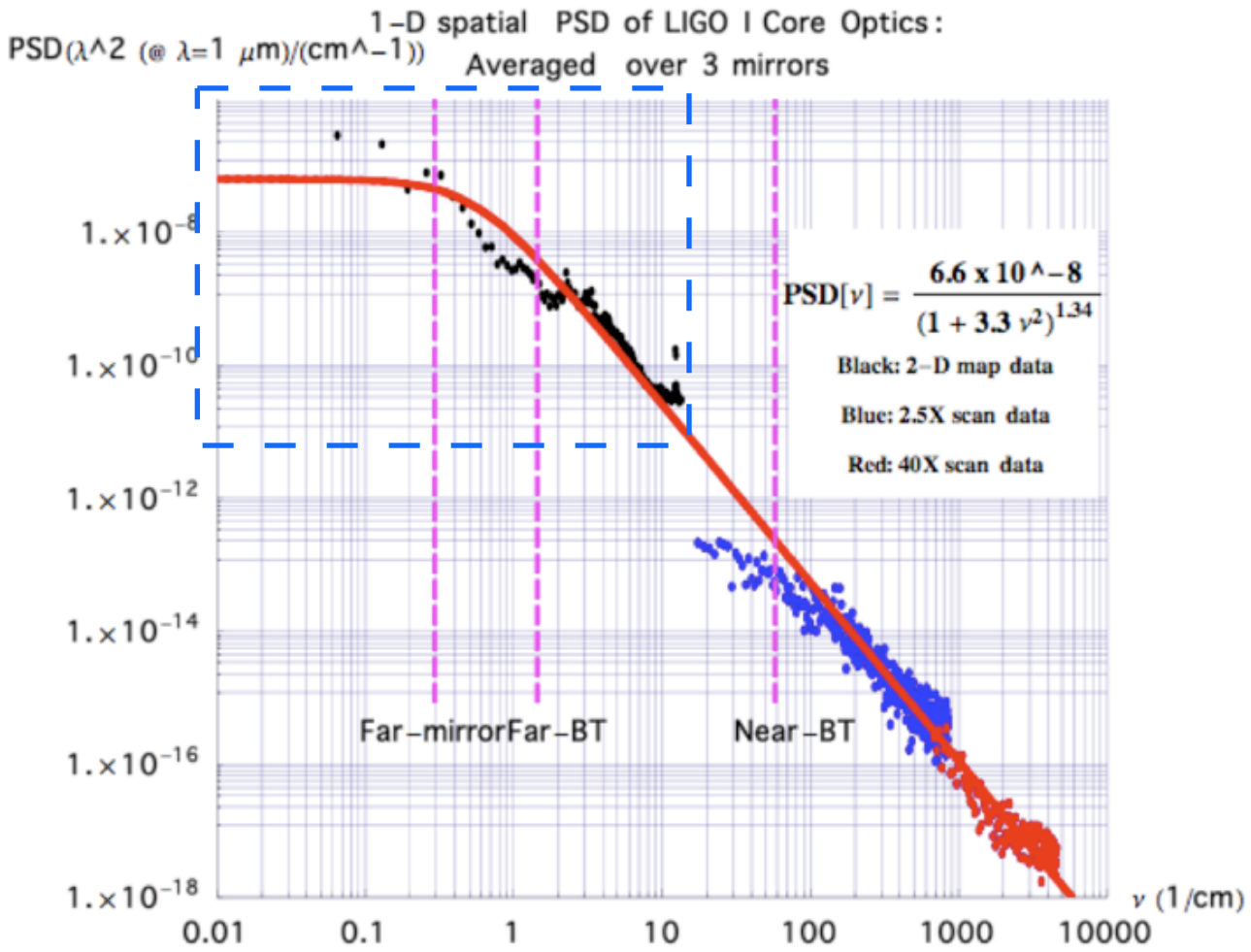

# 1-D spatial PSD
## LIGO I Core Optics vs simulated noise

N = 256
W = 70cm

rms : 0.5nm
2 surfaces
with loss
25ppm & 35ppm

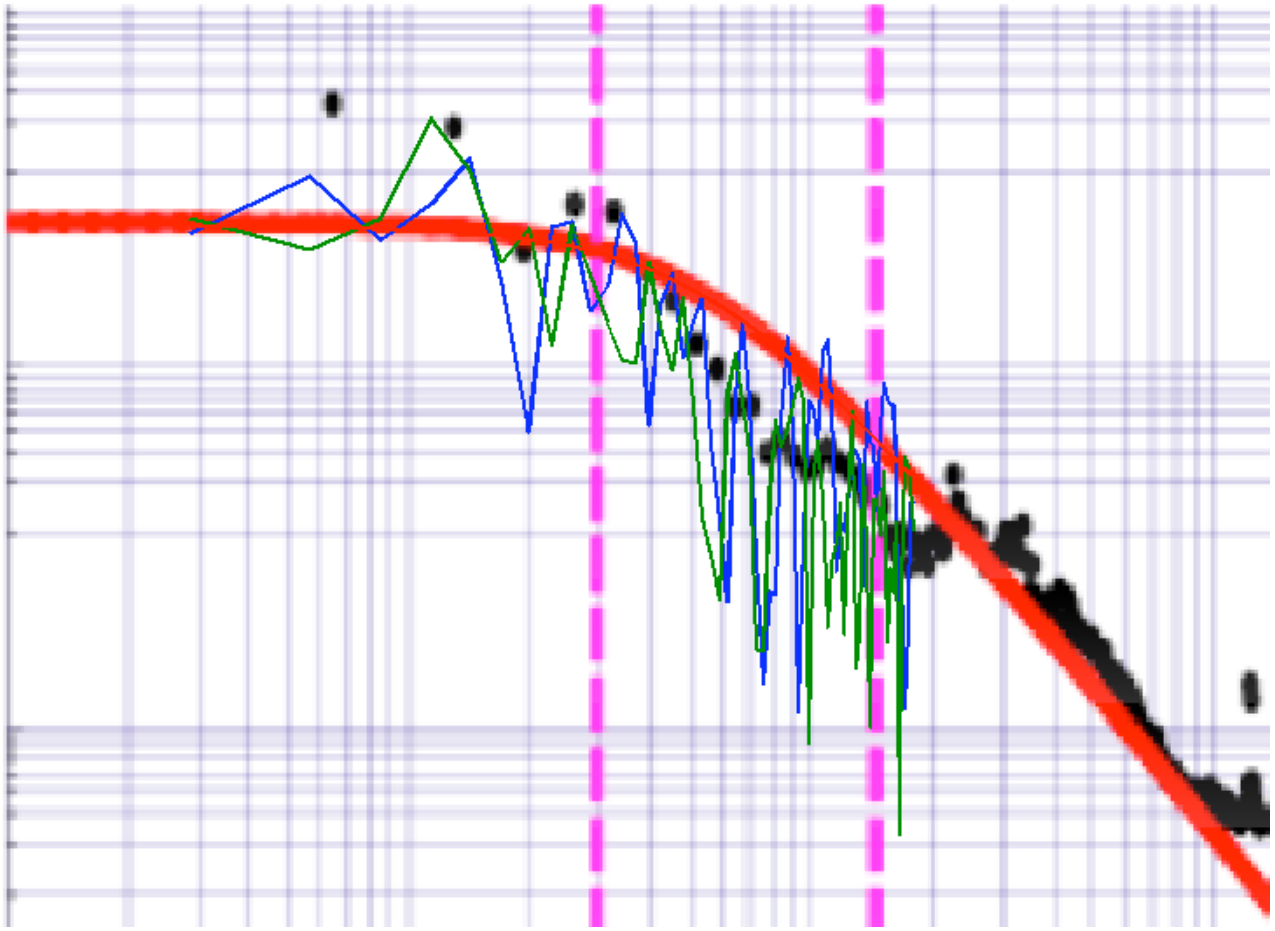

# Loss per mirror

## rms = 1nm vs 0.5nm

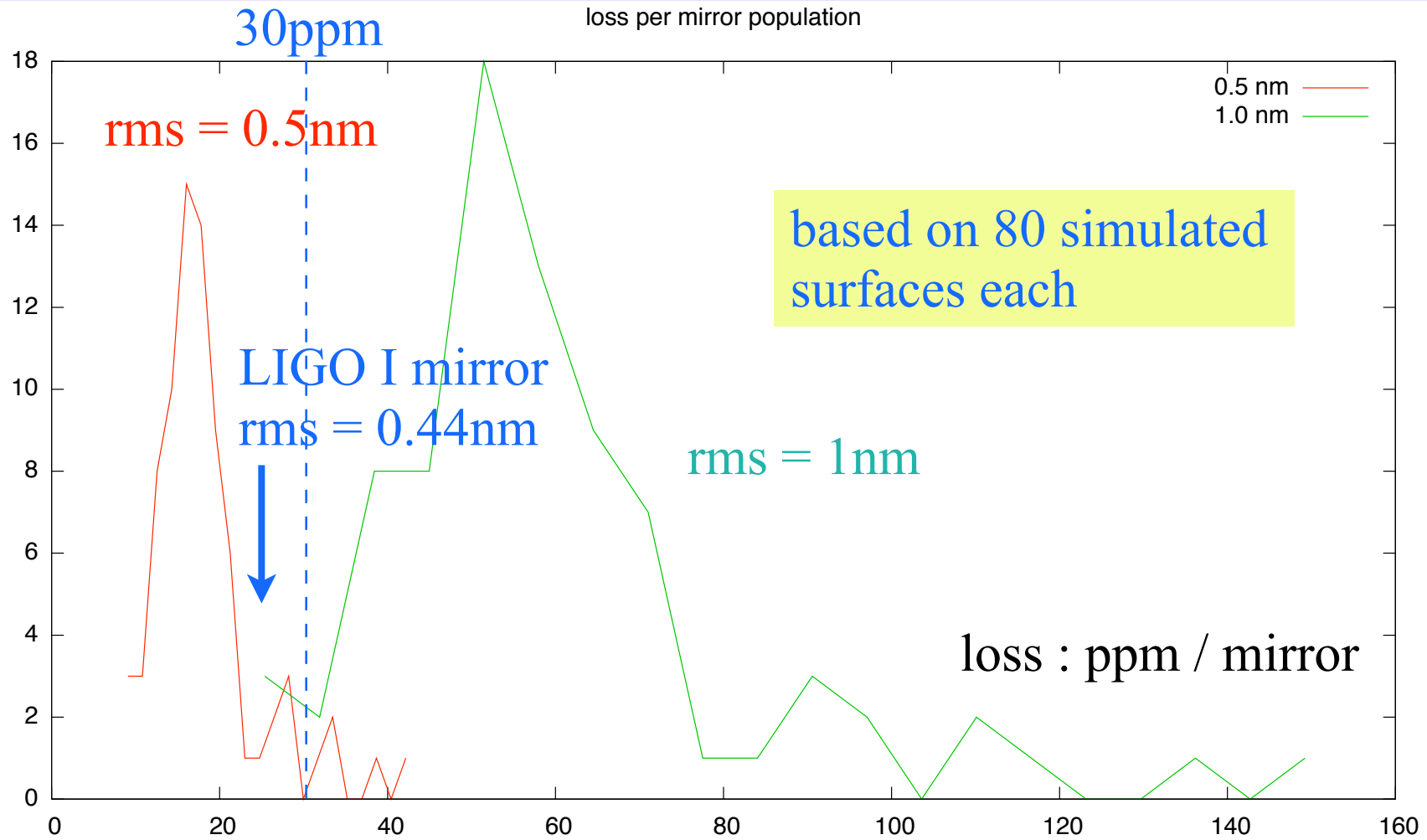

# loss per mirror with different FFT bin size or loss from different frequency

Loss calculated using a bin size : assume no loss with spatial frequency longer than 1/bin size

loss(1/bin2) - loss(1/bin1)
= loss coming spatial freq between 1/bin2 - 1/bin1

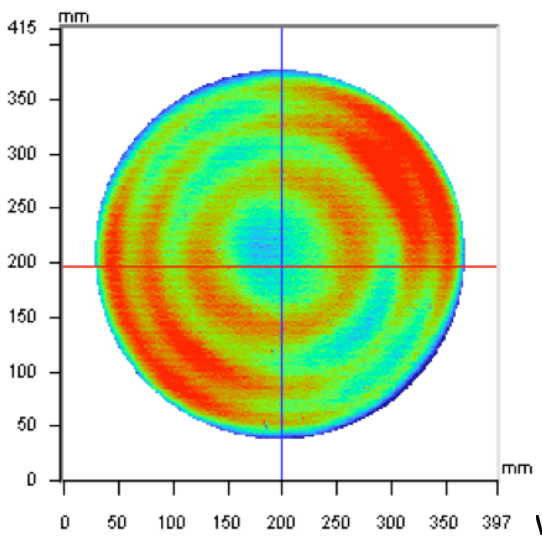


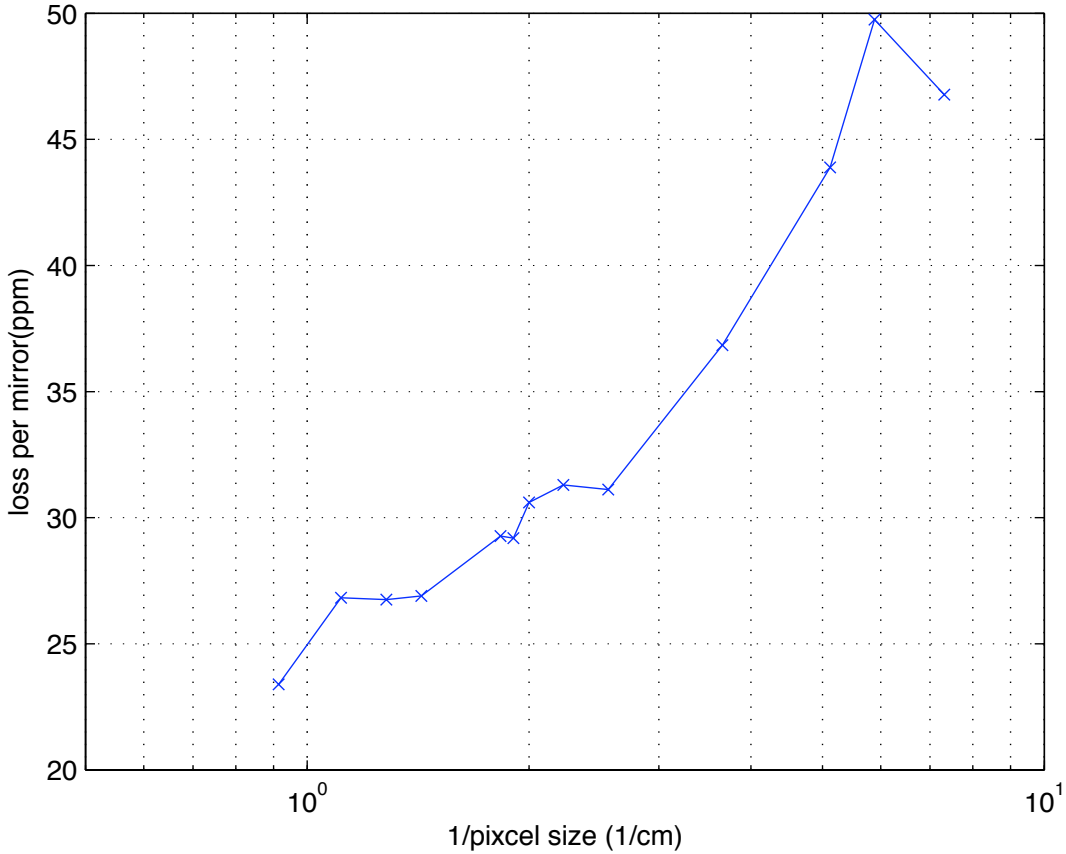


w FFT for advLIGO - Optics mtg @ CIT in Nov06

# Which part of the mirror contribute

loss per mirror in ppm when the central region is suppressed by 0.5

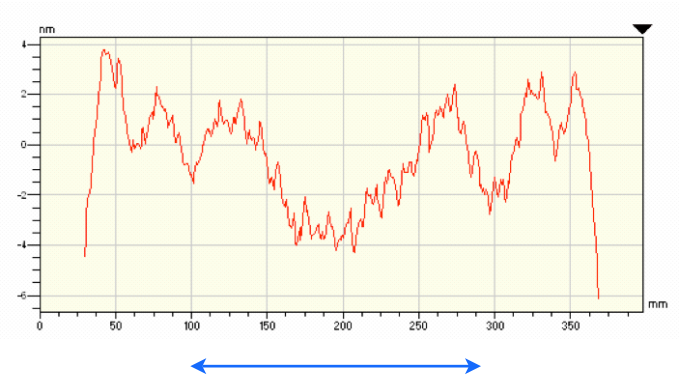


scale by 0.5

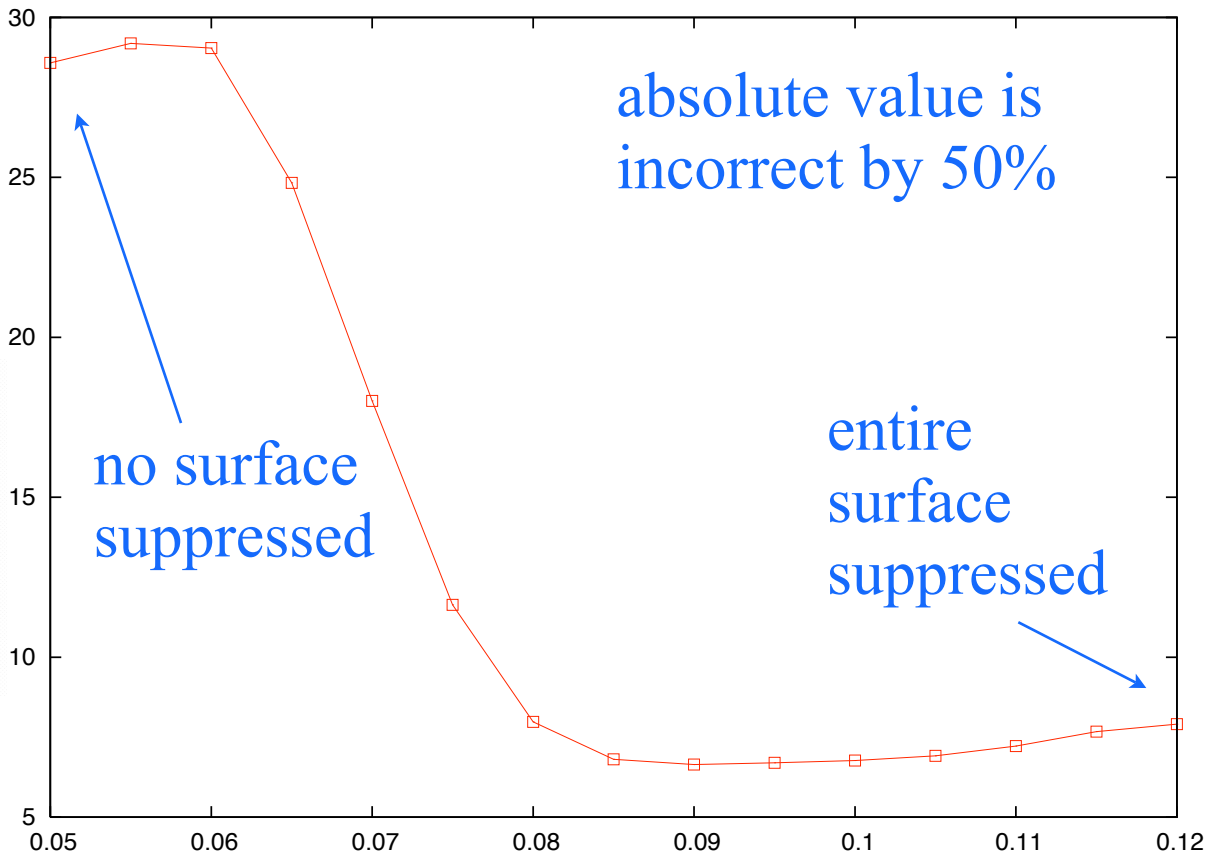

# Marginally stable vs stable recycling cavities

P Fritschel, 9 Nov 2006

# Motivation for stable design

- Greater tolerance to distortions in the recycling cavity
  - Higher order modes not (near)-resonant in the RC
  - Advantage for RF sidebands in the PRC/SRC, and for the GW sidebands in the SRC
- For GW sidebands, does it give a greater tolerance to ITM ROC errors?
  - Common ROC errors: equivalent to the above point
  - Differential ?

# Additional advantages of a stable design

- Simpler handling of RC pick-off beams
  - Pick-off is the leakage through the ‘middle’ RC optic, where the beam is a few mm radius
  - No large beam reducing telescope, only beam dumps
- Recycling mirrors are smaller optics
  - Input mode cleaner optic and suspension
  -

# Disadvantages of a stable design

- Parametric instabilities: does it ‘bottle up’ the higher order modes?
- Alignment sensing: ditto
- Suspensions
  - More intra-cavity optics needing good isolation

# How to choose?

- Distortion comparison: FFT analysis needed to substantiate and quantify
- PI comparison: ditto
- Alignment sensing comparison
- Implementation comparison
  - Layout issues
  - Suspensions
  - Cost

# Stable Recycling Cavities in Advanced LIGO

## LIGO-G060458-00-Z

Muzammil Arain, Guido Mueller

## LSC Meeting
## August 2006

# SRC

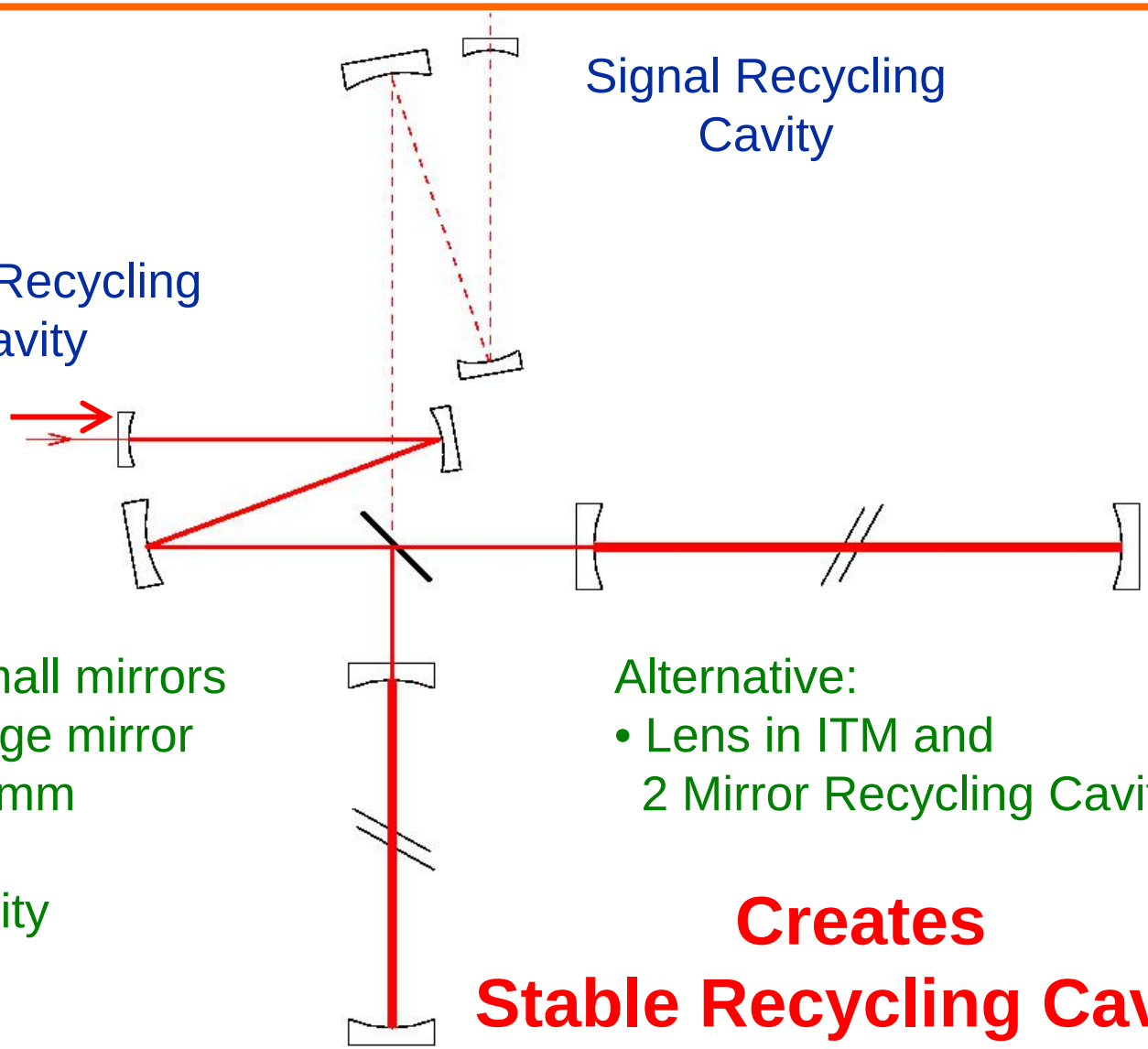


Design adds:

- 2 additional small mirrors
- Removes 1 large mirror
- Beam size > 2mm

Same for SR-Cavity

Alternative:

- Lens in ITM and 2 Mirror Recycling Cavity

**Creates Stable Recycling Cavity**

# SRC

**Current Baseline:**

- **Transversal Mode spacing < FWHM of recycling cavities**

**→ Higher order modes have similar resonance frequencies**

**→ Increased scatter into higher order modes (increased losses)**

**SRC:**

- **Transversal Mode spacing >> FWHM of recycling cavities**

**→ Higher order modes have different resonance frequency**

**→ Suppressed scatter into higher order modes (lower losses)**

**Great! Or?**

# SRC

## Signal Losses:

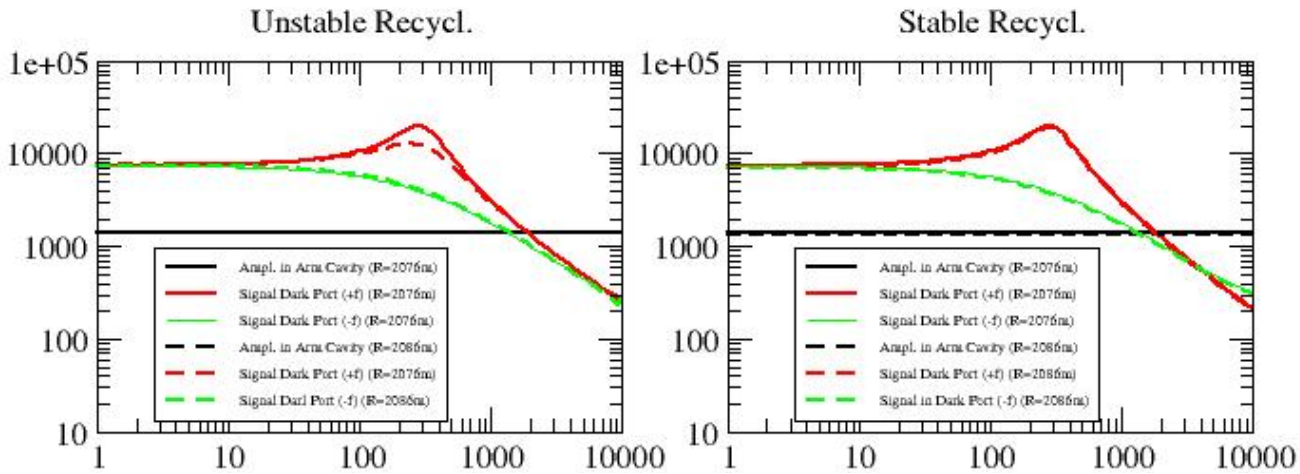


Finesse Results:

- Changed Cavity ROC from 2076m (Optimal) to 2086m
- Confirm signal loss at peak sensitivity
- See also Yi Pan talks on earlier meetings
- Caveat: Thermal Noise dominates in that frequency range. → Signal loss not real

# SRC

## Sideband Losses:

- PM-sidebands scatter into higher order modes in power and combined power-signal recycling cavity → Loss. If higher order modes are
  - resonant → Loss is resonantly enhanced
  - non-resonant → Loss is suppressed
- Effect depends also on:
  - Scatter matrix (Thermal deformation is difficult to predict)
  - Transversal mode spacing between modes (higher is better)

# SRC

## Other areas:

- **Mode matching**
  - » **Carrier between recycling cavities and arms:**
    **HOMs anti-resonant in baseline design**
    **(minor Disadvantage)**
  - » **Stabilizes Sideband spatial mode**
    **→ Improves mode matching with carrier (Advantage)**
    **(double counting: loss)**
- **Parametric Instabilities**
  - » **Under Investigation**

# SRC

## Alignment Sensing:

### Sensing matrix (Amplitude of 10-mode/1e-10 rad)

| AP:$TEM_{10}$ | Unstable | Stable |
|---|---|---|
| ΔITM | 1.8e-2 | 1.1e-3 |
| ΔETM | 1.9e-2 | 1.2e-3 |

| SP:$TEM_{10}$ | Unstable | Stable |
|---|---|---|
| CITM | 5.7e-4 | 8.8e-4 |
| CETM | 6.1e-4 | 9.3e-4 |

- Loose one order of mag in differential alignment signals
  - 10-mode resonant in unstable SR-cavity (near RSE)
- Gain 30% in common alignment signals (Factor 1.5-1.6)
  - 10-mode anti-resonant in unstable PR-cavity
- Gouy-phase difference between ETM and ITM modes: ~$10^0$ in both cases
  - would increase to $16^0$ for 5 cm beam size (16% drop of peak sensitivity)

# SRC

## Alignment Sensing:

**WFS-Signals @ 180MHz**
**Stable Recycling Cavity**

| | WFS1 | | WFS2 | |
|---|---|---|---|---|
| | I | Q | I | Q |
| ΔITM | 1 | -0.01 | 1 | -0.06 |
| ΔETM | 1.1 | -0.08 | 0.79 | 0.22 |
| CITM | 1 | -0.01 | 1 | -0.01 |
| CETM | 1.1 | 0.4 | 0.71 | -0.86 |

# SRC

## Alignment Sensing:

**WFS-Signals @ 180MHz**
**Unstable Recycling Cavity**

| | WFS1 | | WFS2 | |
|---|---|---|---|---|
| | I | Q | I | Q |
| ΔITM | 1 | 0.07 | 1 | 0.02 |
| ΔETM | 1.32 | 0.35 | 1 | 0.05 |
| CITM | 1 | 0 | 1 | 0 |
| CETM | 0.06 | 0.07 | 0 | 0.03 |

CITM: signal generated by 180MHz SB, resonant in PR cavity
→ Dominates the signals

# SRC

## Alignment Sensing:

Mode mismatch degrades ASC signals significantly:

| ROC ITMX/ITMY | Unstab. ΔITM | Stable ΔITM | Unstab. CITM | Stable CITM |
|---|---|---|---|---|
| 2102/2102 | 1.3e-2 | 4.3e-4 | 4.4e-4 | 4.0e-4 |
| 2102/2076 | 4.2e-4 | 2.8e-5 | 9.8e-6 | 2.2e-5 |
| 2076/2076 | 1.8e-2 | 1.1e-3 | 5.7e-4 | 8.8e-4 |
| 2050/2076 | 3.1e-4 | 3.4e-5 | 1.6e-5 | 2.2e-5 |
| 2050/2050 | 1.5e-2 | 3.1e-4 | 7.9e-4 | 2.6e-4 |

- Used X-arm cavity eigenmode to calculate the matrix
- No feedback loops included

# SRC

## Pointing:

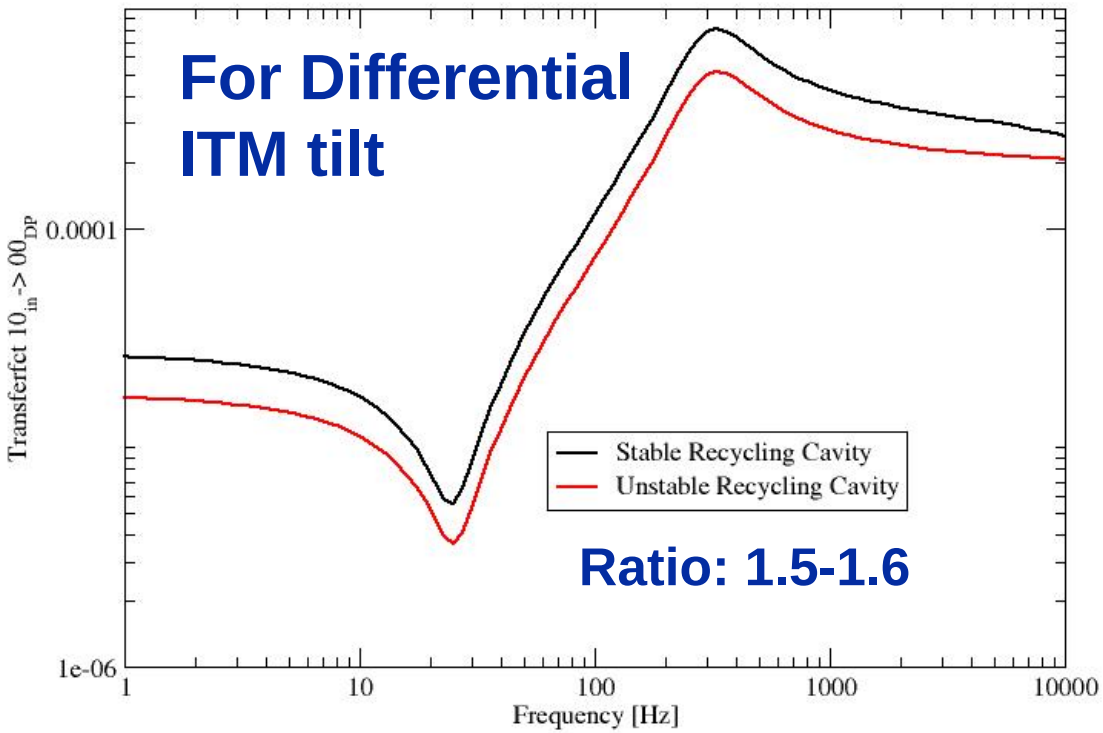


**Transferfunction 10-In → 00-Out.**

**Two critical tilts:**

- **Differential ITM**
  - **most sensitive**
  - **Unstable has slight advantage**
- **SR-mirror**
  - **most difficult to align**
  - **Stable is much better**

# SRC

## Pointing:

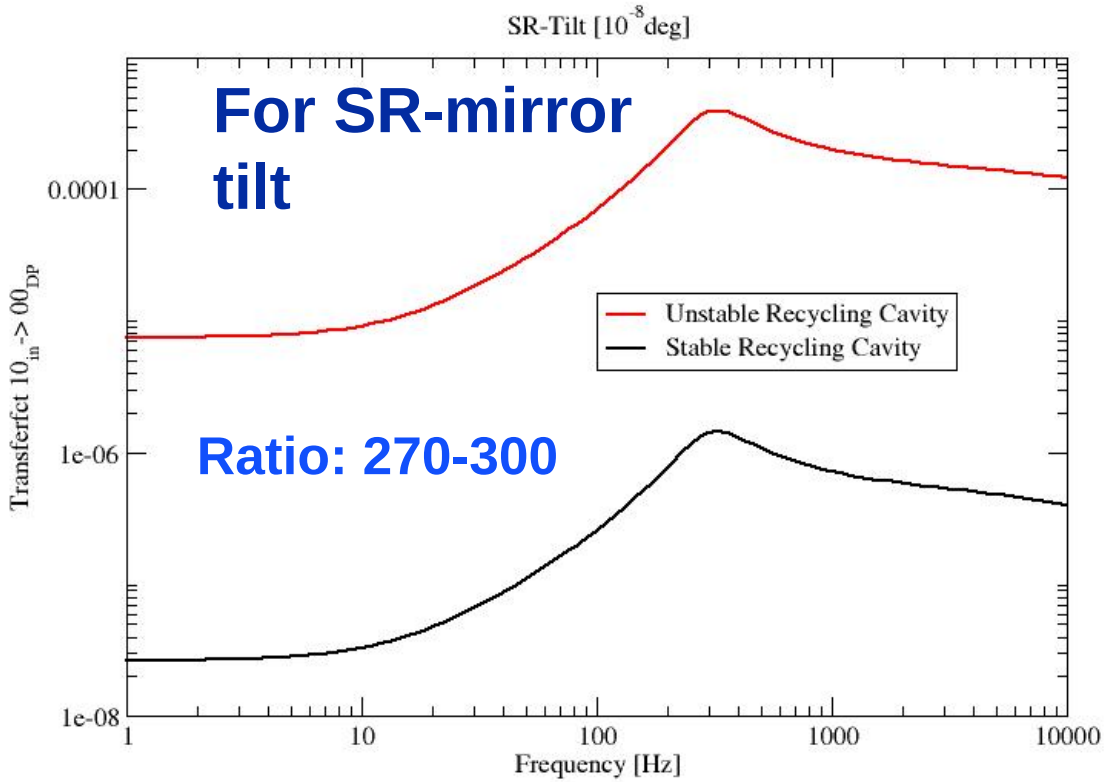


**Transferfunction 10-In → 00-Out.**

**Two critical tilts:**

- **Differential ITM**
  - **most sensitive**
  - **Unstable has slight advantage**
- **SR-mirror**
  - **hardest to align**
  - **Stable is much better**

# SRC

## Advantages/Disadvantages/Unknowns:

- Reduced Signal Loss (Advantage)
  - SR-Cavity (SR tuning)
- Reduced Sideband Loss (Advantage)
  - 9 MHz: PR-Cavity
  - 180 MHz: PR/SR-Cavity
- Mode matching
  - Carrier between recycling cavities and arms (?)
  - Between Carrier and Sidebands inside IFO (Advantage)
- Parametric Instabilities (?)

# SRC

## Advantages/Disadvantages/Unknowns:

- **Alignment Sensing**
  - » Differential ETM/ITM tilt signals are nearly resonant in unstable SR-cavity
  - → Increased Alignment signal in unstable recycling cavity by ~ order of mag in baseline design
  - → But better decoupling of common ITM and ETM alignment signals

- **Pointing Sensitivity (Advantage?)**
  - » Differential ITM tilt requirements about 30% increased in stable recycling cavities
  - » SR-tilt requirements reduced by ~factor 300 in stable recycling cavity (TBC).

**Of Course: Many of these effects or distortions depend on the thermal deformation and the performance of the TCS!**

LIGO

# Time Domain Issues in Parametric Instability

Dave Ottaway

Adv. LIGO Optics Meeting

Caltech

November ‘06

# Starting Evolution of PI

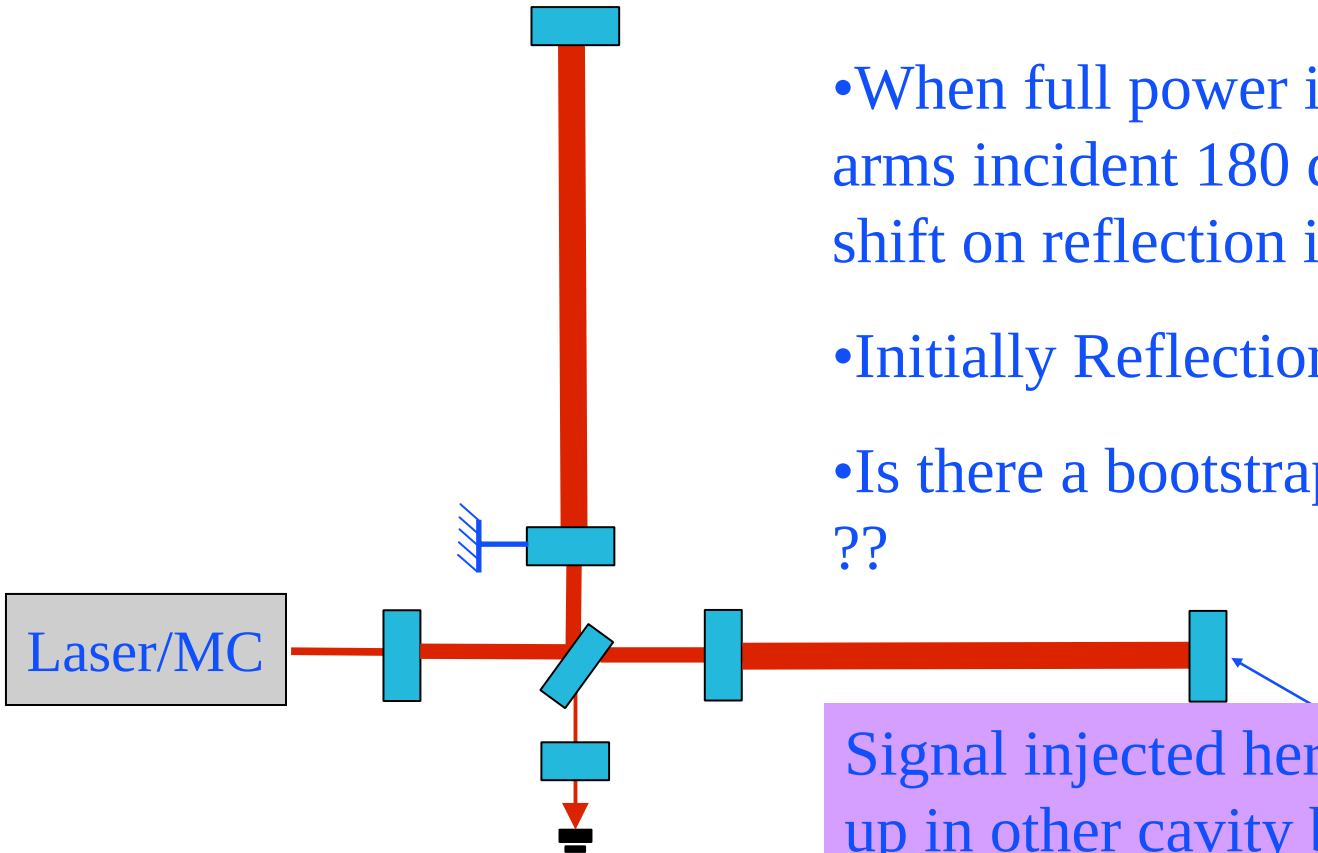


- Arm cavities are over coupled
- When full power is stored in arms incident 180 degree phase shift on reflection is observed
- Initially Reflection in Phase
- Is there a bootstrapping issue ??

Signal injected here, needs to build up in other cavity before full phase shifts are realized

# Time Evolution of Signal Incident on Single Cavity

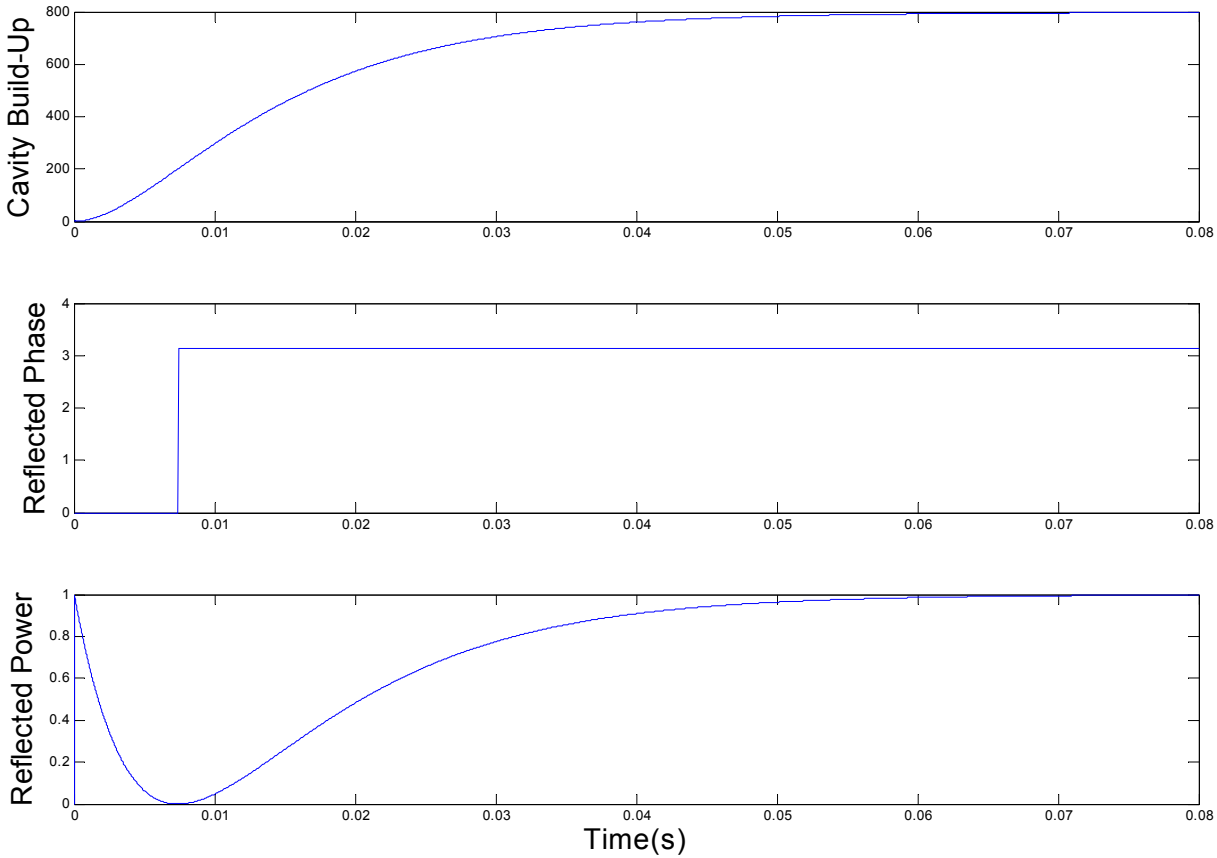

LIGO

# The Model

$E_{BS\_ITMX}(t_n) = E_{PRM\_BS}(t_{n-1})*j*t_{bs}*\exp(j*\Phi_l) + E_{SRM\_BS}*r_{bs}*\exp(j*\Phi_{l\_srm})$

$E_{BS\_ITMY}(t_n) = E_{PRM\_BS}(t_{n-1})*r_{bs}*\exp(j*\Phi_l) + E_{SRM\_BS}(t_{n-1})*j*t_{bs}*\exp(j*\Phi_{l\_srm})$

$E_{BS\_AS}(t_n) = E_{ITMY\_BS}(t_n)*j*t_{bs}*\exp(j*\Phi_{ly}) + E_{ITMY\_BS}(t_{n-1})*r_{bs}*\exp(j*\Phi_{lx})$

$E_{BS\_RM}(t_n) = E_{ITMX\_BS}(t_{n-1})*j*t_{bs}*\exp(j*\Phi_{lx}) + E_{ITMY\_BS}(t_{n-1})*r_{bs}*\exp(j*\Phi_{ly})$

$E_{ITMX\_ETMX}(t_n) = E_{BS\_ITMX}(t_{n-1})*j*t_{itmx}*\exp(j*\Phi_{lx}) + E_{ETMX\_ITMX}(t_{n-2})*r_{itmx}*\exp(j*\Phi_{Lx})$

$E_{ITMX\_BS}(t_n) = E_{BS\_ITMX}(t_{n-1})*ri_{tmx}*\exp(j*\Phi_{lx}) + E_{ETMX\_ITMX}(t_{n-2})*j*t_{itmx}*\exp(j*\Phi_{Lx})$

$E_{ITMY\_BS}(t_n) = E_{BS\_ITMY}(t_{n-1})*j*t_{itmy}*\exp(j*\Phi_{ly}) + E_{ETMY\_ITMY}(t_{n-2})*r_{itmy}*\exp(j*\Phi_{Ly})$

$E_{ITMY\_BS}(t_n) = E_{BS\_ITMY}(t_{n-1})*r_{itmy}*\exp(j*\Phi_{ly}) + E_{ETMY\_ITMY}(t_{n-2})*j*t_{itmy}*\exp(j*\Phi_{Ly})$

$E_{ETMX\_ITMX}(t_n) = E_{ITMX\_ETMX}(t_{n-2})*r_{etmx}*\exp(j*\Phi_{Lx}) + j*t_{etmx}*E_{ETMX\_IN}$

$E_{ETMY\_ITMY}(t_n) = E_{ITMY\_ETMY}(t_{n-2})*r_{etmy}*\exp(j*\Phi_{Ly}) + j*t_{etmy}*E_{ETMY\_IN}$

$E_{PRM\_BS}(t_n) = E_{BS\_RM}(t_{n-1})*r_{rm}*\exp(j*\Phi_l) + E_{IN}*j*t_{rm}$

$E_{PRM\_IN}(t_n) = E_{BS\_RM}(t_{n-1})* *j*t_{rm}*\exp(j*\Phi_l) + E_{IN}*r_{rm}$

$E_{SRM\_BS}(t_n) = E_{BS\_SRM}(t_{n-1})* *r_{srm}*\exp(j*\Phi_{l\_srm}) + E_{AS\_IN}*j*t_{srm}$

$E_{SRM\_AS}(t_n) = E_{BS\_SRM}(t_{n-1})* j*t_{srm}*\exp(j*\Phi_{l\_srm}) + E_{AS\_IN}*r_{srm}$

Evaluate the fields every cavity ½ round trip time

# Example Results

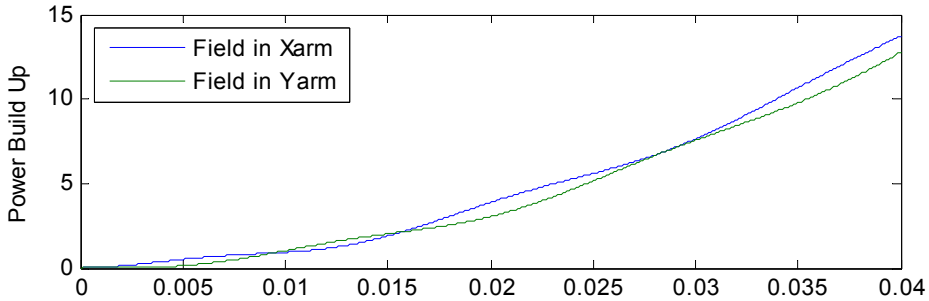


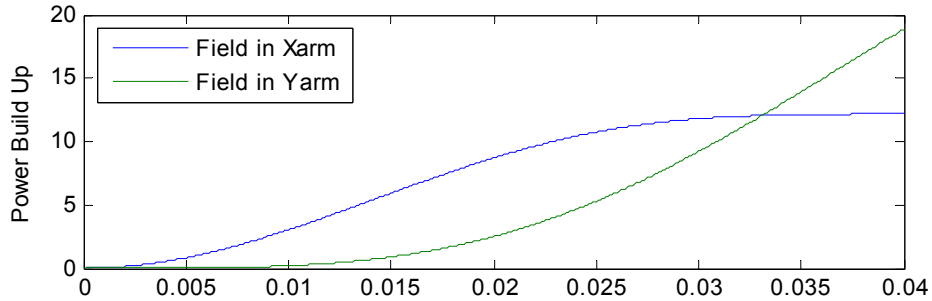


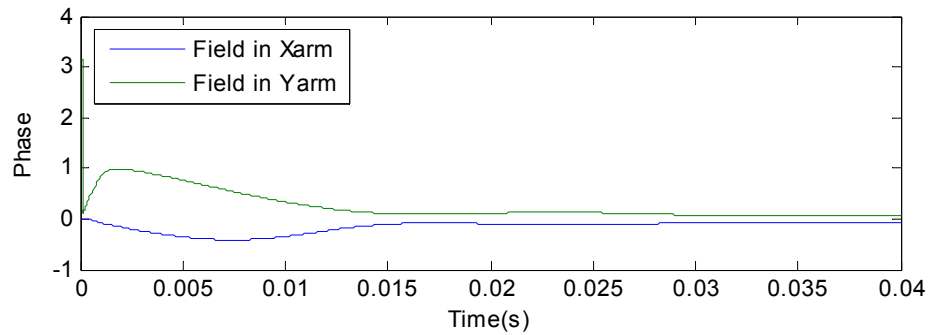


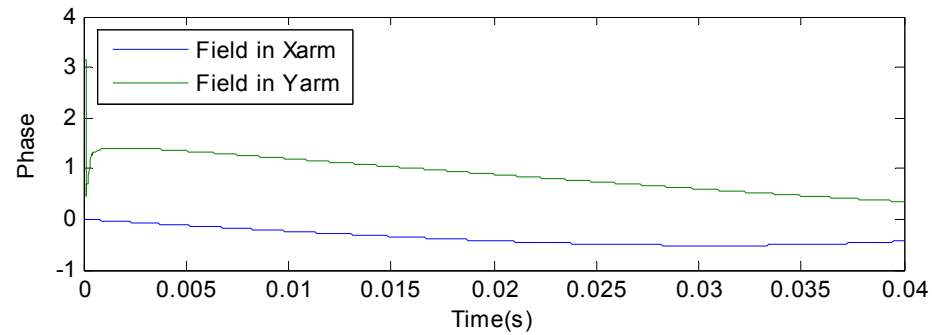


SRC Phases = 0.11 (left) and 4*0.11

Field injected in Xarm ETMX

LIGO

# Comments

- This work is preliminary
- Unlikely that this makes PI worse
- This model has not been fully probed
- The time dynamics of the mechanical modes need to be included

LIGO

# Recycling and Parametric Instability

Bill Kells

Caltech LIGO

# PI "*R*" calculation from entire cavity field

- Previous: model arm cavity field as discreet SHOs

$$R = \frac{4PQ_m}{mL{\omega_m}^2 c}\left(\sum_i \frac{Q_i^s \Lambda_i^s}{1+(\Delta\omega_i^s/\delta_i^s)^2} - \sum_j \frac{Q_j^{as}\Lambda_j^{as}}{1+(\Delta\omega_j^{as}/\delta_j^{as})^2}\right)$$

***Each*** acoustic {m}

***Braginsky, Vyatchanin***

- Cavity specific modes {j}, $Q_j$, $\Lambda_{jm}$ need accurate specification
  - » Proves difficult for modest order HTMs: high loss/distortion
  - » Is a significant "background" PI missed (K. Thorne; W. Kells: aS ~cancels S)?

- Now: build on FFT tool, ideally suited to net SS field from <<λ *static* distortions (acoustic surface amplitude from FEA)

$$R = \frac{4PQ_m}{m{\omega_m}^2 c}\left(\frac{V\int |E_0^s| Im(E_{bk}^s) u_z dA}{\int |E_0^s|^2 dA \int |\vec{u}|^2 dV} - \frac{V\int |E_0^{as}| Im(E_{bk}^{as}) u_z dA}{\int |E_0^{as}|^2 dA \int |\vec{u}|^2 dV}\right)$$

- Instead of SB(+/-$f_m$) modes: FFT cavity length shifted by $\pm\frac{\lambda}{2}\frac{f_m}{FSR}$ for proper Stokes (a-Stokes) simulation

# FFT "*R*" values: AdvLIGO arm

- Complete $R^{S}$-$R^{aS}$ for AdvLIGO arm
  - FEA generated {m}: $f_m$ to few %
  - No flats, ears, wedge
  - ~only 6 R>1
  - No anomalous background
  - All high R value correspond to known HTMs
  - Simple cases agree with analy & previous resu

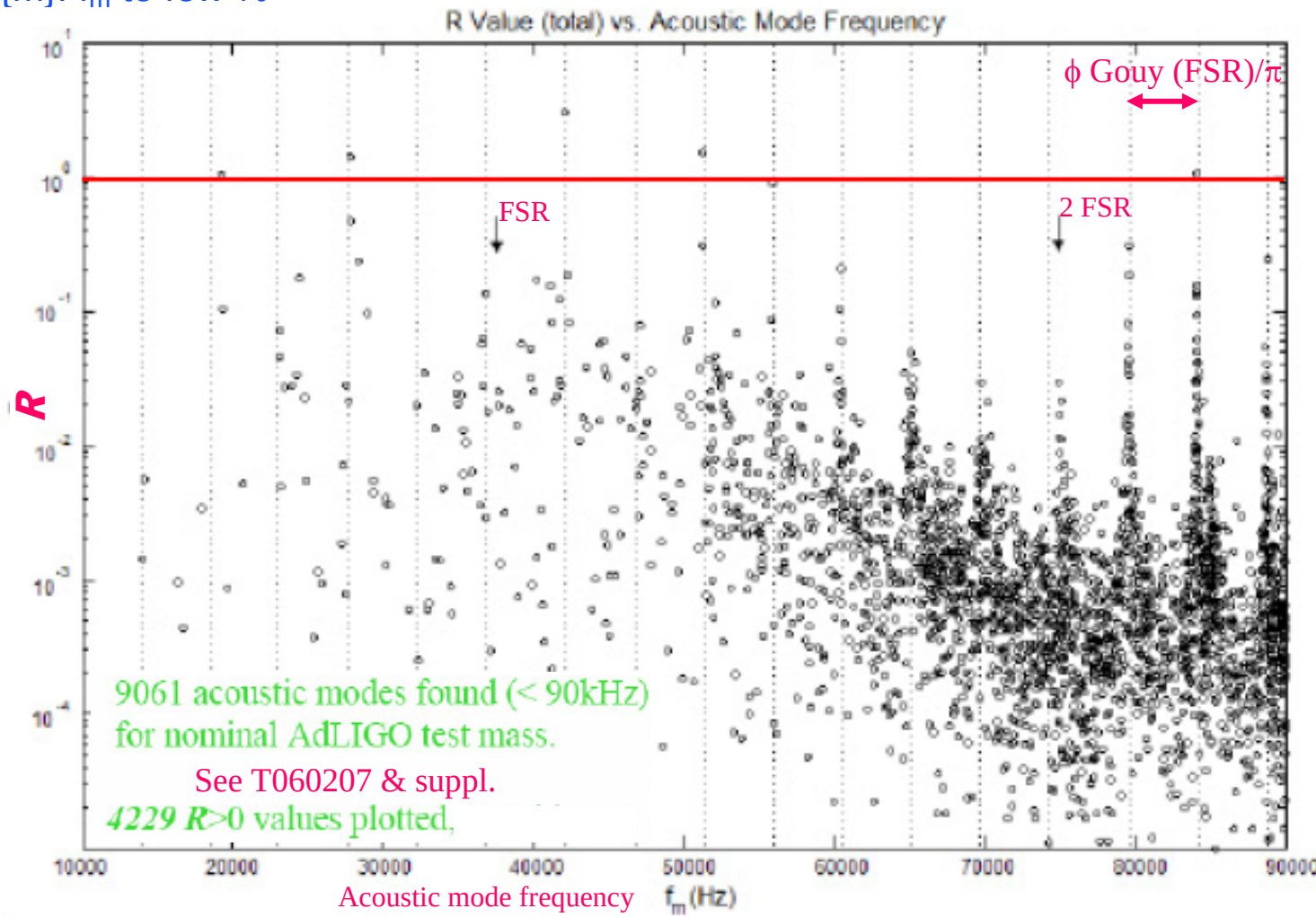

# Full Ifo: essential Features

- Single arm only
  - » PI gain strongly depends on $Q_m$ and $Q_j$
    - – For AdL this limits plausible {m} to $f_m$<90kHz, ~3-4000 Stokes dominated modes
    - – Above at least 6th order {j} cavity loss too high
    - – 1st order (tilt) and perhaps 2nd order (curvature) special (control possible).

⇨ Complete survey Via FFT simulation

- PRC only (AdL parameters)
  - » ~10x recycling enhancement of PI gain. However:
    - – This peaking is ~10x narrower (+/-2 Hz tune of PI mode from arm res.)
    - – Arms must have nearly same Gouy phase (Δ ROC <1-2m)
    - – No enhancement (over arm alone PI gain) for > 3d order Pi modes (too lossy)
- PRC + SRC (AdL parameters) T060159
  - » Same enhancement level (& widths) as PRC
  - » Significant “pulling” of peaks with SRC phasing (GW detuning + Gouy multiplet)
  - » Certain phases are dangerous: Δ ROC “protection” obviated

# Recycled tuning landscape

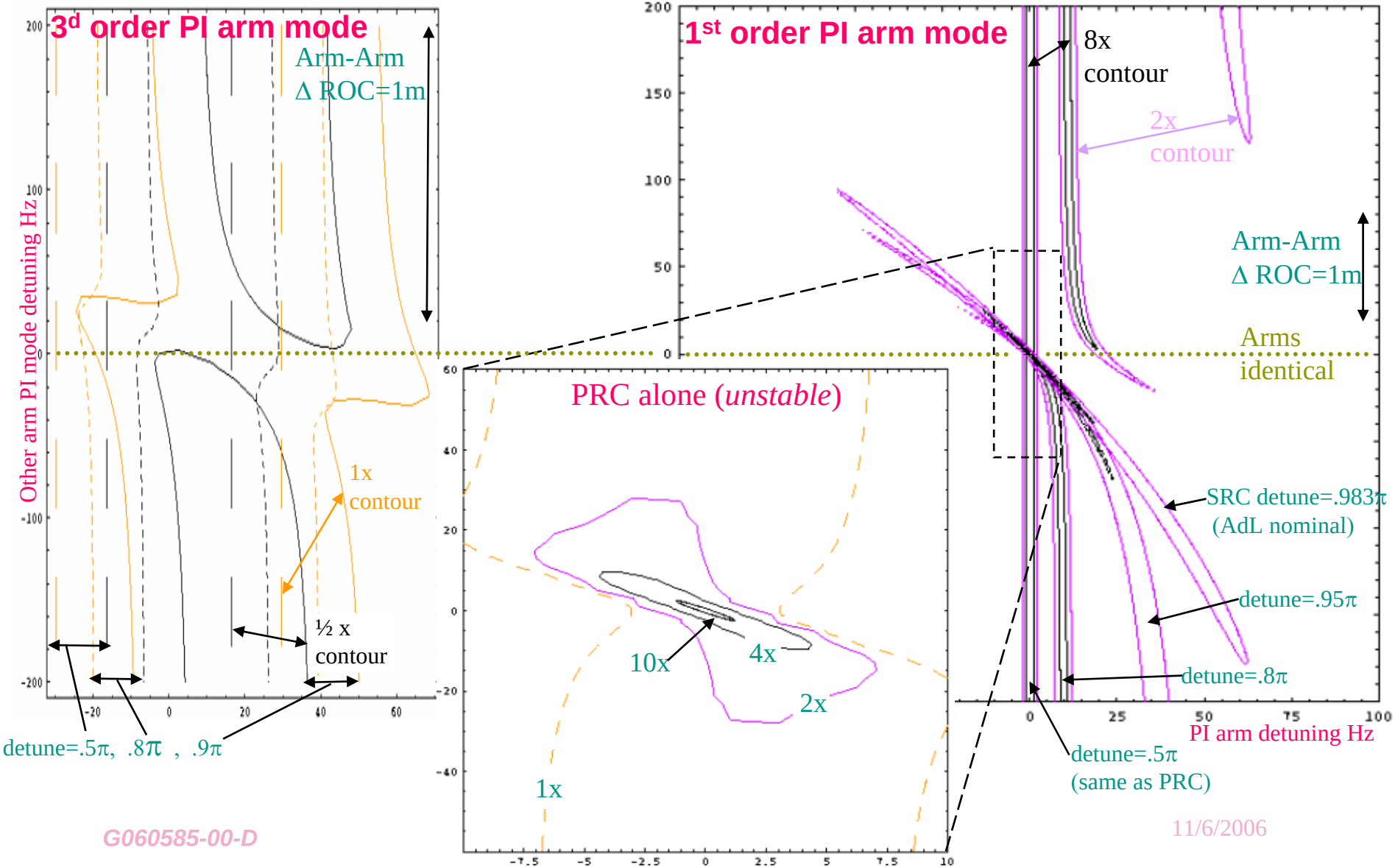

# PI gain widths !

- SRC increases enhancement ridge “area” in 2 arm tuning
- Large SRC Gouy phase range leaves ridge unavoidable for allowed ΔROC

- However, width of ridge is also critical !
  - » Likelyhood of “hitting” enhancement: ~(enhancement width)/FSR =4Hz/38kHz x ~6000/2 acoustic modes x 4 TM x 2-3 HTM = order 3 probable cases

- Already PRC reduces width factor 2

- SRC narrows further, so may actually be Advantageous if a very few exact resonances can be avoided (e.g. thermal tuning)

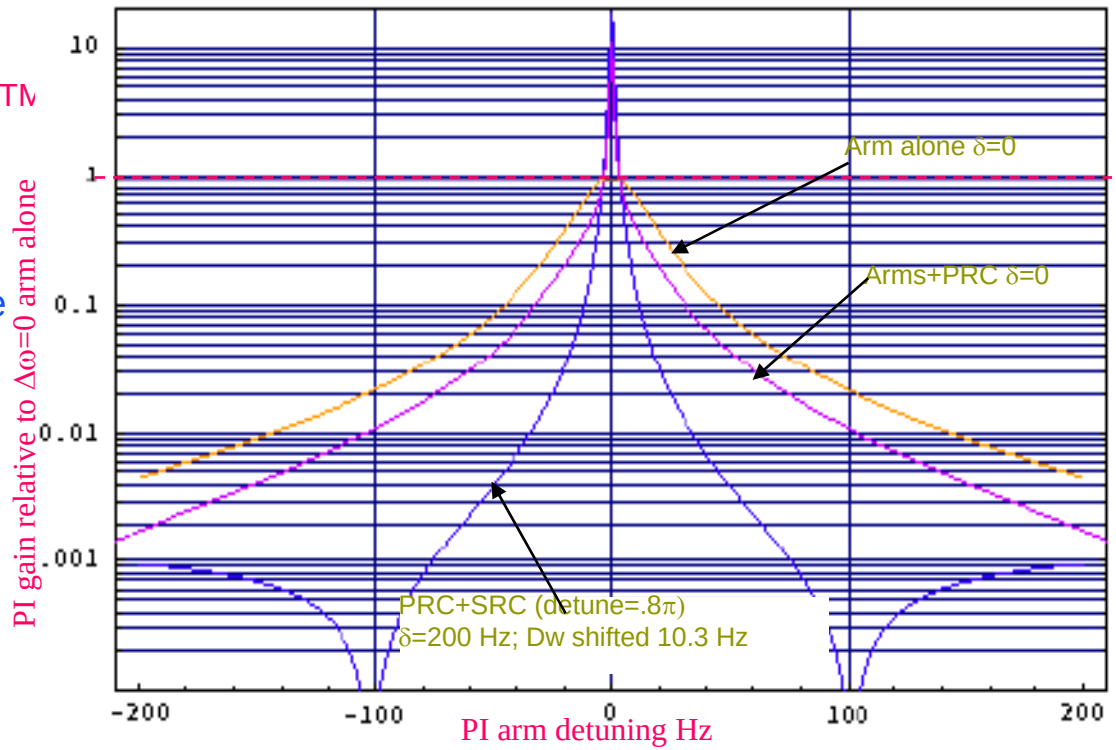

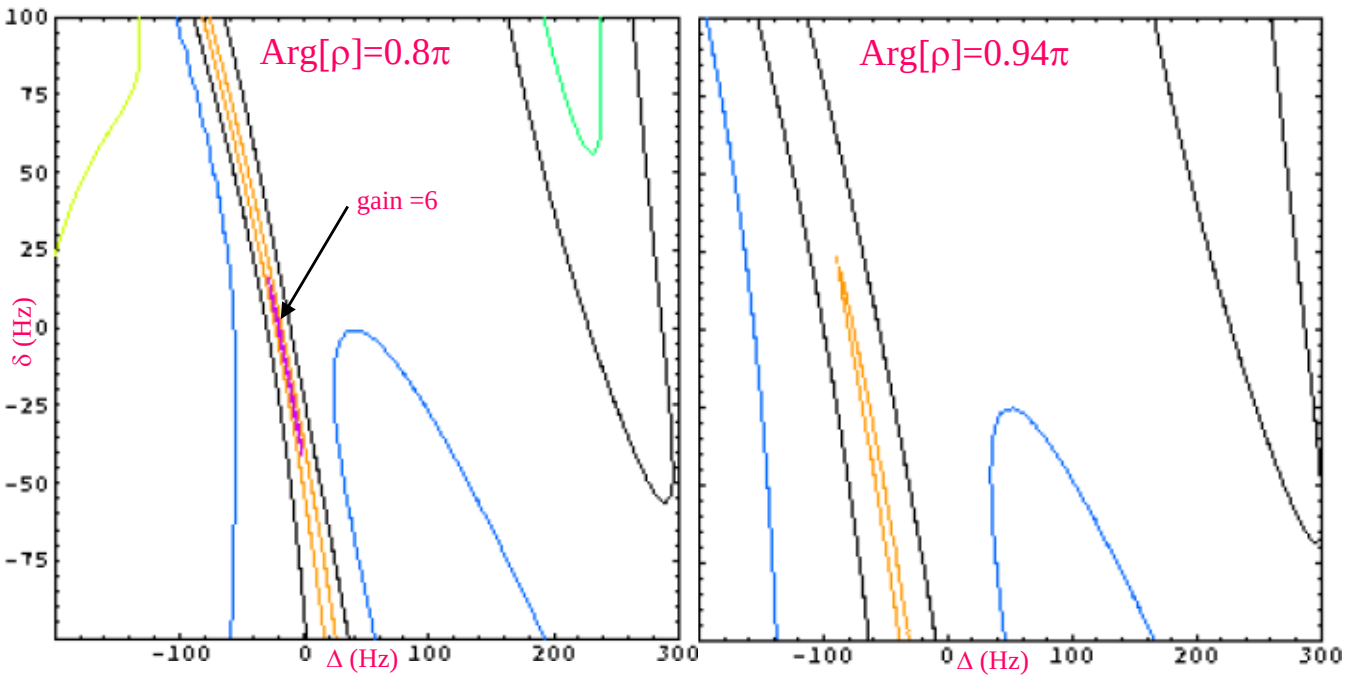
Arg[ρ]=0.8π
Arg[ρ]=0.94π
gain =6
δ (Hz)
Δ (Hz)
Δ (Hz)
100
75
50
25
0
-25
-50
-75
-100
0
100
200
300

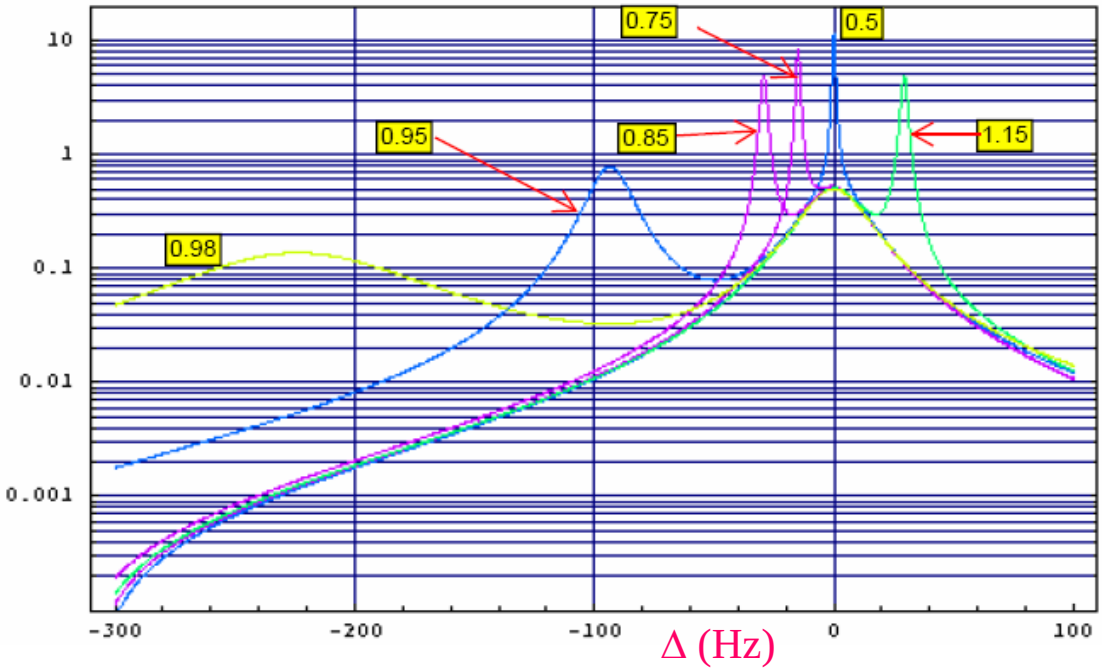
0.75
0.5
0.95
0.85
1.15
0.98
10
1
0.1
0.01
0.001
-300
-200
-100
0
100
Δ (Hz)

# Analysis of Parametric Oscillatory Instability in Signal Recycled LIGO Interferometer with Different Arms

S. E. Strigin and
S. P. Vyatchanin

Faculty of Physics, Moscow State University

Caltech, November 8, 2006

# Outline


1. Introduction
   - Effect of Parametric Oscillatory Instability
   - Account of anti-Stokes Mode
   - Proposed “cures” to avoid the parametric instability
   - PI in Signal Recycled Interferometer
   - Different Arms
2. Parametric Instability in SR Interferometer with Different Arms
   - Sygnal Recycled Interferometer
   - Normal modes
   - Identical mirrors
   - Elastically different mirrors
   - Elastic modes
3. Summary

# Outline


1. Introduction
   - Effect of Parametric Oscillatory Instability
   - Account of anti-Stokes Mode
   - Proposed “cures” to avoid the parametric instability
   - PI in Signal Recycled Interferometer
   - Different Arms
2. Parametric Instability in SR Interferometer with Different Arms
   - Sygnal Recycled Interferometer
   - Normal modes
   - Identical mirrors
   - Elastically different mirrors
   - Elastic modes
3. Summary

# Effect of Parametric Oscillatory Instability in FP Cavity

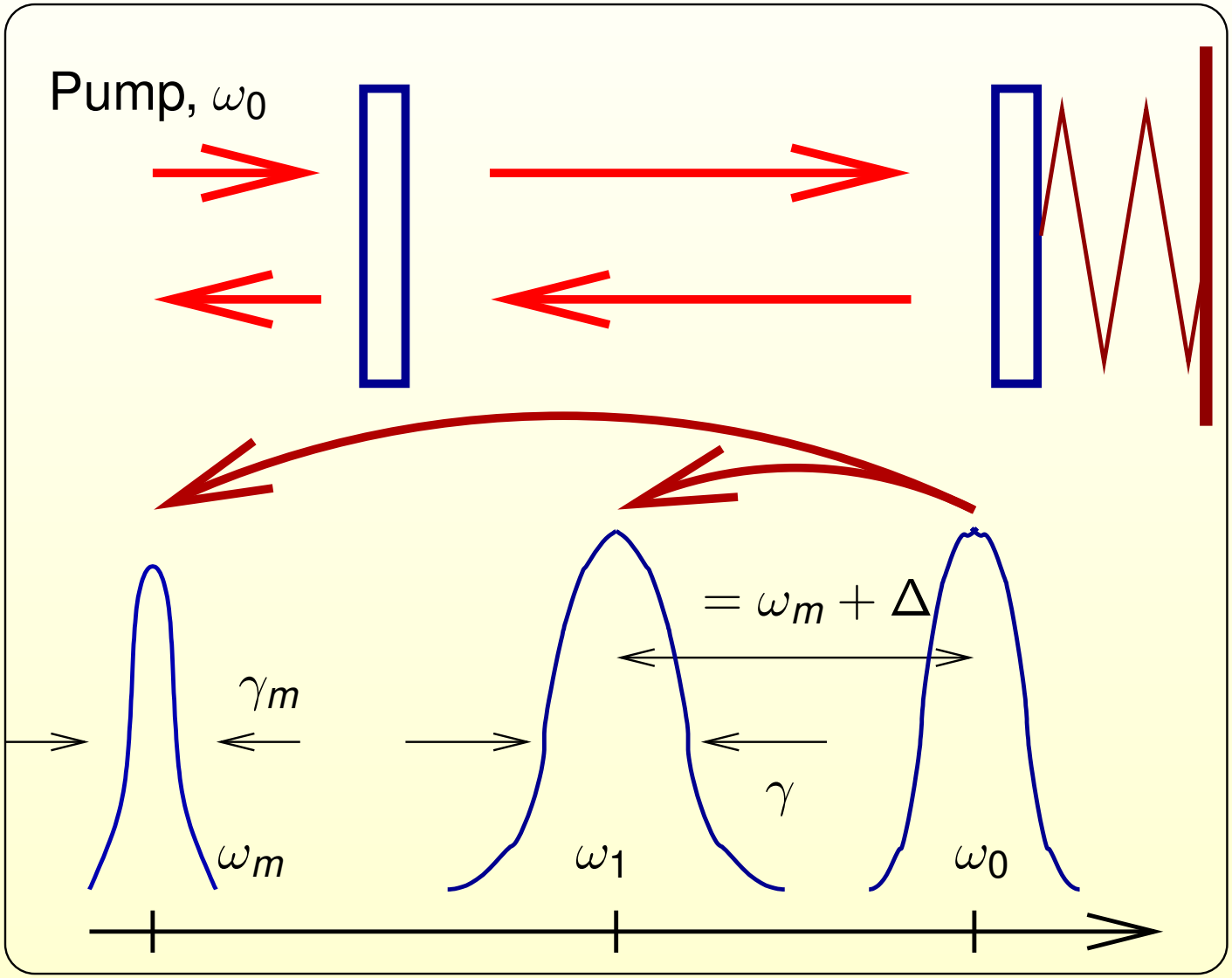

# Condition of Parametric Instability in FP Cavity:

## Qualitative consideration:

- Detuning $\Delta = \omega_0 - \omega_1 - \omega_m$ is small: $\Delta \ll \gamma$.
- We have $\gamma_m \ll \gamma$. Hence, flow of energy partially compensates dissipated power in elastic mode, i.e. efffective relaxation rate $\gamma_m^{\rm eff}$ decreases with pump increase.
- At the threshold value of pump power $W_c$: $\gamma_m^{\rm eff} = 0$.
- Condition of parametric instability[a]:

$$\frac{\mathcal{Q}\gamma}{\gamma_m(\gamma^2+\Delta^2)} > 1\,, \quad \mathcal{Q} \equiv \frac{\Lambda_1 W \omega_1}{cL\omega_m m}\,, \quad \gamma \gg \gamma_m.$$

- In approximation of given amplitude of main mode (i.e. unlimited pump): elastic oscillations amplitude and optical power in Stokes mode rise exponentially.

[a] V. B. Braginsky, S. E. Strigin, and S. P. Vyatchanin, *Physics Letters* **A287**, 331 (2001) [cond-mat/0107070].

# Condition of Parametric Instability in FP Cavity:

## Qualitative consideration:

- Detuning $\Delta = \omega_0 - \omega_1 - \omega_m$ is small: $\Delta \ll \gamma$.
- We have $\gamma_m \ll \gamma$. Hence, flow of energy partially compensates dissipated power in elastic mode, i.e. efffective relaxation rate $\gamma_m^{\text{eff}}$ decreases with pump increase.
- At the threshold value of pump power $W_c$: $\gamma_m^{\text{eff}} = 0$.
- Condition of parametric instability[a]:

$$\frac{\mathcal{Q}\gamma}{\gamma_m(\gamma^2 + \Delta^2)} > 1\,, \quad \mathcal{Q} \equiv \frac{\Lambda_1 W \omega_1}{cL\omega_m m}\,, \quad \gamma \gg \gamma_m.$$

- In approximation of given amplitude of main mode (i.e. unlimited pump): elastic oscillations amplitude and optical power in Stokes mode rise exponentially.

[a] V. B. Braginsky, S. E. Strigin, and S. P. Vyatchanin, *Physics Letters* **A287**, 331 (2001) [...]

# Condition of Parametric Instability in FP Cavity:

## Qualitative consideration:

- Detuning $\Delta = \omega_0 - \omega_1 - \omega_m$ is small: $\Delta \ll \gamma$.
- We have $\gamma_m \ll \gamma$. Hence, flow of energy partially compensates dissipated power in elastic mode, i.e. efffective relaxation rate $\gamma_m^{\rm eff}$ decreases with pump increase.
- At the threshold value of pump power $W_c$: $\gamma_m^{\rm eff} = 0$.
- Condition of parametric instability[a]:

$$\frac{\mathcal{Q}\gamma}{\gamma_m(\gamma^2+\Delta^2)} > 1\,, \quad \mathcal{Q} \equiv \frac{\Lambda_1 W \omega_1}{cL\omega_m m}\,, \quad \gamma \gg \gamma_m.$$

- In approximation of given amplitude of main mode (i.e. unlimited pump): elastic oscillations amplitude and optical power in Stokes mode rise exponentially.

[a] V. B. Braginsky, S. E. Strigin, and S. P. Vyatchanin, *Physics Letters* **A287**, 331 (2001) [illegible]

# Condition of Parametric Instability in FP Cavity:

## Qualitative consideration:

- Detuning $\Delta = \omega_0 - \omega_1 - \omega_m$ is small: $\Delta \ll \gamma$.
- We have $\gamma_m \ll \gamma$. Hence, flow of energy partially compensates dissipated power in elastic mode, i.e. efffective relaxation rate $\gamma_m^{\rm eff}$ decreases with pump increase.
- At the threshold value of pump power $W_c$: $\gamma_m^{\rm eff} = 0$.
- Condition of parametric instability[a]:

$$\frac{\mathcal{Q}\gamma}{\gamma_m(\gamma^2+\Delta^2)} > 1\,, \quad \mathcal{Q} \equiv \frac{\Lambda_1 W \omega_1}{cL\omega_m m}\,, \quad \gamma \gg \gamma_m.$$

- In approximation of given amplitude of main mode (i.e. unlimited pump): elastic oscillations amplitude and optical power in Stokes mode rise exponentially.

[a] V. B. Braginsky, S. E. Strigin, and S. P. Vyatchanin, *Physics Letters* **A287**, 331 (2001) [illegible]

# Parametric condition in FP Cavity (cont.)

**The more realistic approximation of given pump $P$.**

We can consider the parametric instabiility as phase transition of system consisted of three oscillators nonlineary coupled with each other.
Phase transition takes place when $W = W_c$.

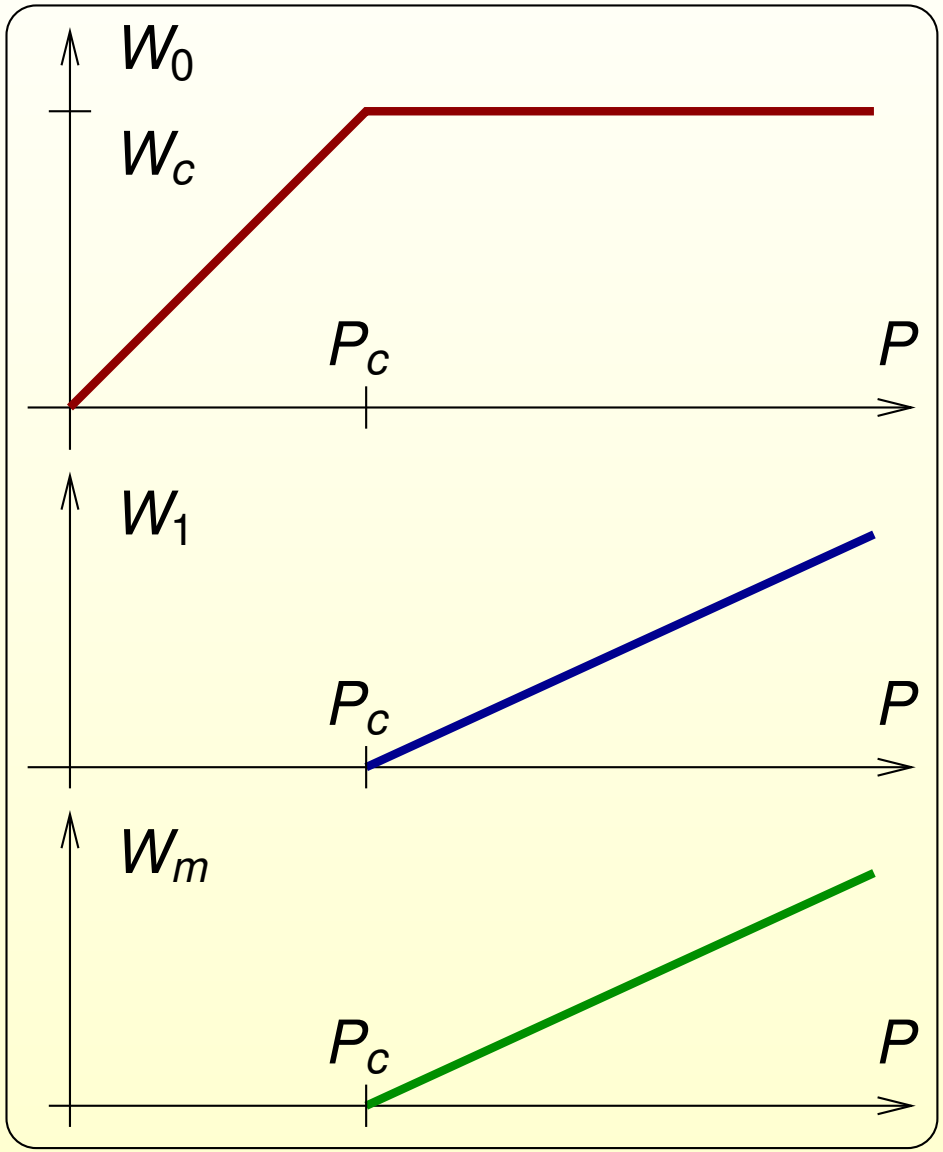

# Outline


1. Introduction
   - Effect of Parametric Oscillatory Instability
   - Account of anti-Stokes Mode
   - Proposed “cures” to avoid the parametric instability
   - PI in Signal Recycled Interferometer
   - Different Arms
2. Parametric Instability in SR Interferometer with Different Arms
   - Sygnal Recycled Interferometer
   - Normal modes
   - Identical mirrors
   - Elastically different mirrors
   - Elastic modes
3. Summary

# Anti-Stokes Mode

Existence of the anti-Stokes mode with frequency $\omega_{1\,a} = \omega_0 + \omega_m$ will substantially dump the effect of parametric instability[a]. However, the probability that suitable anti-Stokes mode exists is relatively small[b].

---

[a] E. D'Ambrosio and W. Kells, *Physics Letter* **A299**, 326 (2002). LIGO-T020008-00-D

[b] V. B. Braginsky, S. E. Strigin and S. P. Vyatchanin, *Physics Letters* **A305**, 111 (2002).

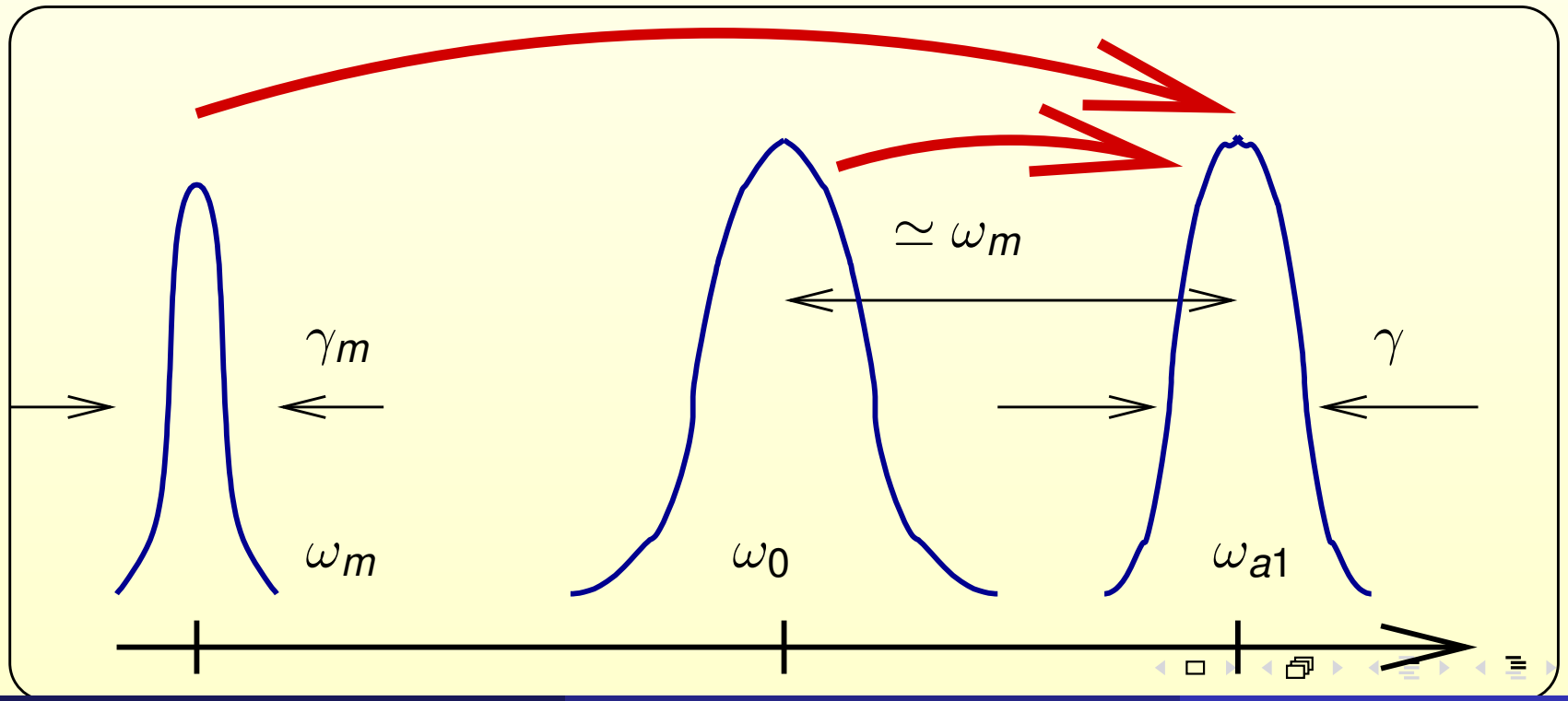

# Outline


1. Introduction
   - Effect of Parametric Oscillatory Instability
   - Account of anti-Stokes Mode
   - Proposed “cures” to avoid the parametric instability
   - PI in Signal Recycled Interferometer
   - Different Arms
2. Parametric Instability in SR Interferometer with Different Arms
   - Sygnal Recycled Interferometer
   - Normal modes
   - Identical mirrors
   - Elastically different mirrors
   - Elastic modes
3. Summary

## Proposed “cures” to avoid the parametric instability:

(i) to change the mirror shape[a];
(ii) to introduce low noise damping[b];
(iii) to heat the test masses in order to vary curvature radii of mirrors and hence to control detuning and decrease overlapping factor[c].

---

[a] V. B. Braginsky, S. E. Strigin and S. P. Vyatchanin, *Physics Letters* **A305**, 111 (2002).

[b] V. B. Braginsky and S. P. Vyatchanin, *Physics Letters* **A293**, 228 (2002).

[c] C. Zhao, L. Ju, J. Degallaix, S. Gras, and D. G. Blair, Phys. Rev. Lett. **94**, 121102 (2005).

# Outline


1. Introduction
   - Effect of Parametric Oscillatory Instability
   - Account of anti-Stokes Mode
   - Proposed “cures” to avoid the parametric instability
   - PI in Signal Recycled Interferometer
   - Different Arms
2. Parametric Instability in SR Interferometer with Different Arms
   - Sygnal Recycled Interferometer
   - Normal modes
   - Identical mirrors
   - Elastically different mirrors
   - Elastic modes
3. Summary

# Signal Recycled LIGO Interferometer

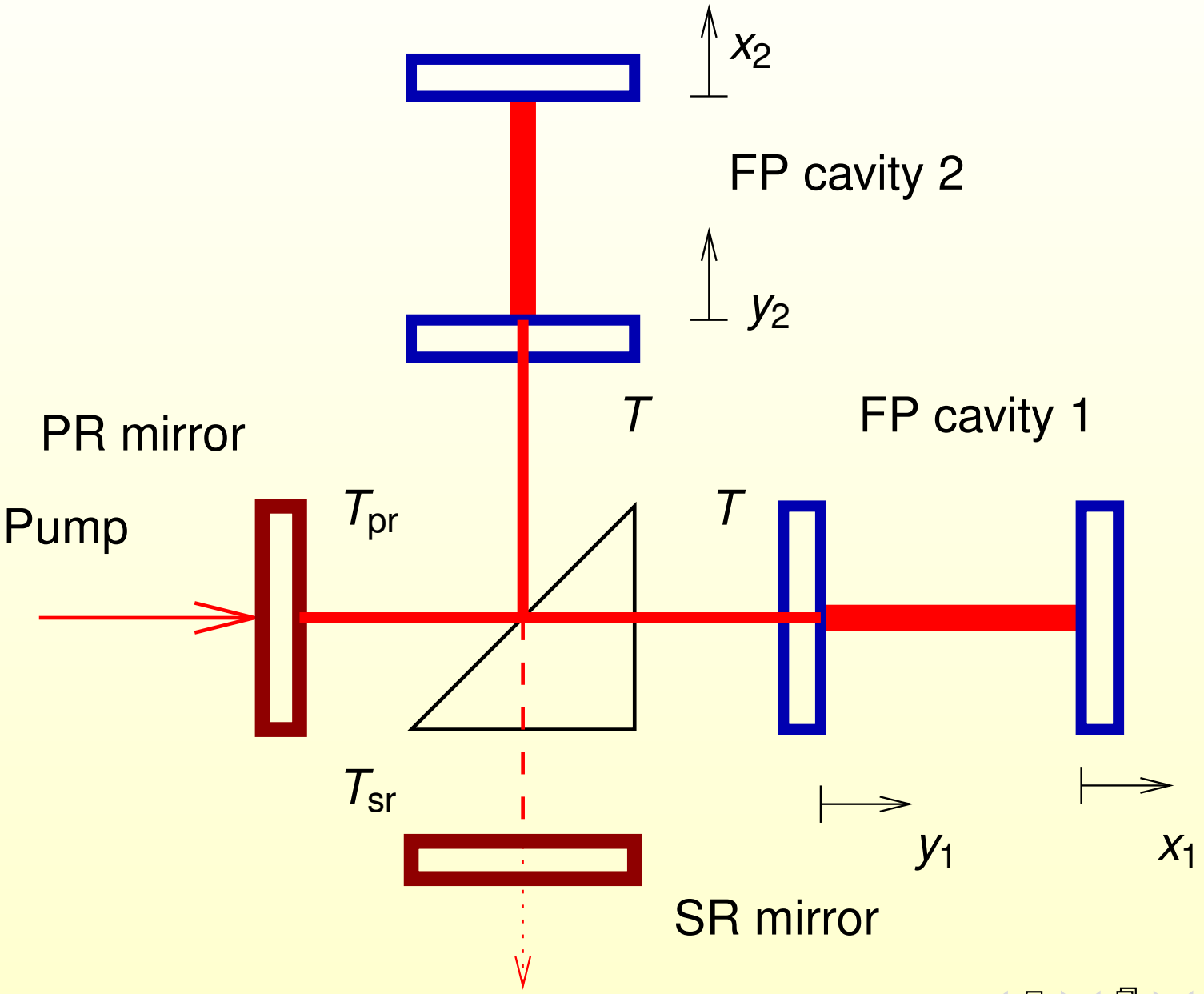

# Instability Condition in SR LIGO Interferometer

## There are two modes: symmetric and antisymmetric.

The symmetric mode is tuned in resonance and detuning $\delta$ of anti-symmetric depends on SR mirror's position. The relaxations rates of modes are $\gamma_{0+}$, $\gamma_{0-}$

## We have inequality: $\gamma_m \ll \gamma_{0+}$, $\gamma_{0-}$

$\gamma_m \simeq 10^{-3}\ \mathrm{s}^{-1}$, $\quad \gamma_{0+}, \gamma_{0=} \simeq 1 \ldots 10\ \mathrm{s}^{-1}$.

## Instability condition

See [a]

$$\frac{\mathcal{Q}}{2\gamma_m}\left(\frac{\gamma_{0+}}{\gamma_{0+}^2+\Delta^2}+\frac{\gamma_{0-}}{\gamma_{0-}^2+(\Delta+\delta)^2}\right)\geq 1\,, \quad \mathcal{Q}\equiv\frac{\Lambda_1 W\omega_1}{cL\omega_m m}\,. \qquad (1)$$

[a] A.G. Gurkovsky, S.E. Strigin, A. and S.P. Vyatchanin, arXive: gr-qc/0608007, accepted to *Physics Letters*.

# Instability Condition in SR LIGO Interferometer

## There are two modes: symmetric and antisymmetric.

The symmetric mode is tuned in resonance and detuning $\delta$ of anti-symmetric depends on SR mirror's position. The relaxations rates of modes are $\gamma_{0+},\ \gamma_{0-}$

## We have inequality: $\gamma_m \ll \gamma_{0+},\ \gamma_{0-}$

$\gamma_m \simeq 10^{-3}\ \mathrm{s}^{-1}, \quad \gamma_{0+}, \gamma_{0=} \simeq 1 \ldots 10\ \mathrm{s}^{-1}.$

## Instability condition

See [a]

$$\frac{\mathcal{Q}}{2\gamma_m}\left(\frac{\gamma_{0+}}{\gamma_{0+}^2+\Delta^2}+\frac{\gamma_{0-}}{\gamma_{0-}^2+(\Delta+\delta)^2}\right) \geq 1\,, \quad \mathcal{Q} \equiv \frac{\Lambda_1 W \omega_1}{cL\omega_m m}\,. \qquad (1)$$

[a] A.G. Gurkovsky, S.E. Strigin, A. and S.P. Vyatchanin, arXive: gr-qc/0608007, accepted to *Physics Letters*.

# Instability Condition in SR LIGO Interferometer

## There are two modes: symmetric and antisymmetric.

The symmetric mode is tuned in resonance and detuning $\delta$ of anti-symmetric depends on SR mirror's position. The relaxations rates of modes are $\gamma_{0+},\ \gamma_{0-}$

## We have inequality: $\gamma_m \ll \gamma_{0+},\ \gamma_{0-}$

$\gamma_m \simeq 10^{-3}\ \mathrm{s}^{-1}, \quad \gamma_{0+}, \gamma_{0=} \simeq 1 \ldots 10\ \mathrm{s}^{-1}.$

## Instability condition

See [a]

$$\frac{\mathcal{Q}}{2\gamma_m}\left(\frac{\gamma_{0+}}{\gamma_{0+}^2+\Delta^2}+\frac{\gamma_{0-}}{\gamma_{0-}^2+(\Delta+\delta)^2}\right)\geq 1\,, \quad \mathcal{Q}\equiv\frac{\Lambda_1 W\omega_1}{cL\omega_m m}\,. \qquad (1)$$

[a] A.G. Gurkovsky, S.E. Strigin, A. and S.P. Vyatchanin, arXive: gr-qc/0608007, accepted to *Physics Letters*.

# Outline


1. Introduction
   - Effect of Parametric Oscillatory Instability
   - Account of anti-Stokes Mode
   - Proposed “cures” to avoid the parametric instability
   - PI in Signal Recycled Interferometer
   - Different Arms
2. Parametric Instability in SR Interferometer with Different Arms
   - Sygnal Recycled Interferometer
   - Normal modes
   - Identical mirrors
   - Elastically different mirrors
   - Elastic modes
3. Summary

# W. Kells: the arms may be detuned (!)

## The frequencies of Hermite-Gauss modes in FP cavity

depends on with curvature radii $R_1, R_2$ of mirrors and cavity's length $L$ Main modes with indeces $m = n = 0$ are tuned in resonance and other modes differ. For Advanced LIGO parameters

$$R_{1,2} = 2\,076 \pm 3\ \mathrm{m}, \quad L = 4\ \mathrm{km},$$
$$\Delta f_{qmn} \simeq \pm(m+n+1)\,100\ \mathrm{Hz}\,.$$

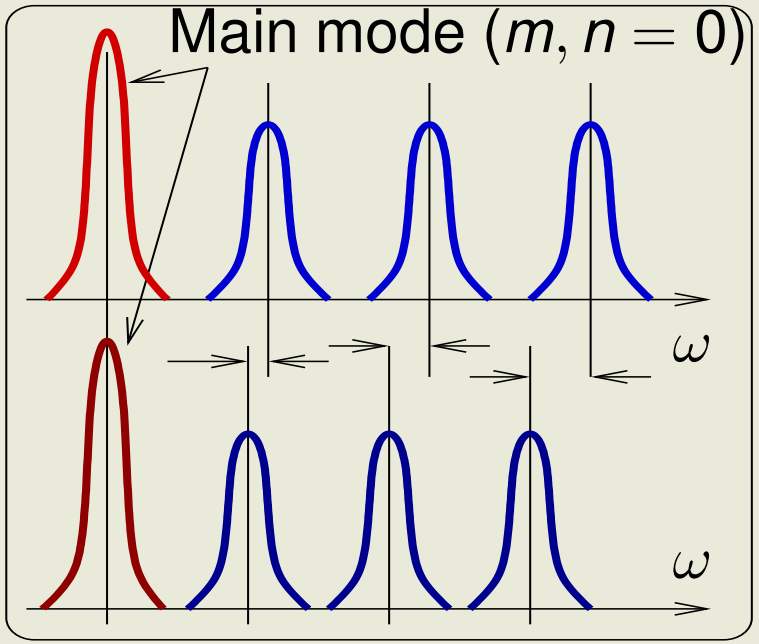


## It is large value!

Frequency range of Advanced LIGO: 50 . . . 500 Hz;
bandwidthes: $\gamma_{0+},\ \gamma_{0-} \simeq 1 \ldots 10\ \mathrm{sec}^{-1}$.
FP cavities in arms are not optically identical ones !.

# Outline


1. Introduction
   - Effect of Parametric Oscillatory Instability
   - Account of anti-Stokes Mode
   - Proposed “cures” to avoid the parametric instability
   - PI in Signal Recycled Interferometer
   - Different Arms
2. Parametric Instability in SR Interferometer with Different Arms
   - Sygnal Recycled Interferometer
   - Normal modes
   - Identical mirrors
   - Elastically different mirrors
   - Elastic modes
3. Summary

# Signal Recycled LIGO Interferometer

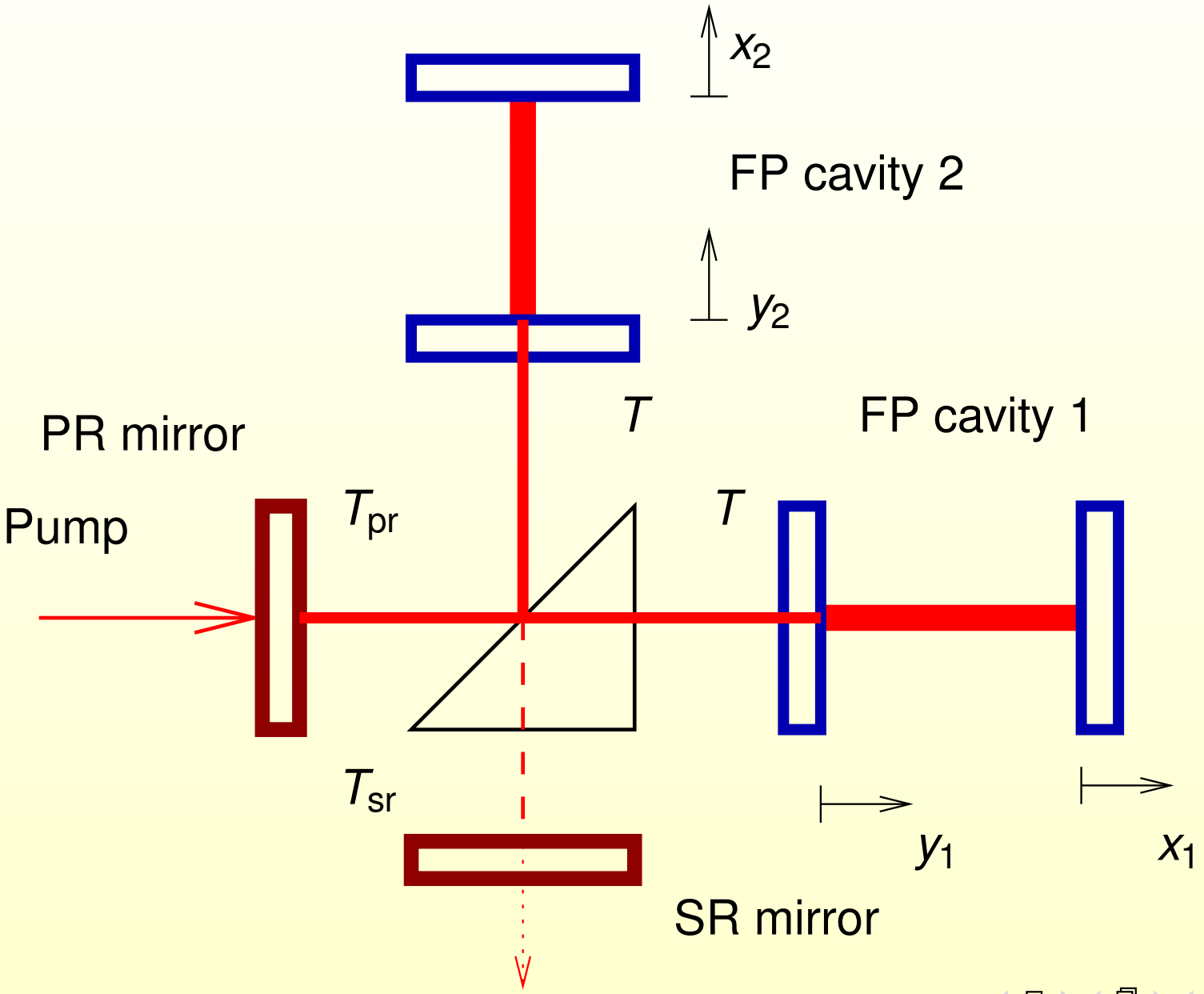

# Assumptions

## No losses, no noises

No optical losses in mirrors. No suspension noise in mirrors.

## Non-identical arms

Different frequences of the Stokes modes in FP cavities. Arms are tuned in resonance with the main mode. $\omega_s = (\omega_1 + \omega_2)/2$, $d = (\omega_1 - \omega_2)/2$.

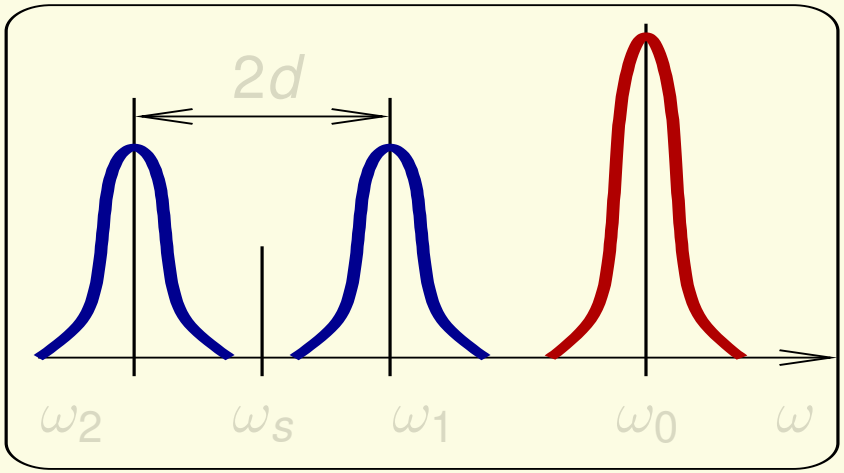


## Approximation of constant field

Optical power $W$ circulating inside the arms is a constant.

# Assumptions

## No losses, no noises

No optical losses in mirrors. No suspension noise in mirrors.

## Non-identical arms

Different frequences of the Stokes modes in FP cavities. Arms are tuned in resonance with the main mode. $\omega_s = (\omega_1 + \omega_2)/2$, $d = (\omega_1 - \omega_2)/2$.

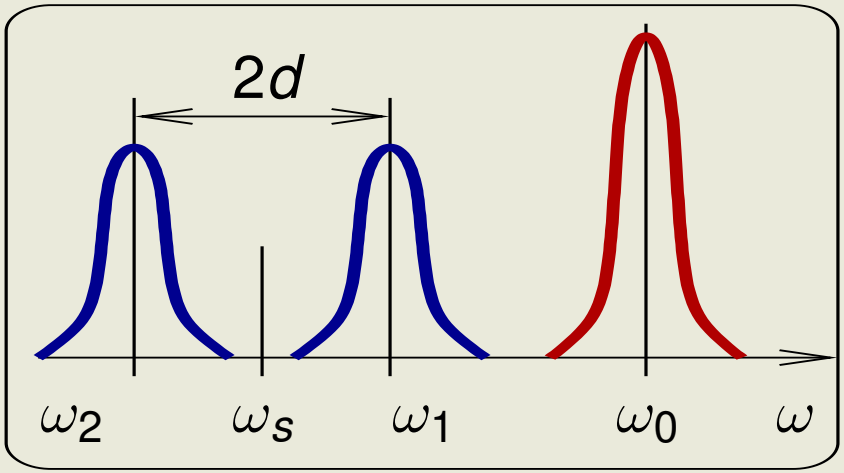


## Approximation of constant field

Optical power $W$ circulating inside the arms is a constant.

# Assumptions

## No losses, no noises

No optical losses in mirrors. No suspension noise in mirrors.

## Non-identical arms

Different frequences of the Stokes modes in FP cavities. Arms are tuned in resonance with the main mode. $\omega_s = (\omega_1 + \omega_2)/2$, $d = (\omega_1 - \omega_2)/2$.

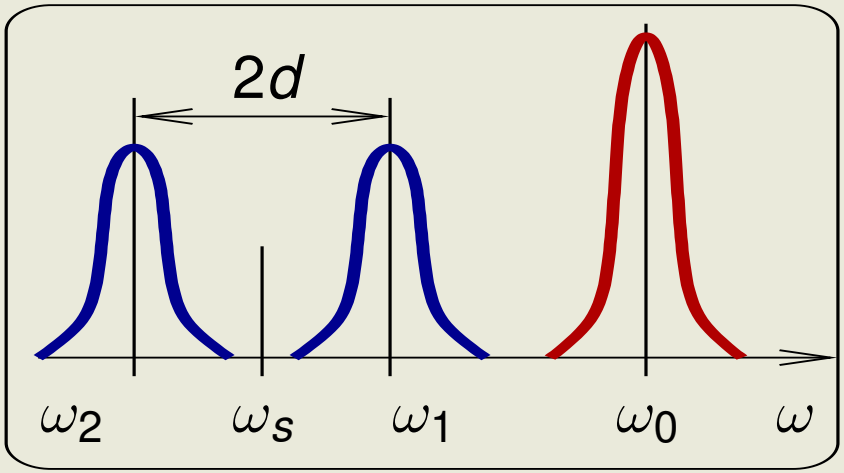


## Approximation of constant field

Optical power $W$ circulating inside the arms is a constant.

# Outline


1. Introduction
   - Effect of Parametric Oscillatory Instability
   - Account of anti-Stokes Mode
   - Proposed “cures” to avoid the parametric instability
   - PI in Signal Recycled Interferometer
   - Different Arms
2. Parametric Instability in SR Interferometer with Different Arms
   - Sygnal Recycled Interferometer
   - Normal modes
   - Identical mirrors
   - Elastically different mirrors
   - Elastic modes
3. Summary

# Normal modes

## For detuned arms ($d \neq 0$) — two normal modes: $\xi,\ \eta$

$$\xi = \frac{f_1 - \varkappa f_2}{1+\varkappa^2}, \quad z_\xi = \mathcal{Z}_1 - \varkappa \mathcal{Z}_2, \qquad \eta = \frac{\varkappa f_1 + f_2}{1+\varkappa^2}, \quad z_\eta = \varkappa \mathcal{Z}_1 + \mathcal{Z}_2,$$

$$\varkappa = \sqrt{1 - \left(\frac{2d}{\gamma_+ - \gamma_- + i\delta}\right)^2} + \frac{2id}{\gamma_+ - \gamma_- + i\delta},$$

$$\lambda_{\xi,\eta} = -\frac{\gamma_+ + \gamma_- - i\delta}{2} \pm \sqrt{\left(\frac{\gamma_+ - \gamma_- + i\delta}{2}\right)^2 - d^2}$$

## Recall, for optically identical arms ($d = 0,\ \varkappa = 1$)

mode $\eta$ transform into symmetric mode: $\eta \sim f_1 + f_2,\ \lambda_\eta = -\gamma_+$
and mode $\xi$ — into anti-symmetric mode: $\xi \sim f_1 - f_2,\ \lambda_\xi = -\gamma_- + i\delta$
(detuting $\delta$ is controlled by position of SR mirror).

# Outline


1. Introduction
   - Effect of Parametric Oscillatory Instability
   - Account of anti-Stokes Mode
   - Proposed “cures” to avoid the parametric instability
   - PI in Signal Recycled Interferometer
   - Different Arms
2. Parametric Instability in SR Interferometer with Different Arms
   - Sygnal Recycled Interferometer
   - Normal modes
   - Identical mirrors
   - Elastically different mirrors
   - Elastic modes
3. Summary

# Instability condition for elastically identical mirrors

## Generalization for detuned arms.

We assume $-\mathrm{Re}\lambda_{\xi,\eta} \gg \gamma_m$,

$$\frac{2\mathcal{Q}}{\gamma_m}\left(\frac{-\mathrm{Re}(\lambda_\xi)}{\left[\mathrm{Re}(\lambda_\xi)\right]^2+\left[\Delta+\mathrm{Im}(\lambda_\xi)\right]^2}\right)\geq 1, \tag{2}$$

Or $$\frac{2\mathcal{Q}}{\gamma_m}\left(\frac{-\mathrm{Re}(\lambda_\eta)}{\left[\mathrm{Re}(\lambda_\eta)\right]^2+\left[\Delta+\mathrm{Im}(\lambda_\eta)\right]^2}\right)\geq 1,$$

$$Q=\frac{\Lambda W\omega_s}{cLm\omega_m},\quad \Delta=\omega_0-\omega_s-\omega_m$$

# Outline


1. Introduction
   - Effect of Parametric Oscillatory Instability
   - Account of anti-Stokes Mode
   - Proposed “cures” to avoid the parametric instability
   - PI in Signal Recycled Interferometer
   - Different Arms
2. Parametric Instability in SR Interferometer with Different Arms
   - Sygnal Recycled Interferometer
   - Normal modes
   - Identical mirrors
   - Elastically different mirrors
   - Elastic modes
3. Summary

# Instability condition for elastically different mirrors

## We consider elastic mode of one mirror only

We assume $-\mathrm{Re}\lambda_{\xi,\eta} \gg \gamma_m$,

$$\frac{\mathcal{Q}}{(1+\varkappa^2)\gamma_m}\left(\frac{-\mathrm{Re}(\lambda_\xi)}{\left[\mathrm{Re}(\lambda_\xi)\right]^2+\left[\Delta+\mathrm{Im}(\lambda_\xi)\right]^2}+\right. \tag{3}$$

$$\left.+\frac{-\varkappa^2\mathrm{Re}(\lambda_\eta)}{\left[\mathrm{Re}(\lambda_\eta)\right]^2+\left[\Delta+\mathrm{Im}(\lambda_\eta)\right]^2}\right)\geq 1.$$

$$Q=\frac{\Lambda W\omega_s}{cLm\omega_m},\quad \Delta=\omega_0-\omega_s-\omega_m$$

# Dependence of $\gamma_-$ and $\delta$ on SR mirror's position. No arms detuning $d = 0$

Close to resonance

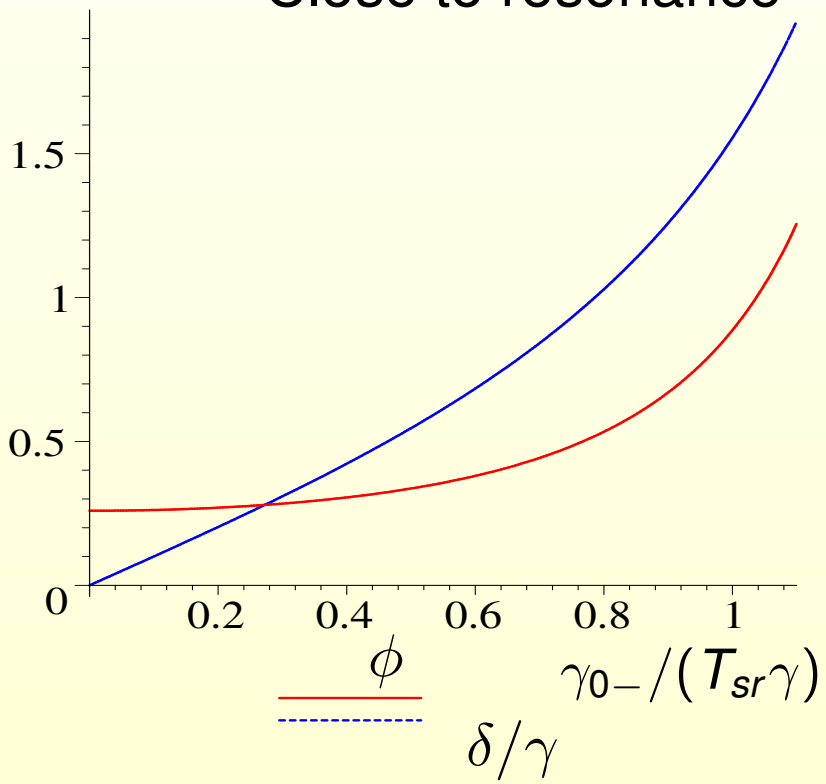


Close to anti-resonance

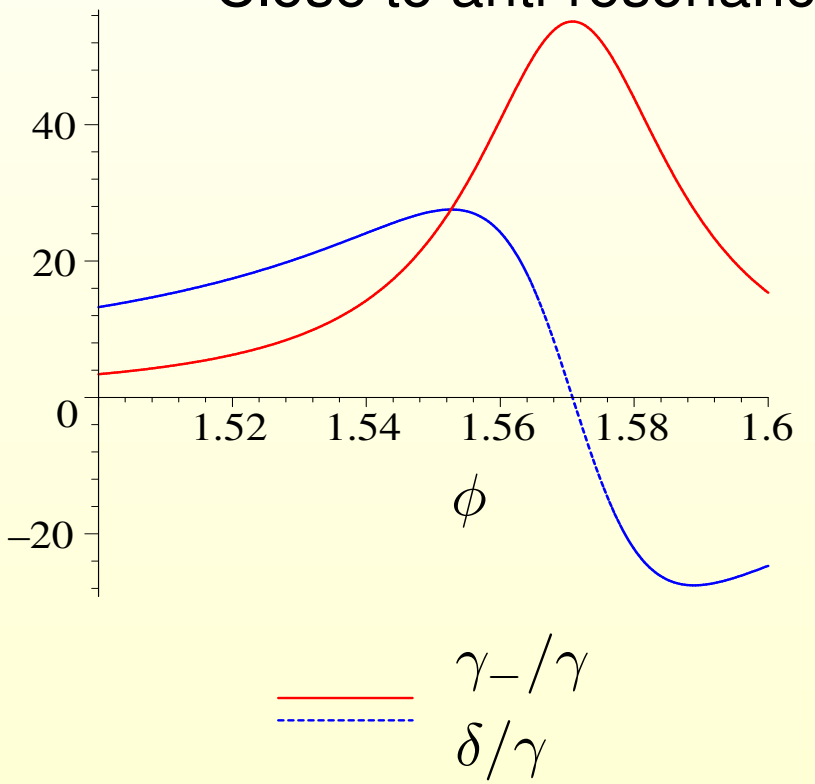

# The chance to fall into the trap of parametric instability

We assume the following parameters:

$$\gamma_m \simeq 10^{-3}\text{sec}^{-1},$$
$$\gamma_+,\ \gamma_- \simeq 2 \ldots 10\ \text{sec}^{-1},$$
$$\delta \simeq 100 \ldots 1000\ \text{sec}^{-1}.$$

## The chance to fall into the trap of parametric instability

depends on value Re$\lambda_{\xi,\eta}$.
Does Re$\lambda_{\xi,\eta}$ for detuned interferometer differ dramatically from $\gamma_+,\ \gamma_-$?

# Dependence of Re$\lambda_{\xi,\eta}$ and Im$\lambda_{\xi,\eta}$ on arms detuning $d$

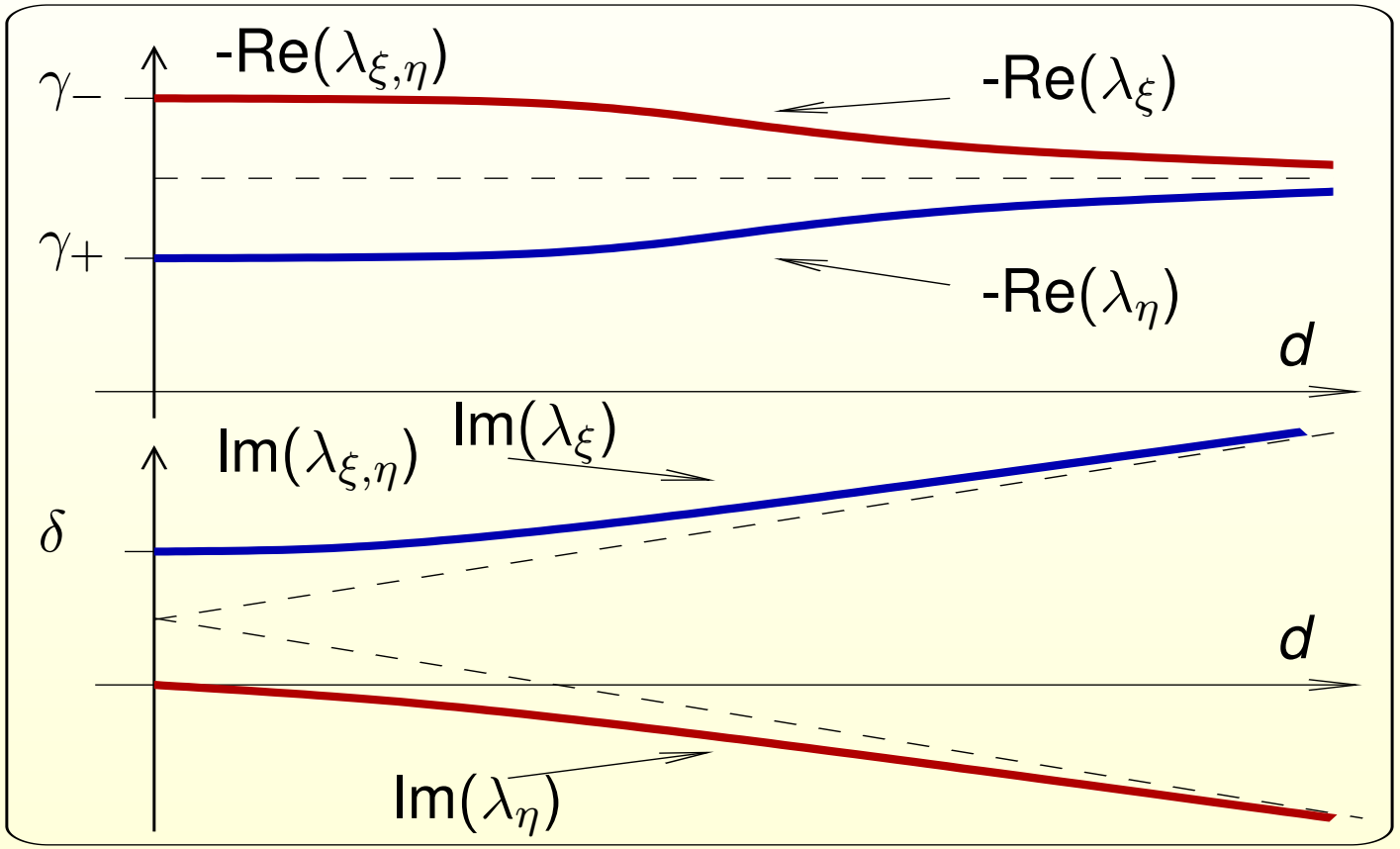


**Answer:**

Re$\lambda_{\xi,\eta}$ does not differ dramatically from $\gamma_+$, $\gamma_-$.
Hence the chance to fall into PI is practically the same.

# Resipes

## We can "scan" the frequency range

to find instability (or its precursors) by the followig ways:
a) variation of the SR mirror position (change of SR detuning $\delta$).
b) inhomogenious heat of mirrors to vary their curvature radii — it allow to control arms tuning $d$.
It provides us *in situ* with very valuable information about the possible danger of parametric instability.

## Precursors

Registration of Stokes modes provides information about the resonance frequencies of elastic modes with "suitable" spatial distributions. These Stokes modes may be the modes of higher orders (dipole, quadrupole and so on).

# Estimates

## Small Detuning — Small Chance to Fall into Trap

Let $\Delta \ll \gamma_{0+} \simeq 2\ \mathrm{s}^{-1}$ and $\delta \gg \gamma_{0-} \simeq 2 \ldots 10\ \mathrm{s}^{-1}$. Then parametric instability will take place at power $W_c \simeq 5$ W (!) (if $\omega_m = 10^5\ \mathrm{sec}^{-1}$, $\gamma_m = 6 \times 10^{-4}\,\mathrm{sec}^{-1}$, $\Lambda_1 \simeq 1$). However, there is small chance that such small detuning takes place.

## Large detuning ($|\Delta| > \gamma_{0+}$)

The realization of parametric instability for large detuning requires dramatically larger optical power: $W_c \sim \Delta^2/\gamma_{0+}^2$. For example, if detuning is about 1 kHz and other parameters are the same one can obtain $W_c \simeq 10^8$ W (!). Advanced LIGO plans to use $W \simeq 10^6$ W.

# Outline


1. Introduction
   - Effect of Parametric Oscillatory Instability
   - Account of anti-Stokes Mode
   - Proposed “cures” to avoid the parametric instability
   - PI in Signal Recycled Interferometer
   - Different Arms
2. Parametric Instability in SR Interferometer with Different Arms
   - Sygnal Recycled Interferometer
   - Normal modes
   - Identical mirrors
   - Elastically different mirrors
   - Elastic modes
3. Summary

# Insufficient Accuracy of Numerical Calculation of Elastic Modes

## Insufficient Accuracy

Accuracy of standard packages FEMLAB or ANSYS
is about several percents only (!).
We need the accuracy at least $\gamma_{0+}/\omega_m \simeq 10^{-7} \div 10^{-5}$ (!).

## Numerical calculations have some sence

Nevertheless, such calculations have sense:
(i) to estimates of overlapping factors;
(ii) to get approximate information about frequency and structure of the elastic modes.

# Even improved numerical methods can not solve the problem completely:

## Not a cylindric shape of mirrors

For example, the pins to attach fiber may produce the shift of elastic mode frequency up to 100 $\sec^{-1}$[a].

[a] V. B. Braginsky, S. E. Strigin and S. P. Vyatchanin, *Physics Letters* **A305**, 111 (2002).

## The inhomogeneity of Young modulus and density of fused silica

may provide an uncontrollable relative shift of elastic mode frequency about percents[a]

[a] V. B. Braginsky, S. E. Strigin and S. P. Vyatchanin, *Physics Letters* **A305**, 111 (2002).

# Summary

## Chance to trap into parametric instability

in detuned interferometer does not differ dramaticaly as compared with non-detuned interferometer.

## We can “scan” the frequency range

to find instability (or its precursors)
by variation of the SR mirror position
and by variation of curvature radius of mirrors in arms.

## Outlook

Numerical calculation of elastic modes frequencies
with relative error $< 10^{-5}$

# Acknowledgments


## Many thanks

to Bill Kells **for statement of problem,**

to Vladimir Braginsky,
Bill Kells,
David Ottaway **for fruitful discussions.**

# Passive Parametric Instability Control

Slawek Gras

The University of Western Australia



sgras@cyllene.uwa.edu.au

# Test mass model

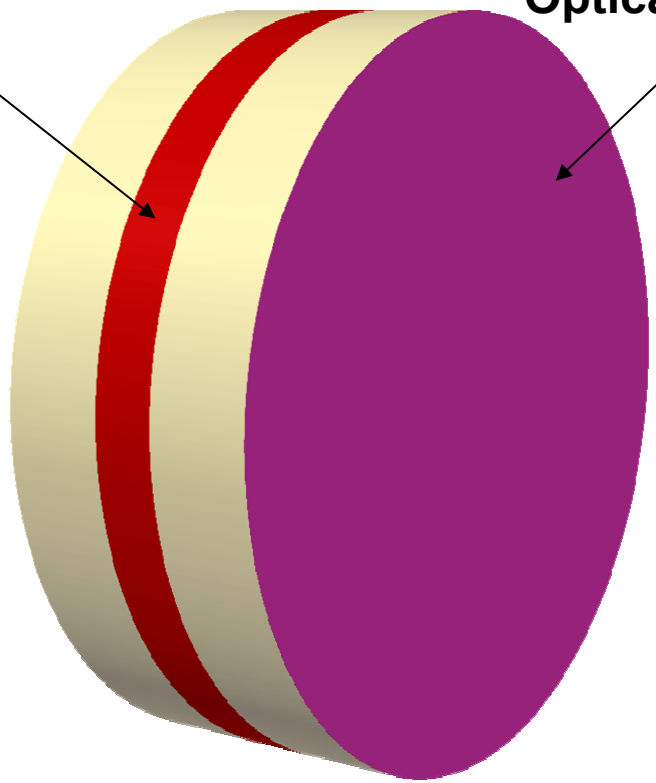


**Sapphire:**
**Test mass radius r = 0.16m**
**Thickness d = 0.13m**

$$R \propto Q_m$$

$$RoC\_ETM = RoC\_ETM + n \cdot \Delta RoC\_\max$$

$$\Delta RoC\_\max = 40\,m, \quad n \in \langle 0 : 0.2 : 1 \rangle$$


sgras@cyllene.uwa.edu.au

# Ring damper modelling

**a) thermal analysis** **+** **modal analysis**

$$S(f) = \frac{4k_B T}{\pi f F_0^2} \int E(\vec{r}) \left[ \frac{\phi(\vec{r})}{\sqrt{\phi^2(\vec{r}) + 1}} \right] dv$$

-FEM (coating, substrate and side wall strain energy)
- TN for various beam spot sizes
(position with a minimum contribution to the TN)
- optimal configuration (ring width, thickness and loss angle)

$$Q_n = \frac{\int E_n(\vec{r}) dv}{\int E_n(\vec{r}) \left[ \frac{\phi(\vec{r})}{\sqrt{\phi^2(\vec{r}) + 1}} \right] dv}$$

- FEM (coating, substrate and side wall strain energy for acoustic modes)
- acoustic mode damping

**b) parametric instability**

$$\Lambda_{1(a)} = \frac{V \left( \int f_0(\vec{r}_\perp) f_{1(a)}(\vec{r}_\perp) u_z d\vec{r}_\perp \right)^2}{\int |f_0|^2 d\vec{r}_\perp \int |f_{1(a)}|^2 d\vec{r}_\perp \int |\vec{u}| dv_\perp}$$

**c) NS/NS range**

-combination of Bench with TN form FEM

-FEM (frequency, mode shape ->overlapping parameter, effective mass)
- diffraction losses for different RoC (eigenvalue method)
- R gain estimation (with\without the ring)
- selection of unstable mode for different RoC


sgras@cyllene.uwa.edu.au

# Analysis Scheme

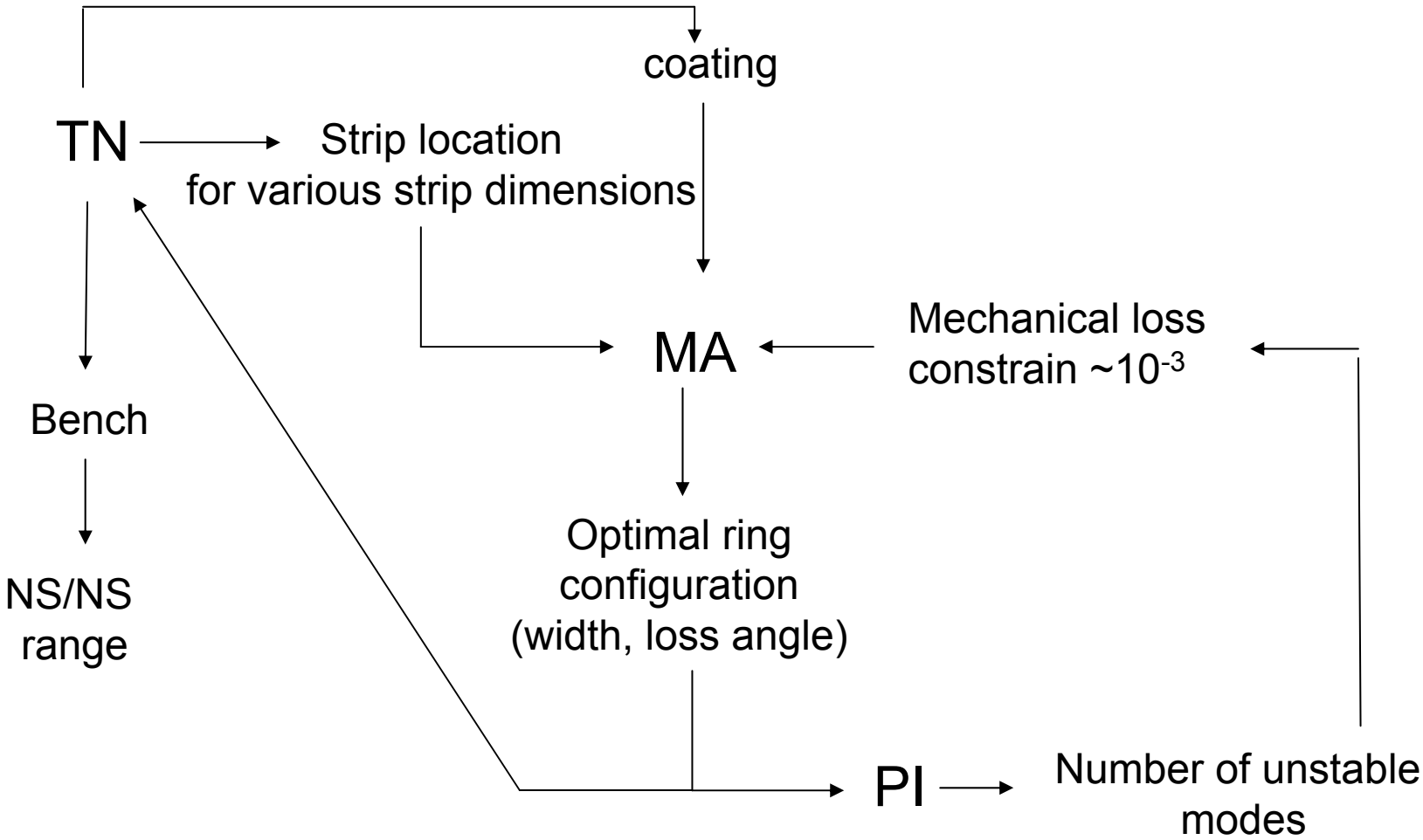



sgras@cyllene.uwa.edu.au

# FEM Strip Model

## Model A


-part of substrate
- the same elastic properties as substrate

## Model B ?


-strip with various elastic properties
-required to know priory minimum position

## Model C?

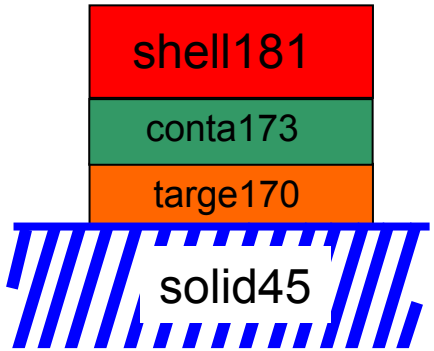


-strip with various elastic properties
-possible simulation of friction between strip and substrate
-required to know priory minimum position
-non-linear solution (time consuming)


sgras@cyllene.uwa.edu.au

# FEM model

solid45, 21725 elements
solid46, 869 elements

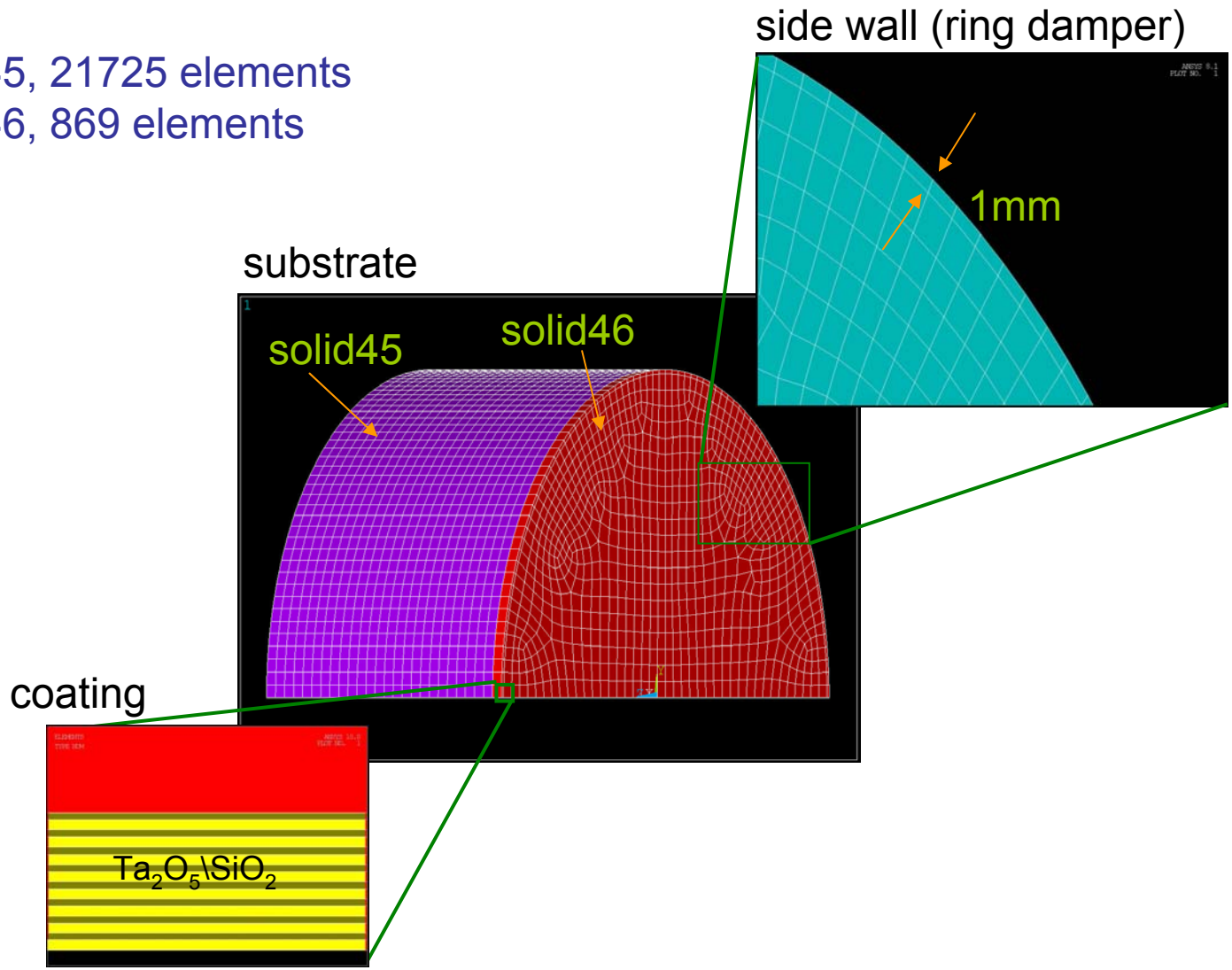






sgras@cyllene.uwa.edu.au

# Ring damper modeling

**Thermal analysis**

- ring position with minimal contribution to TN for different geometries
- ring thickness vs. loss angle

**Modal analysis**

- optimal width of the ring in respect to the mode suppression


sgras@cyllene.uwa.edu.au

# Null position

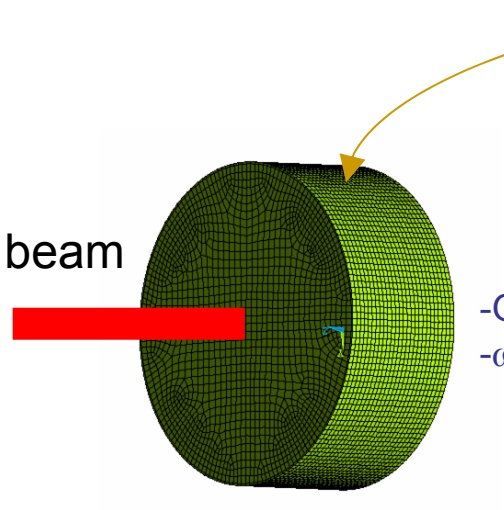


-Gaussian pressure profile
-$\omega$ = 6e-2 cm ($1/e^2$)

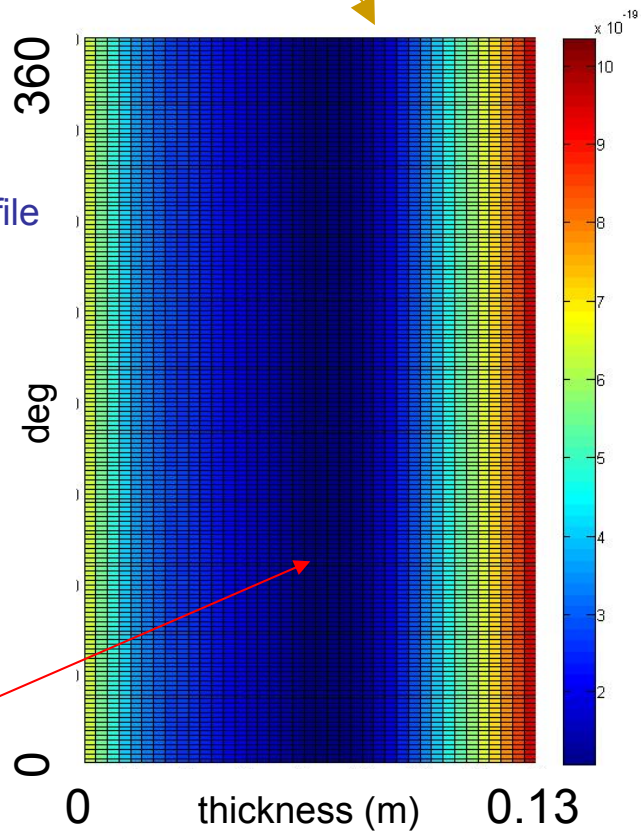


The front face edge has smaller energy concentration than the back face of the test mass

Minimum Strain Energy

$$\Delta E = \omega E \cdot loss$$

at $E_{min} \rightarrow \Delta E_{min} \rightarrow TN_{min}$


sgras@cyllene.uwa.edu.au

# Thermal noise at the null position

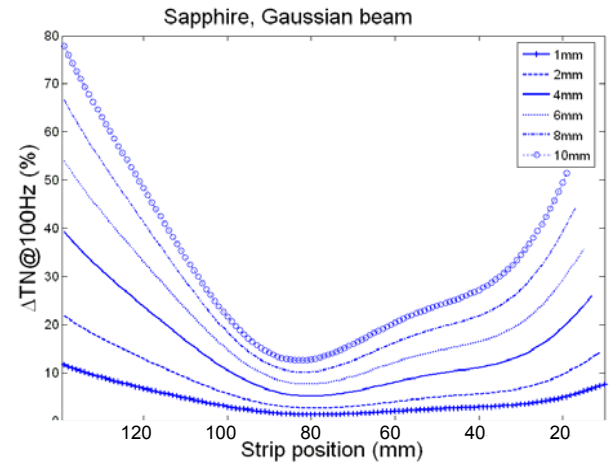


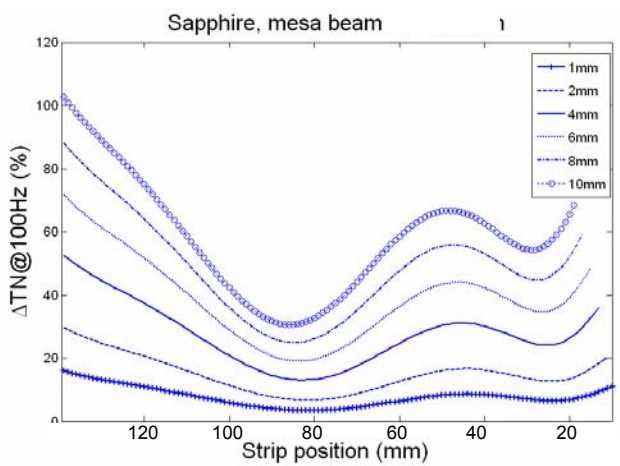


-beam spot size with 1ppm diffraction loss

- loss angle φ=2e-2

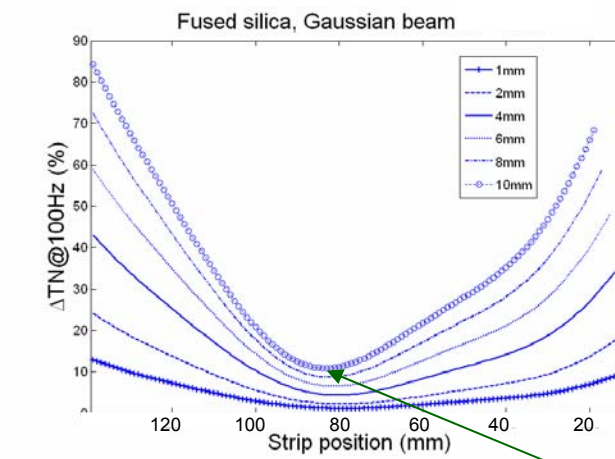


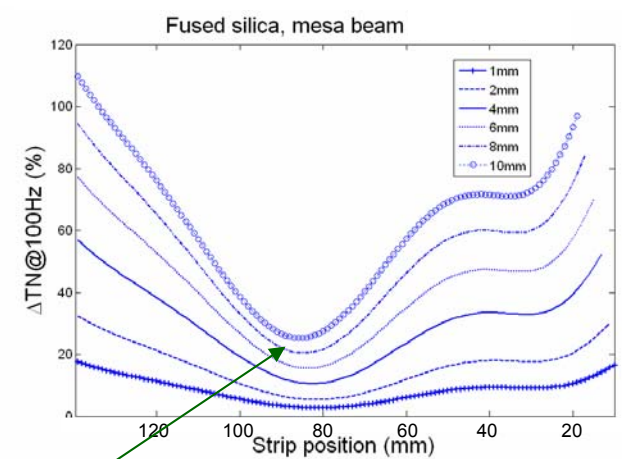


ΔTN – Brownian thermal noise degradation due to the ring in respect to the Brownian thermal noise of the substrate itself

Ring position with minimum contribution to the TN



sgras@cyllene.uwa.edu.au

# Ring damper modeling

## Optimal ring damper position

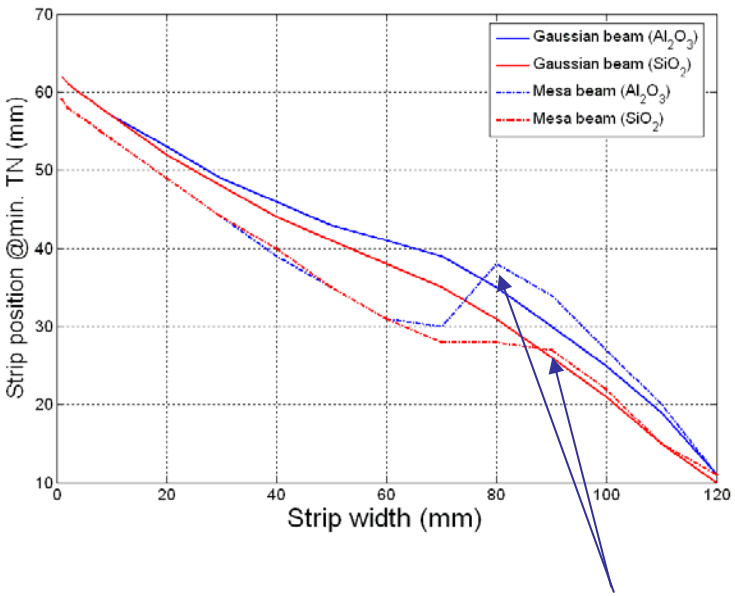


## Ring thickness map - fixed TN level

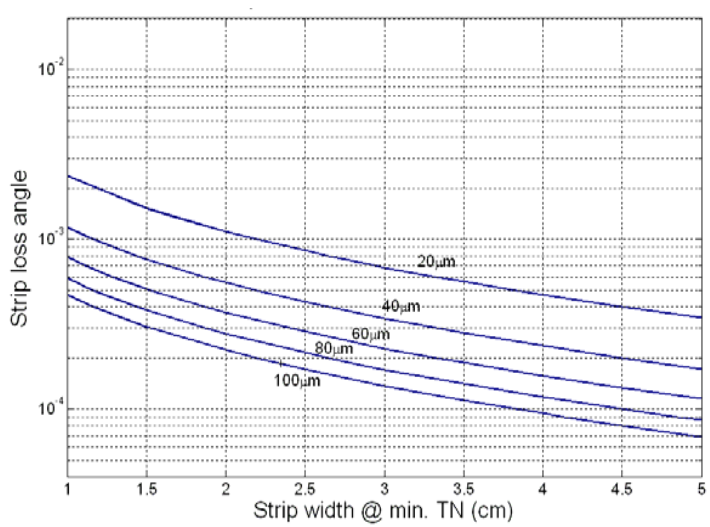


due to the secondary minima


sgras@cyllene.uwa.edu.au

# Ring damper modeling

$$\phi_r = 1e-2$$

For the ring at the null position:

$$\phi \cdot V_{ring} = const$$

~ 20 mm (Gaussian,1ppm )
~ 10 mm (Messa,1ppm)

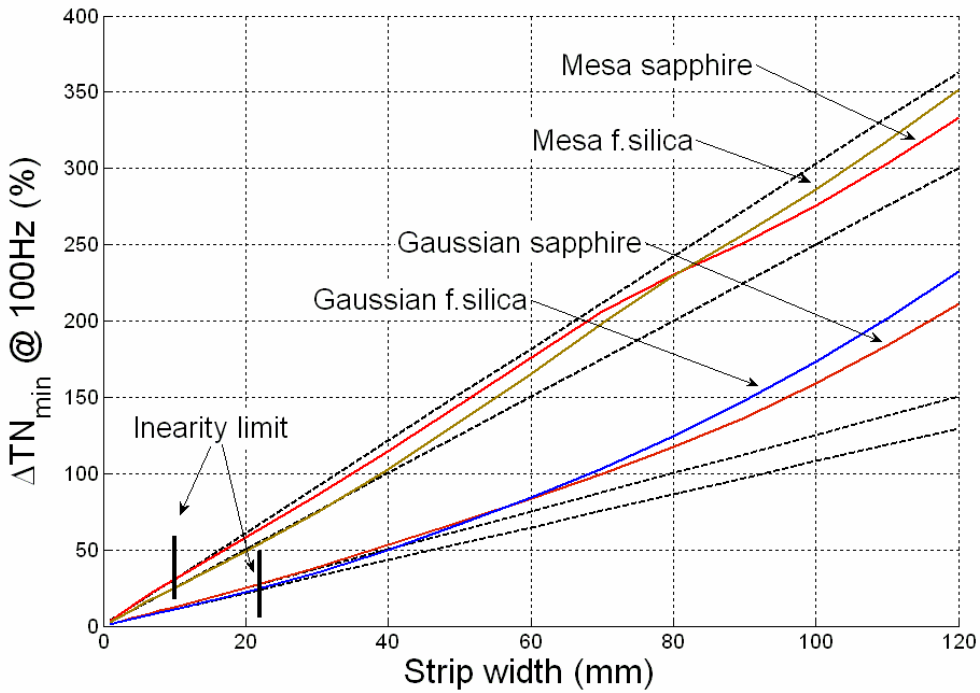



sgras@cyllene.uwa.edu.au

# Q-suppression due to the strip for the first 160 modes

Fixed thermal noise level $\Rightarrow \quad \phi_{eff} = 1.1e-8$
(different strip width with corresponding strip loss angle)

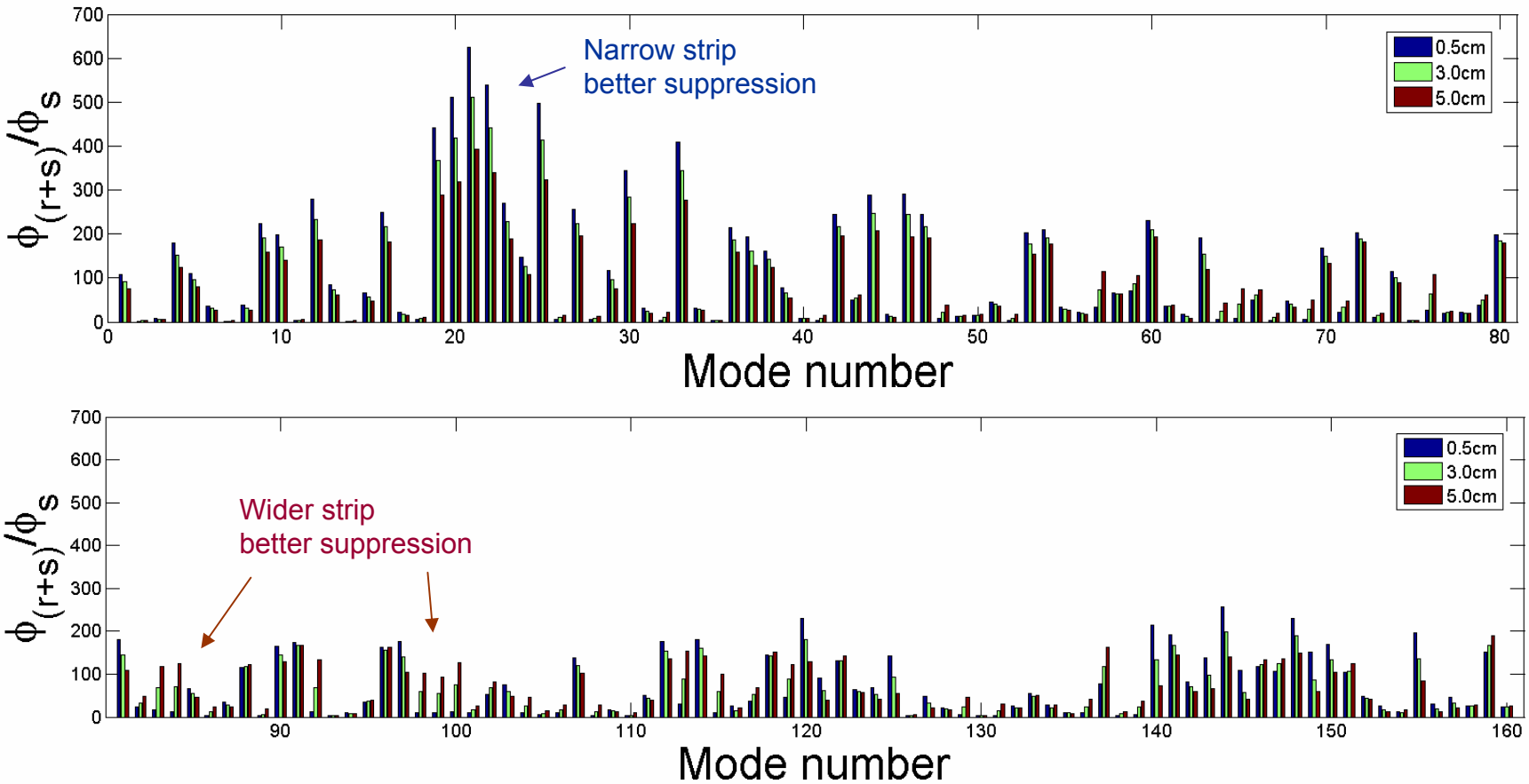


3 cm wide ring seems to be a good compromise


sgras@cyllene.uwa.edu.au

# Mode damping

Q-suppression is highly dependent on a mode shape.
Different modes have different energy concentration on the side wall of the test mass. Only modes with high strain energy located at the ring position are substantially damped.

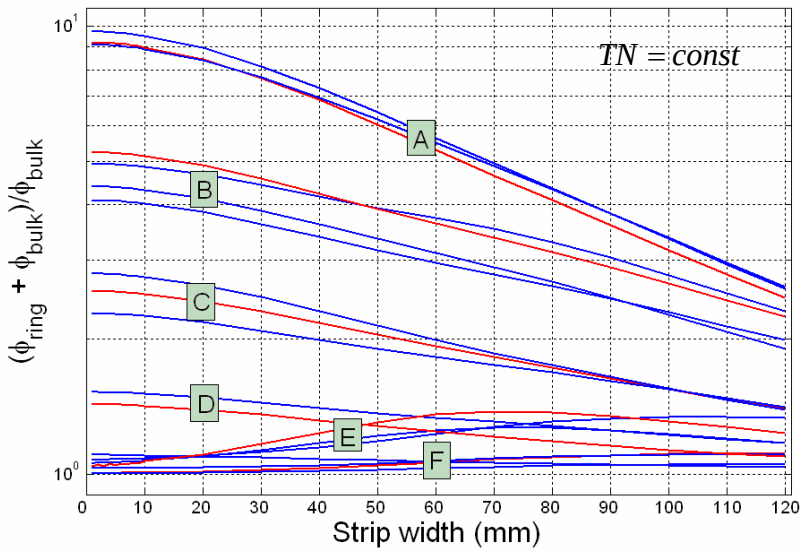


barrel side wall strain energy distribution:

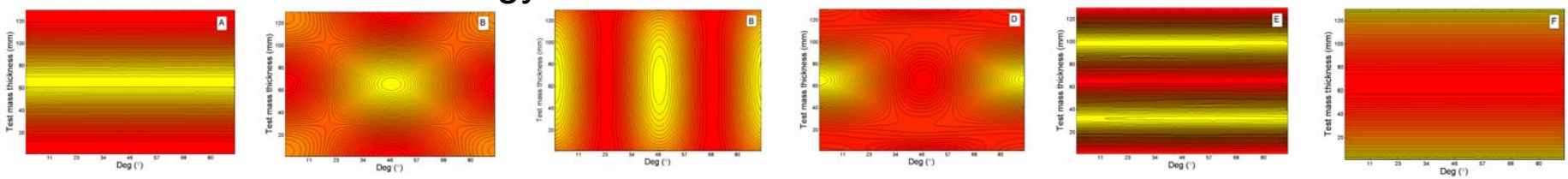

A B C D E F

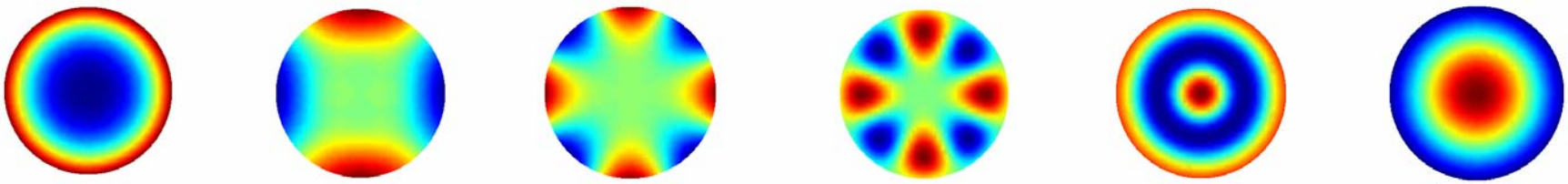

34.4kHz 36.6kHz 9.4kHz 39.3kHz 40.6kHz 13.7kHz


sgras@cyllene.uwa.edu.au

# Optimal ring damper


sgras@cyllene.uwa.edu.au

# Q-suppression due to the mirror coating

-18 layers of SiO2/Ta2O5 (ETM)

- 8 layers of SiO2/Ta2O5 (ITM) -

assumed loss isotropy $\varphi_{\parallel} = \varphi_{\perp}$

-loss frequency dependent (*)

$\varphi$ = 4.0E-05 + f 2.7E-09

$\varphi$ = 4.2E-04 + f 0.4E-09

SiO2: Young modulus E = 70E09
Poisson ratio p = 0.17
Density ρ=2200 kg/m3

Ta2O5: Young modulus E = 140E09
Poisson ratio p = 0.23
Density ρ = 8200 kg/m3

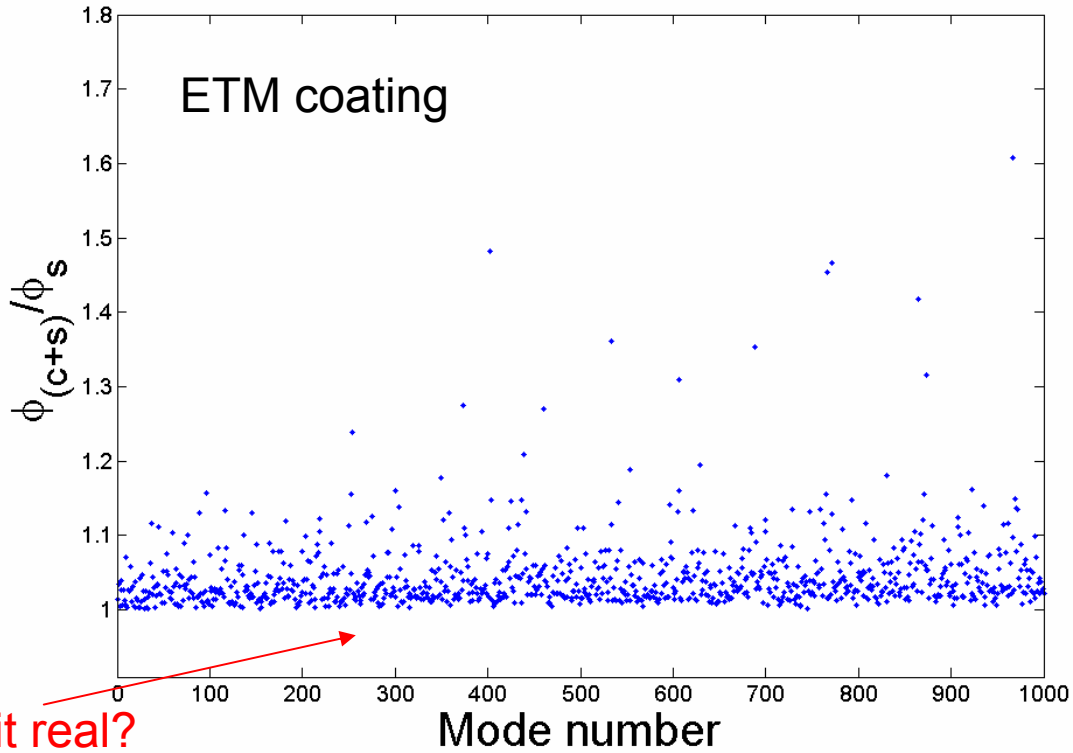


Is it real?

Almost no suppression

trivial check: what if cylinder would be not 13cm thich but only 1mm thick?

1.9579e+008 (130mm thick) $\xrightarrow{\text{by scaling}}$ 4.5079e+007 (1mm thick)


sgras@cyllene.uwa.edu.au

# IFO Brownian thermal noise amplification

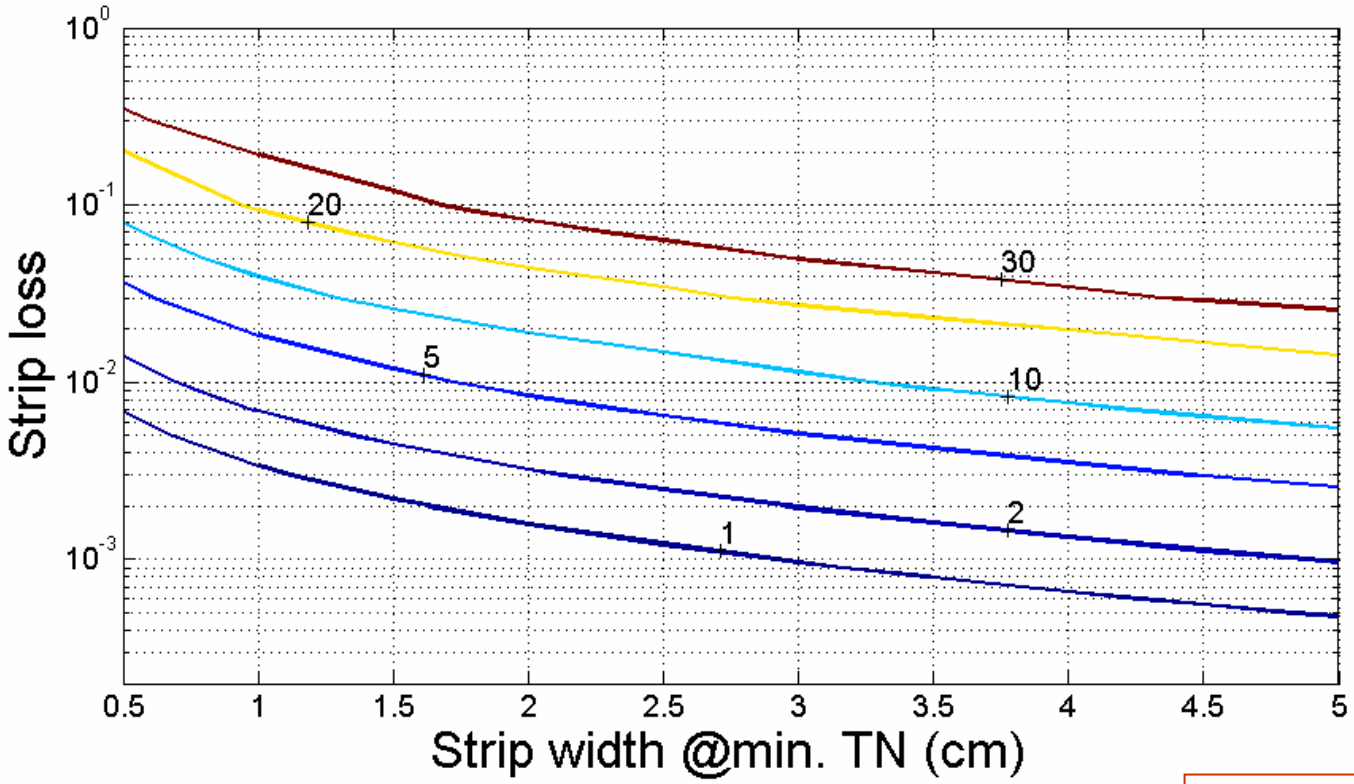


-all four test masses with same ring damper
-ITM/ETM coating included
-lines correspond to the the IFO thermal noise degradation with respect to the Brownian TN without rings

| TN | Require ring loss |
|---|---|
| 1% | 9.65e-4 |
| 2% | 1.98e-3 |
| 5% | 5.14e-3 |
| 10% | 1.14e-2 |
| 20% | 2.27e-2 |


sgras@cyllene.uwa.edu.au

# Thermal noise results

**Brownian Noise at 100Hz with RoC = 2076 m (FEM result ): m/√Hz**

| | ITM | ETM |
|---|---|---|
| **Coating** | **2.7242e-21** | **4.0936e-021** |
| Substrate | 1.4448e-21 | 1.4448e-21 |
| Ring | 1.2380e-21 | 1.2380e-21 |
| **Total (ifo,without ring)** | **7.5304e-21** | |
| **Total (ifo, ring)** | **7.9270e-21** ΔTN=+5% | |

Bench (coating):

2.9693e-021 ~8%

4.3685e-021 ~6%



sgras@cyllene.uwa.edu.au

# Ring damper thermal noise

TN=+5%

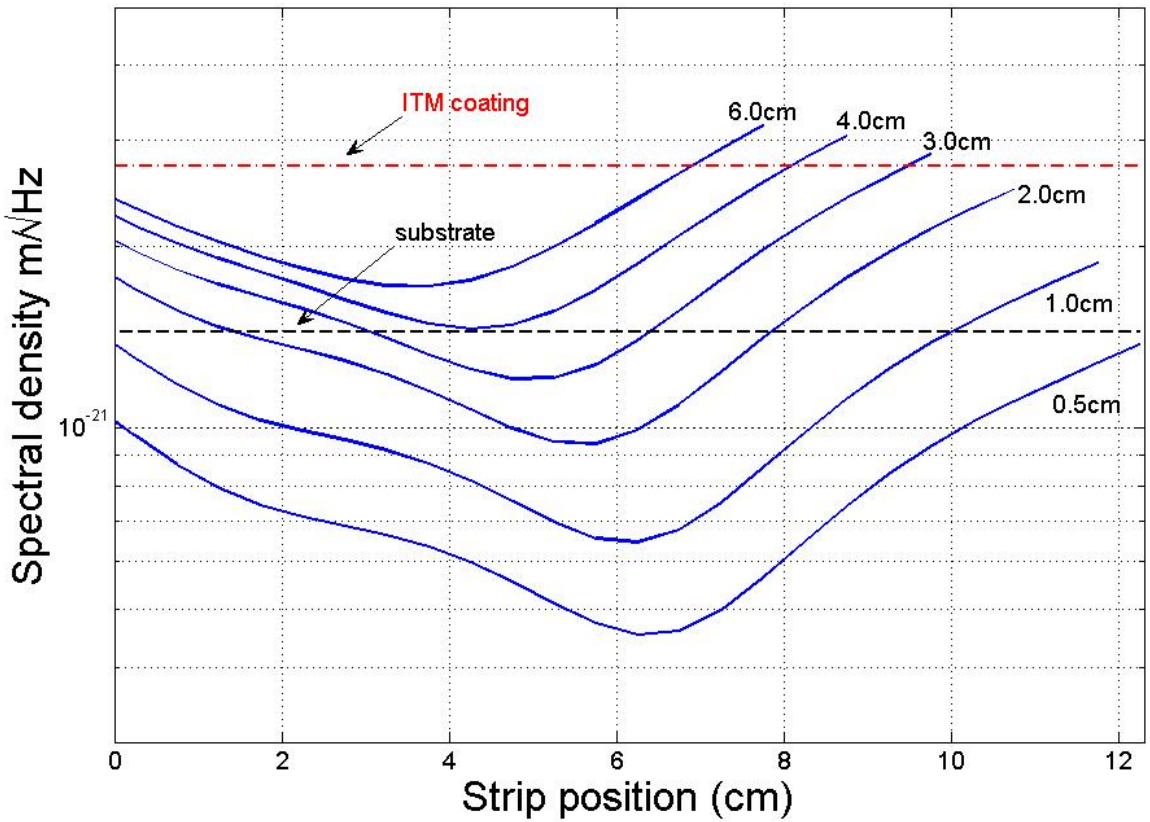


$$\phi_s = 5e-9$$

$$\phi_r = 5.14e-3$$



sgras@cyllene.uwa.edu.au

# Q-damping (ring + coating)

highly loss dependent

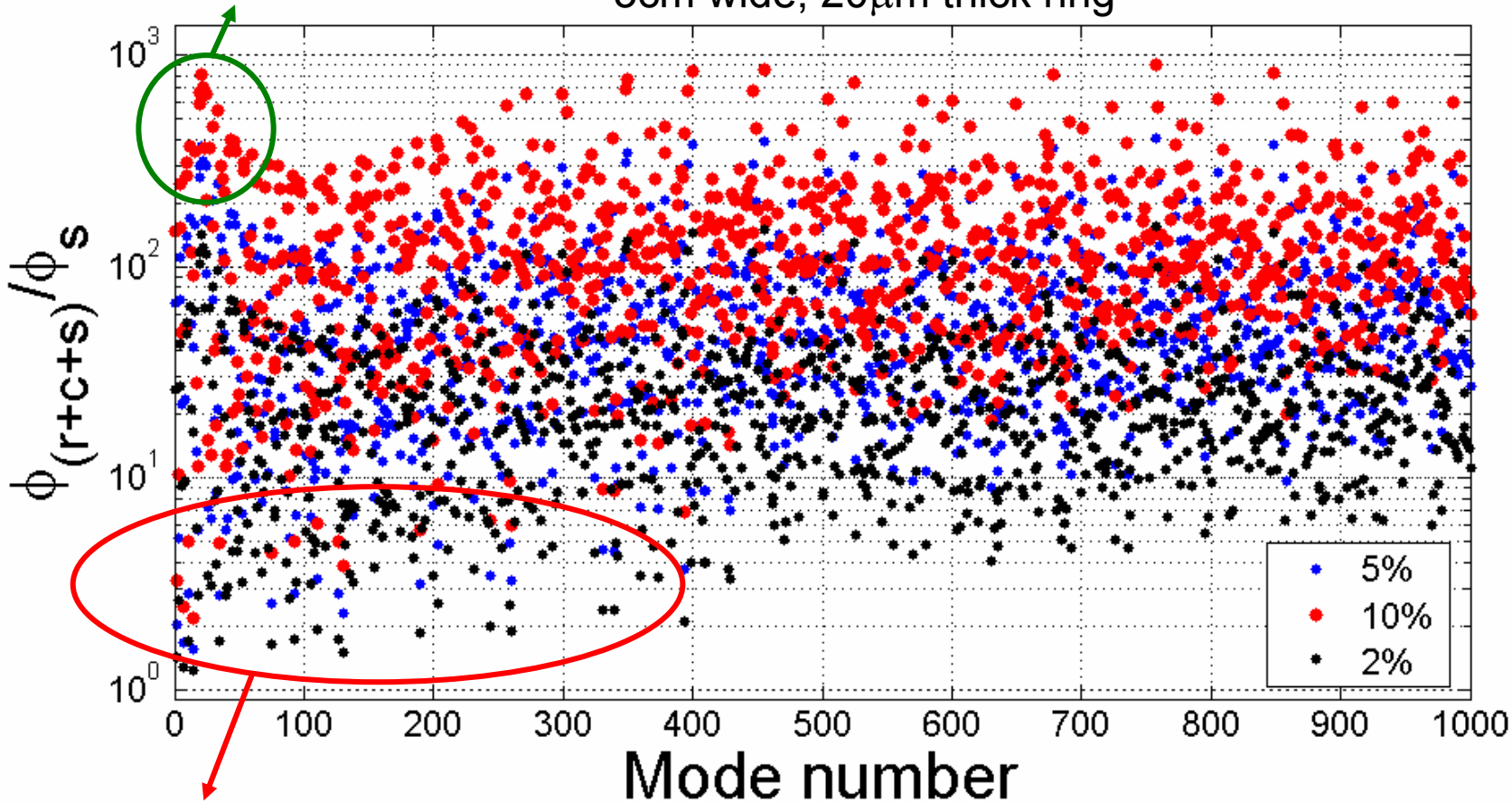


weakly loss dependent

Mean suppression value:
2% 27 5% 68 10% 151


sgras@cyllene.uwa.edu.au

# Parametric Instability

+

# Ring damper


sgras@cyllene.uwa.edu.au

$$R_j = \frac{4PQ_{m\,j}}{McL\omega_{mj}^2}\left(\frac{Q_{1i}\Lambda_{1i}}{1+\Delta\omega_{1i}^2/\delta_{1i}^2}\times\Omega_{1i} - \frac{Q_{1ai}\Lambda_{1ai}}{1+\Delta\omega_{1ai}^2/\delta_{1ai}^2}\times\Omega_{1ai}\right)$$

Acoustic mode quality factor suppressed by a strip

**PARAMETERS:**

T_ETM = 0.05%
T_ITM = 15ppm
T_PRM = 6%
Wavelength = 1.064e-06 m
Arm length = 4000 m
Mirror radius = 0.16 m (coated 0.157m)
Optical mode order –> up to the 9th
Total number of optical modes = 22
Optical mode family : LGM
Axial mode order = 5
Total number of acoustic modes = 1000
(range: 9.42kHz – 165.6KHz)
RoC step: 0.2m

PRC contribution to the R

$$\Omega_{1(a)i} = \frac{2+\delta_{1(a)i}/\delta_{pr}+\Delta\omega_{1(a)i}^2/\delta_{pr}^2}{2\left(1+\Delta\omega_{1(a)i}^2/\delta_{pr}^2\right)}$$

Overlapping parameter

$$\Lambda_{1(a)} = \frac{V\left(\int f_0(\vec{r}_\perp)\, f_{1(a)}(\vec{r}_\perp)u_z d\vec{r}_\perp\right)^2}{\int|f_0|^2 d\vec{r}_\perp \int|f_{1(a)}|^2 d\vec{r}_\perp \int|\vec{u}|dv}$$


sgras@cyllene.uwa.edu.au

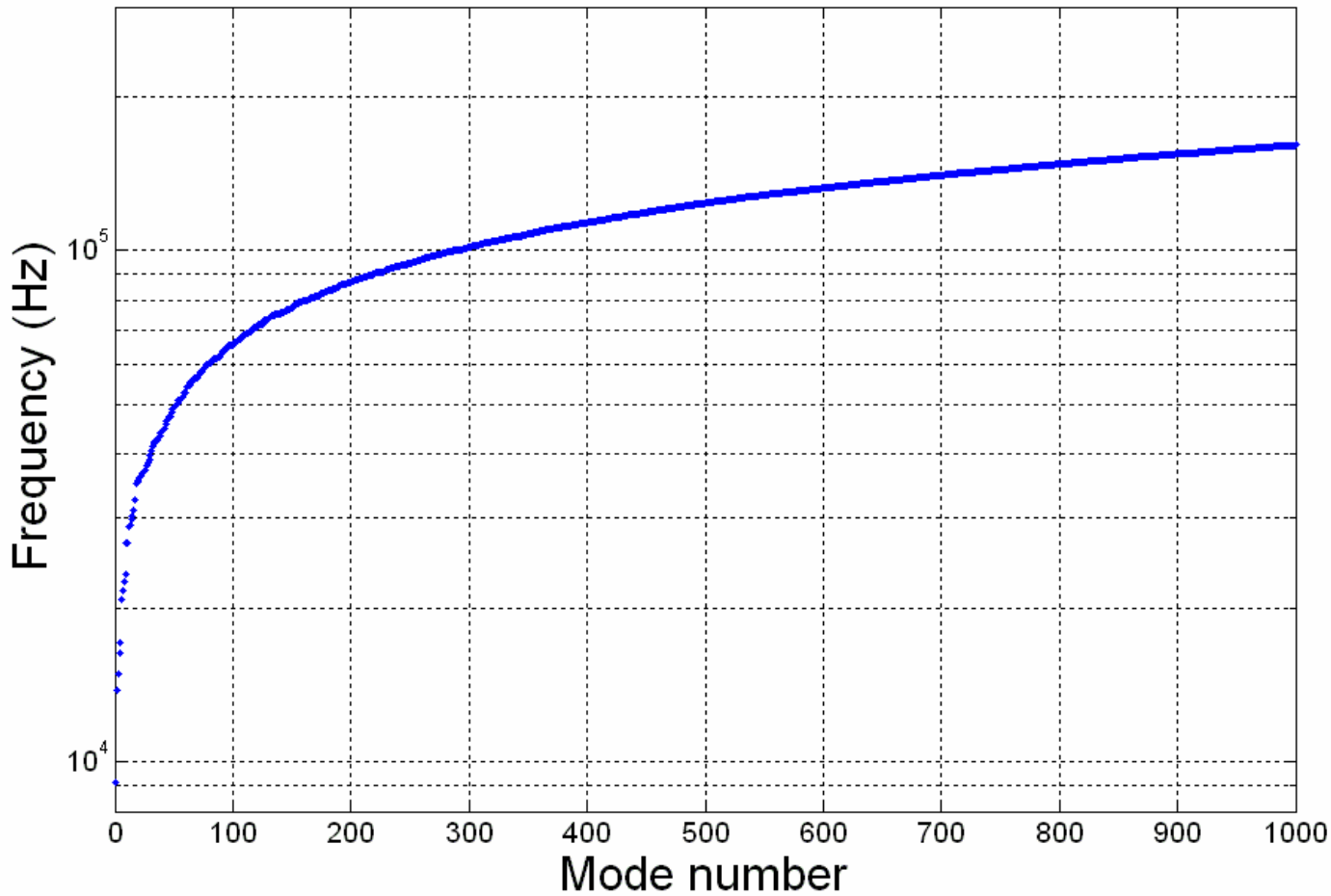



sgras@cyllene.uwa.edu.au

# Diffraction Losses

$$E_{12}[n,m] = \frac{ik}{2\pi}\iint_{Sm} E_1[m]\frac{\exp(-ik\rho)}{\rho}\,ds$$

$$K(\vec{r},\vec{r}') = \frac{ik}{2\pi\rho}e^{-ik\rho}$$

$$\rho = \sqrt{\delta^2 + \left|\vec{r}-\vec{r}'\right|^2}$$

$$\delta = L - h(\vec{r}) - h(\vec{r}')$$

$$E_{12} = A_{12}E_1$$

$$E_2[n] = E_{12}[n,m] = A_{12}[n,m]E_1[m]$$

$$E_2 = A_{12}E_1$$

$$E_1 = A_{21}E_2 = A_{21}A_{12}E_1 \Leftrightarrow E_1 = \gamma E_1$$

-fast
-allows calculate many modes simultaneously
-required high density mesh
-limited to mirror with big spot size

Yuanying Ch,…,Opt. Communications 234 (2004) 1


sgras@cyllene.uwa.edu.au

# Diffraction Losses

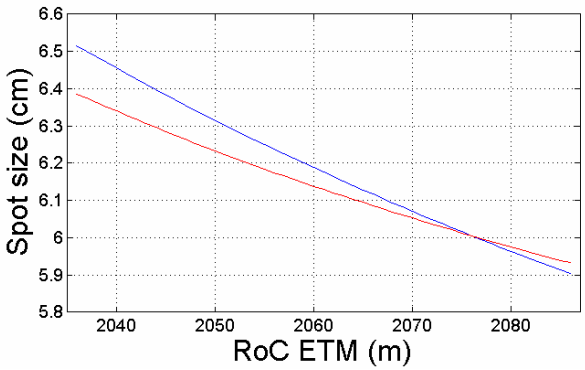


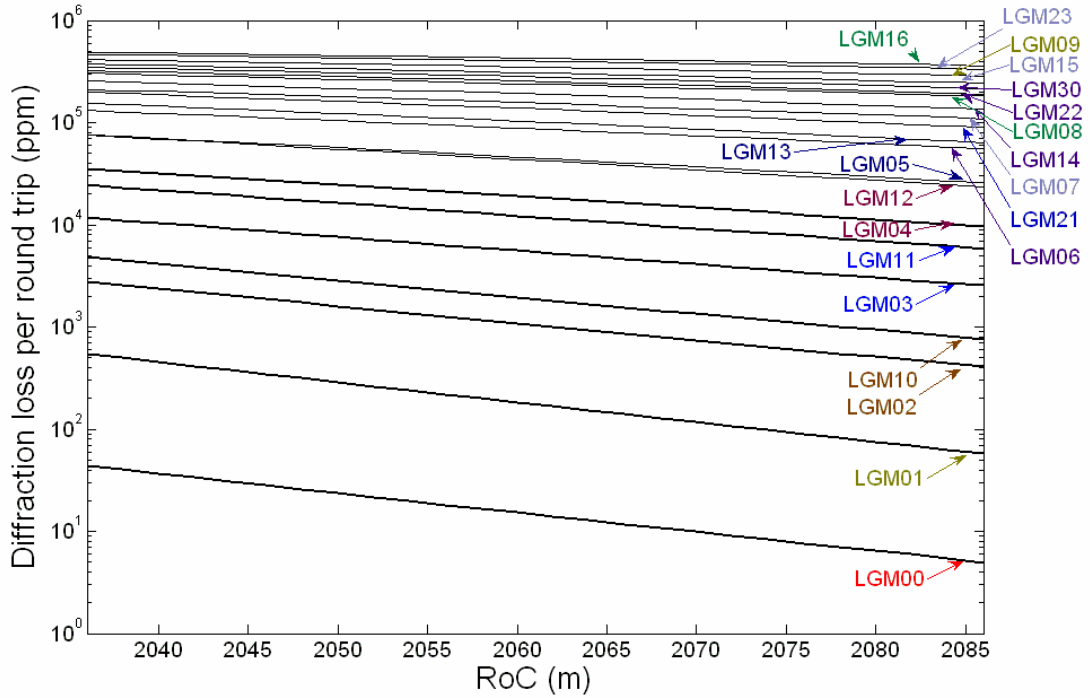


Results consistent with FFT


sgras@cyllene.uwa.edu.au

# Diffraction losses

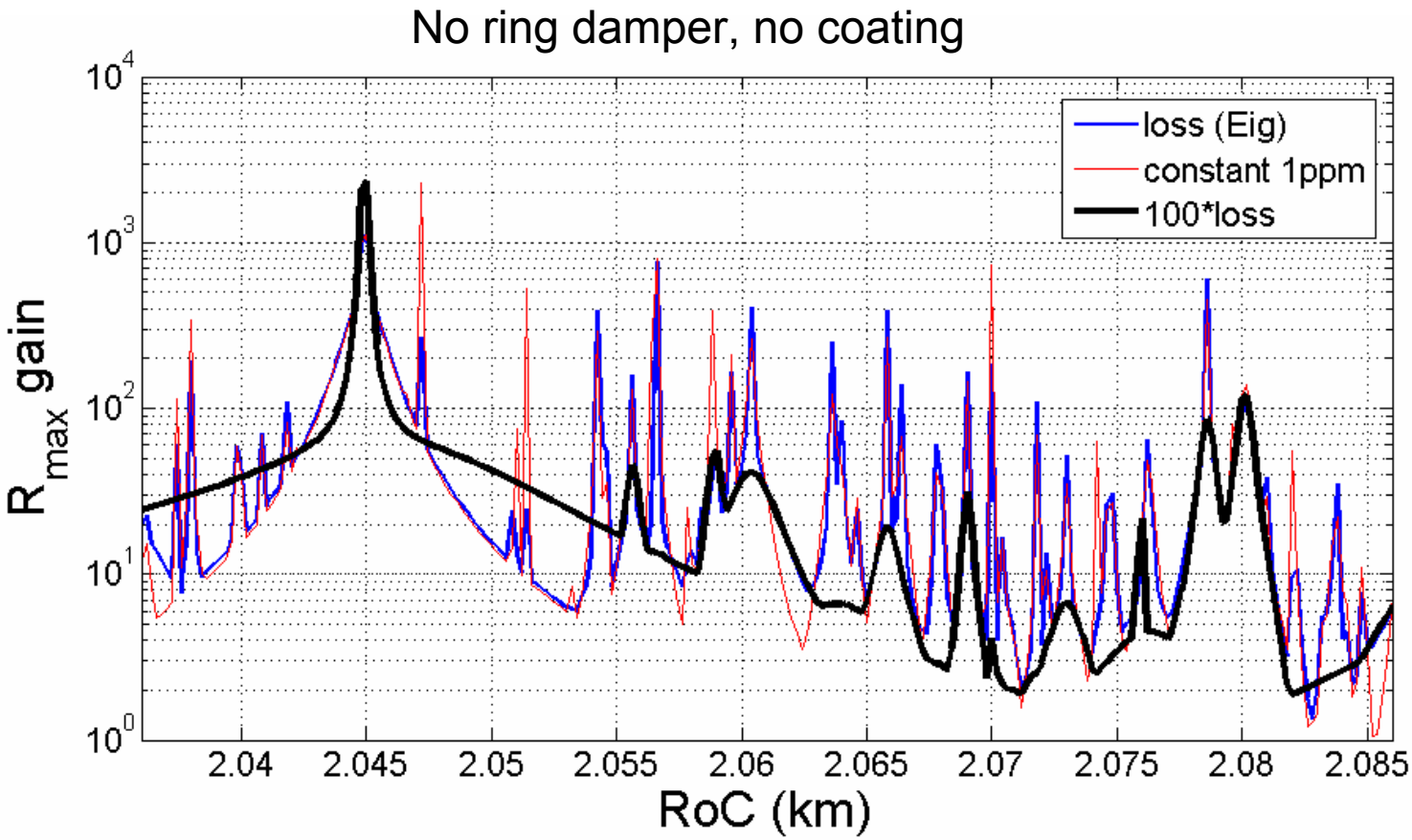


Underestimation ⟶ higher resonance peaks
Overestimation ⟶ higher off-resonance


sgras@cyllene.uwa.edu.au

# PRC (unstable)

$R_{max}$=2207, Freq=33.39kHz (17)

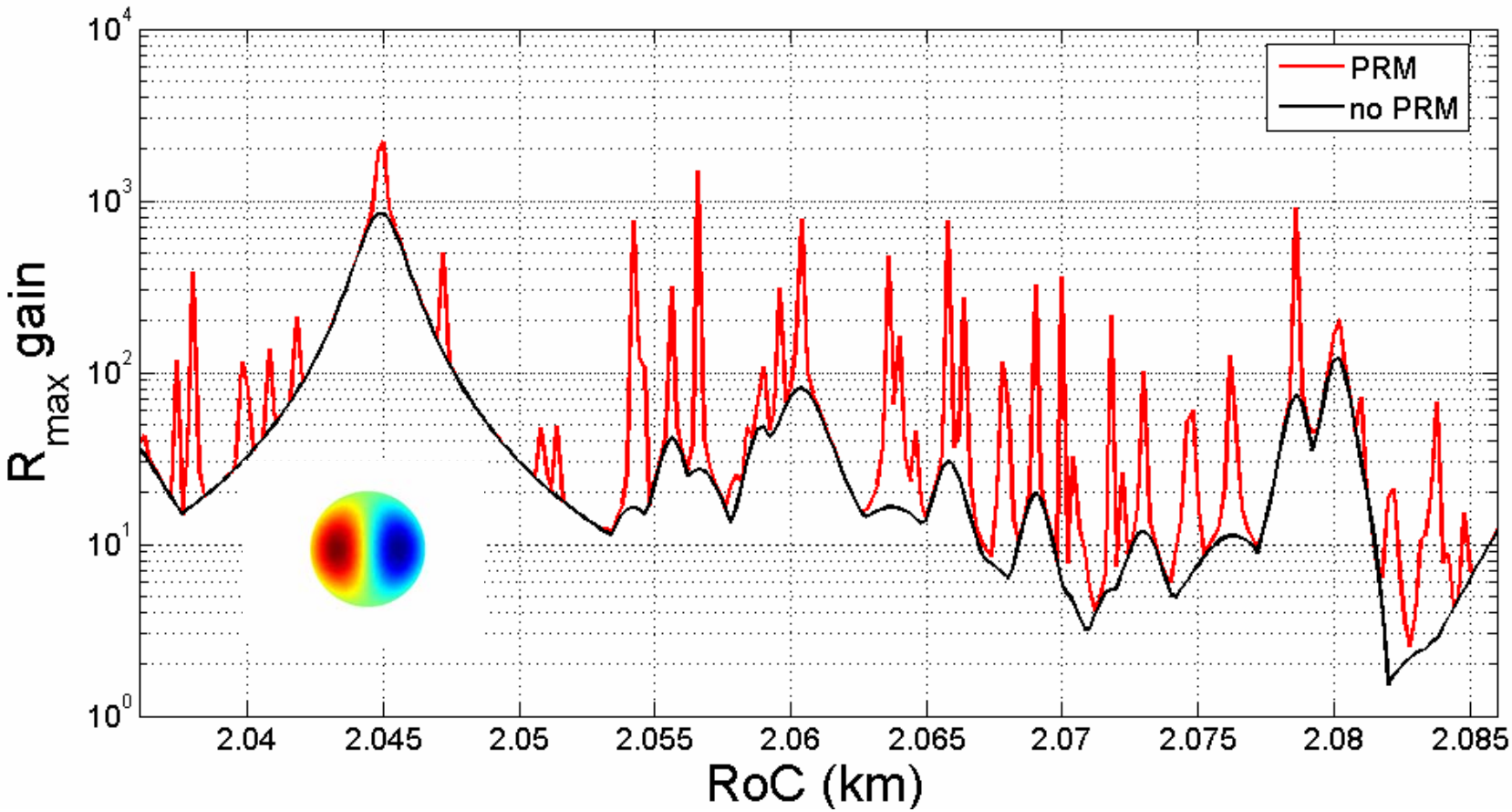


Power Recycling Mirror ⟶ resonance amplification


sgras@cyllene.uwa.edu.au

# Passive control with ring damper

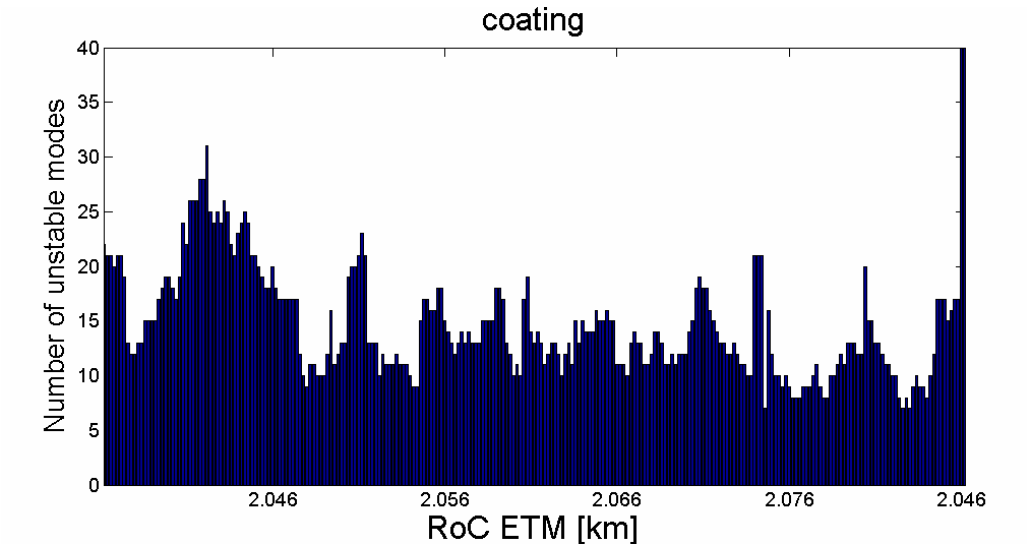


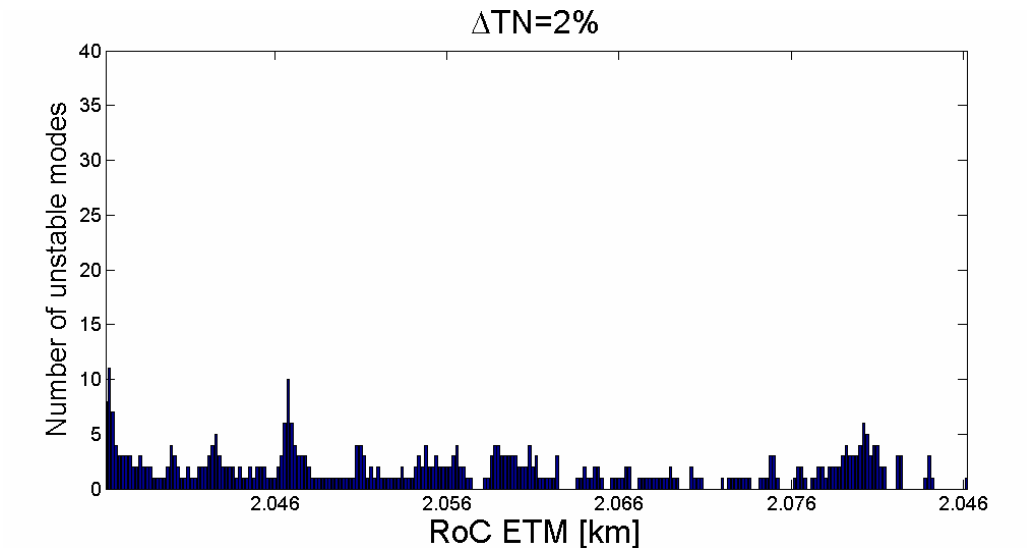



sgras@cyllene.uwa.edu.au

# Passive control with ring damper

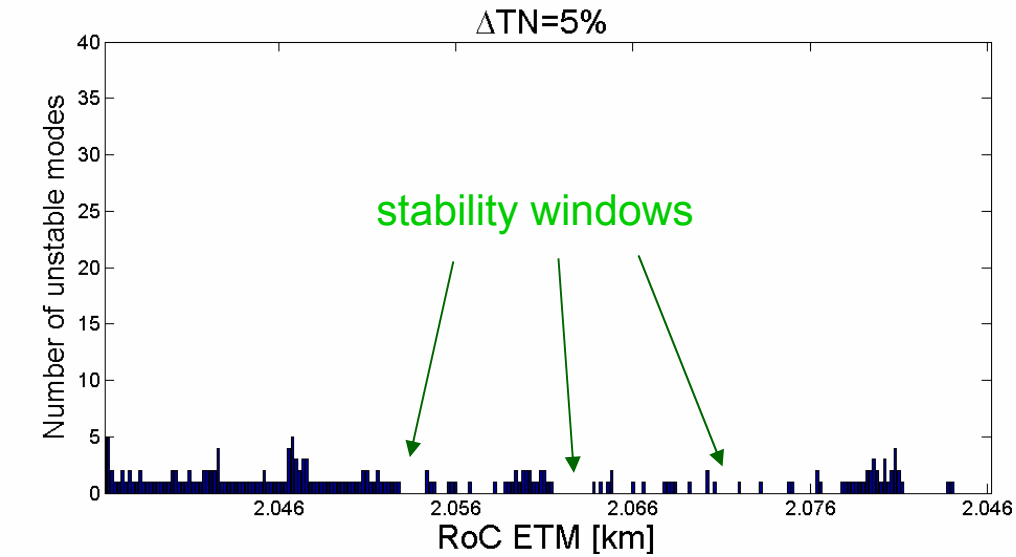


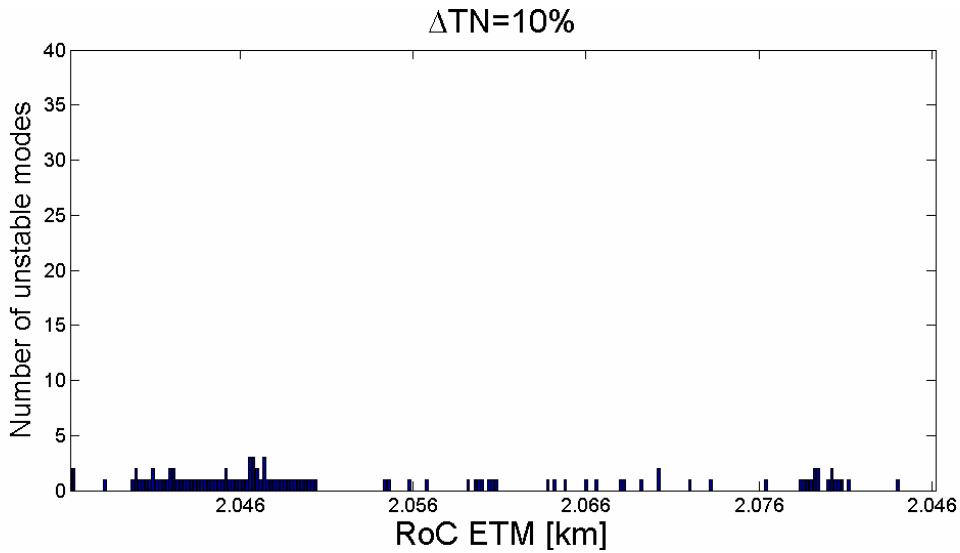



sgras@cyllene.uwa.edu.au

# Passive control with ring damper

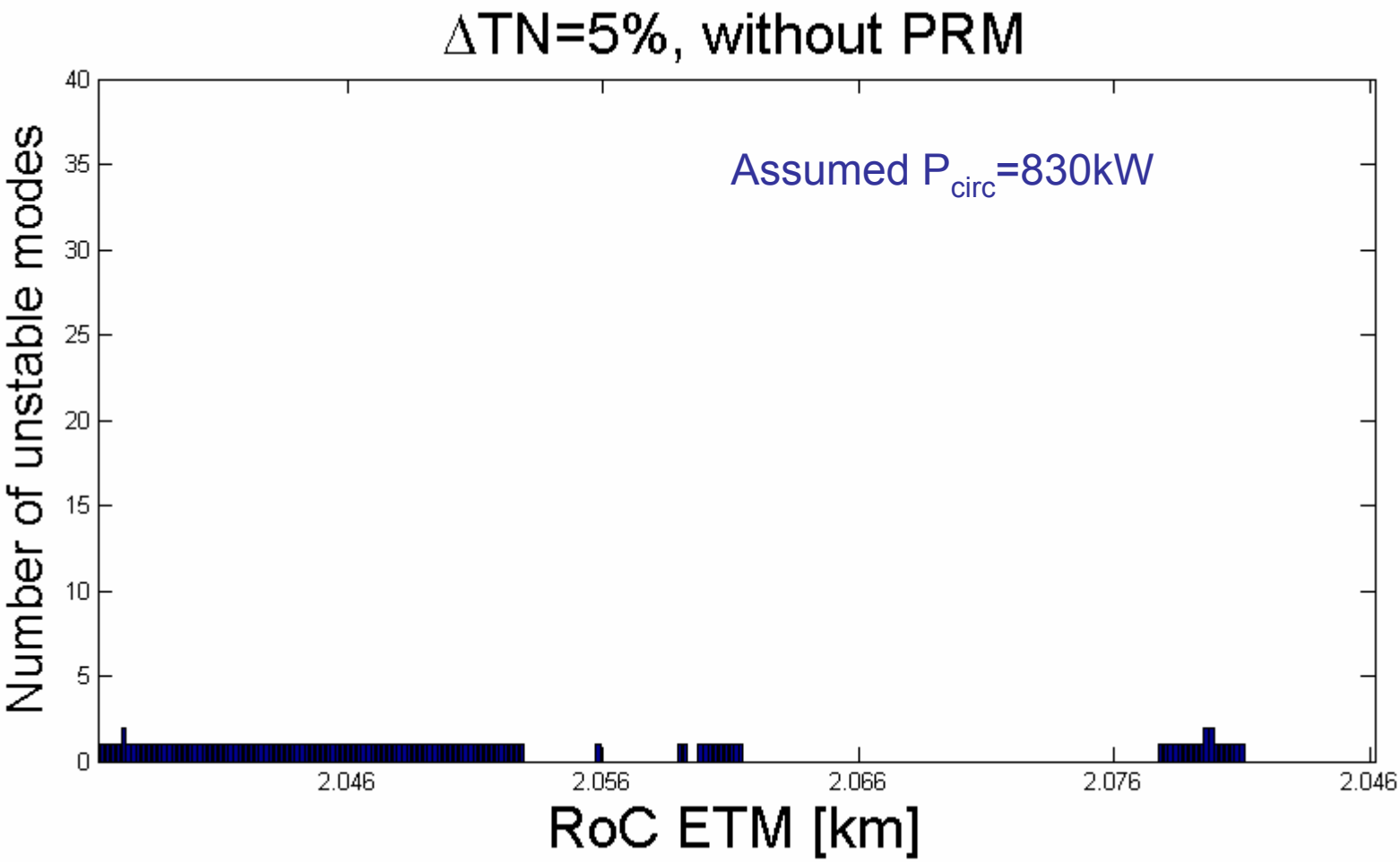



sgras@cyllene.uwa.edu.au

# NS/NS range

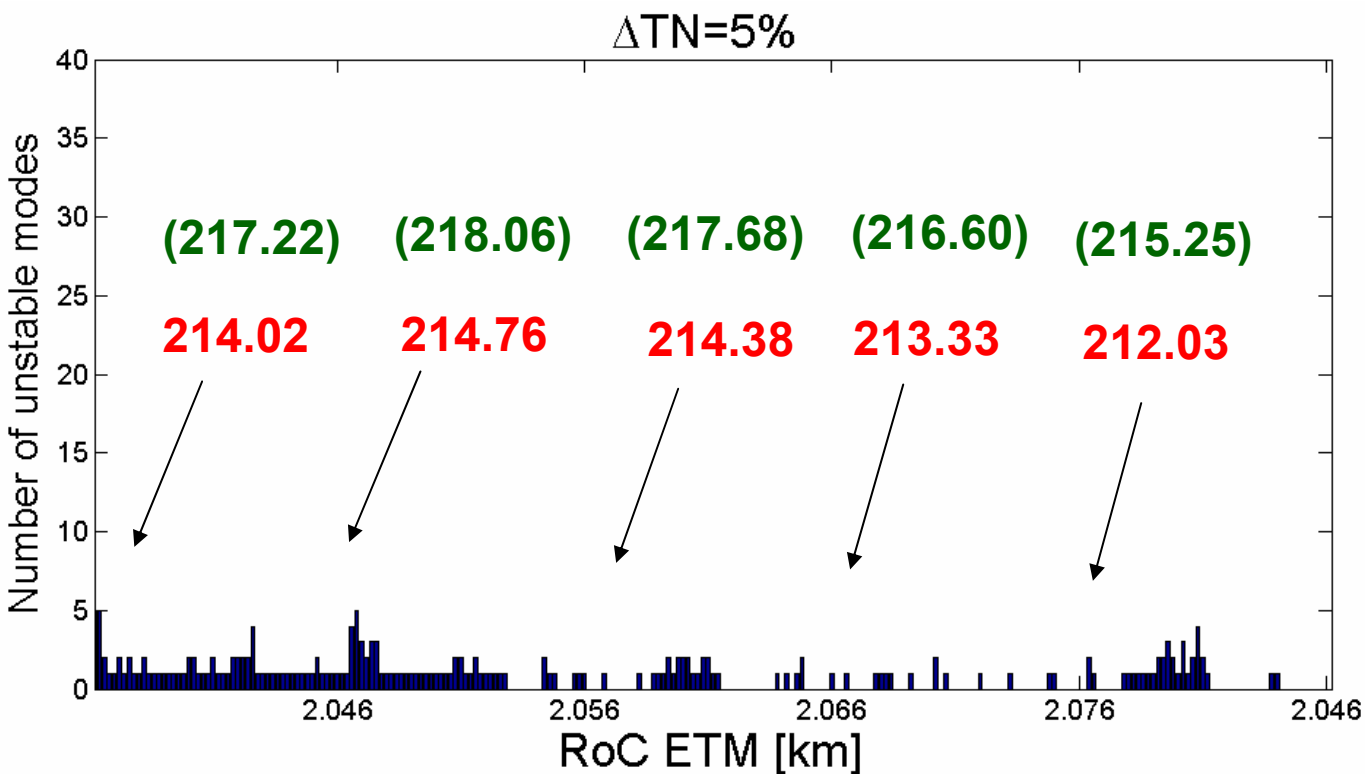


The NS/NS range was estimated using the Bench code (**switched off**: Residual gas, Seismic, Suspension, **FEM input**: Brownian TN of the substrate, coating and the ring).

**5% increase of the Brownian TN results in 1.6% degradation of the NS/NS range.**


sgras@cyllene.uwa.edu.au

LIGO

# Ring Dampers at the TNI

Akira Villar

LIGO Optics Meeting

November 9, 2006

Eric D. Black, Greg Ogin, Kenneth G. Libbrecht

# Instability Condition: R>1

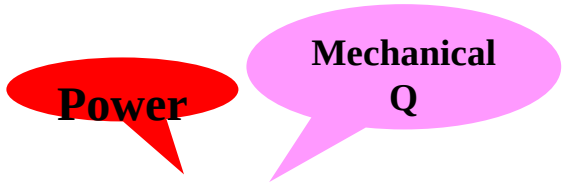


$$R \approx \frac{2PQ_m}{McL\omega_m^2}\left(\frac{Q_1\Lambda_1}{1+\Delta\omega_1^2/\delta_1^2} - \frac{Q_{1a}\Lambda_{1a}}{1+\Delta\omega_{1a}^2/\delta_{1a}^2}\right) > 1$$

Ju, et al. G050325-00 who got it from
Braginsky, et al. Phys. Lett. A 305, 111 (2002)

# Reducing Q's
# without affecting thermal noise (much)



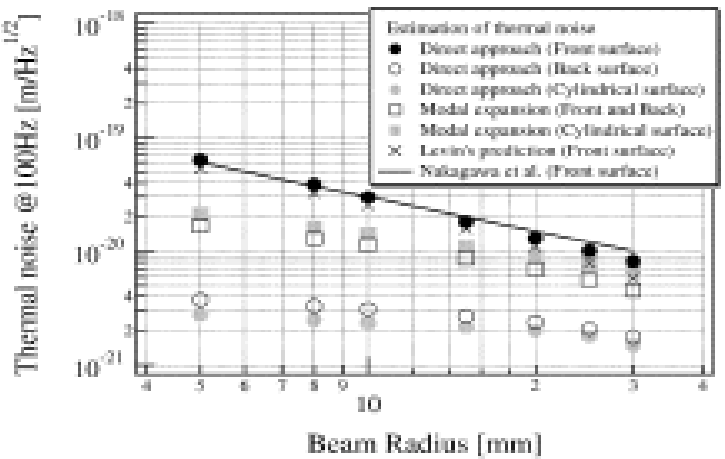


Fig. 3. Thermal fluctuations of surface models. This graph shows the dependence of the amplitude of the thermal noise at 100 Hz on the beam radius. The closed, open, and grey circles represent the thermal motions of the Front, Back, and Cylindrical surface models calculated from the direct approaches, respectively. The open squares are an estimation of the Front and Back surface models from the modal expansion. The estimations from the modal expansion in both cases are the same because the -values are the same. The grey squares show the evaluation of the Cylindrical surface models derived from the modal expansion. The crosses represent Levin's prediction about the Front surface model. The line shows an analytical estimation by Nakagawa et al. of the thermal noise of the Front surface model.

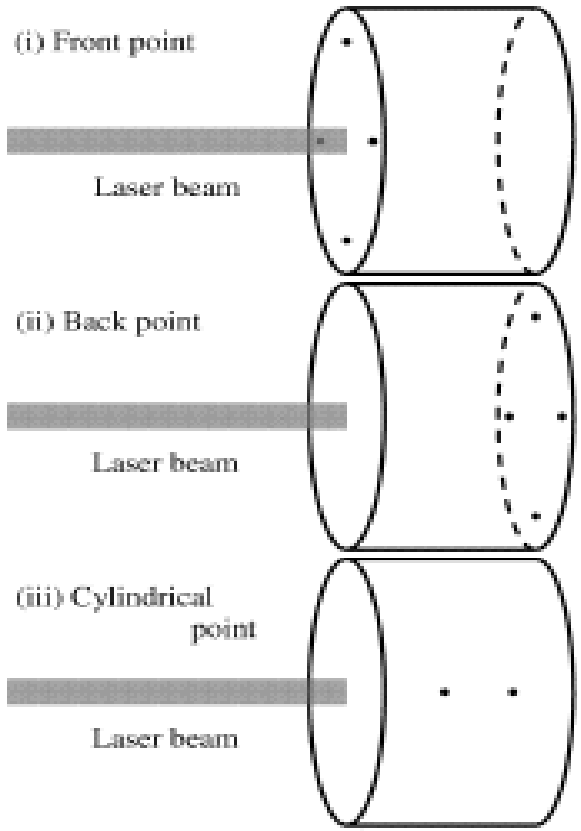


Fig. 4. Dissipation concentrated at points. The black dots indicate points at which the loss was concentrated. The other part had no

LIGO

# Ring Damper

Idea: Lossy ring around mirror barrel could suppress mechanical Q's of many modes, without affecting thermal noise on the face (much)

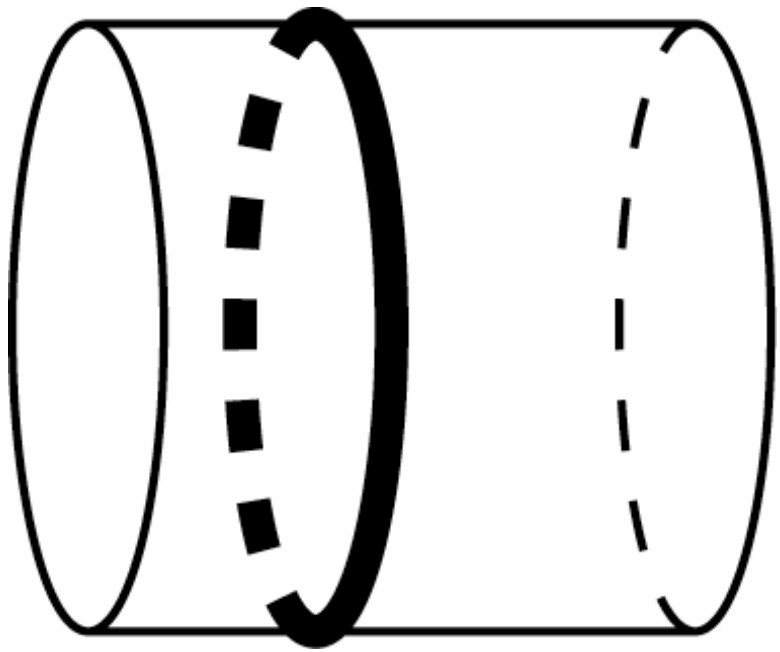

# FEA Model 1

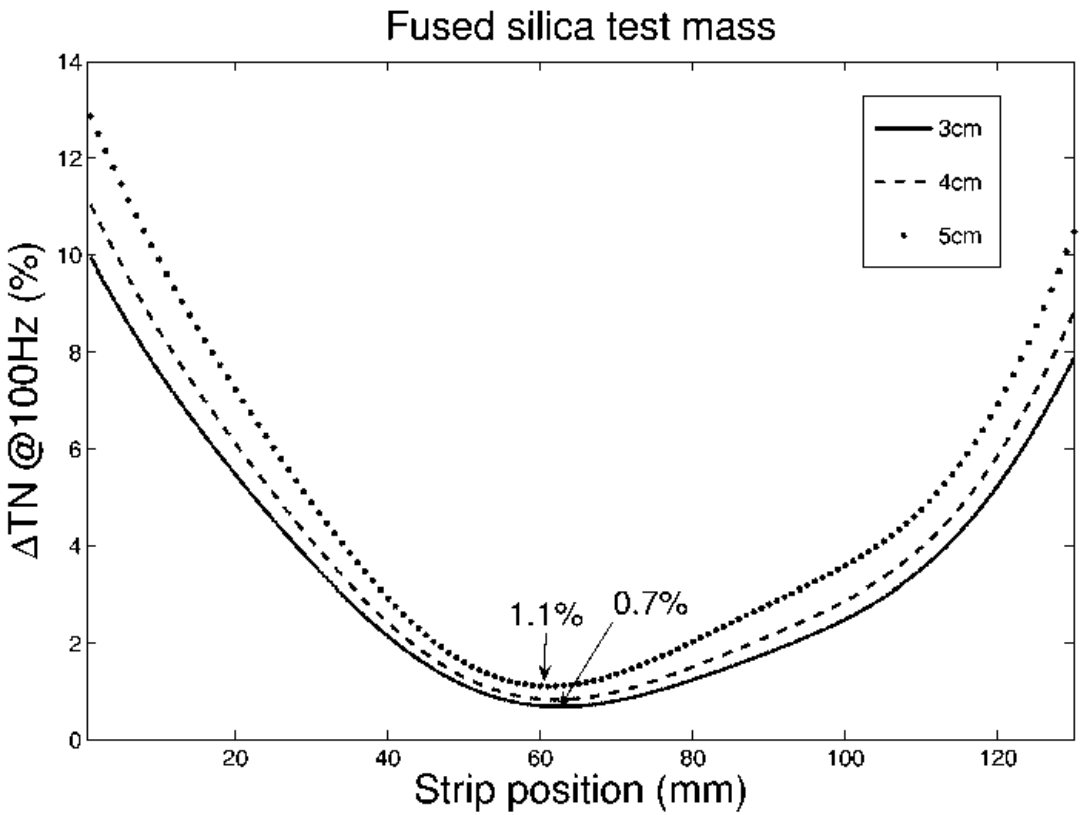


Gras, et al. preprint

*Test Mass Ring Dampers with Minimum Thermal Noise*

# FEA Model 2

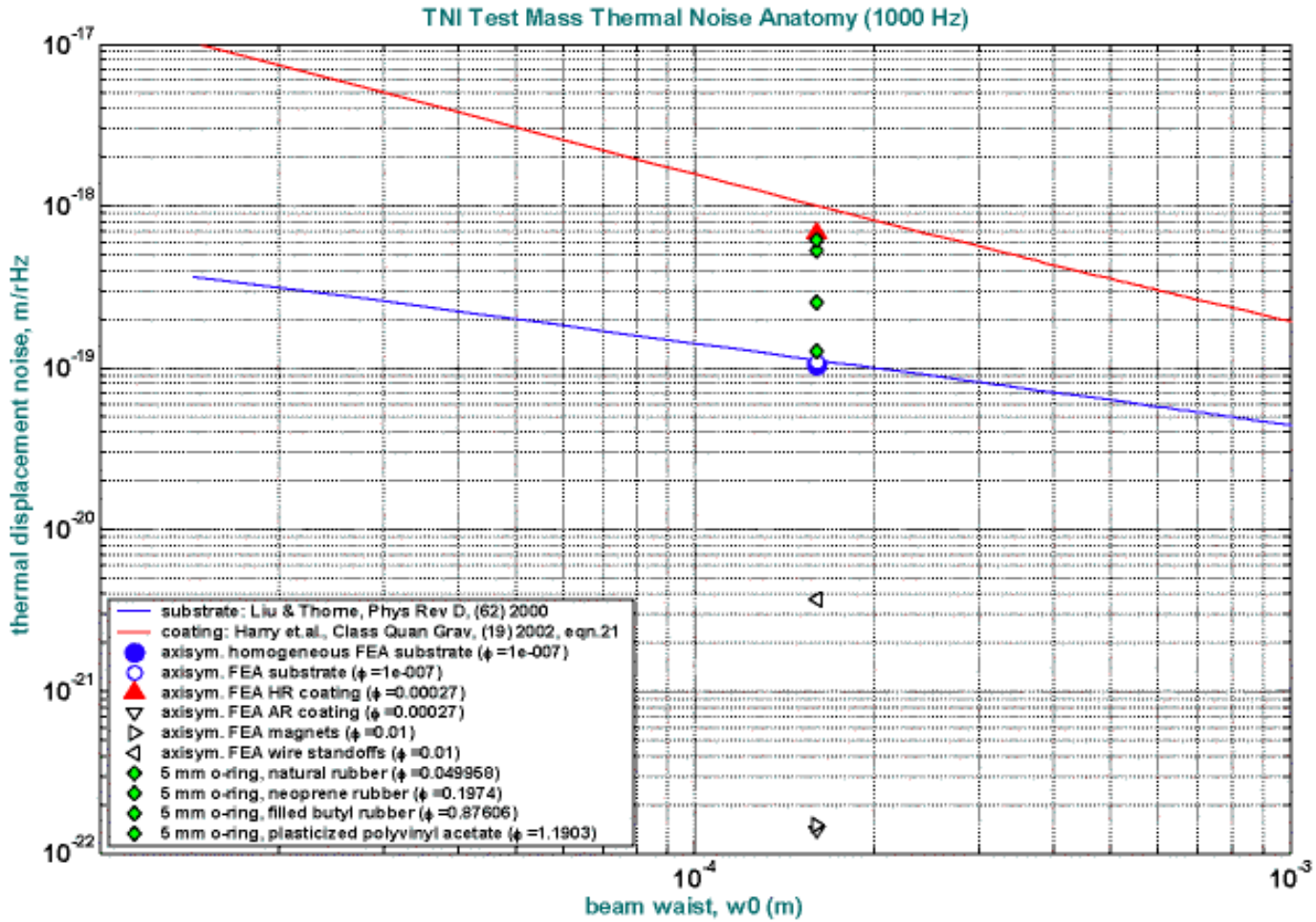


D. Coyne, T050173-00

# TNI Without Rings

- Fundamental-noise limited interferometer (thermal and shot).
- Test Cavities:
  - Fused silica substrates, 4” x 4” cylinder
  - Titanium doped silica tantala coatings
  - Ring dampers to be placed around SAC output mirror only

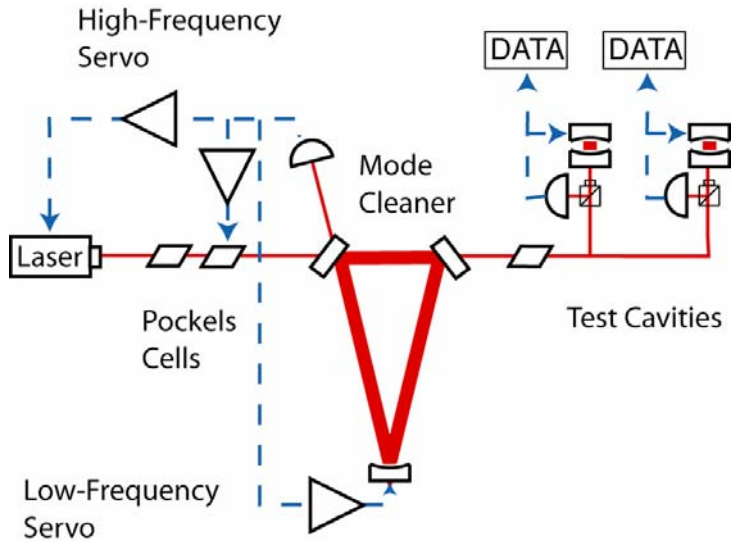


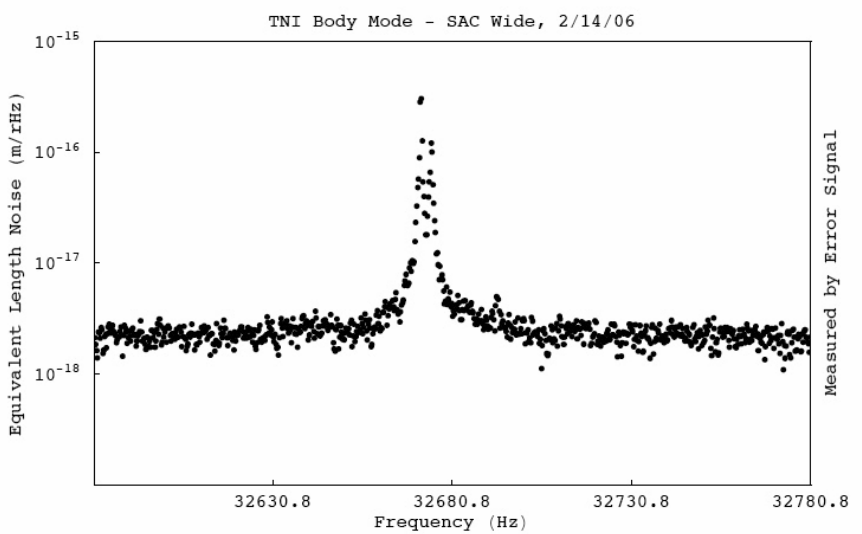


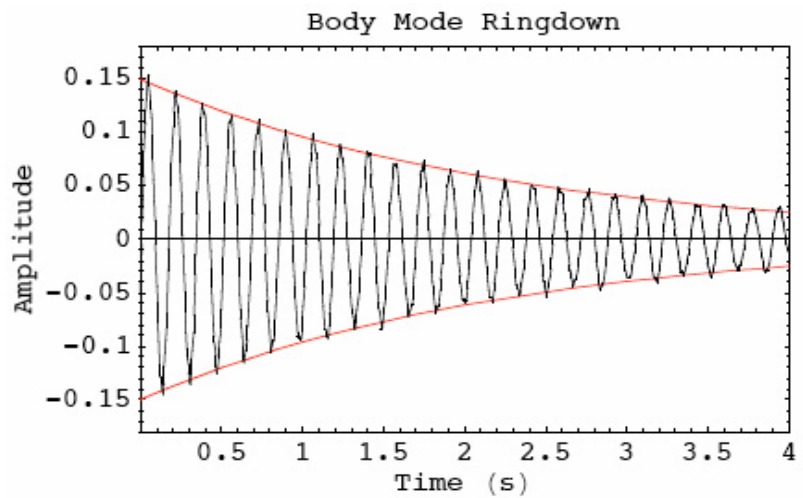

# TNI Without Rings

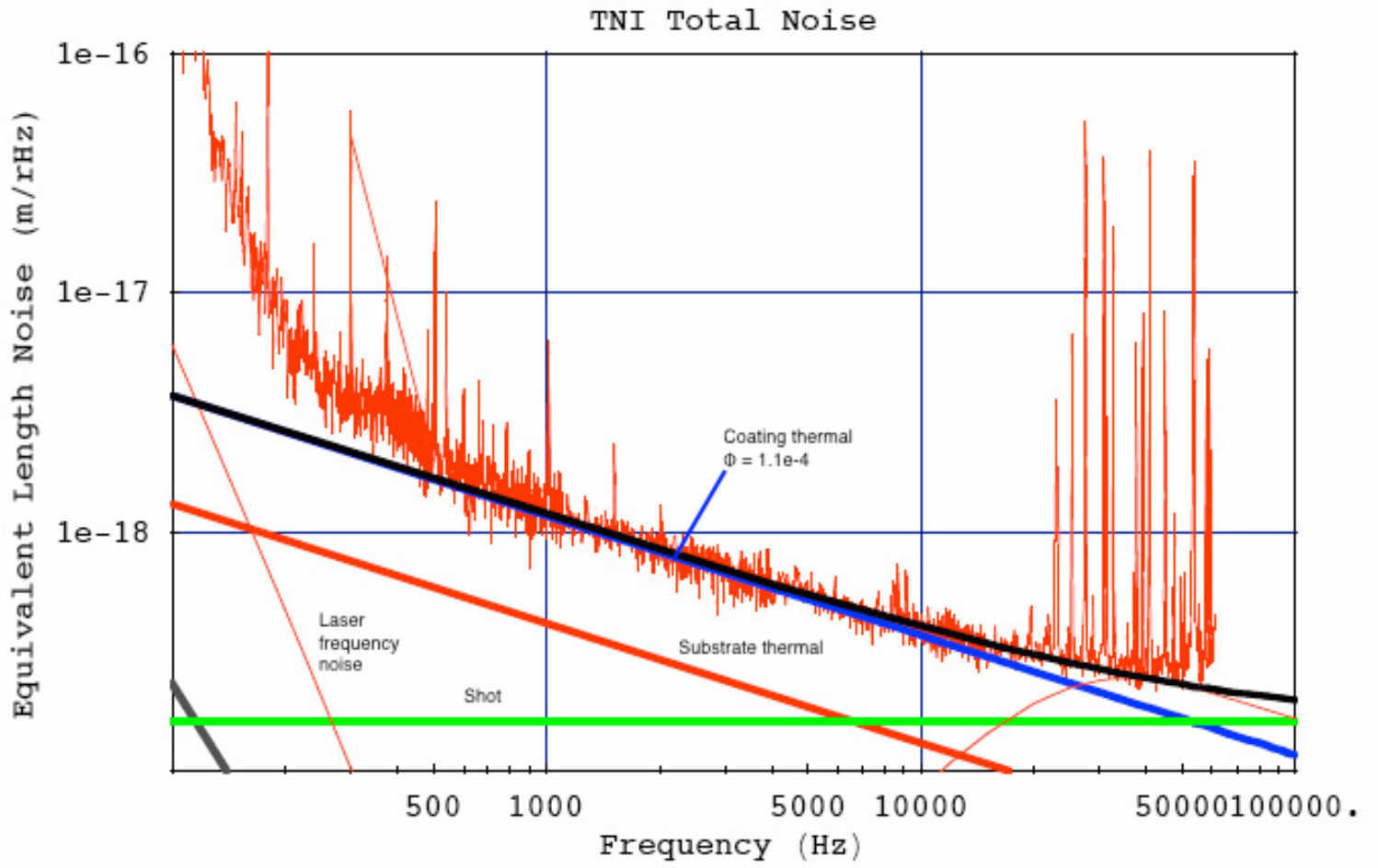

# Buna O-Rings

- Buna, 1/8” thick, undersized diameter (3.25”)
- Large Q reduction, Q’s now to small to measure by ringdown: can’t excite modes

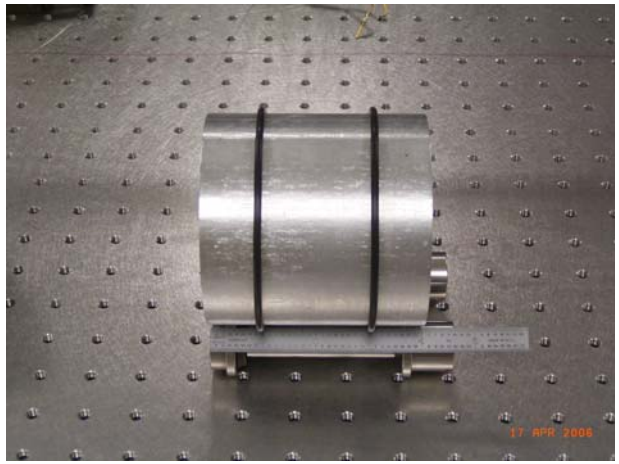

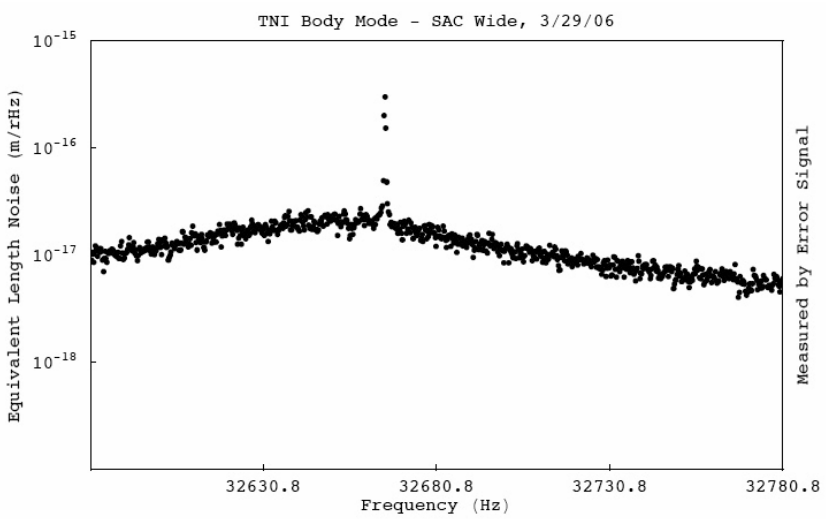


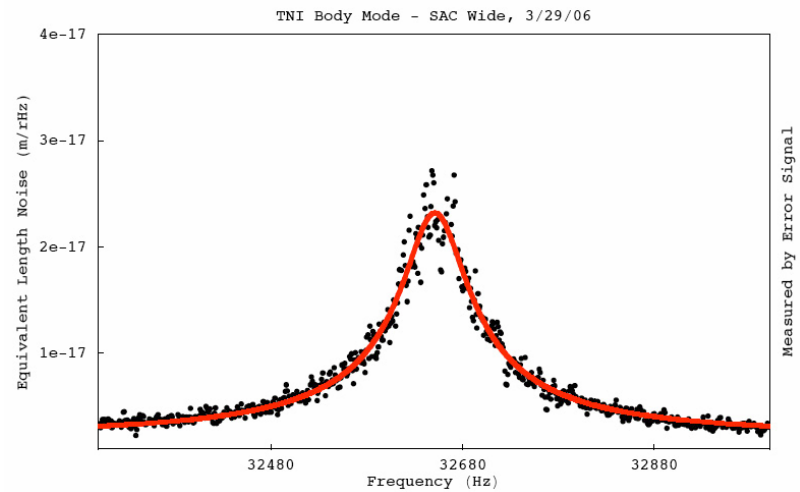

# Buna O-Rings

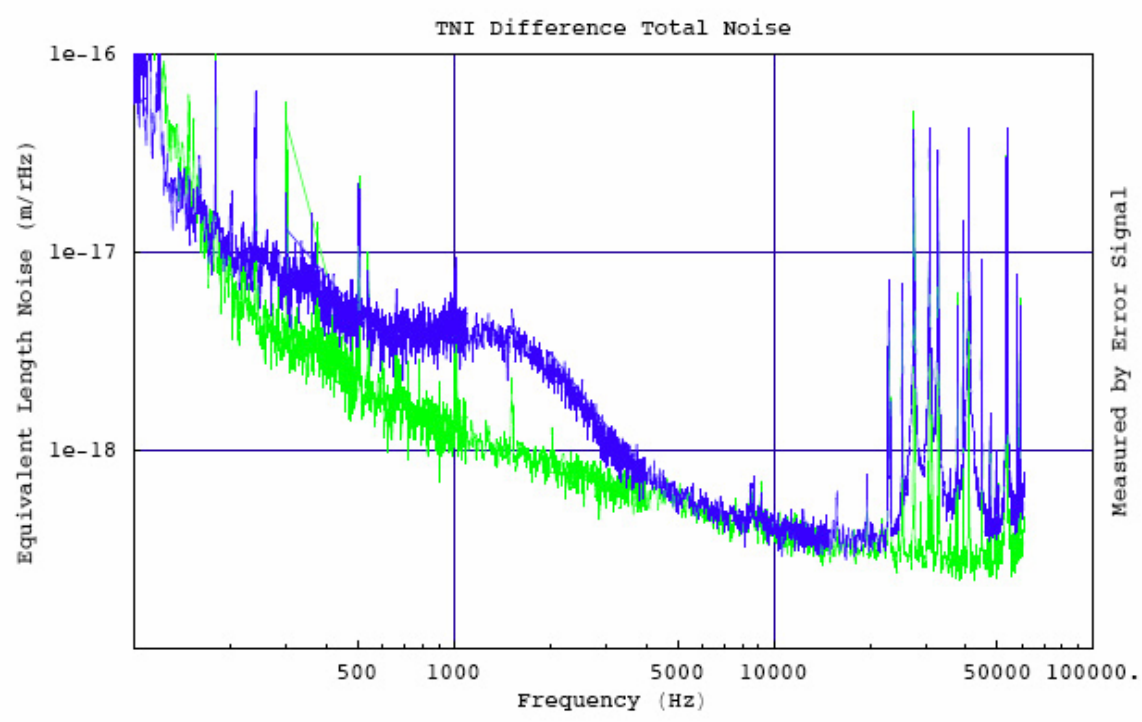


- Substantial increase in noise floor from 200 Hz to 4 kHz
- Still thermal noise limited above 5 kHz

# FEA Modal Analysis

- Dennis Coyne did a rough FEA modal analysis and found mechanical modes at a few kilohertz (wiggle modes of a square o-ring).
- Riccardo Desalvo and Phil Willems independently showed that low-Q modes at a few kilohertz could lead to the “shelf” observed in our broadband noise floor.
- Precise calculation would require detailed knowledge of o-ring shape when stretched, as well as contact area with the mirror.

Dennis’
“back of the envelope”
model

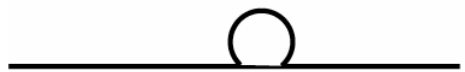

Actual o-ring geometry
not too different

# Kapton Tape

- Essentially massless, to avoid “waving” modes seen with buna.
- Lossy strip closely approximates models of Gras, Blair, et al.
- Q reductions range from factor of 2 to none at all

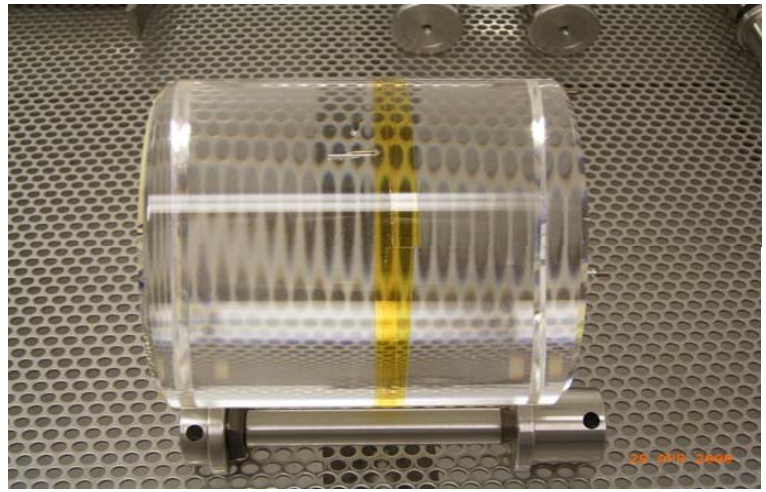

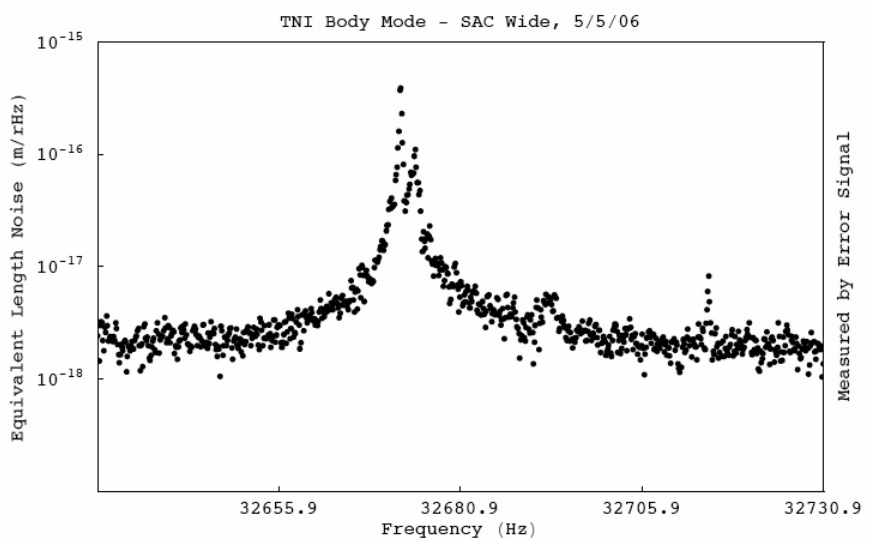


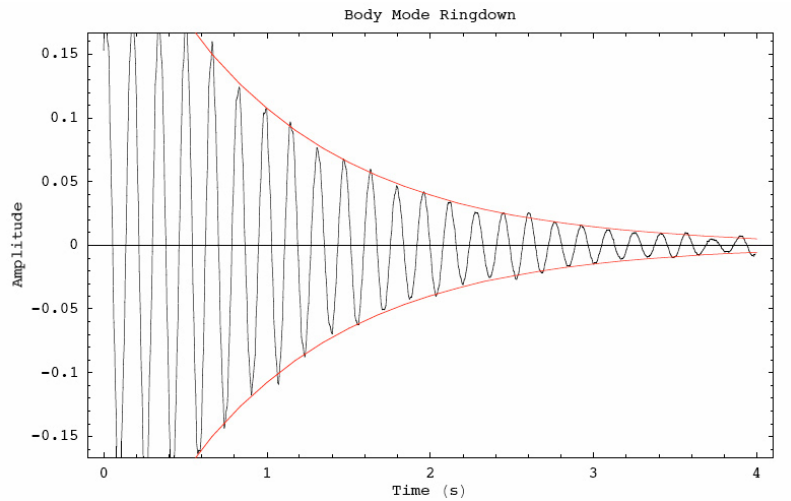

# Kapton Tape

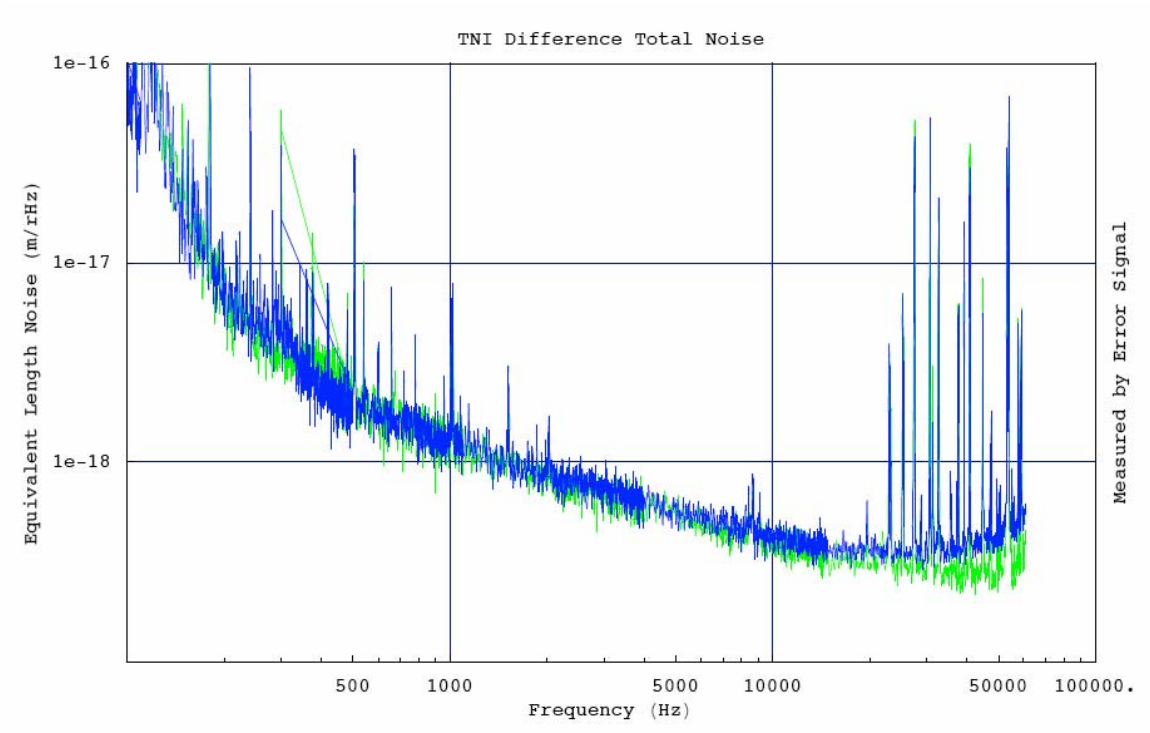


- No change in noise floor

# Q-Spoiling Oscillator Probably Needs Mass

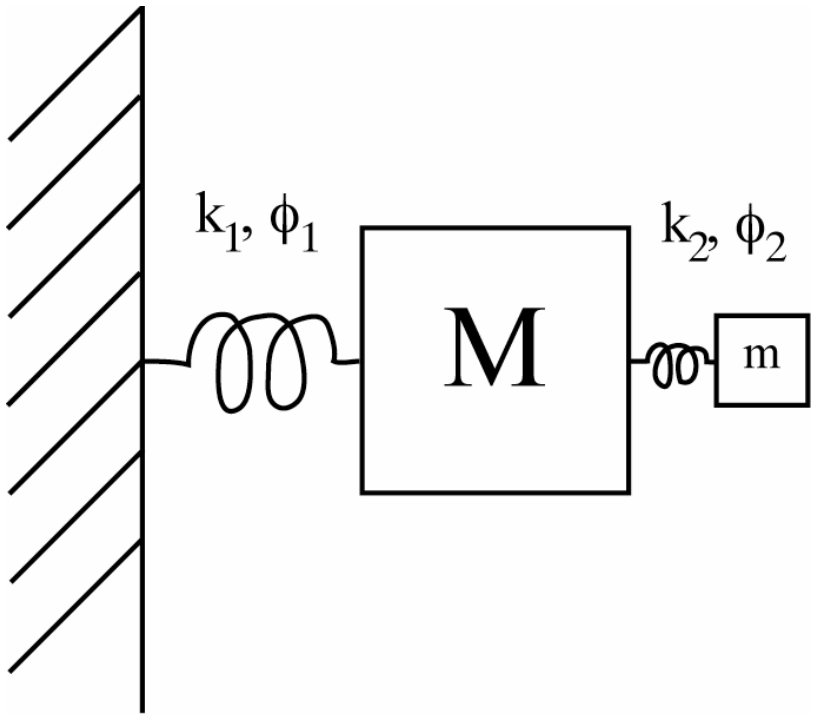


Bill Kells, private communication

# Copper rings I: Screw-tensioned

- Buna, kapton results tell us
  - Need mass to damp mirror Q's
  - Need "waving" mode well above the measurement band
- For expediency screw the rings on
- Q's were reduced below our ability to excite the modes, as with buna
- Noise floor increased, showing both new modes and additional broadband noise

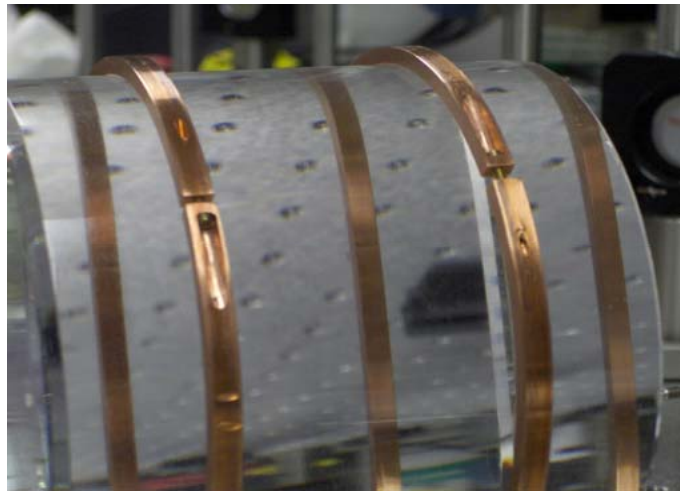

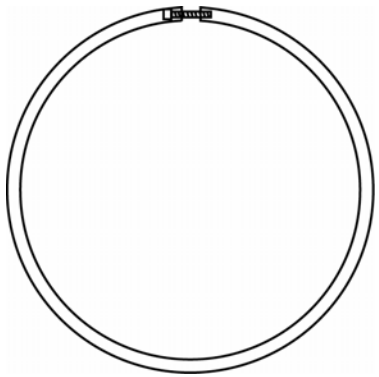

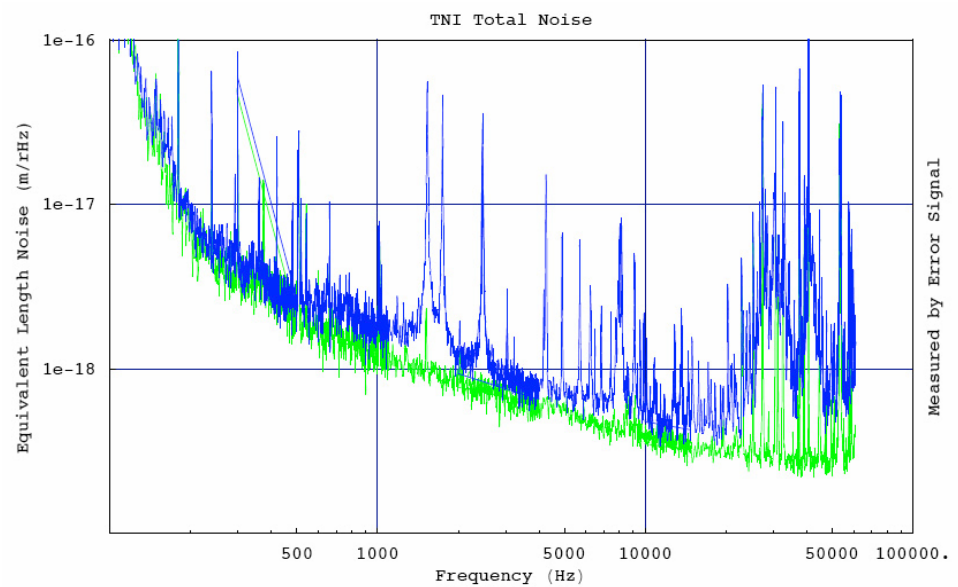

# Copper Rings II: Monolithic

- Monolithic copper rings machined undersized, heated for expansion, then placed around the barrel of the optic.
- At room temperature, 4.000” rings are 0.0025” undersized.
- Heating to 100°C expected to expand them to 0.0026” oversized.
  - Tabulated (Atomic Mac)

$$\alpha = 1.7 \times 10^{-5} K^{-1}$$

- Observed expansion is consistent with expectations.
- Rings slipped over mirrors easily, with no apparent damage to the optic.
- Q reduction still good, as with buna and screw-tensioned rings.
- Broadband noise floor ~unaffected below ~20kHz.

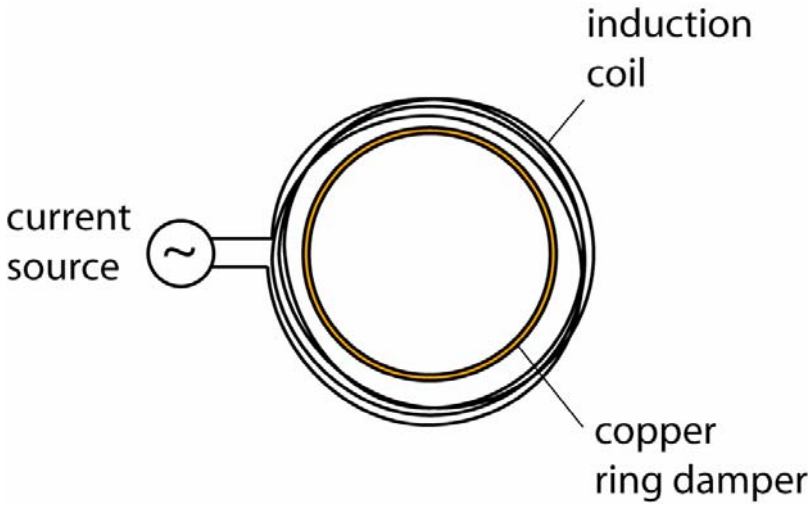

# Copper Rings II: Monolithic

- Q's were reduced.
- Small increase in thermal noise?

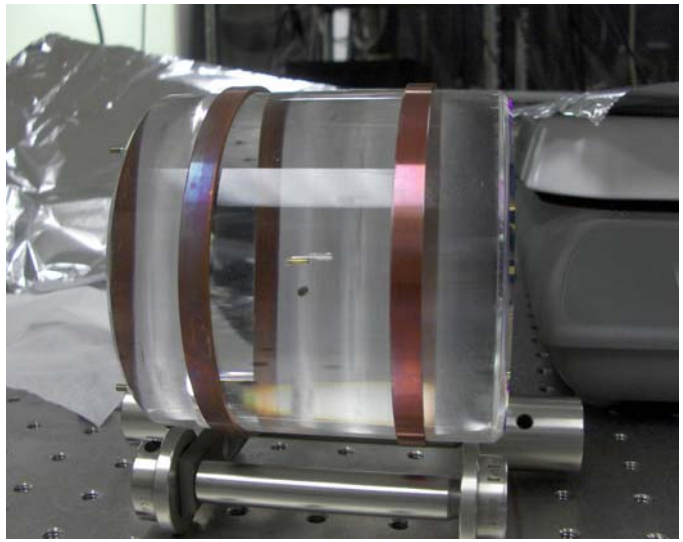

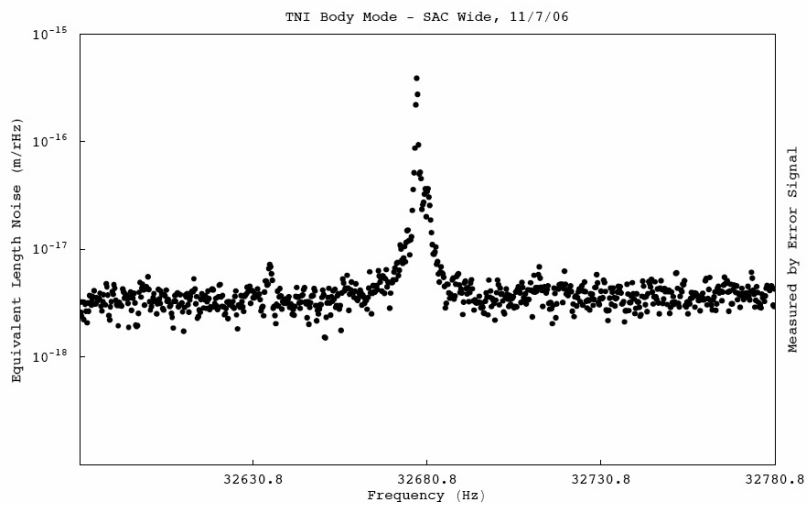


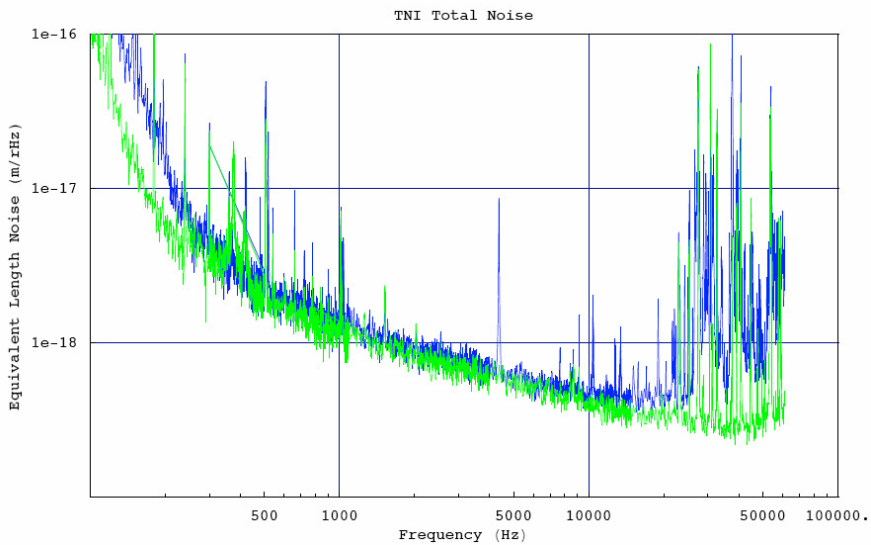

LIGO

# Conclusions

- Ring dampers need both loss and mass for effective Q reduction.
- Screws appear not to provide enough tension for the rings to contact the mirror everywhere around the barrel.
- Monolithic rings work better, appear to damp Qs without spoiling the noise floor in the TNI, up to the first body mode of the mirrors.
- Inductive heating works well, and hot rings do not appear to damage the optic during installation.
- Need to quantify Q reduction for different modes. FEA model?

# Experimental Investigation of Parametric Instabilities at Gingin Facility

ACIGA
University of Western Australia

L. Ju, C. Zhao, S. Gras, S. Schediwy, P. Barriga,
Y. Fan, Z. Yan, D. G. Blair,

# Gingin Cavity

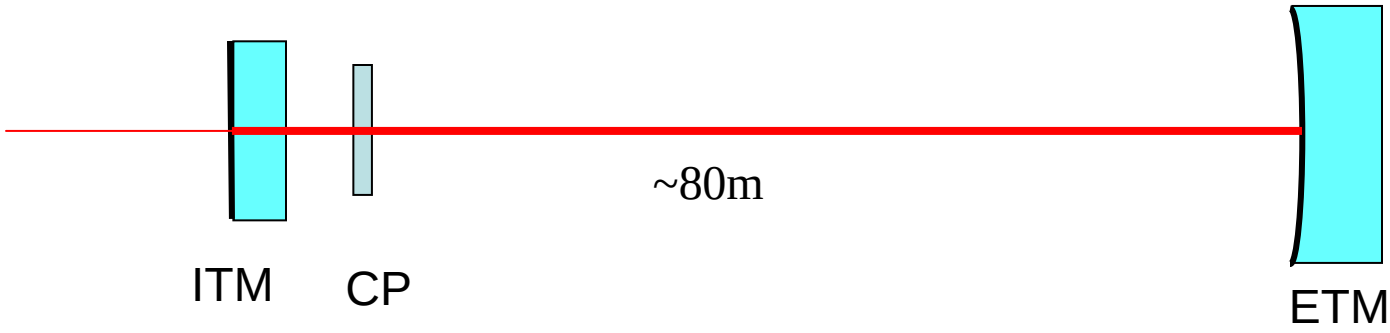


- ITM—a-axis Sapphire, 100×46, RoC=∞, Substrate reversed, absorption~ 50ppm
- ETM—m-axis Sapphire, 150×80 RoC=720m
- Compensation Plate—Fused silica
- Cavity waist—8.7mm (cold),
- Finesse—1300

# Gingin Cavity vs Parametric Instability

- FSR of Gingin cavity—1.95 MHz
- Mode spacing
  - Cold cavity,

    $\Delta f_{LG41}$=89kHz, $\Delta f_{LG01}$=206kHz
  - Hot cavity with 1kW power

    $\Delta f_{LG41}$=86kHz, $\Delta f_{LG01}$=256kHz
  - Compensation plate thermal tuning-> $\Delta f_{LG01}$=63kHz

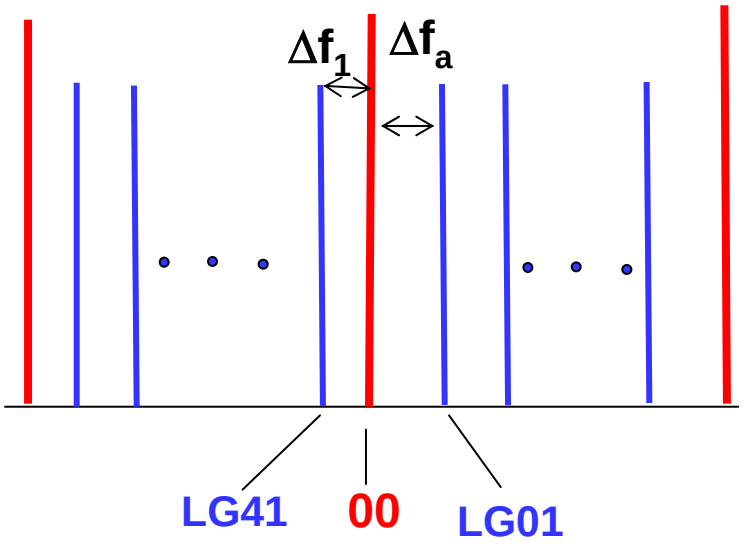

# Four Stage Plan for Parametric Instability Experiments

1) Thermal tuning of high order optical modes
2) Observe 3 mode interactions using externally excited acoustic modes
3) Observe acoustic mode Q changes to determine R
4) Test control techniques

# Thermal tuning of optical mode spacing between LG00 and LG01

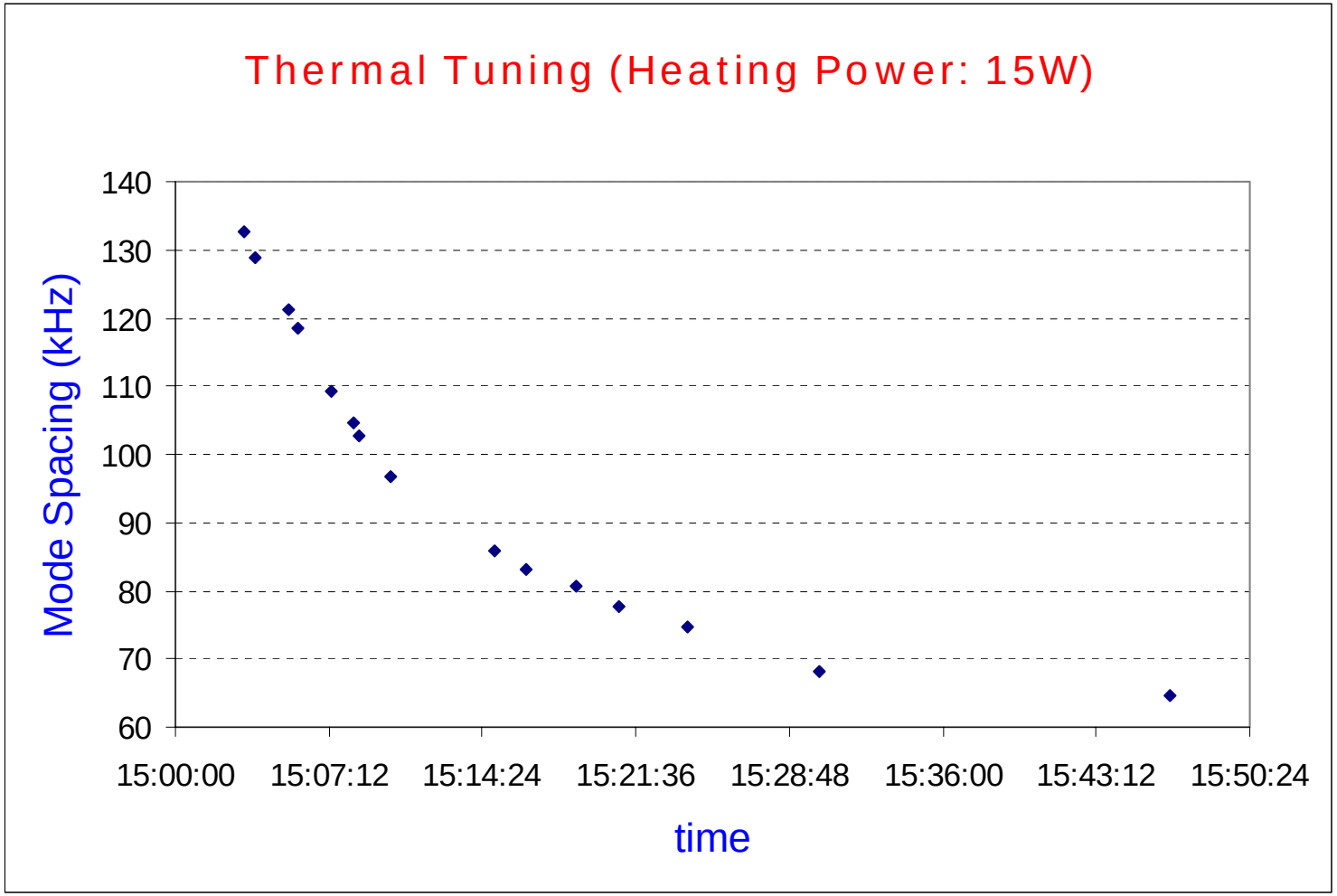

# 3 mode & 2 mode interactions

- 2 mode interactions
  - Short cavity, large FSR
  - Sidebands within cavity bandwidth
  - optical spring effect
  - Observed (MIT group, 40m, Caltech microcavities, UWA Niobe, Moscow RF )
  - Potentially useful method of damping instabilities
- 3 mode interactions
  - Long cavity, small FSR
  - 30kHz-140kHz test mass acoustic modes
  - parametric instability
  - Not yet observed

# 2 mode interaction: damping tool

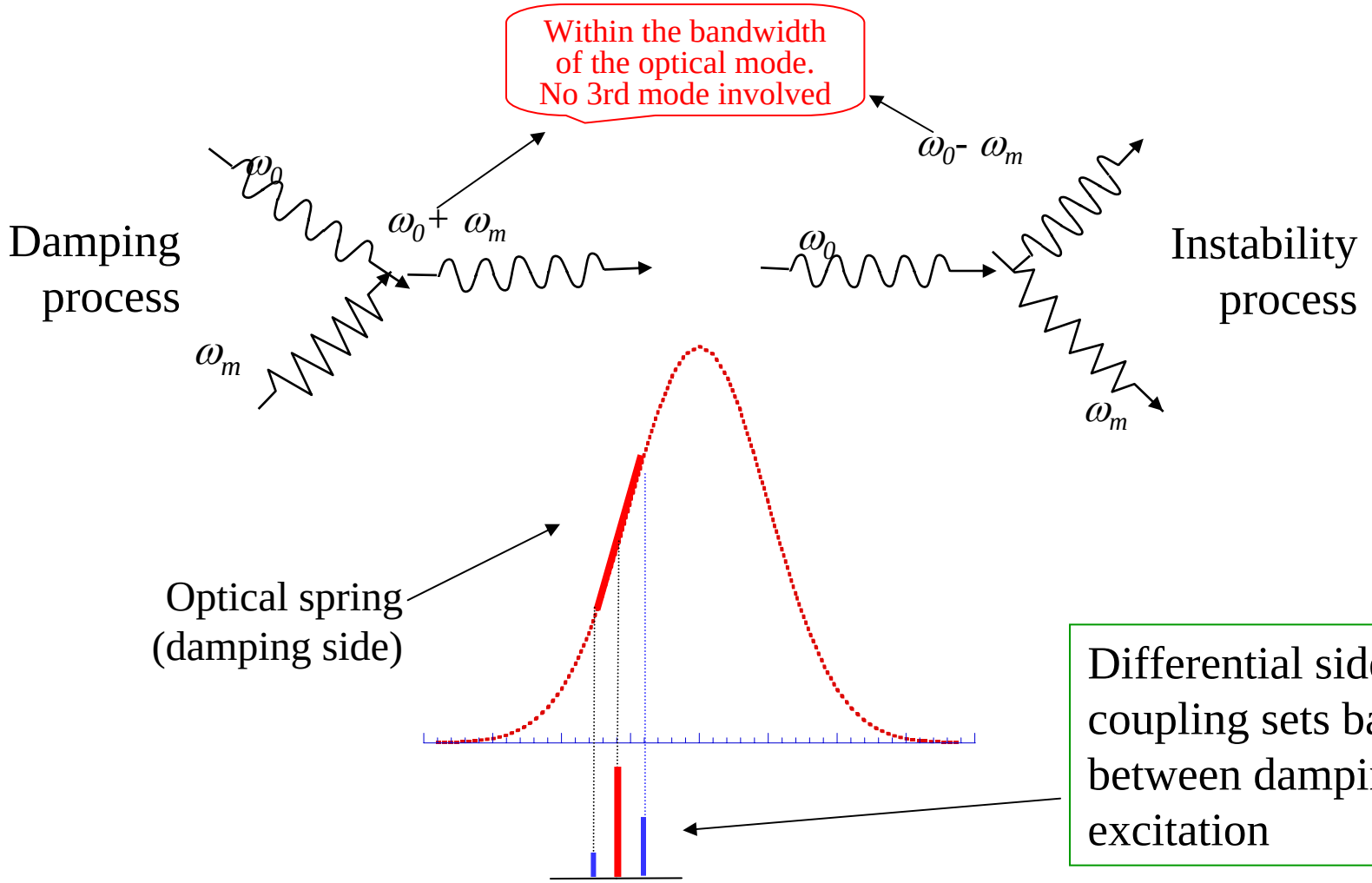


Differential side band coupling sets balance between damping and excitation

# 3 mode interactions

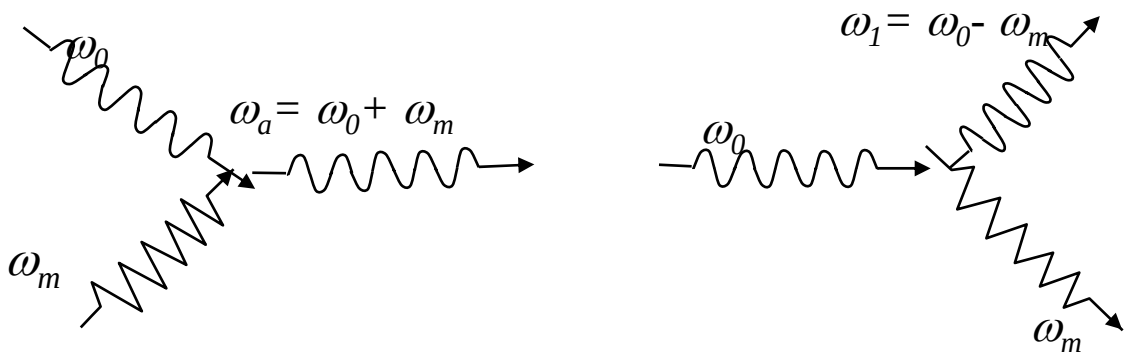


- Narrow lines acoustic frequency
- Sideband power flow determined by existence of extra cavity modes
- Intrinsic asymmetry of mode structure

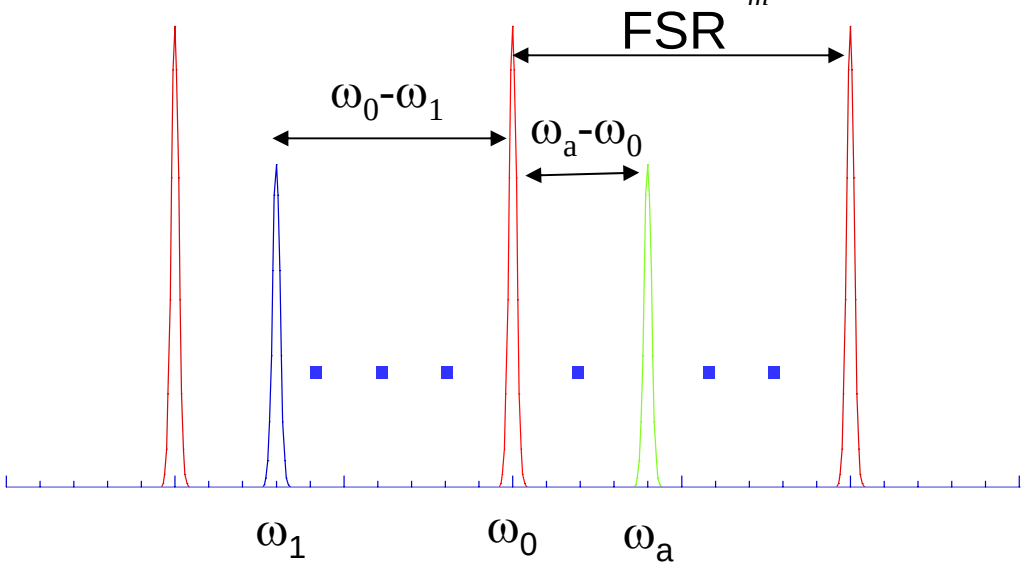

# Gingin 3 modes interaction observation (planned)

- Excite the target acoustic modes (electrostatically or magnetically)
- Observe the high order mode resonance as the HOM offset is thermally tuned

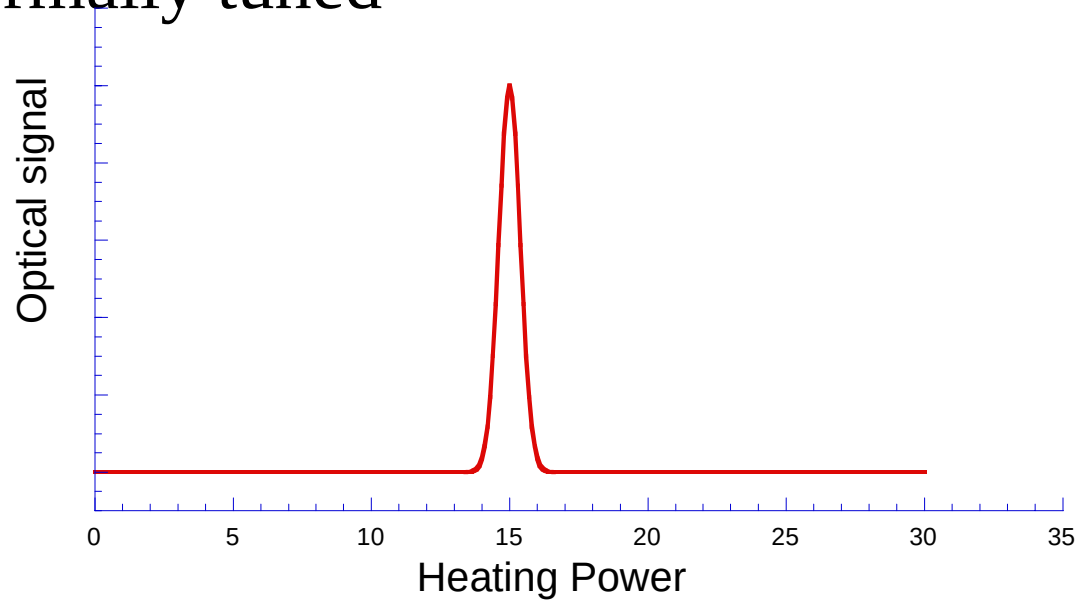

# Candidate modes

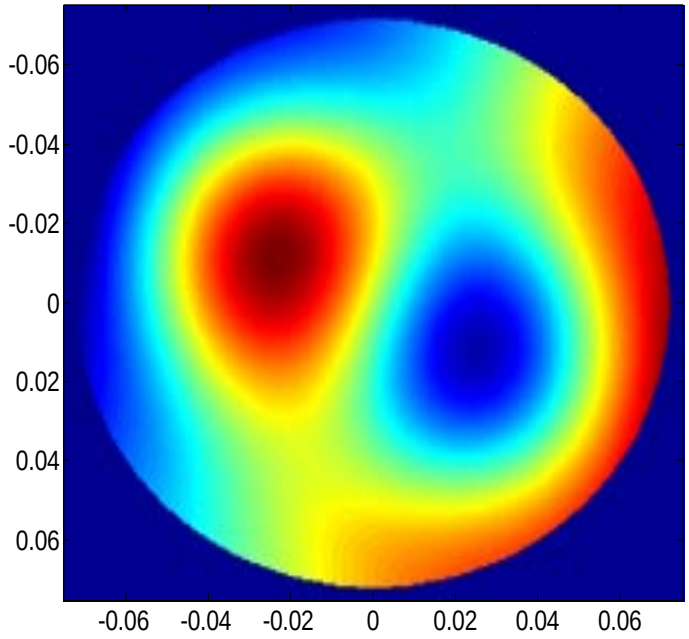


Acoustic mode $f_m$=62.1 kHz

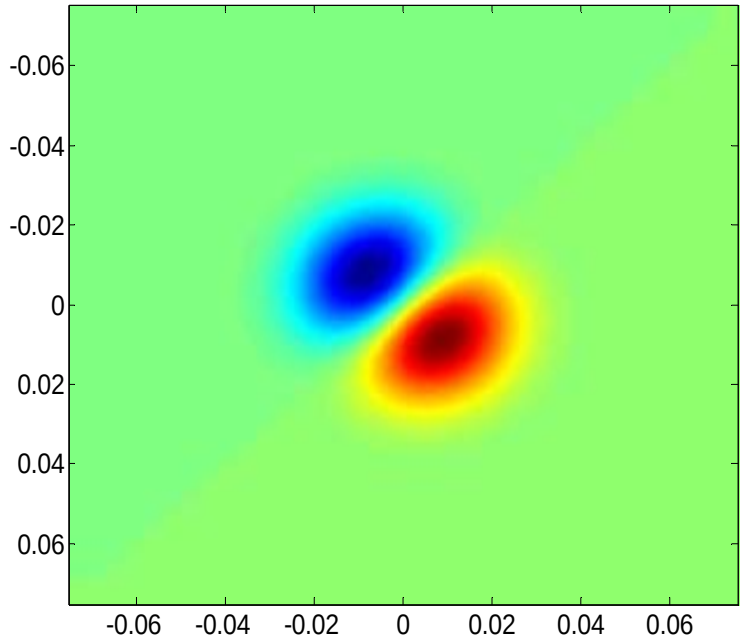


Optical mode, LG01 (w=17mm with compensation plate thermal tuning)

B=0.29, $\Lambda=B^2\times M/M_{eff}=0.4$,

P=1 kW, $Q_m=10^7$

**R= -0.19** Anti-Stokes

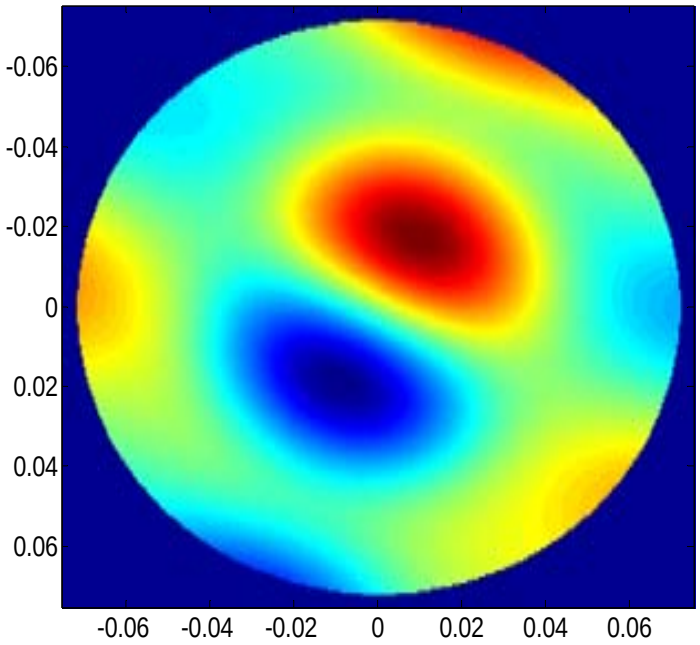


Acoustic mode $f_m$=86.2 kHz

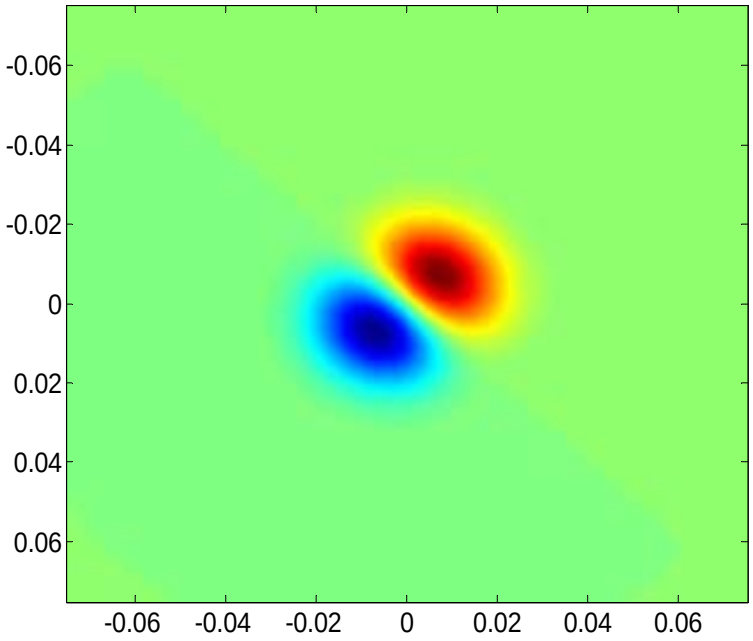


Optical mode, LG01 (w=14mm)

B=0.29, $\Lambda$=0.32,
P=1 kW, $Q_m=10^7$
**R= -0.16** Anti-Stokes

* Mechanical modes calculation taking into account anisotropic mechanical properties of sapphire

# Current Status

- Confirmation of observed acoustic modes shape to modelled modes—modeling accuracy.
- Acoustic excitation attempted by both electrostatic comb and using OSEM actuator
  - Excitation difficulties: magnet stand-off is a low pass filter. Electrostatic comb a bit too far from substrate.
- Still searching for mode that matches the Stokes mode with a reasonable overlap factor.
- New calculation of mechanical modes uses anisotropic mechanical properties of sapphire; substantial change in mode frequencies and mode shapes.

# Study 3: Mechanical Q change

**What we expect**

| | | |
|---|---|---|
| **R=1** | **Q= infinity** | **Unstable** |
| **R=0.1 (-0.1)** | **~10% increase (decrease) in $Q_m$** | |
| | **Detectable** | |
| **R=0.01(-0.01)** | **~1% increase (decrease) in $Q_m$** | |
| | **Hard to detect** | |

**To observe the Q change of the two mechanical modes mentioned above need Q-factor to be high enough. There may be large suspension losses.**

# Experimental Set Up

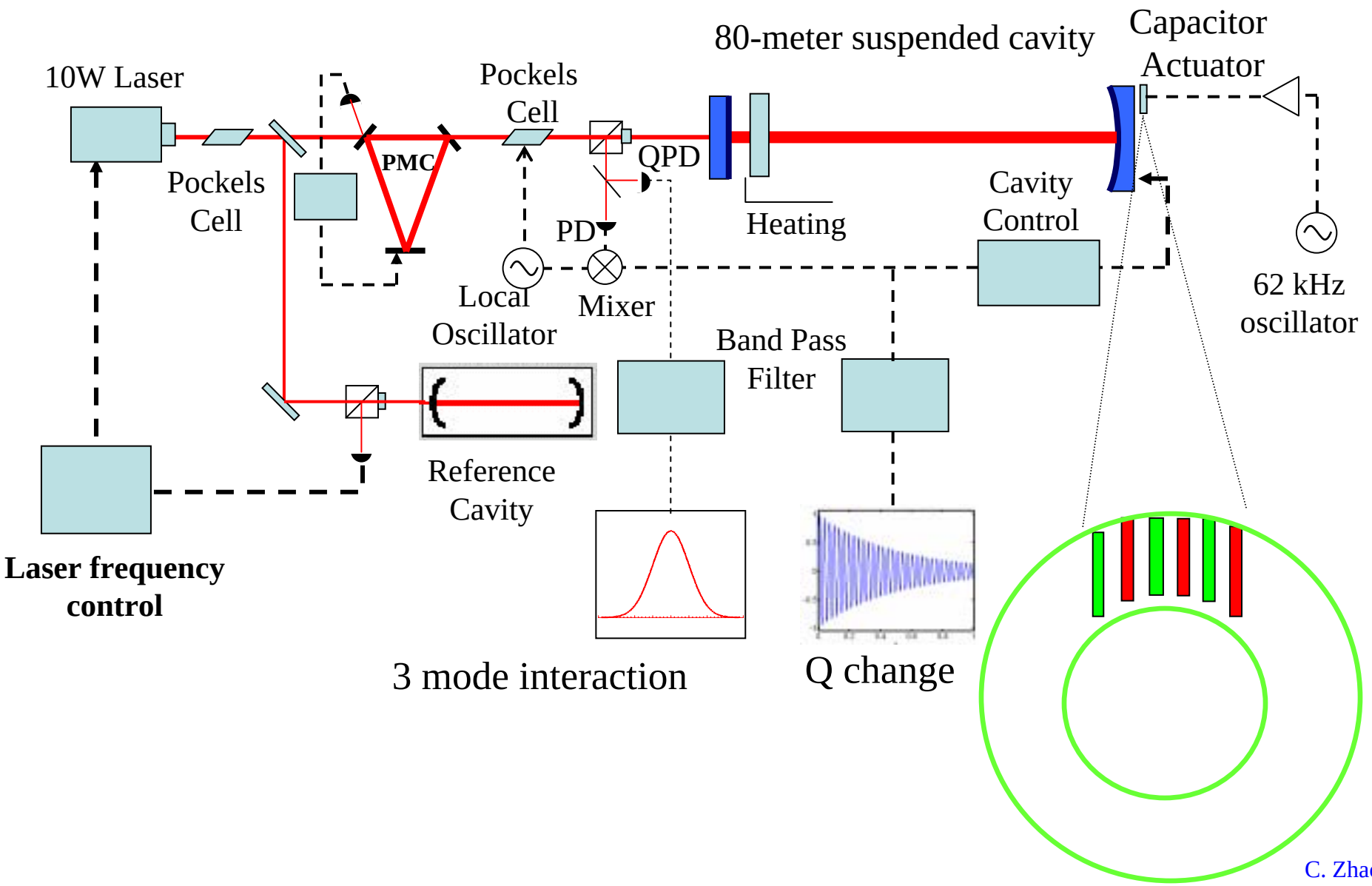


C. Zhao

# Optical tranquilizer ?

Braginsky's proposed Tranquilizer (*Phys. Lett. A 293, 228,2002*)
--2 modes interaction

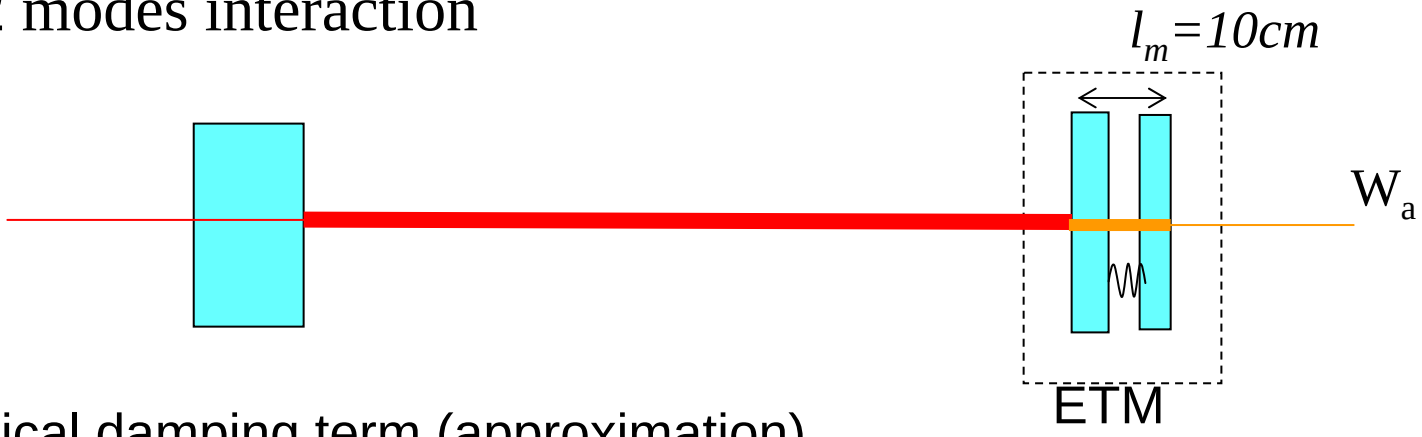


Optical damping term (approximation)

$$\delta_l \cong -\frac{64 W_a \omega_a}{mc^2 \delta_a} \frac{1}{T_a^2 (1+\rho^2)^3} \frac{\xi}{(1+\xi^2)^3} \longrightarrow 5.5\ s^{-1}$$

$W_a = 1W$ $\quad \omega_a = 2\times10^{15} s^{-1}$
$T_a = 3\times10^{-5}$ $\quad L_a = 1\times10^{-4}$
$l_m = 10cm$ $\quad \delta_a \approx 1\times10^{5} s^{-1}$
$m = 10kg$ $\quad \xi = -0.45$

Compared with mechanical $\delta_m \sim 5\times10^{-3} s^{-1}$

# Optical Spring Constant

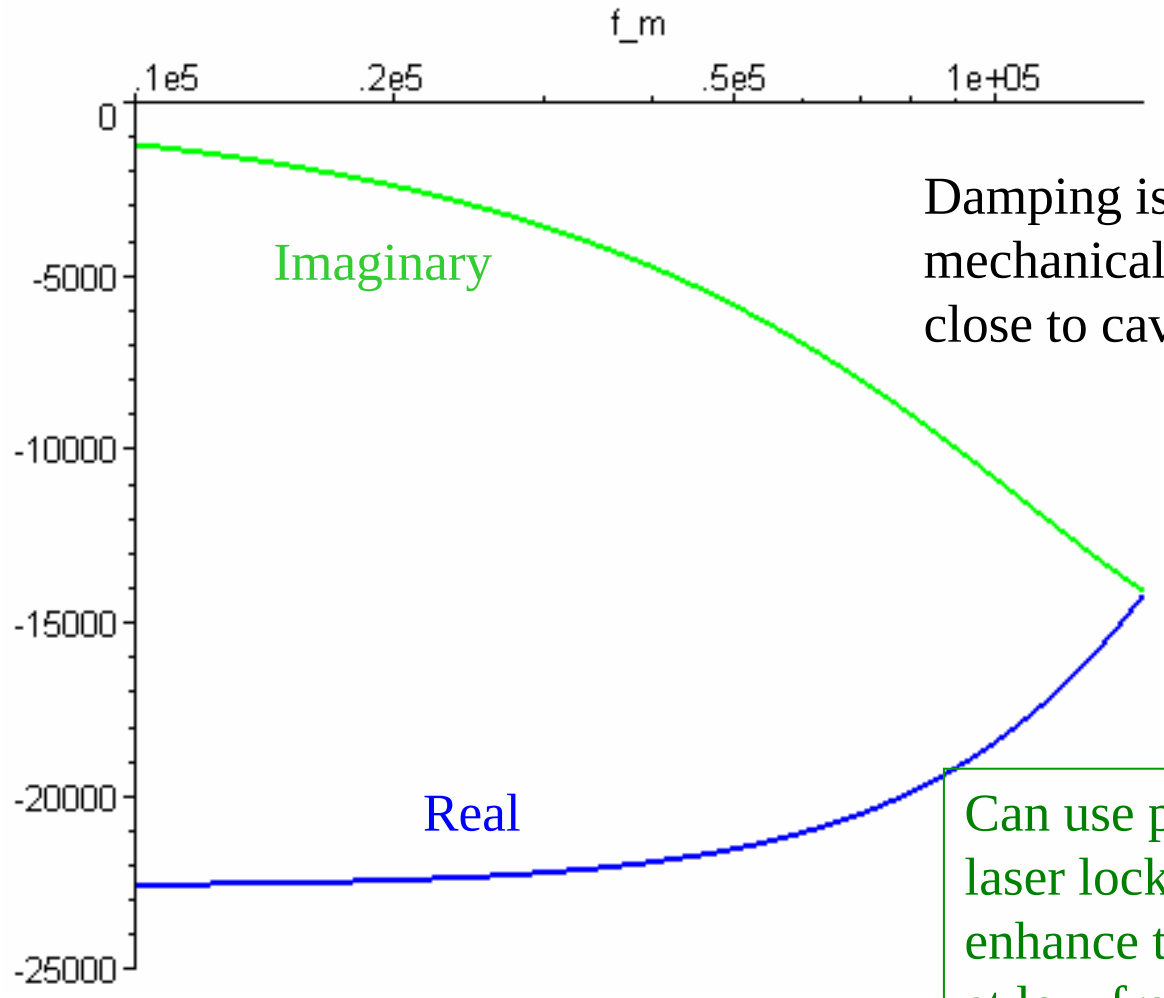


Damping is only large when mechanical frequency is close to cavity linewidth

Can use phase shift in laser locking servo to enhance the damping term at low frequency at the expense of the real term.

# Enhanced Optical spring damping
## --a 10cm cavity result

748Hz

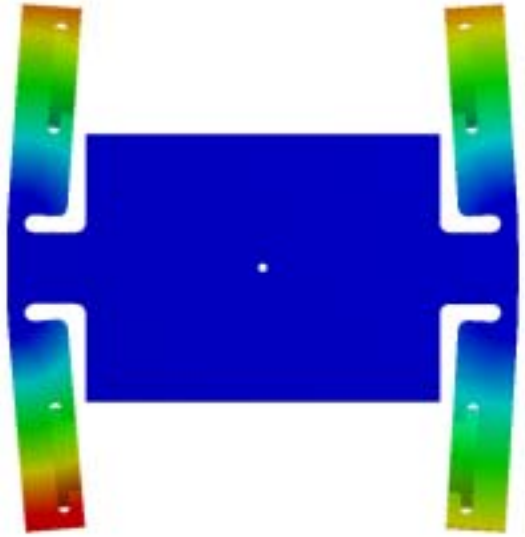

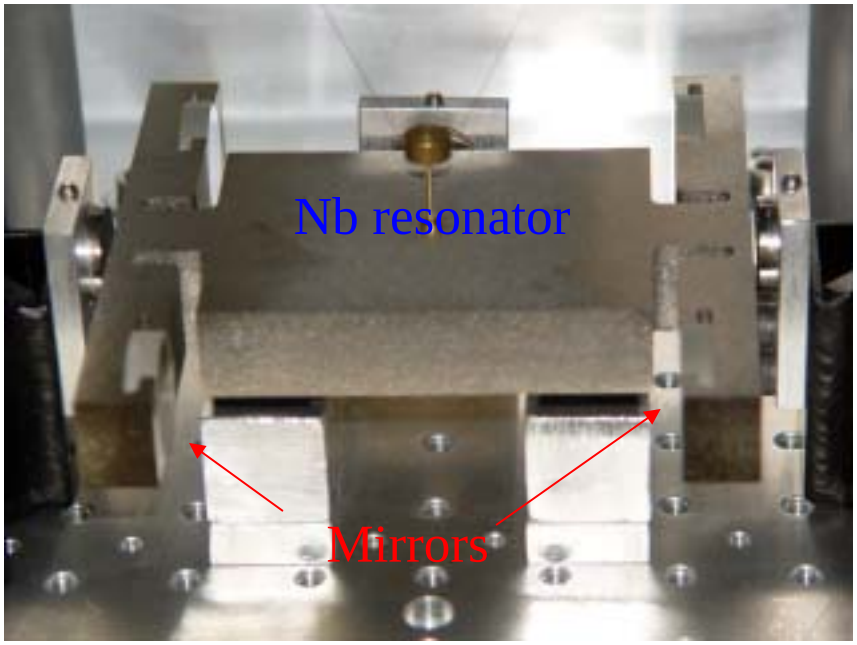


Cavity frequency ~ $10^{-2}$ Advanced LIGO instability frequency

Effective mass ~ $10^{-2}$ Advanced LIGO test mass

input power up to 30mW, Finesse ~4500

# Schematic servo system for the 10cm cavity

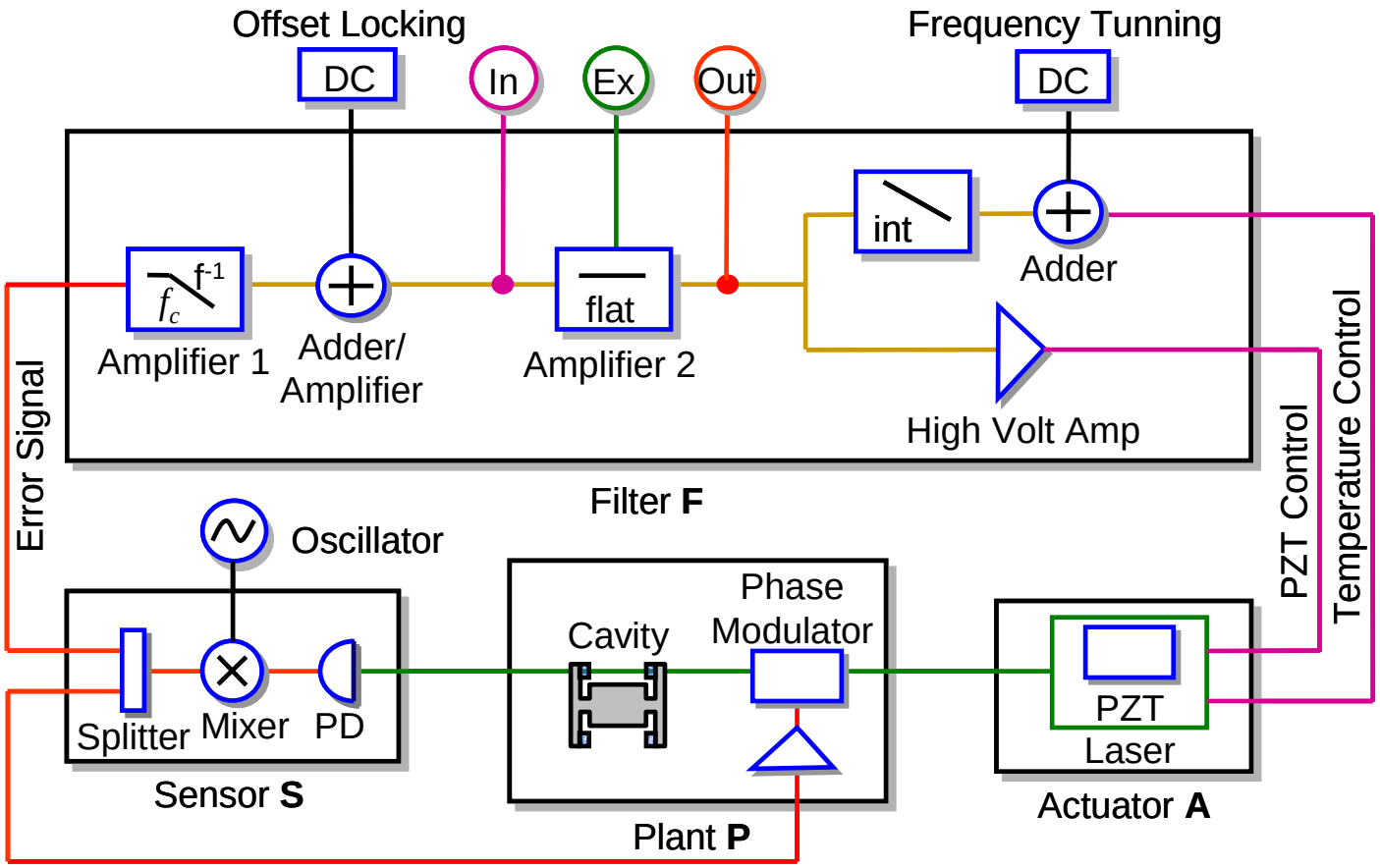

# Enhanced Optical Spring Effect

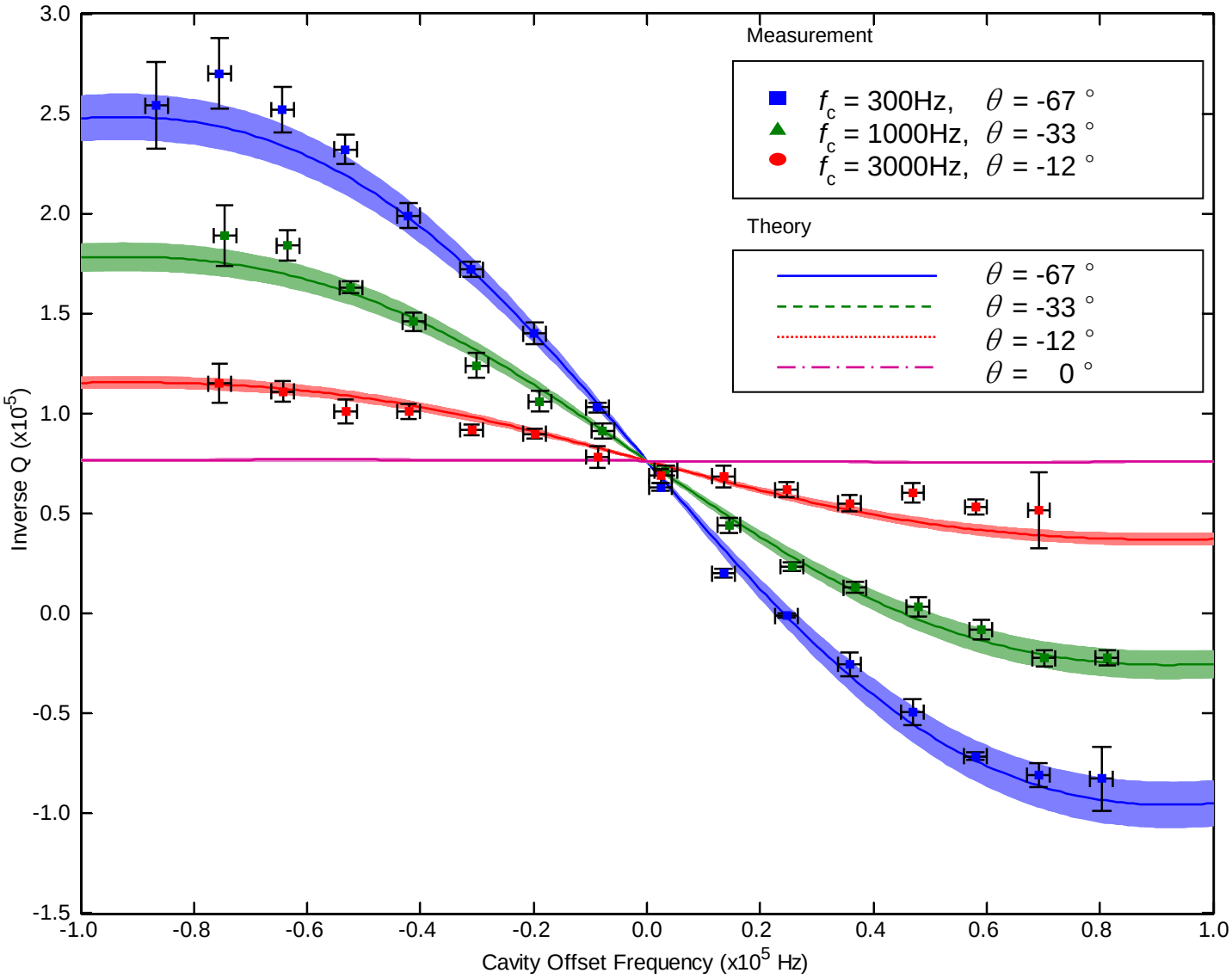

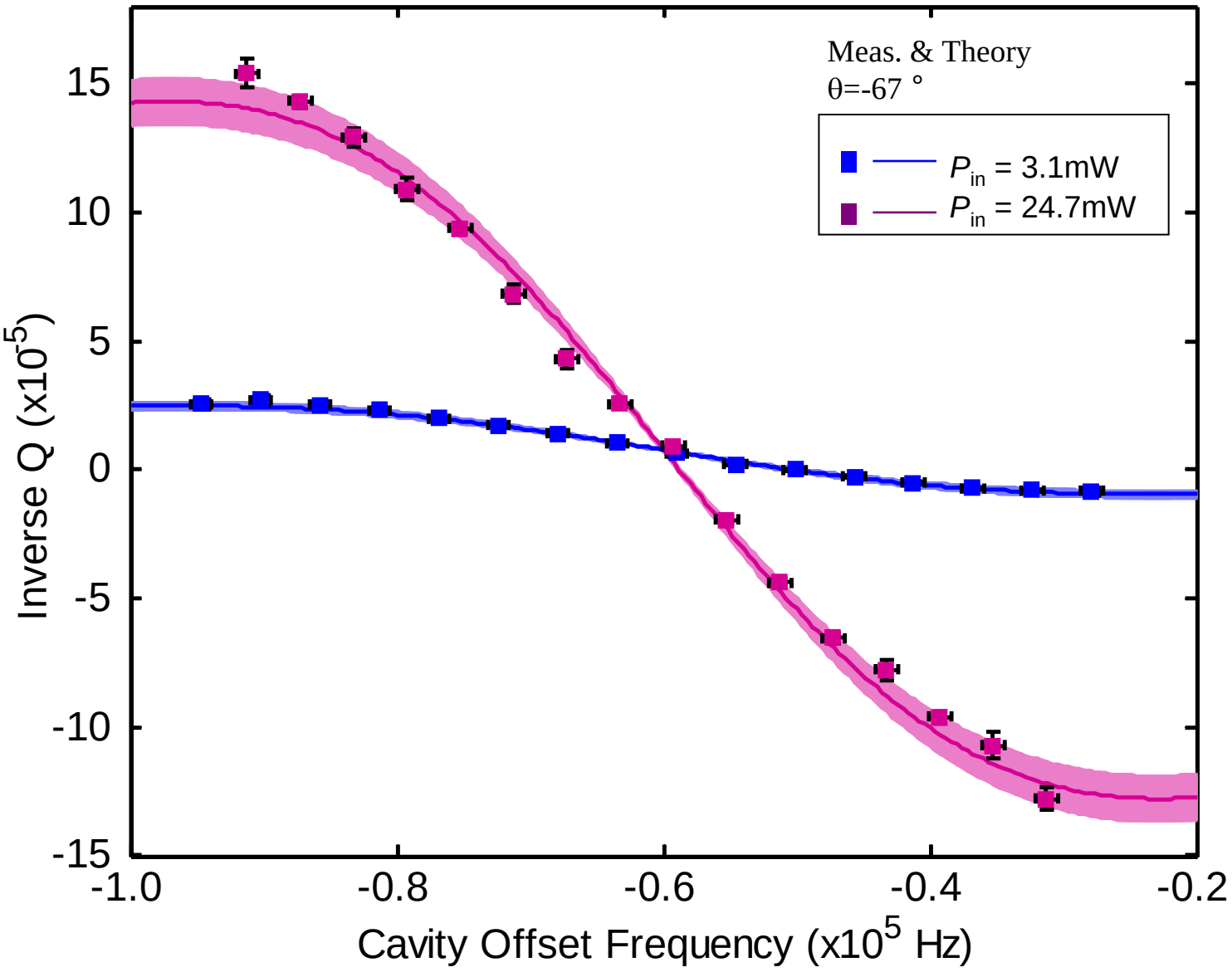
Meas. & Theory
θ=-67 °
$P_{in}$ = 3.1mW
$P_{in}$ = 24.7mW
Inverse Q (x10$^{-5}$)
15
10
5
0
-5
-10
-15
-1.0
-0.8
-0.6
-0.4
-0.2
Cavity Offset Frequency (x10$^{5}$ Hz)

# Braginsky's Tranquiliser Paper

- 10cm cavity linewidth too narrow for $f_m$>30kHz: must use shorter cavity or lower finesse.
- Linear approximation not valid.
- Linewidth requirement means more difficult to create significant damping at high frequency.
- Power densities too high unless cavity g-factor is extremely close to unity! eg > 0.9999

# Two possible tranquiliser designs

1) 10cm cavity, F=2500, linewidth 600kHz.

2) 3cm cavity, F=20,000

In both cases need very large spots to cope with the power required.

Near unstable cavity: very susceptible to thermal lensing and alignment noise.

Case 1 needs unacceptable high laser power.

Case 2 needs lower power.

Both have impossible power densities unless spot size is very large ….g~.99999.

# Reduced $\mathcal{F}$ and the Power Requirement

- To reduce parametric gain 10-fold

requires $Q_m = 3\times10^7$ reduced to $3\times10^6$

- Effective mass: $m_{eff} = 10\text{kg}$
- Cavity length: $l_m = 10\text{cm}$
- $FWHM = 600\text{kHz}$
- Cavity pole: $f_p = 300\text{kHz}$
- $\mathcal{F} = 2500$
- Input mirror transmission:
  $T_{in} = 8.9\times10^{-4}$
- All other cavity losses:
  $L_{cav} = 16.2\times10^{-4}$
- Mechanical frequency:
  $f_m = 10\text{kHz} \rightarrow 150\text{kHz}$

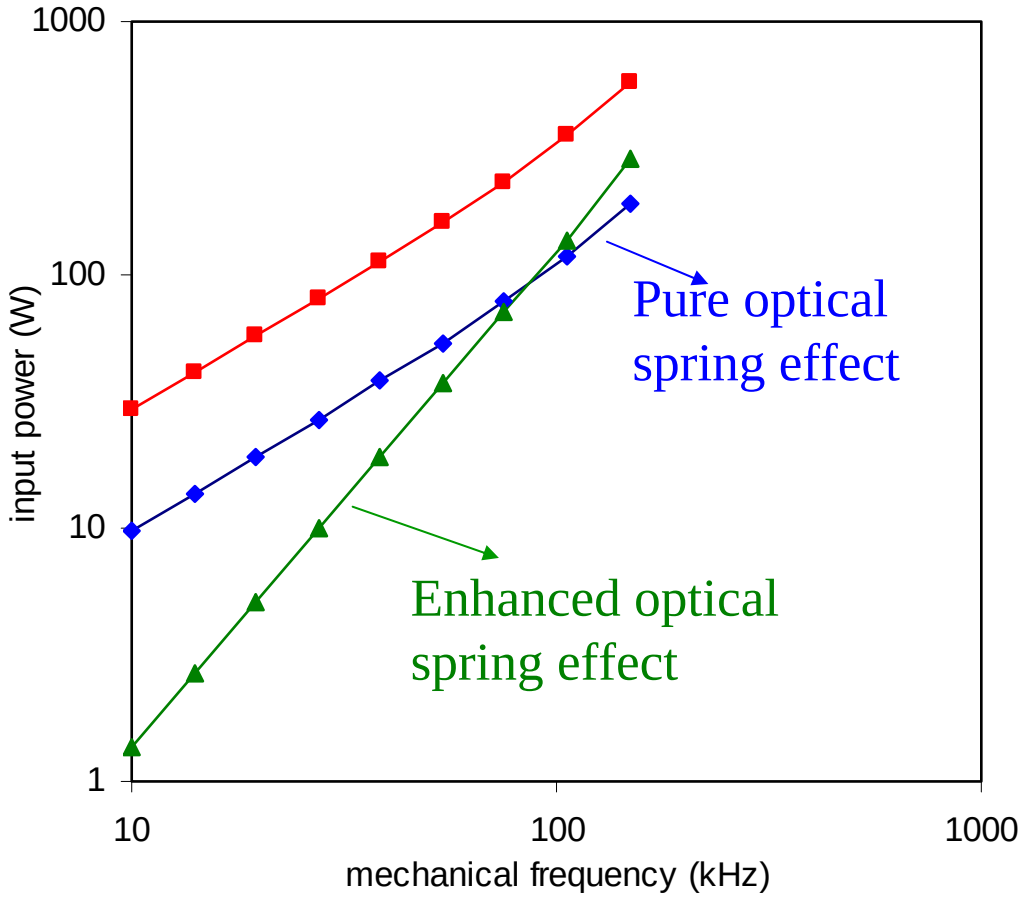


Unacceptable input power required for high frequency suppressing!

# Reduce cavity length

Example:

$l_m$=3cm

$\mathcal{F}$=20000

g=0.9999

Beam size~2mm

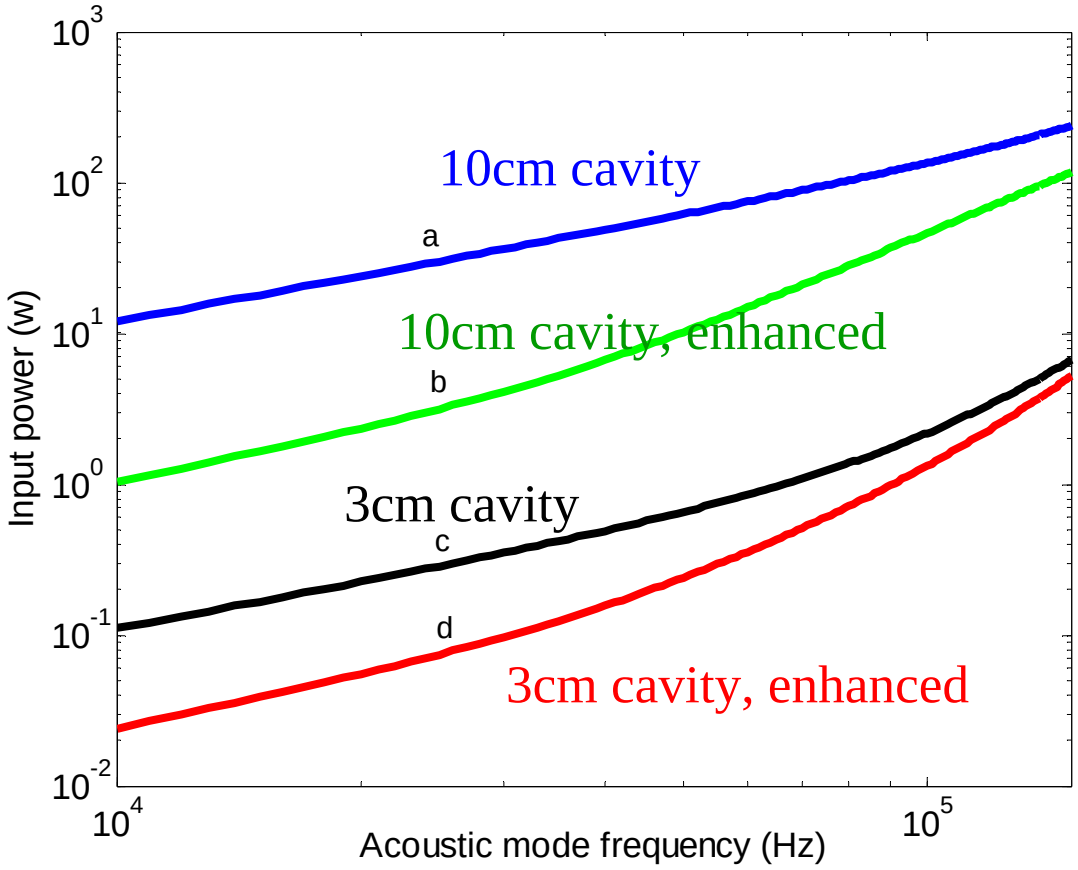


Input power: 1W

Circulating Power: 8.7kW

Too high power density!! Too close to flat-flat cavity

# summery

- Expect to observe 3-mode interactions in near future.
- PI observations depend on test mass high order mode Q-factors
- Tranquiliser cavity demonstrated at low frequency but seems impractical for AdvLIGO
- Next PI workshop at Gingin after Amaldi conference.

# Satellite Workshop of Amaldi 7

## Stabilisation of Parametric Instabilities in Advanced Gravitational Wave Detectors

## Perth, 17-19, July 2007

(exact time will be determined according to feedback)

a) to reach a consensus on the magnitude of the PI problem
b) to determine the level of risk PI poses to advanced detectors
c) to understand limitations in the theory and modelling of PI,
d) to assess methods for controlling PI and
e) to identify priorities for the next phase of research and
f) propose possible implementation strategies.